Investigation of hemicellulose biomaterial approaches : the extraction and modification of hemicellulose and its use in value-added applications

Wissam Farhat

N°d'ordre NNT : 2018LYSES032

THESE de DOCTORAT DE L'UNIVERSITE DE LYON
opérée au sein de
Université Jean Monnet – Saint-Étienne

réalisée en cotutelle internationale avec l'Université North Caroline State - Raleigh

Ecole Doctorale N° 488
Sciences Ingénierie Santé

Spécialité de doctorat :
Chimie et Sciences des Matériaux Polymères

Soutenue publiquement le 31/08/2018, par :
Wissam Farhat

Investigation of Hemicellulose Biomaterial Approaches: The Extraction and Modification of Hemicellulose and its Use in Value-added Applications

---

Devant le jury composé de :
Khan, Saad Professeur North Caroline State University (NCSU). Président, Rapporteur

Ford, Ericka Maîtresse de conférence HDR NCSU. Rapporteure

Venditti, Richard Professeur NCSU. Directeur de thèse
Ayoub, Ali Docteur NCSU. Co-directeur de thèse
Becquart Frédéric Maître de conférence HDR Université Jean Monnet (UJM). Directeur de thèse
Mignard, Nathalie Maîtresse de conférence HDR UJM. Co-directrice de thèse

L'Université de Lyon, Université Jean Monnet Saint-Etienne
&
North Carolina State University

DOCTORAL THESIS

(Joint Supervision PhD Program)

Specialty
Chemistry and Materials Science

By
Wissam FARHAT

To receive the
Doctorate Degree

Investigation of Hemicellulose Biomaterial Approaches: The Extraction and Modification of Hemicellulose and its Use in Value-added Applications

---

Dissertation Defense Date: August 31, 2018

Thesis Committee Members:

Ericka FORD	**Asst. Prof. at NC State University**	**Reviewer**
Saad KHAN	**Prof. at NC State University**	**Reviewer**
Nathalie MIGNARD	**Assoc. Prof. at Université Jean Monnet**	**Co-advisor**
Ali AYOUB	**Adj. Asst. Prof. at NC State University**	**Co-advisor**
Frédéric BECQUART	**Assoc. Prof. at Université Jean Monnet**	**Advisor**
Richard VENDITTI	**Prof. at NC State University**	**Advisor**

ABSTRACT

Wissam FARHAT**. Investigation of Hemicellulose Biomaterial Approaches: The Extraction and Modification of Hemicellulose and its Use in Value-added Applications.** (Joint supervision between the department of Forest Biomaterials, North Carolina State University, USA and Lyon University, Jean Monnet University, Laboratory of Polymer Materials Engineering, France).

The increased use of renewable materials is considered as one of the key issues of sustainable development. Carbohydrates are renewable materials that are readily biodegradable and tend to degrade in biologically active environments. Hemicelluloses (HC) are one of the most common polysaccharides next to cellulose and chitin, representing about 20-35% of lignocellulosic biomass, and have not yet found broad industrial applications as does cellulose. Hemicellulose is a hetero-polysaccharide and a green substitute for petroleum based polyols and is a non-food-based substitute for starch polyols. The aims of this project are to develop an optimized strategy for the extraction of hemicellulose and the use of the extracted hemicellulose in value-added biomaterials. The extraction of hemicellulose would have great potential to supply raw materials for the new bio-economy.

In this research, we have used the alkaline method to extract long chain hemicellulose from switchgrass (SWG) and bleached pulp (B-HWP). The hemicellulose extracted by aqueous NaOH solutions (3–17% $NaOH_{aq}$) from B-HWP was relatively pure with near 0% lignin and 90% xylose content, whereas the partially delignified SWG hemicellulose contained about 3-6% lignin on a weight basis and 72–82% xylose, depending on the NaOH concentration during extraction. A maximum molecular weight of SWG hemicellulose of 64,300 g/mol was achieved for the 10% NaOH solution extraction. The residual lignin showed was associated with a reduction in the system T_g. For instance, the T_g of pure hemicellulose is significantly reduced from 147°C to 132°C with 4.8% lignin.

The techno-economical feasibility of building a commercial biorefinery for the production of hemicellulose using bleached pulp as a starting raw material was examined. Our preliminary

results showed that the designed refinery requires 101 tons/day bleached pulp, 268 tons/day acetic acid, and 37 tons/day makeup ethanol to produce 88 tons/day dissolving pulp, 10 tons/day hemicellulose, and 376 tons/day sodium acetate. The capital investment was was indicated to be U$ 184.6 million. The operations involved with the sodium acetate contributes costs of $ 52.8 million, which represents about 28.6% of the total investment. However, the cost of the production of hemicellulose is $10.4, which represents 5.6% of the total investment. Our results revealed that this technology is not well suited for large scale up and other process alternatives should be developed.

To expand its applications to the field of stimuli-responsive hydrogels, coating and adhesives, polymer networks, as well as drug-delivery systems, hemicellulose was functionalized by introducing reactive groups onto its main chain. A hemicellulose based water resistant gel for coating applications has been synthesized. The hemicellulose crosslinked with 5-10% ammonium zirconium carbonate (AZC) shows promising potential for coating applications and may be an important higher valued product. We have reported that the loading stress required to break a hemicellulose-based adhesive connection between two paper surfaces was 0.89, 2.02, 2.75, 3.46, and 3.11 (MPa) for 2, 4, 6, 8 and 10% AZC samples, indicating that up to about 8% AZC crosslinker in the hemicellulose increases the adhesive strength behavior of the material.

In addition, hydrogels were formed from the macromolecules: starch, hemicellulose, and lignin using reactive extrusion in the presence of citric acid with and without SHP catalyst. The water uptake of the hydrogels was determined for a pH range from 4 to 9 and a temperature of 37°C, similar to physiological conditions. The swelling behavior of the designed hydrogels is dependent on the pH of the surrounding environment. Hydrogels swelling degree increased at high pH values. Equilibrium swelling of the hydrogels was as high as 1400% at pH 9. This is due to electrostatic repulsion generated by the ionized citric acid moieties grafted to the polymer. This repulsion results in a very loose structure capable of absorbing relatively high amounts of the fluid from the external environment.

The interest in stimuli-responsive natural polymers has entirely expanded in this century as a way to eliminate discarded plastic and polymer wastes. We have prepared thermally reversible

hemicellulose-based networks, crosslinked by means of Diels-Alder chemistry. Hemicellulose was first converted into a thermoplastic material via ring-opening graft polymerization of caprolactone to enhance the material processability. The grafting of PCL onto the hemicellulose was confirmed by ^{1}H-NMR by the presence of protons signals that correspond to PCL side chains and PCL substituted XylP protons. Hemicellulose grafted PCL showed an improved thermoplastic characteristic in comparison with pure hemicellulose as evidenced by a high tendency toward film formation and T_g reduction from 144.3°C (pure hemicellulose) to 84.1°C (HC_gPCL, DP4.26). The thermoplastic hemicellulose (hemicellulose-grafted-poly(caprolactone) was functionalized with different amounts of furan rings and allowed to react with bismaleimide through Diels-Alder reaction. The temperature dependent reversibility of the designed networks was evaluated by solubility and rheological assessments. The creep-recovery tests were applied to the designed networks at two different temperatures; (80°C) and (150°C), respectively. At low temperature (80°C) the samples exhibited a complete recovery due to the solid viscoelastic behavior of the crosslinked materials; however, at higher temperature (150°C) the tested specimens lost part of their elastic behavior and were converted to a liquid viscoelastic materials in response to the de-crosslinking as induced by the opening of the DA adduct at such high temperature. Also, temperature-sweep tests indicated that the temperature at which the networks disassemble varies based on the amount of the furan moieties in the initial copolymer and can range between 108.6 and 127.6°C. The designed networks display promising molecular and synthetic features for the production of high-performance temperature-responsive polymers from renewable resources.

Finally, the worldwide potential demand for replacing petroleum-derived raw materials by renewable resources in the production of valuable biodegradable polymeric materials is significant from both social and environmental viewpoints fuel and will predominate in the coming periods.

Keywords: Biomaterials, Sustainable polymers, Green chemistry, Hemicellulose, Bioeconomy

RESUME

Wissam FARHAT**. Stratégies d'Investigation de Biomatériaux à base d'Hémicellulose: Extraction et Modification de l'Hémicellulose et son Utilisation pour Applications à Haute Valeur Ajoutée.** (Cotutelle entre le Department of Forest Biomaterials, North Carolina State University, USA et l'Université de Lyon, Université Jean Monnet, Laboratoire Ingénierie des Matériaux Polymères, France).

L'utilisation de matériaux renouvelables est considérée comme l'un des points clés du développement durable. Les glucides sont facilement biodégradables et ont tendance à se dégrader dans les environnements biologiquement actifs. L'hémicellulose (HC) est l'un des polysaccharides les plus courants, représentant environ 20 à 35% de la biomasse lignocellulosique, et n'a pas encore trouvé sa place dans de larges applications industrielles comme la cellulose. L'hémicellulose est un hétéro-polysaccharide. C'est aussi un substitut vert pour les polyols issus du pétrole ainsi qu'un substitut non alimentaire des polyols d'amidon. Les objectifs de ce projet sont le développement d'une stratégie optimisée pour l'extraction de l'hémicellulose et l'utilisation de l'hémicellulose dans les biomatériaux à valeur ajoutée. L'extraction de l'hémicellulose aurait un grand potentiel pour fournir des matières premières à la nouvelle bio-économie. Pour étendre ses applications au domaine porteur des hydrogels, comme aux revêtements et adhésifs sensibles aux stimuli, des réseaux de polymères ou des systèmes de relargage de médicaments, les propriétés de l'hémicellulose ont été modifiées en introduisant des groupes réactifs sur sa chaîne principale avant de mettre au point les matériaux souhaités. Enfin, le potentiel de remplacement des matières premières dérivées du pétrole par des ressources renouvelables pour la production de précieux matériaux polymères biodégradables est important du point de vue social et environnemental..

Keywords: Biomatériaux, Polymères renouvelables, Chimie verte, Hémicellulose, Bioéconomie

DEDICATION

To my father Ali and my mother Neamat

To my Sisters Riham, Weam, Rayan, and Leen

To my Niece Lamis and my Nephew Hadi

To all my family members and loved ones

Thank you for your sacrifices

Thank you for your Support

Billion thanks for your Love

BIOGRAPHY

On August 15th, 1992, Wissam A. Farhat was born and raised in a calm and lovely town near the sea called Ansariyeh, South Governorate in Lebanon. His Dad Ali, has his own business of blacksmithing. During his childhood, Wissam used to help his father in his work, mainly during the rush time. After high school, he decided to move to Beirut to start a new journey as a future scientist. He was encouraged to pursue a Bachelor degree in Biochemistry at the Lebanese University. In 2013, he received the Bachelor of Science Degree in Biochemistry, followed by the Master's degree in Oncology and Cancer Biology in 2015. During his Master studies, Wissam completed nine months of internship at the American University of Beirut (AUB). For professional growth as an academic scholar and researcher in science, he was encouraged to pursue his Doctoral studies in polymer and materials science, under a joint supervision between Lyon University, laboratory of Polymer Materials Engineering (IMP), France and North Carolina State University, department of forest biomaterials, USA. As graduate student, Wissam has showed a high level of performance, as evident in his list of awards and publications, including the prestigious Eiffel Excellence Scholarship (awarded in 2017), issued by the French Ministry of Europe & Foreign Affairs that has funded part of his dissertation work.

ACKNOWLEDGMENTS

My educational and professional journey is full of intellectual and personal connections from around the world. The work presented in this dissertation is made possible with the following people who have been supportive in my academic and personal life.

I would like to express my sincere gratitude and appreciation to my advisors and co-advisors, Drs Ali Ayoub, Frederic Becquart, Nathalie Mignard, and Richard Venditti, who have been patient about giving perfect directions, allowing independence as a graduate student and generous support, so I am deeply appreciative of all their time. The collaboration between NC State University and Lyon University was led by Dr. Ayoub who gave special directions during my PhD journey. Dr. Becquart and Dr. Mignard guided my work at IMP, France as they have inspired numerous ideas toward my advancement. Dr. Venditti's mentorship and guidance during my work at NCSU had a tremendous impact on my professional career.

Besides my advisors, I would like to thank the rest of my thesis committee, Drs Saad Khan and Ericka Ford for their insightful comments and for the questions which incented me to widen my research from various perspective. Also, Thanks to Dr. Mohamed Taha for his help in initiating my scientific research and thanks to Drs Christian Carrot and Jean-Charles Majesté for allowing me to pursue part of my research at their laboratories at IMP.

Similar, profound gratitude goes to Mr. Tiago De Assis, for his guidance and assistance in the techno-economic analysis and useful discussions. I am particularly grateful to Tiago and Camilla Abbati de Assis for their heart-warming support at Raleigh, North Carolina. I have very fond memories of my time there. Special mention goes to all of the department members from NC State and IMP mainly to Carolina Londono Zuluaga, Sachin Agate, Remil Aguda, Matthew Kollman, Ilhem Charfeddine, Caroline Pillon, Alessandro Fouilloux, Xiang Li, Bastien Bessaire, Benjamin Risse, Teddy Tichane, and Xavier Dreux, for the stimulating discussions, and for all the fun we have had in the last three years. Also, I would like to thank my friends in particular Dr. Karim El Roz for his support and the adventures we experienced together while at NC State.

I take this opportunity to acknowledge the French Ministry of Europe & Foreign Affairs for the awarded Eiffel Scholarship that has funded a part of my PhD thesis. Finally, but by no means least, thanks go to my parents for the unceasing encouragement, support and attention. Million thanks to my Dad Ali, my Mom Neamat and my Sisters, Riham, Weam, Rayan, and Leen. They are the most important people in my universe and I dedicate this PhD dissertation to them. This accomplishment would not have been possible without them. Thank you for your sacrifices. Billion thanks for your love.

Table of Contents

General Introduction: A Brief Summary of the Doctoral Dissertation

Currently, there is a very strong interest to replace synthetic polymers with natural polymers for applications that interact with humans or the environment. This is based on human health, environmental impacts at end of life, the use of renewable resources, and for national security. The advancement in the scope of sustainable biomaterials is an essential step to solve echological and economic issues currently impacting present and future generations. Hemicelluloses (HC) are arguably the second most abundant polysaccharides after cellulose, representing about 20-35% of lignocellulosic biomass, and have not yet incorporated in a broad industrial applications.

Chapter one of this dissertation is a bibliographic research devoted to the methods used to extract hemicellulose, the structural properties of hemicellulose, and the use of hemicellulose in value-added biomaterials. In fact, hemicelluloses, due to their hydrophilic and physical crosslinked (H-bonds) nature, may tend to be overlooked as a component in water-resistant product applications. However, their domains of use can be greatly expanded by chemical derivatization. Research in which hydrophobic and processable derivatives of hemicellulose are used with to prepare films and composites are considered in this chapter. Isolation methods that have been used to separate hemicellulose from biomass are also reviewed. In addition, the most useful pathways to alter the hemicelluloses into hydrophobic and processable material are reviewed. In this way, the derivatization can increase the applications of themicelluloses. Several applications of these materials are discussed

The extraction of hemicellulose would have great potential to supply raw materials for the new bio-economy. We have recently conducted an optimized hemicellulose extraction technology from different starting materials as discussed in Chapter two. In this strategy, the starting raw materials were subjected to an alkaline treatment for both delignification and hemicellulose extraction. This strategy was adopted to extract high molecular weight polymeric hemicellulose. In addition, the technical and economical analysis for this extraction process was examined to provide a

preliminary results about the feasibility of commercial biorefinery for the production of hemicellulose using bleached pulp as a starting raw material.

To expand its applications to the field of stimuli-responsive hydrogels, coating and adhesives, polymer networks, as well as drug-delivery systems, the properties of hemicellulose were modified by introducing reactive groups onto its main chain. Hemicellulose based materials were prepared and characterized for their suitable application. In Chapter three, we have synthesized a water resistant gel for coating applications. The natural polymer hemicellulose crosslinked with ammonium zirconium carbonate shows a promising potential for coating applications and maybe an important higher valued byproduct for the coating industries.

Recently, we have incorporated the reactive extrusion as a green technology for the synthesis of pH-sensitive gel materials from natural polymers for the potential use as drug delivery vectors. This novel technology is presented in Chapter four of this dissertation. The designed hydrogels were formed using citric acid (CA) as a non-toxic cross-linker. The gels showed a strong swelling ability dependent on the pH. The sensitivity of the hydrogels to pH can be rationalized to the ability of the carboxyl groups of CAs to ionize with increased pH forming a loose structure as caused by the electrostatic repulsion of the ionized CA. This repulsion results in the formation of a very loose structure capable of absorbing a relatively high amounts of the fluid from the surrounding medium.

In Chapter five, we have conducted a synthetic method for the conversion of hemicellulose into a thermoplastic material. This method embrace ring opening graft polymerization of the cyclic ε-caprolactone (CL) onto the hemicellulose backbone. The various characterization analysis of the structure, physicochemical and mechanical properties of the copolymers revealed a successful grafting. The grafted materials exhibited interesting “thermoplastic features” as evidence in the reduction in the glass transition temperature sand the ability to form a continuous film compered to the unmodified hemicellulose. These materials showed great tendency to degrade under aerobic conditions, enhancing their use in bioplastic industry.

In our group, we have recently synthesized a stimuli-responsive hemicellulose based thermo-reversible polymeric gels by means of Diels-Alder (DA) chemistry as discussed in Chapter six.

This study was conducted to enable in-depth understanding of the various molecular and synthetic routs for the production of high-performance temperature-responsive polymers from renewable resources. Thermomechanical analysei and rheology measurements were used to authenticate the thermoreversible properties of the manufactured gels.

To sum, the global impending demand for substituting fossil fuel based materials by sustainable resources for the design of valuable eco-friendly polymeric materials is important from both public and ecological viewpoints and will dominate in the coming decades. Our results in all the investigation areas presented here shed light on vital features of the use of hemicellulose in sustainable and renewable biomaterials, representing a step forward towards the expansion of value-added biomaterials that might solve future economical and ecological problems.

Chapter 1: Introduction to Hemicellulose: A Renewable and Sustainable Material

1. Bioeconomy: Research and Innovation

Fossil materials and energy resources such as petroleum, gas, and coal are the major reason for heating up the global climate. They are the main reason of several challenges including; climate change, food security, health, and energy security. Securing the universe from these challenges require new economic sectors that depend preferably on the use of renewable and sustainable resources for materials and energy production. Bio-based economy or "*bioeconomy*" is a strategy adopted to reduce the environmental hazards the world is facing already today [1]. It is envisioned that this strategy will deal with other problems related to food security, health, industrial restructuring, and energy security. In general, the term "*bioeconomy*" represent a part of the economic cycle that inspire the use of sustainable bio-resources from land and sea (biomass), including crops, wood, fish, and microorganisms to design and produce bio-based materials and energy (Figure 1) [2].

The goal of the low-emissions-bioeconomy is more innovative and deal with merging the need for renewable agriculture and the sustainable use of biological resources for industrial practices, while ensuring biodiversity and ecological security. The bioeconomic policy depends on several crucial factors that embrace the evolution of new technologies, developing new markets, and competitiveness with petroleum-based economy [2]. The transition towards a larger and more advanced bioeconomy will influence many aspects of the economy, society in general, and the

environment. To achieve this transition, the European Commission has arranged a strategy to shift the European economy towards a superior and more sustainable consumption of renewable resources [3]. The National Renewable Energy Action Plans (NREAPs), suggested that the European Union (EU's) electricity production from renwable resourses will increase from 90 TWh in 2006 to around 230 TWh in 2020 [4].

In addition, according to the U.S. Department of Agriculture (USDA), the bio-based products already contribute $369 billion to the U.S. economy each year and employment of four million workers [5]. Also, it has been envisioned that the bioeconomic contribution for the production of chemicals and materials will increase from 30 billion pounds or 12% of the current production of target United States chemical commodities in 2010, to 45 billion pounds (18%) in 2020, and 62.5 billion pounds (25%) in 2030 [6].

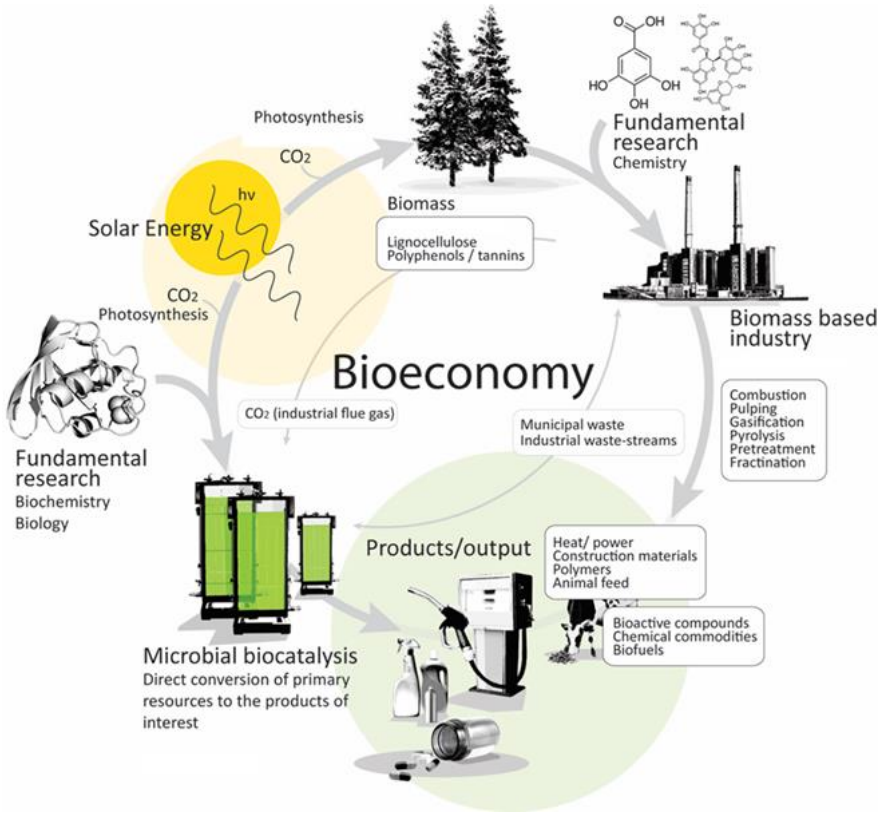

Figure 1. Schematic overview of the bioeconomic policy. Towards economically competitive and sustainable solutions to global challenges. Reproduced from [7].

The awareness about bio-based economy have attracted the governments and industries in the globe. For instance, the topic of bioeconomy have gained significant interest over the last several years as indicated by the steadily increasing number of publications and citations on the topic (Figure 2).

The concept of bioeconomy comprise several scientific disciplines. In fact, it is likely possible to differentiate between three ultimate visions of what a bioeconomy constitute. These visions based on the scientific contribution and the significance of bioeconomy studies in the fields of natural and engineering science [1]. These visions are:

a. The ***bio-technology*** vision highlights the significance of bio-technology studies and its commercialization in the different economic sectors.
b. The ***bio-resource*** vision explores the importance of the research and advancements in the conversion of biological raw materials in sectors such as agriculture, marine, forestry, and bioenergy, as well as on the development of innovative value chains.
c. The ***bio-ecology*** vision investigates the influence of ecological routes to tune the use of energy and nutrients, allow biodiversity, and evade monocultures and soil degradation.

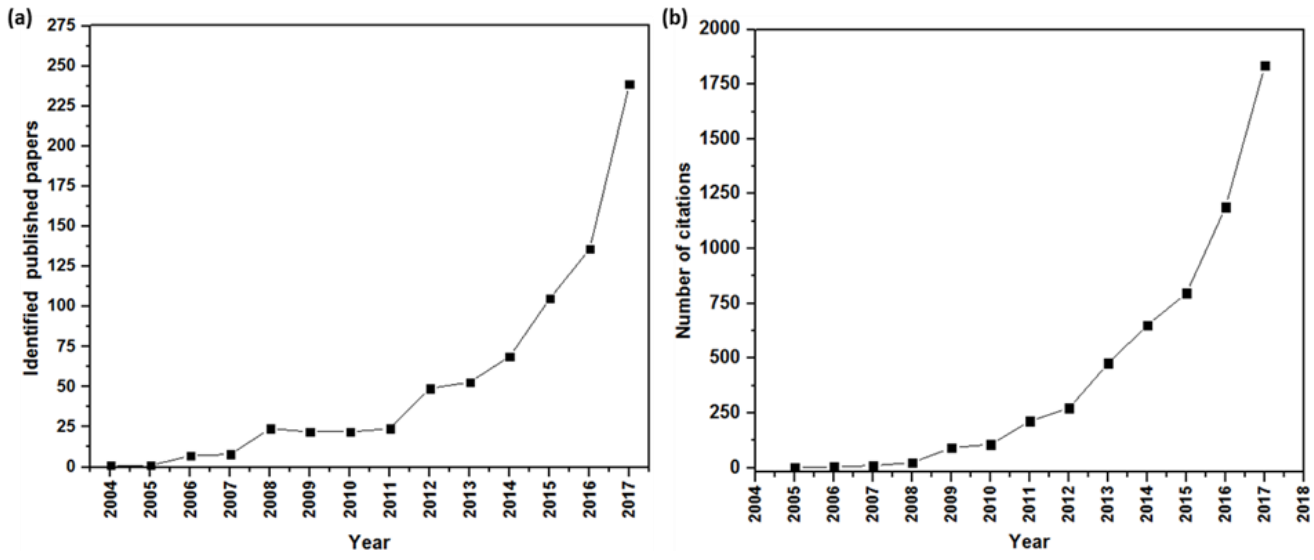

Figure 2. Graph showing Web of Science search results for the key word "bioeconomy" from 2004 to 2017. (a) is the identified published papers and (b) is the number of citations achieved. (We did not include 2018 to allow the papers published in the last year to gather citations in 2018. Results collected: April 23, 2018).

Finally, it is anticipated that the overall success of the bioeconomic approaches require a substantial support that involve the proposition of new policies and financial tools to be investigated for allowing and facilitating the investments by industrial sponsors in this sector.

2. Biomass resources and biorefinery approach

Bioeconomy concept depends on the availabiliy of the biomass. A biomass is all plants and plant derivatives that has already played an important role in the production of biofuel and biobased products. Several reports have predicted an increase in the future dependence on biomass for the production of energy, chemicals, and bio-based materials. For example, in 1992, the Renewable Intensive Global Energy Scenario (RIGES) suggested that, by 2050, biomass could supply approximately half of the world's energy needs [8]. In its Bioenergy for Heat and Power Technology roadmap in 2012, the International Energy Agency (IEA) has indicated that the potential utilization levels of biomass for energy by 2050 could be in the range of 100 to 300 EJ per year, compared to 50 EJ in 2012 [9].

In addition, with expanding concerns about ecological conservation and waste management, naturally occurring renewable materials such as carbohydrates, proteins, and others have become well known in the production of biobased products. The expression 'biobased products' refers to a diverse class of products including: biofuels (biodiesel and bioethanol), bio-energy (heat and electricity), and biobased chemicals and materials (succinic acid, polylactic acid, formic acid, fatty acid derivatives, and others) that can be produced by a biorefinery [10]. According to IEA Bioenergy Task 42 Biorefinerie, "Biorefining is the sustainable processing of biomass into a spectrum of marketable products and energy" [11]. Biorefinery systems work by processing the input (biomass) to generate an output (fuel, chemicals, heat, electricity) (Figure 3) [12]. The ideal outcome would be to accomplish all of these objectives with the least impact on wildlife, water, soil, or air quality.

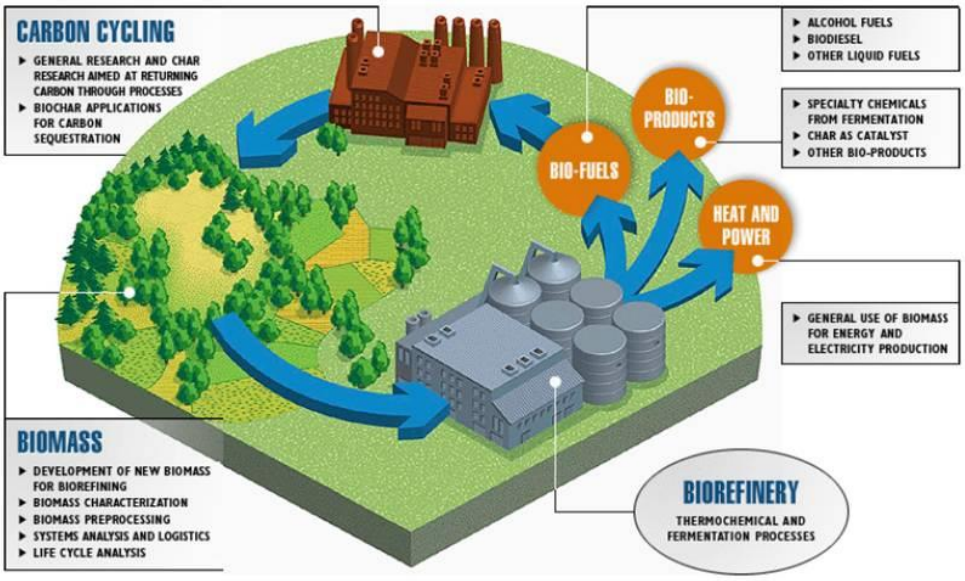

Figure 3. The biorefinery concept. Towards sustainable and eco-friendly products [13].

Two categories of biomass have been used as input to a biorefinery, classified as first and second generation. In the former, they are edible biomass based-products mostly composed of starch-rich plants [10]. However the need for food and improved economic benefits of starch has captured the attention of many to move towards second–generation biorefinery routes that consists of residual non-food parts of the current crops or other non-food sources (lignocellulosic biomass) [10]. An example of this would be the use of hemicellulose for starch non-food applications. The use of the environmentally friendly lignocellulosic biomass (cellulose, hemicellulose, and lignin), structure shown in Figure 4, as a source of chemicals and other materials, replaces the oil-based, fossil hydrocarbon to create green products. The low cost, availability, renewability, and the eco-friendly characteristics of bio-based raw materials are promising factors in chemicals and materials production [14].

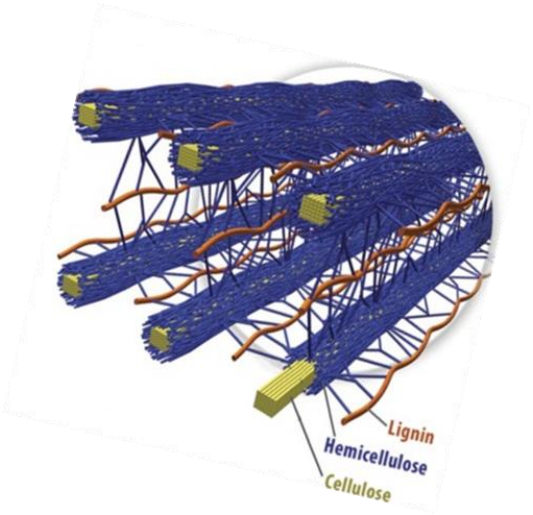

Figure 4. Microscopic structure of lignocellulosic biomass [15].

3. Hemicellulose: An added-value material in the bioeconomic cycle

The US Department of Energy reported that about 1.3 billion dry tons of biomass could be available for large-scale bioenergy and biorefinery industries in the U.S. alone [16]. Based on the 1.3 billion tons of biomass, it can be estimated that about 400 million tons of hemicelluloses are available in the United States each year. Also it is reported that about 15 million tons of hemicelluloses are produced per annum from the pulp and paper industry, which gives about 415 million tons of hemicellulose available every year for utilization in bioenergy and biorefinery industries in the U.S. [16]. However, this hemicellulose is not utilized for value-added applications. Rather, it is primarily incinerated to produce energy. In the paper industry much of the hemicellulose remains in the fibers, which provides a strength benefit to the paper product. However, another portion is discarded as waste material during bleaching and other operations. Also, in the kraft pulping processes, the majority of hemicellulose are degraded into a low molecular weight isosaccharinic acid, dissolved with lignin in the black liquor, and then burned as a fuel [16][17]. However, since the heating value of hemicellulose is approximately half that of lignin [18] and because of its availability, it would be beneficial to develop a number of bioproducts such as biochemical and biomaterials to enhance the value extracted from wood. This could be an important part of a forest-based biorefinery that offers technologies and enabling the

conversion of biomass into a wide range of marketable products such as fuel, chemicals, food, and materials.

Moreover, in the recent years hemicelluloses attracted the research on ist use in certain applications such as hydrogels, cosmetics, drug carriers, and others [19][20][21]. However due to its hydrophilic nature, hemicelluloses show phase separation and poor mechanical properties when blended with hydrophobic polymers. Also, as other polysacharides, hemicellulose shows extensive hydrogen bonding that convert it into a non-processable thermoset material. These properties limit the use of hemicellulose for added-value applications. To overcome such issues, hemicelluloses can be chemically modified by incorporating a hydrophobic and/or a thermolastic group into its back bone and thus enhance its structural features and open new windows for applications of hemicelluloses.

3.1.Hemicellulose structural features

Hemicelluloses are arguably the second most abundant renewable component of lignocellulosic biomass after cellulose [22][23]. However, unlike cellulose in which the monomer units are chemically homogenous, hemicelluloses are a heterogeneous branched group of polysaccharides made up of pyranoses and furanoses sugar units including: xylose, mannose, arabinose, glucose, galacturonic acid, and others. Different hemicellulose composition, structure, and amount could be obtained from different sources of biomass. For example, in hardwoods, the major hemicellulose component is *O-acetyl-4-O-methyl-glucuronoxylan*, in which one-tenth of the xylopyranose backbone units are substituted at C-2 with α-(1→2)-linked 4-O-methyl-glucuronic acid residues; whereas, occurring in about 70% of the xylopyranose backbone is a hydroxyl group that is acetylated at C-2 or C-3 (Figure 5) [24][25].

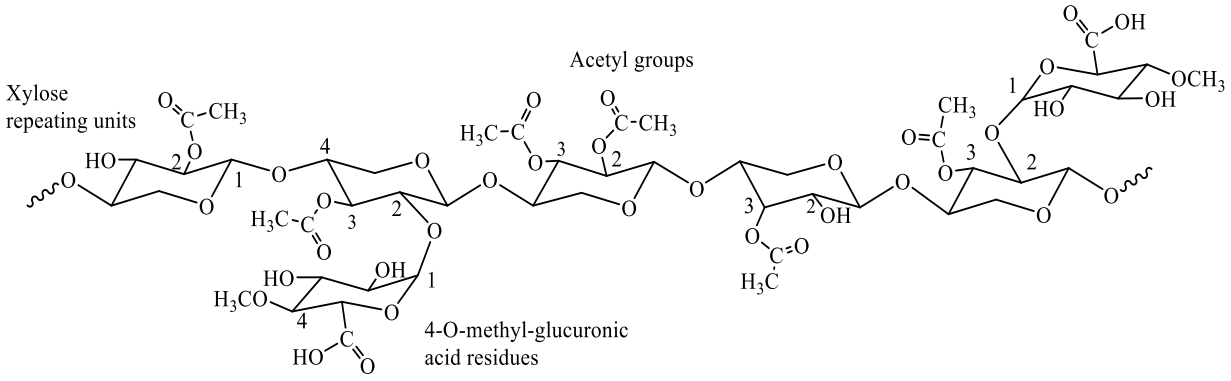

Figure 5. O-acetyl-4-O-methyl-glucoronoxylan: The major hemicellulose component in hardwoods

This is different from softwood, in which the major hemicellulose component is *O-acetyl-galactoglucomannan*. This has a backbone consisting of a randomly distributed β (1→4) linked mannose and glucose units with α-(1→6) linked galactose units attached to the mannose and glucose units. Depending on the source of the polysaccharide, the mannose/galactose ratio can vary from 1.0 to 5.3 [26]. For example, the mannose/glucose ratio is 3.3 in *Senna occidentalis* and 1.6 in *Cyamopsis tetragonoloba* [27]. The hydroxyl groups at C-2 and C-3 in the mannose units are partially substituted by acetyl groups with a degree of acetylation of 20% [28][16][29]. (Figure 6)

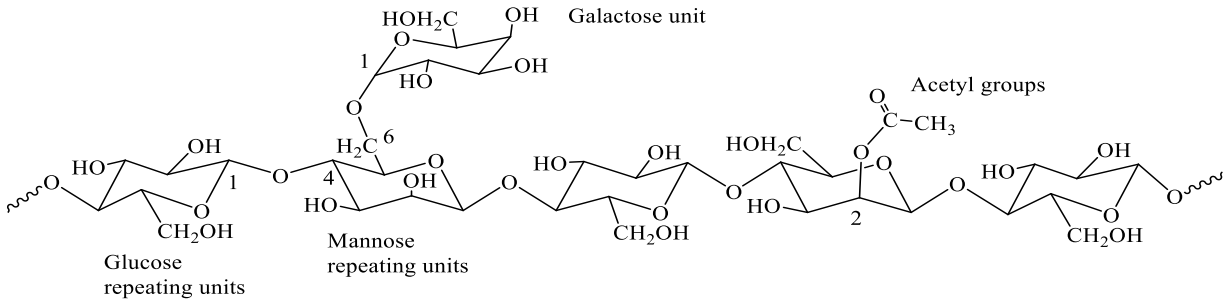

Figure 6. O-acetyl-galactoglucomannan: The major hemicellulose component in softwoods

Moreover, a*rabinoxylan* is the predominant component of hemicellulose in grasses including switchgrass and others [30]. It is a hemicellulose that consists of β-(1→4) linked xylose units, with α-(1→2) and α-(1→3) linked arabinose units (Figure 7) [31].

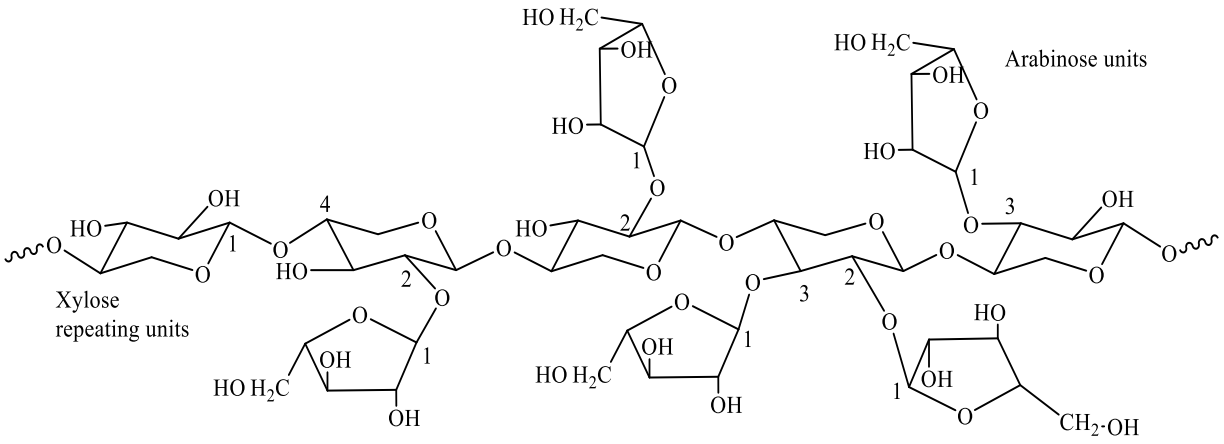

Figure 7. Arabinoxylan: The major hemicellulose component in switchgrass

Other less abundant hemicelluloses, including mannan, arabinan, galactan, arabinogalactan, rhamnogalactan, and others are present in the plant cell walls. They may be present in the plant as a complex mixture. These hemicelluloses are abundant in the soft tissues of some fruit and sugar beet pulp, but they are less frequent in wood tissues. Figure 8 shows the main monomeric sugars of hemicellulose

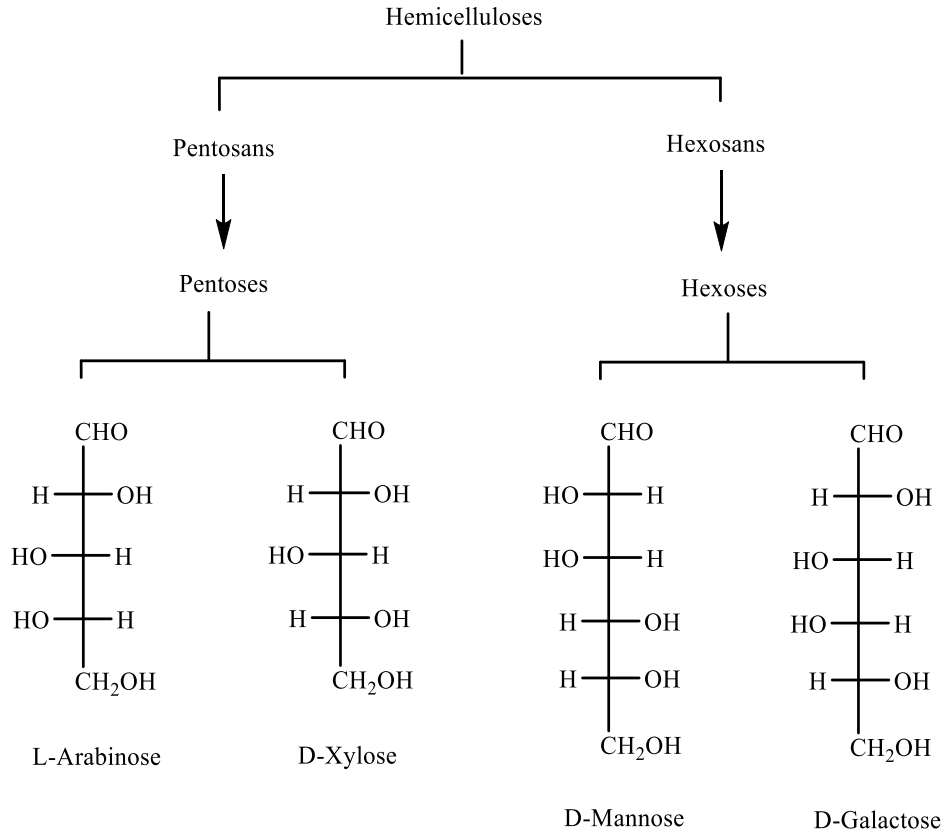

Figure 8. Main monomeric sugars of hemicelluloses

3.2. Hemicellulose Extraction Methods

Several methods have been explored to extract hemicellulose from woody and non-woody tissues. Those methods include dilute acid pretreatments [32][33][34], alkaline extraction [35], alkaline peroxide extraction [36], liquid hot water extraction [37][38], steam treatment [39], microwave treatment [40], ionic liquid extraction [41], and others [42].

Dilute acid pretreatment, often involving about 0.5-1% sulfuric acid, is a useful procedure for hemicellulose isolation [34]. By this method the majority of the original amount of hemicellulose from the poplar tree (hardwood) can be recovered as dissolved sugar (Figure 9) [34]. However, in the course of such treatment a high amount of the hemicellulose monomers are degraded, leading to the generation of byproducts [32][33]. On the other hand, extraction of hemicellulose from sugarcane bagasse using hot water extraction at a temperature of 150 to 170^{o}C recovers almost

90% of the hemicellulose as dissolved sugar, but with relatively less monomer degradation compared to the dilute acid method [38]. Because hot water treatment cleaves some of the acetate groups from hemicellulose, the pH decreases. The reduced pH results in additional generation of acetic acid, leading to a phenomenon called “auto-hydrolysis”. It has been shown that auto-hydrolysis can be promoted by irradiating the wood with microwaves in water [39].

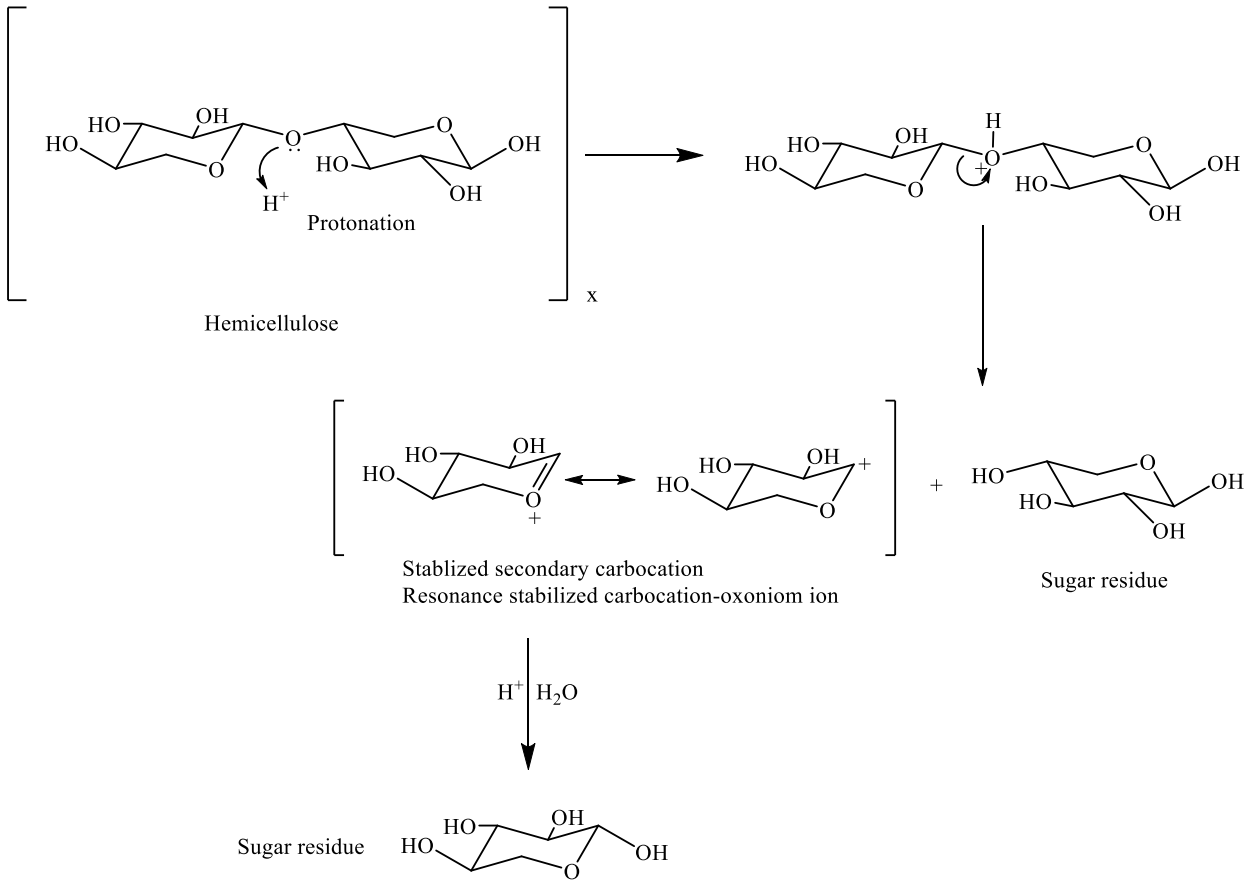

Figure 9. Schematic illustration of the dilute acid extraction mechanism of hemicellulose

Due to severe treatments caused by acidic and partly applied heated extraction processes, hemicellulose degrades by losing its chain length and consequently exhibits high polydispersity [38][39]. Steam and microwave treatment are combined with chemicals to dissolve the hemicellulose; however, due to the complexity of those methods, they have been applied mainly at a small scale for hemicellulose extraction**.** In steam treatment, ester bonds in the hemicelluloses will be cleaved; then the wood is treated with steam, resulting in the formation of acetic acid. This will lower the pH and thus induce auto-hydrolysis of the glycosidic bonds in the hemicelluloses.

Such a process will generate a low molecular weight, water-soluble hemicellulose. From this method one can get a low % yield of hemicellulose with significant contamination of dissolved cellulose and lignin and degradation products of the hemicellulose**.**

An ionic liquid/cosolvent extraction system has been used by Froschauer and his colleagues [41] to separate hemicellulose and cellulose from wood pulp. In this study hemicellulose-rich birch kraft pulp were selectively separated, with high levels of purity, into pure cellulose and a hemicellulose fractions using mixtures of cosolvents (water, ethanol, or acetone) and the cellulose dissolving ionic liquid 1-ethyl-3-methylimidazolium acetate (EMIM OAc) with reaction conditions of temperature 60°C for 3 h of stirring (Figure 10). This process was used to generate dissolving pulp that meet the manufacture of revived cellulose products and cellulose derivatives because of its extraordinary cellulose content which is assumed to be more than 90%, as well as the product's high brightness and a uniform molecular-weight distribution [41].

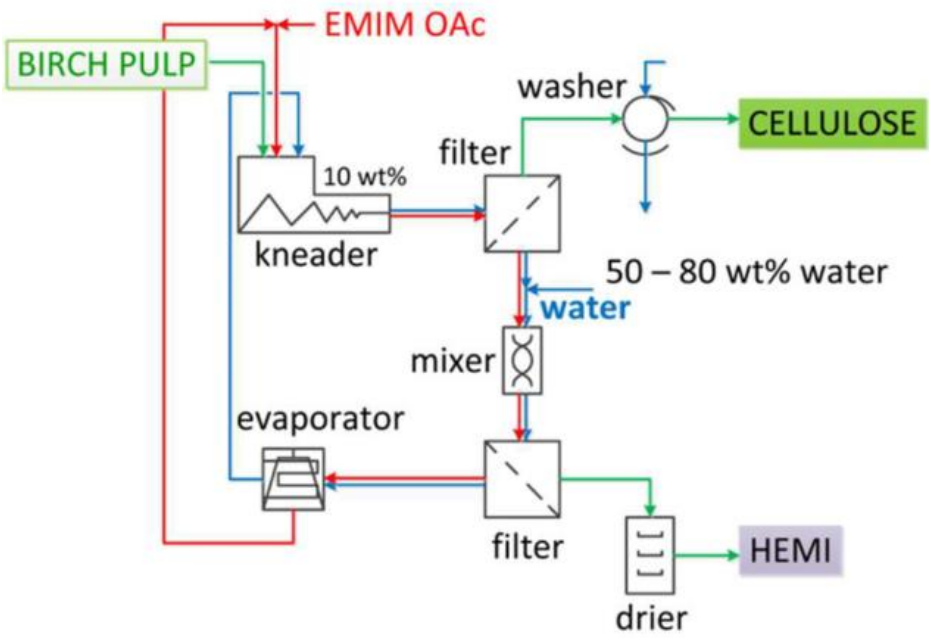

Figure 10. Schematic Illustration of the Fractionation of Hemicellulose-Rich Pulp into Cellulose and Hemicellulose [41].

Alkaline extraction is well studied approach, and it is known as a strong and efficient method for hemicellulose extraction [43] [44]. Alkaline treatment can cleave the ester linkage between the ferulic acid of the lignin and the glucan and arabinan residues of hemicellulose in the cell wall,

thus releasing oligomeric and polymeric hemicellulose rather than sugars as obtained from dilute acid extraction or hot water extraction (Figure 11) [29]. The extraction of hemicelluloses from various biomasses is expected to be closely related with the amount of lignin-carbohydrates complexes (LCCs) [16].

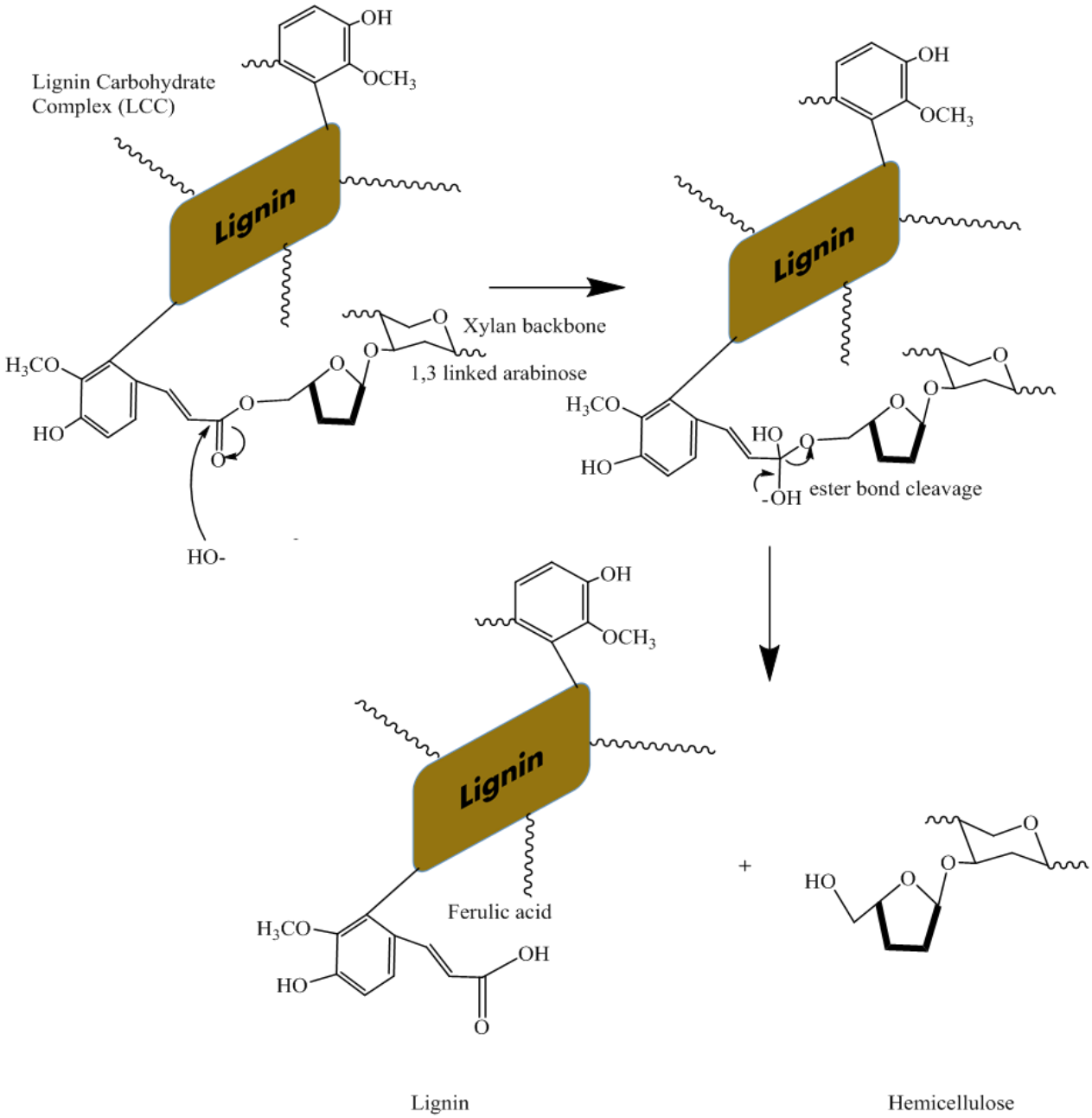

Figure 11. Schematic illustration of the mechanism of alkaline extraction of hemicellulose

The LCCs entail covalent linkages between lignin and carbohydrates, mainly hemicelluloses [45]. The major types of LCCs includes: phenyl glycoside, benzyl ether, and benzyl ester types of linkages [16][45]. Different biomasses have different frequencies of the LC complexes, for example the amount of ether and esters LCC linkages in pine and aspen CEL (cellulolytic enzyme lignin) has been reported as circa 2.2–2.5 and 0.3–0.6 per 100 monomeric lignin units, respectively [45].

The decision on which method would be used for hemicellulose extraction is highly dependent on the final application of the recovered hemicellulose. For example, if the extracted hemicellulose is targeted for the production of bioethanol, then the monomeric form of sugars is required, and thus it may be preferred to use dilute acid or hot water. In addition, xylose monomeric sugars are the major source of the natural food sweetener xylitol [46]. Xylitol is a naturally occurring five-carbon polyalcohol and has important properties that make it appropriate for sugar-free confections: It is entirely not dangerous for the teeth because of its anticaries characteristics and it is tolerated by diabetics. It is also widely distributed in the plant kingdom, especially in certain fruits and vegetables [47]. However, the small amounts present in these sources render its quantitative extraction difficult and uneconomical. In industrial scale, xylitol is consequently produced through chemical reduction of xylose derived from hemicellulosic hydrolysates of birchwood or other xylose rich materials [47].

Many yeast species, particularly *Candida* species, are good xylitol producers [46]. Xylitol is produced as a metabolic intermediate of D-xylose fermentation; D-xylose can be transformed to xylitol by NADPH-dependent aldehyde reductase, or can be isomerized to D-xylose by D-xylose isomerase, and then reduced to xylitol by NADH-dependent xylitol dexhydrogenase. A major source of D-xylose is sugarcane bagasse, the fibrous residue obtained after the extraction of sugar from sugarcane. This waste has been used as raw material for hydroxymethyl furfural production, paper pulp, acoustical boards, press woods, and agriculture mulch. Sugarcane bagasse can be hydrolyzed by dilute acid with high-solid, low-liquid ratio to get a mixture of fermentable sugars with xylose as the main constituent [48].

In the hydrolysate, some byproducts generated in the hydrolysis, such as acetic acid, furfural, phenolic compounds, or lignin-degradation products can be present. These are potential inhibitors

of the microbial metabolism. In order to provide hydrolysates suitable as fermentation substrate, other treatments, such as acidified activated charcoal or cation-exchange resins, can used to eliminate these toxic elements [48].

Some other applications require a high molecular weight polymer (blended plastics, hydrogels, and others). For those applications it may be extremely important to use the alkaline method for the isolation of hemicellulose from the biomass.

3.3. Differences between Hemicellulose Extraction Methods

Dilute acid pretreatment is one of the most significantly applied methods for hemicellulose isolation. By this method approximately 100% of hemicelluloses are broken down into monomeric sugars and sugar degradation products, including weak acids, furan derivatives, and phenolics, which considerably increases the vulnerability to hydrolysis of cellulose. The sugar degradation products are known to be inhibitors of fermentation, which limits the utilization of cellulose for bioethanol production. In addition, acid usage is often very costly due to the high cost of equipment required to be resistant to acid. Acid use is not always ecofriendly and can result in waste disposal problems [49].

Alkaline extraction is another widely used hemicellulose extraction method. However, during alkaline extraction, the usage of high alkaline concentrations may present environmental concerns and may lead to prohibitive recycling and wastewater treatment. In contrast to acid technologies, the reactor costs for alkaline extractions are lower. Alkaline methods greatly improve extraction performance by favoring lignin removal while leaving the hemicellulose in a polymeric form, not the individual sugars [49][50].

High molecular weight polymeric forms of hemicelluloses have been used in a wide range of applications, including resins, hydrogels, drug carriers, food additives, and many others [19][51][52][53]. On the other hand, the alkaline method for hemicellulose extraction can induce significant modifications to the extracted polysaccharide. Indeed; alkali extractions have the drawbacks of removing acetyl groups from the polymeric chains. Furthermore, a relatively high quantity of the hexuronic acid residues in 4-O-methylglucuronoxylans are cleaved and alkaline degradation occurs at the reducing ends of the polysaccharides [35][36].

Despite being currently at the laboratory/pilot stage, auto-hydrolysis methods for hemicellulose extraction could become commercially available. By this method, about 90% of the hemicelluloses can be recovered in the oligomeric form. This method does not require a catalyst for hemicellulose recovery. Auto-hydrolysis has a similar mechanism as the dilute acid method for hemicellulose extraction. Both processes are catalyzed by the hydronium ion. However, unlike the dilute acid method, auto-hydrolysis uses only water as the extraction medium. With increased temperature, the water auto-ionizes, releasing hydronium ion which induces a slight drop in the pH; this leads to a partial hemicellulose depolymerization by selective cleavage of both O-glycosidic linkages and acetyl groups. With time, acetic acid ionizes and releases hydronium ions, and thus improves extraction kinetics. The contribution of hydronium ions from acetic acid is higher than that from water auto-ionization [54][55]. Unlike the dilute acid pretreatment, in auto-hydrolysis as well as in steam explosion methods, low amounts of lignin can be solubilized and relatively small amounts of the monomeric residues are decomposed into sugar degradation products. Therefore the product is a liquid fraction without numerous amounts of inhibitor compounds. In both the steam explosion and auto-hydrolysis methods, hemicelluloses are recovered in an oligomeric form. This oligomeric form of hemicellulose has been used in some industrial applications including pharmaceuticals, chemicals, or food additives [50][56][57]. The main operational difference between these processes is that the steam explosion method utilizes a higher temperature for a shorter amount of time.

Extraction of hemicellulose from the non-delignified biomass (lignocellulosic materials) yields polysaccharides that are contaminated with high proportions with lignin, whereas hemicellulose separation from bleached pulps results in a relatively pure hemicellulose [58][59]. Several delignification methods have been reported, such as organosolv treatments where lignin removal is promoted by direct action of an organic solvent (ethyl acetate, acetic acid, acetone, methanol and others) [60]. These procesess can be catalyzed by acids or salts for selective delignification [61]. Another method is bio-delignification, in which the microorganism, including certain fungi and bacterial species, are used for the degradation of lignin. This method has advantages of low energy use and mild environmental conditions [62]. Table 1 provides the major differences between the extraction methods and their effects on the hemicellulose structure.

Table 1. Effects of extraction methods

Extraction Method	Recovered hemicellulose form	Formation of Sugar degradation products	Cost and environmental hazards
Dilute acid	Monomeric Sugars	High quantity	Expensive and waste disposal problems
Auto-hydrolysis	Oligomeric form	Low quantity	Inexpensive with low environmental hazards
Steam explosion	Oligomeric form	Low quantity	Inexpensive with low environmental hazards
Alkaline treatment	Polymeric form	Low quantity	Less expensive than dilute acid but with relatively high environmental problems

3.4. Structural Characterization of Hemicellulose: Analytical and Spectroscopic Techniques

The great interest in converting lignocellulosic biomass into valuable, green fuels and chemicals have challenged researchers to develop methods for determining the structure, the accurate chemical composition, the quantity, as well as the potential uses of hemicellulose in the lignocellulosic biomass.

Several analytical methods have been used to characterize hemicellulose [63][64]:

- High performance liquid chromatography (HPLC),
- Size exclusion chromatography (SEC),
- Gas chromatography-mass spectrometry (GC-MS),
- NMR spectrometry 1D and 2D,
- Matrix assisted laser desorption ionisation-time of flight (MALDI-TOF) mass spectrometry.

a. High Performance Liquid Chromatography (HPLC): Is a technique in analytical chemistry used to separate, identify, and quantify each component in a mixture. A hemicellulose polysaccharide can be subjected to hydrolysis into its sugars moieties by means of dilute acid treatment. The monosaccharide compositions of the hydrolyzed hemicellulose can be analyzed by HPLC [65].

b. Size Exclusion Chromatography (SEC): this technique, also known as Gel permeation Chromatography (GPC), is a commonly used polymer characterization method because of its capability to afford good molar mass distribution (Mw) results for polymers. This method typically requires aqueous solution to permit the transport of the polymer through the GPC column. However, due to the poor solubility of hemicelluloses in the most of organic solvents, hemicelluloses can be modified typically by esterification (e.g. acetylation) to increase their hydrophobic properties and hence, their solubility in organic solvents [29].

c. Gas Chromatography coupled Mass Spectroscopy (GC-MS): It is an analytical method that combines the features of gas-chromatography and mass spectrometry to identify different substances within a test sample. GC-MS has numerous advantages in carbohydrate analysis, generating well resolved chromatograms that allow the identification and quantification of the studied compounds, even if they are present in very small amounts [66].

d. 1D and 2D NMR spectrometry: NMR analysis is the method of choice for the structural analysis of polysaccharides including hemicellulose. It is a fast, reliable, and nondestructive technique. For unknown structure, NMR can either be used to match against spectral libraries or to infer the basic structure directly. Once the basic structure is known, NMR can be used to determine molecular conformation in solution as well as studying physical properties at the molecular level such as conformational exchange, phase changes, solubility, and diffusion [67]

e. MALDI-TOF Mass Spectroscopy: It is an ionization method that uses a laser energy absorbing matrix to create ions from large molecules with minimal fragmentation. The major advantages associated with the use of MALDI-MS include a high level of sensitivity; applicability to molecules exhibiting a wide range of masses; little or no fragmentation of the molecules being analyzed and the rapidity with which results can be obtained. Data analysis is enhanced by the fact that nearly only single-charged ions are generated. This fact also indicates that the mass to charge ratios of the ions formed in connection with MALDI analysis are directly related to the absolute molar masses of the molecules present (bio-macromolecules) [68][69]

In fact, there is no unique method that can fulfill all requisite parameters required to predict the structural features of the hemicellulosic material. But combination of the gamut of analysis techniques as already elaborated can provide a clear and trusted characterization.

In the research of Mazumder and his colleagues [63], hemicellulose was extracted from *Benincasa hispida* fruit with 1- and 4-M KOH, generating dual fractions, so-called B1OH and B4OH, respectively. The SEC analysis of the extracted hemicellulose indicated that both fractions are highly polydispersed, with one wide peak between 0.2 and 0.5 Kav for B1OH and 0.3 and the other peak between 0.6 Kav for B4OH fraction. Thus the apparent molecular weight of the extracted carbohydrates was assumed to be around 130 kDa. Compositional assessment of both fractions revealed the existence of both biopolymers, xyloglucan and xylan. Enzymatically hydrolyzed polymers by endo-β-(1→4)-D-glucanase, an enzyme known to cleave the β-(1→4)-D-glucosidic linkages of xyloglucan next to an unbranched glucose residue, were then analyzed by MALDI-TOF-mass spectrometry. The xyloglucan residues had the following m/z peaks values 1087, 1247, 1393 and 1555 (Th) which correspond to XXXG, XXLG and/or XLXG, XXFG and XLFG oligosaccharides respectively. Those oligosaccharides are labeled according to Fry nomenclature for xyloglucan-derived oligosaccharides (Tables 2 and 3) [70]. It has been indicated that those fucogalactoxyloglucan hold O-acetyl substituents absolutely on galactose-units of the xyloglucan oligosaccharide [63]. The results obtained by MALDI spectrometry were confirmed by HPAE-PAD chromatography. Indeed three elution peaks with retention times similar to those of XXXG, XXFG, and XLFG + XXLG, were obtained respectively.

Table 2. One-letter codes for the differently-substituted β-D-glucosyl residues of xyloglucan-derived oligosaccharides. (*) Or reducing terminal D-glucose moiety [70].

Code letter	Structure represented	Mnemonic
G	β-D-Glc$p$*-	Glucose
X	α-D-Xyl$p$-(1→6)-β-D-Glc$p$*-	Xylose
L	β-D-Gal$p$-(1→2)-α-D-Xyl$p$-(1→6)-β-D-Glc$p$*-	gaLactose
F	α-L-Fuc$p$-(1→2)-β-D-Gal$p$-(1→2)-α-D-Xyl$p$-(1→6)-β-D-Glc$p$*-	Fucose
A	$\left.\begin{matrix}\alpha\text{-L-Ara}f\text{-(1→2)}\\ \alpha\text{-D-Xyl}p\text{-(1→6)}\end{matrix}\right\}$-$\beta$-D-Glc$p$*-	Arabinose
B	$\left.\begin{matrix}\beta\text{-D-Xyl}p\text{-(1→2)}\\ \alpha\text{-D-Xyl}p\text{-(1→6)}\end{matrix}\right\}$-$\beta$-D-Glc$p$*-	Beta-xylose
C	$\left.\begin{matrix}\alpha\text{-L-Ara}f\text{-(1→3)-}\beta\text{-D-Xyl}p\text{-(1→2)}\\ \alpha\text{-D-Xyl}p\text{-(1→6)}\end{matrix}\right\}$-$\beta$-D-Glc$p$*-	follows A and B
S	α-L-Ara$f$-(1→2)-α-D-Xyl$p$-(1→6)-β-D-Glc$p$*-	Solanaceae

Table 3. Abbreviated nomenclature of some xyloglucan oligosaccharides. Sugar residues and their linkages are represented as follows: Ara α-L-arabinofuranosyl-(l→2)-, Fuc α-L-fucopyranosyl-(l→2)-, Gal β-3-D-galactopyranosyl-(l→2)-, Glc β-D-glucopyranosyl-(I→4) [or reducing D-glucose], Xyl α-D-xylopyranosyl-(l→6) [70].

Structure	Abbreviations		Structure	Abbreviations	
	Old	New		Old	New
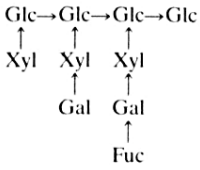	XG10	XLFG	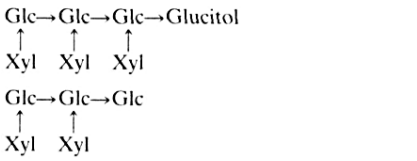	XG7-ol	XXXGol
					XXG
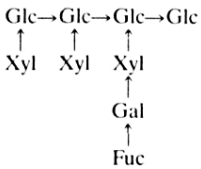	XG9	XXFG			FG
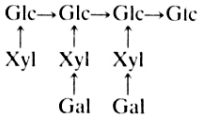	XG9n	XLLG	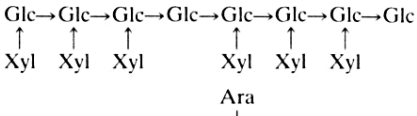		XXXGXXXG
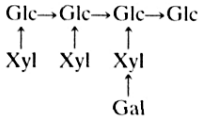	XG8	XXLG	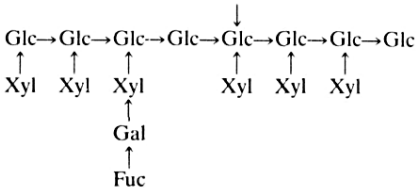		XXFGAXXG
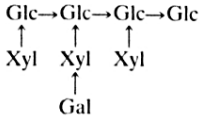		XLXG			

Finally sugar analysis of enzymatically hydrolyzed xylan with endo-β-(1→4)-xylanase, an enzyme specific for the cleavage of the glucosidic linkages of β-D- xylan, showed that the xylan in *Benincasa hispida* fruit is primarily comprised of xylose monomers (84.5%) and a minor quantity of mannose (1.7%), glucuronic acid (4.6%), glucose (2.5%), and galactose (3.5%) residues and trace amounts of arabinose and 4-O-methyl glucuronic acid (4-O- MeGlcA) residues. The MALDI-TOF-mass spectrometric and HPAE-PAD chromatography analysis of the obtained fragments indicated that the xylans, existing in both fractions the B1OH and B4OH, shows the conventional structure of linked β-(1→4) xylopyranosyl main chain, substituted with three 4-O-methyl glucuronic acid per 97 xylopyranosyl unit [63].

In the research of Sun and his coworkers [71], several fractions of dewaxed wheat straw hemicellulose were extracted successively with sodium hydroxide at increasing strength from 0.25 to 2.0 M. Sugar analysis by HPLC showed that xylose was the predominant sugar residue in all the hemicellulosic fractions, comprising about 70-80% of the whole sugars in these fractions. Moreover, the analysis indicated that as the sodium hydroxide strength increased from 0.25 to 2.0 M, the quantity of arabinose was reduced from 16.5 to 9.2%, while the glucose amount increased from 3.6 to 6.2%. Regarding the uranic acid, its amount varied between 3.8 and 5.4% for the various fractions. In this study, Sun's group indicated that the dewaxed wheat straw hemicellulose absolutely comprises an extraordinary quantity of arabinose and low amount of xylose compared to the high xylose and low arabinose content hemicelluloses isolated from straw holocelluloses. This observation reveals that the arabinose in the wheat straw cell walls most likely comprises a part of the sidechain of hemicelluloses, is linked to ferulic acid or straightforward to lignin, and is easily detached and released. However the xylose residues constitute the key chain of hemicellulose and are not extracted unless delignification has occurred.

Furthermore the data of Sun's group indicated that besides the ester linkage among ferulic acid and polysaccharide, or *p*-coumaric acid and lignin, the high quantity of lignin is directly ether-linked to arabinose in hemicelluloses [71]. For the ease of its characterization, the extracted hemicellulose fraction 2 (this is the fraction of hemicellulose extracted with 0.5 M sodium hydroxide) was methylated and used for further studies. Methylation of the fraction 2 hemicellulose gave a product with an $[\alpha]_D^{17}$ value of -87^o indicative of ß-linkages, which was

confirmed by the ^{13}C NMR spectrum (δ 104.8 ppm for C-1). In addition to that, the reduction and hydrolysis of the methylated hemicellulose releases the following methylated sugars:

- 2,3,5-tri-O-methyl-L-arabinose (6.8%),
- 2,3,4-tri-O-methyl-D- xylose (4.9%),
- 2,3-di-O-metyl-D-xylose (77.4%),
- 2-O- methyl-D-xylose (7.2%),
- 3-O-methyl-D-xylose (3.7%).

Indeed, 2,3,5-tri-O-methyl-L-arabinose formation reveals the presence of one terminal arabino-furanosyl group per thirteen xylose monomers. On the other hand, the existence of 2,3,4-tri-O-methyl-D-xylose indicated that there is a terminal sugar and for every 18 xylose monomers in the backbone chain, there was one xylopyranosyl group. Also it was deduced that the backbone consisted of β-D-(1→4) linked xylose monomers by the formation of a large proportion of 2,3-di-O-metyl-D-xylose. The side-chains were linked to positions two and three of the xylopyranose monomers, as designated by the establishment of 3- or 2-O-methyl-D-xylose, due to the double content of 2-O-methyl-D-xylose relative to 3-O-methyl-D-xylose. They concluded that the L-arabinose and 4.9% D-xylose residues appear as side-chains bonded to the main β-D-(1→4) xylopyranose residues through position 3 of xylose. Also it was shown that the molar ratio of uranic acid:xylose in the polysaccharide fraction 2 was 1.9:50. This indicates that for every twenty-six D-xylopyranosyl residues in the backbone, there was one uranic acid unit.

Combining all the data together, it might be concluded that the extracted dewaxed wheat straw hemicellulose fraction 2 had a structure composed of a main chain of β-D-(1→4) xylopyranosyl residues, with D-(1→2) linked glucopyranosyluronic acid (or 4-O-methyl-α-D-glucopyranosyluronic acid), and L-(1→3) linked arabino-furanosyl or D-xylopyranosyl residues at the branch points [71].

4. Hemicellulose modification

Due to their high stability, presence of polar hydroxyl (OH) groups, and biodegradability, hemicelluloses have been considered for their utilization in industrial applications based on the hydrophilic nature of the materials. Hemicelluloses are used in value-added industrial applications

including hydrogels, additives in papermaking, in cosmetics and in pharmaceutical applications. [19][72][51]. For instance, arabinogalactans are used as emulsifiers, stabilizers, and binders in the food, pharmaceutical, and cosmetic industries. Arabinogalactan has properties that make it suitable as a carrier for delivering diagnostic or therapeutic agents to hepatocytes (liver cells) *via* the asialoglycoprotein receptor [73]. Arabinogalactan also can stimulate natural killer (NK) cell cytotoxic activity, and thus activate the immune system against tumor cells by inhibiting their metastasis to the liver [74]. Xylans have numerous medical applications. For instance, xylan has been considered as a suitable raw material to produce colonic drug delivery systems due to the ability of enzymes produced by the colonic microflora to degrade the glycosidic bonds between the sugar units of the polymer backbone [75].

As stated in the applications listed above, hemicelluloses are hydrophilic polymers with extensive H-bonding; however, the majority of the synthetic polymers used in industrial applications are hydrophobic, so the hydrophilicity of hemicellulose limits the range of its industrial applications [53][76]. Also, the physical H-bonding convert the hemicellulose to a crosslinked material and limits its processability. When it is blended with hydrophobic plastics, the hydrophilic character of hemicellulose results in poor mechanical properties due to poor interfacial adhesion. The hydrophilicity of hemicelluloses results in an inability to form a continuous miscible phase with synthetic hydrophobic polymers**.**

Due to its hydroxyl groups, which can serve as a reaction site, hemicellulose properties can be modified by reactions with numerous chemical agents. In order to broaden its application, hemicellulose has been chemically modified using a variety of chemical reactions including [77] [78] [79].

- oxidation,
- reduction,
- esterification (e.g. acetylation, propionylation, oleoylation, lauroylation, benzolation, and crosslinking),
- etherification (e.g. alkoxylation, cationization, or carboxymethylation),

The aim of those modifications is to attach a hydrophobic group onto the hemicellulose chains and thus, improve its hydrophobicity and processability by reducing the H-bonds. Generally, grafting of a hydrophobic group to hemicellulose improve its water resistance, thermal stability, thermoplastic properties, and its solubility in organic solvents [78]. Moreover, interest in the modification of hemicellulose is growing rapidly and this is reflected by the increasing number of published and cited papers concerning this field (Figure 12). Part of this growth stems from the environmental need to produce hydrophobic materials that are biocompatible and may degrade over time in nature.

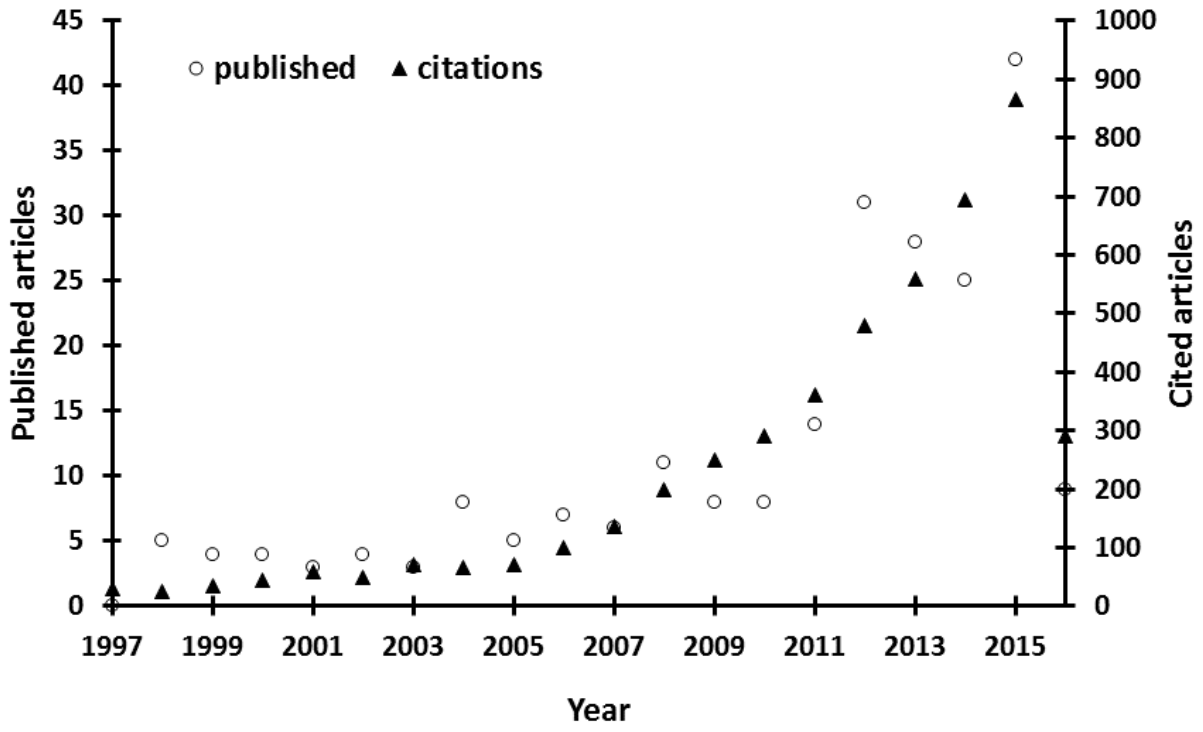

Figure 12. Number of published and cited articles related to hemicellulose hydrophobization from 1997 to 2016 (WEB OF SCIENCE with the search words of hydrophobic and hemicellulose, April 27, 2016).

The following sections describe the most important chemical modifications that have been used to improve hemicellulose water resistance and the changes in properties and intended applications of those hemicellulose derivatives.

4.1.Esterification: A simple chemistry for hemicellulose modification

Esterification is the reaction between alcohols and carboxylic acids or one of its derivatives to form an ester. The derivatives could be either acid chlorides or acid anhydrides. Different types of esterification reactions (acetylation, propionylation, oleoylation, and many others) have been used to modify the hemicelluloses. Therse reactions generate hemicellulose derivatives with different characteristics, useful in tailoring the hemicellulose for its intended application (Figure 13) [25] [80] [81]. For example, hemicellulose miscibility and phase adhesion with plastic polymers could be improved by reacting its hydrophilic hydroxyl with hydrophobic groups through esterification.

Fang and his coworkers performed the esterification of wheat straw hemicellulose using different R groups of the acyl chloride (R ranged from C_3: Propionyl chloride (PC) to C_{20}: Oleoyl chloride (OLC) [80]. In the research of Fang, it was shown that by changing the molar ratios of acid chloride/anhydroxylose, concentrations of the catalyst (TEA: triethylamine), reaction times, and reaction temperatures, the degree of substitution (DS) of hemicellulose could be altered [80]. For example, fixing the temperature and the reaction time shows that the DS of stearoylated hemicellulose is strongly affected by %TEA and the molar ratio of stearoyl chloride/anhydroxylose, with the DS ranging between 0.38 and 1.75.

One way to determine the hydrophobicity of a molecule is to study its solubility in organic solvents. It has been shown that the solubility of the esterified hemicellulose significantly depends on the DS of the sample. Fang and his coworkers studied the solubility of the stearoylated hemicellulose in several organic solvents; their results indicated that stearoylated hemicellulose with DS 0.88 revealed a high solubility in pyridine at 80°C and was partially soluble in dimethylsulfoxide (DMSO), tetrahydrofuran (THF), toluene, chloroform, and dichloromethane compared to the poor solubility of the unmodified hemicellulose in those solvents [80].

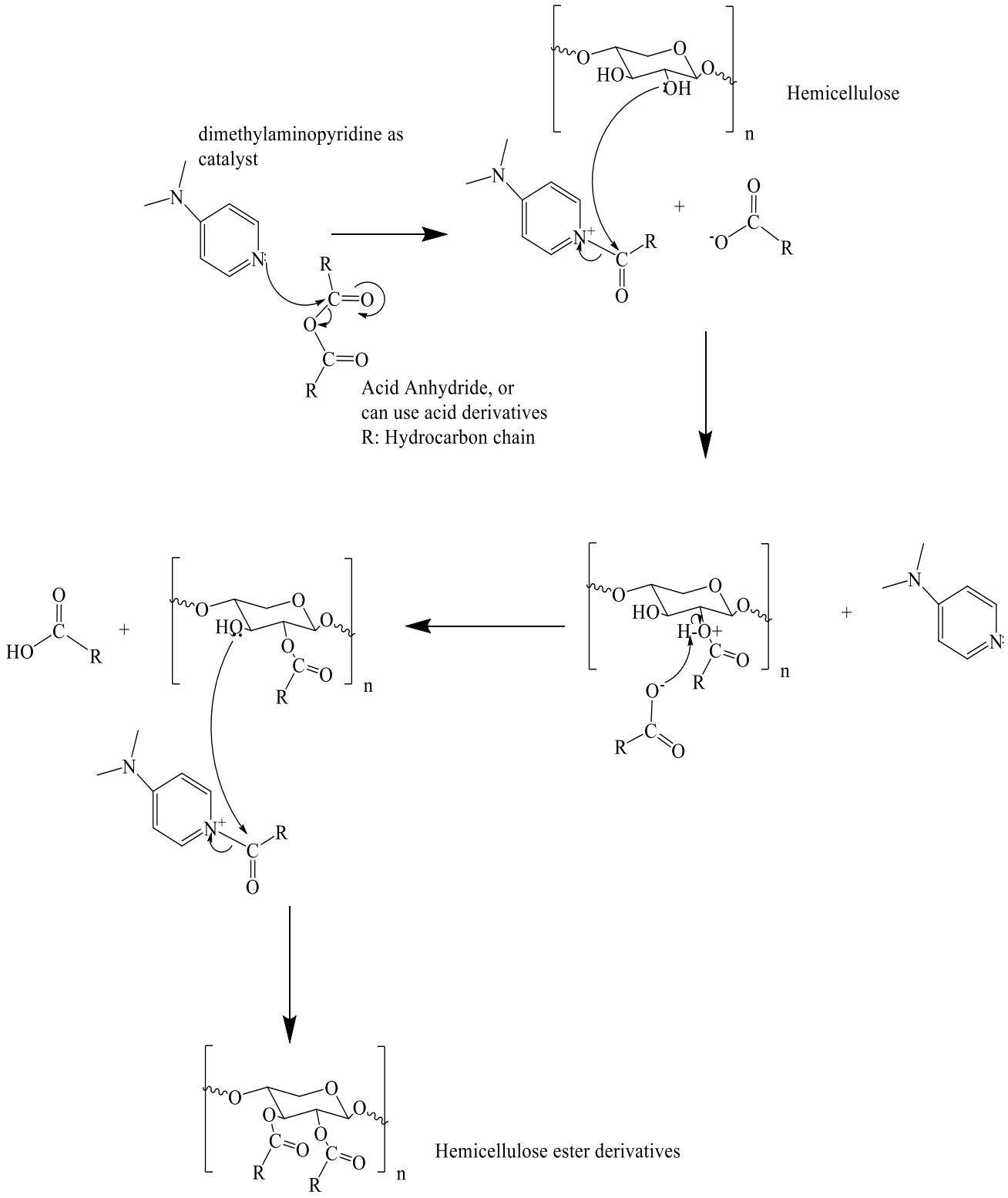

Figure 13. Mechanism of hemicellulose esterification with an acid anhydride and catalyst

Interestingly, in another study, Sun and his coworkers [79] showed that esterified hemicelluloses from poplar using different R groups of acyl chloride were soluble in organic solvents, and all hemicellulose esters were soluble in pyridine at 80°C [79]. Other samples were also somewhat soluble in chloroform, dichloromethane, toluene, and tetrahydrofuran at room temperature. Fang studied the thermal stability of octanoylated hemicelluloses and compared it to the native hemicellulose in nitrogen [80]. The octanoylated hemicelluloses had three major thermal decompositions at temperatures of 260, 330, and 370°C, which represented about 6, 40, and 30% of the total weight loss, respectively. This is different from the native hemicellulose, which showed only two major thermal decomposition temperatures at 280 and 370°C, representing 40 and 20% weight loss, respectively [80]. Fang and his colleagues showed that the native hemicellulose and the octanoylated hemicelluloses were totally volatized at 400°C and 500°C, respectively. The hemicellulose esters showed higher thermal stability than the native hemicellulose and thus provide the potential for hydrophobic hemicellulose as biodegradable plastics, resins, films, and coatings.

Hemicellulose esterification with maleic anhydride in ionic liquid was performed by Peng [82]. In this study, xylan-rich hemicelluloses (XH) were isolated from *Dendrocalamus membranaceus* Munro (DmM) by an alkaline extraction. The extracted hemicellulose was subjected to an esterification reaction with maleic anhydride (MA) in 1-butyl-3-methylimidazolium chloride ([BMIM]Cl) ionic liquid using lithium hydroxide (LiOH) as catalyst. In this study, based on the reaction time, temperature, dosage of catalyst, and the molar ratio of maleic anhydride to anhydroxylose unit in the hemicellulose, the DS can range between 0.095 and 0.75. In addition, the thermal stability of the modified hemicellulose (MXH) with DS 0.75 was lower than that of XH. Indeed, the decomposition temperatures corresponding to the maximum rate of weight loss of XH and MXH were 278 and 238 °C, respectively. Also the 50% weight loss temperatures were observed at 287 and 274 °C for XH and MXH, respectively. The reduction in the thermal stability of MXH relative to XH is due to more hydrogen bonds being destroyed during dissolution [82]. The importance of this type of esterification reaction is the insertion of the carbon-carbon double bond into the hemicellulose chains. For instance, the unsaturated double bonds can function as a desired site for polymerization which can be used for further modification or crosslinking of the hemicellulose polymeric chains.

4.1.1. Hemicellulose modification by acetylation

Hemicellulose acetylation has been frequently reported [29][25][83]. Hemicellulose acetylation is a chemical modification that links an acetyl group to the hemicellulose chain through esterification reactions as mentioned above. Acetylation of hemicellulose can be achieved by using similar conditions to that used for cellulose with an expected increase in hydrophobicity. The acetylation reaction is shown in Figure 14:

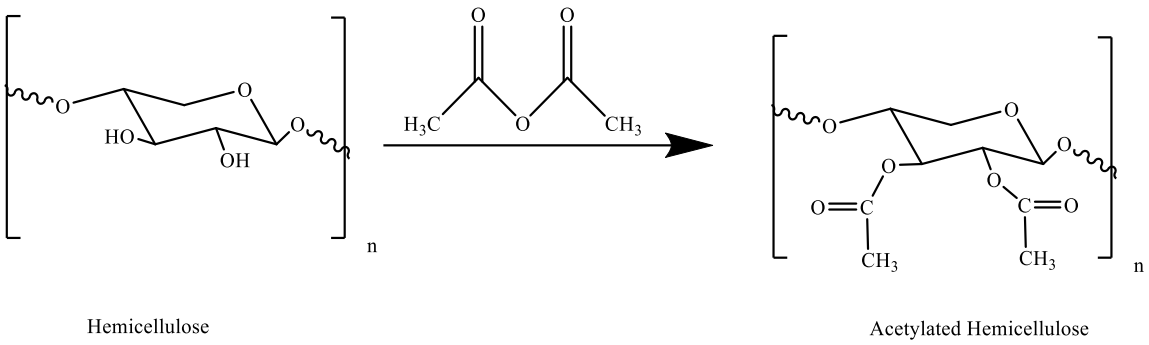

Figure 14. Acetylation of hemicellulose with acetic anhydride

Acetylation of hemicellulose has been carried out by several approaches and under several reaction conditions; however, the most common reaction to attain hemicellulose acetate still utilizes acetic anhydride as an acetylating agent. The reaction conditions can be altered based on the targeted degree of substitution of the final product [29][25] [83][84]. The thermal stability and hydrophobicity of the acetylated hemicellulose depends strongly on the degree of substitution (DS).

Acetylation of hardwood kraft pulp and wheat straw hemicelluloses has been created using the DMA/LiCl/pyridine system [25][85]. The efficiency of this reaction (DS can vary between 0.6 and 2) increases with temperature and the time of the reaction [25][85]. The thermo-gravimetric analysis (TGA) of the acetylated xylan reveals an increase in the decomposition temperature compared to the native xylan. For instance, 50% of the weight of the native xylan from hardwood kraft pulp is lost at 297°C in nitrogen. However, in the case of xylan acetate with a DS of 0.6, 1.1, 1.6, and 2.0, the 50% weight loss decomposition temperatures were 294, 312, 348, and 355°C,

respectively [25]. This increase in the xylan thermal stability after acetylation can be explained by the decreased content of the hydroxl groups after its modification; those groups are usually oxidized during heating [86]. Also the solubility of the acetylated hemicellulose in organic solvents (chloroform, DMSO, THF, and others) increases with the increase in the DS [85].

Ionic liquids with or without catalyst have been used to perform the acetylation of hemicellulose [83][29]. Ayoub and coworkers have acetylated hemicellulose from switchgrass in ionic liquid without catalyst [29]. In that research, DS of 0.21 to 1.25 could be obtained by varying the time of the acetylation reaction between 60 to 1200 min at 80°C. They have shown that 40% of the weight of the native hemicellulose and that of acetylated hemicellulose with (DS = 1.25) was lost at 279°C and 310°C, respectively, indicating that the thermal stability of the acetylated products increased upon acetylation. It was shown that switchgrass hemicellulose acetates with DS of 0.78 and greater were rapidly dissolved in DMSO and THF at room temperature. Acetylated hemicellulose with DS of 1.25 had a contact angle of 83° at a 5s contact time, which was significantly higher than the unmodified hemicellulose at 47° [29].

Acetylated hemicellulose films have been used for food packaging [87][88]. Besides offering an open door for marketing renewable and biodegradable materials, chemical and physical protection of food can be achieved through food packaging with hemicellulose-based materials. For example, spoiling of food can be the result of oxygen-induced damage, especially to fatty acids and vitamins, which affects taste and nutritional benefits. Thus, packaging food with materials from hemicellulose can protect against spoiling.

Hemicellulose-based films can have low oxygen transmittance, and are biodegradable, making for useful barrier films for food products. Though hemicellulose-based films are sensitive to water, the sensitivity can be overcomed by esterification of the hemicellulose, such as acetylation [89]. Hemicellulose *O*-acetyl-galactoglucomannan (AcGGM) has been used as oxygen barrier films [87]. It has been shown that AcGGM is soluble in water and organic solvents. The solubility properties can be attributed to a high degree of acetylation in combination with a low molecular weight. AcGGM films have been obtained from a physical blend with plasticizers such as glycerol, sorbitol and xylitol, and the biobased polymers such as alginate and carboxymethylcellulose

(CMC). Of those, the oxygen permeabilities have been found to be the lowest for AcGGM-alginate and AcGGM-CMC films [52]. The addition of plasticizers resulted in increased hybrid film flexibility and moisture sensitivity and reduction of oxygen permeability. Plasticized AcGGM films showed weaker mechanical properties compared to the films of blended polymer; the hybrid films of polymer blends retains their mechanical properties at elevated humidity as well as generally having larger storage moduli. AcGGM film plasticized with glycerol was determined to have the highest elongation at break (up to 195%) by DMA measurements, but lower elongations of about 3% and 4% of the blended polymers containing CMC and alginate, respectively. AcGGM film plasticized with sorbitol exhibited an oxygen permeability of 2.0 cm^3 µm m^{-2} d^{-1} kPa^{-1}, which is relatively lower than the oxygen permeability of xylitol-containing AcGGM film of values of 4.4 cm^3 µm m^{-2} d^{-1} kPa^{-1}.

Another study performed by Stepan investigated the thermal and mechanical properties of acetylated arabinoxylans films [88]. Using the tensile test, his results indicated that the higher arabinosyl substitution level induces an increase in the film flexibility. Also it has been recommended that the elastic Young's modulus was not considerably affected, even though a bent was observed toward a less rigid material at advanced arabinosyl substitution. TGA tests confirmed that the arabinose content contributed to the thermal stability of the acetylated arabinoxylans. In this experiment, the acetylation of all free hydroxyl groups of both xylose and arabinose were confirmed by NMR. With these results, hydrophobized hemicellulose by acetylation were concluded to have potential as a material to develop oxygen barrier film with high thermal stability and water resistance characteristics.

On the other hand, hydrogels based on acetylated galactoglucomannan (AcGGM) were developed by Voepel [90]. Because hydrogels are polymeric materials that swell in water without being dissolved, they can be synthesized and evaluated for drug delivery systems application. Novel hemicellulose-containing hydrogels have prospects in oral drug administration technology [90]. In the cited study, neutral and ionic hydrogels based on (2-hydroxyethylmethacrylate) HEMA-Im–modified AcGGM (M-AcGGM) and maleic anhydride modified M-AcGGM (CM-AcGGM) were produced and inspected for their chemical, physical, and drug release properties. The neutral hydrogels were produced from functionalized AcGGM using 2-hydroxyethylmethacrylate

(HEMA) coupled *via* carbonyldiimidazole (CDI) and a co-monomer in a radical-initiated polymerization. The ionic hydrogels were prepared through a second modification reaction between the HEMA-modified AcGGM and maleic anhydride, a "double-modified" hemicellulose and an ionic poly (CM-AcGGMco-HEMA) hydrogels were successfully formed [90]. In neutral hydrogels the drug release rate decreased with an increase in the relative amount of the methacrylated AcGGM and its corresponding degree of methacrylation. Results indicated a faster release of drugs at pH 7.0 in comparison to pH 3.0. This can be attributed to the dissociation of the carboxylic groups by which it induces swelling of the hydrogel matrix due to the electrostatic repulsion. The increase in the ionic strength will hide the charges and thus contribute to reduced swelling.

4.1.2. Hemicellulose Modification by Oleoylation

Oleoylation of hemicellulose is an esterification reaction characterized by the replacement of the hydroxyl groups with a hydrophobic oleoyl group, Figure 15. The oleoylation of wheat straw hemicellulose was studied by Sun's group [91][92]. Their research showed that in order to get a very high oleoylation yield of wheat straw hemicellulose (above 86%) with a degree of substitution (DS) of 1.67, the reaction conditions must be optimized as follows. The molar ratio of moles of xylose in hemicelluloses/mol of oleoyl chloride must be 1/3 at a temperature of 75ºC for 35 min, with weight percentage of hemicellulose (w/w) equal to 174%. This reaction was carried out in N,N-dimethylformamide (DMF) and lithium chloride system with 4-dimethylaminopyridine as a catalyst [92].

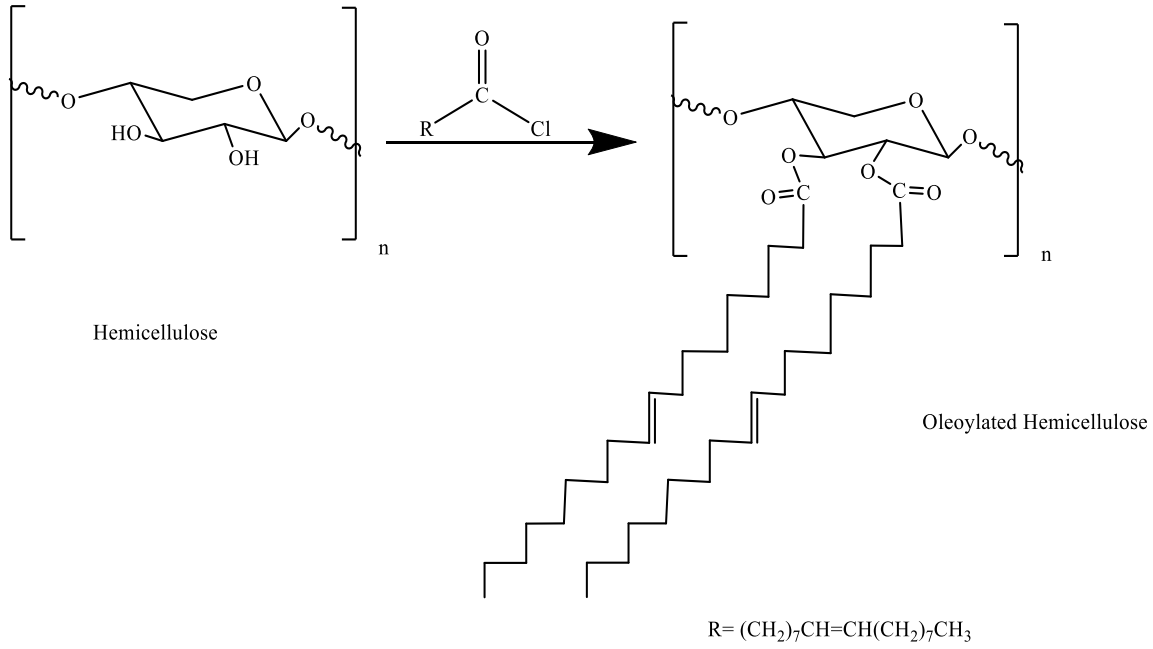

Figure 15. Oleoylation of hemicelluloses in N,N-dimethylformamide (DMF) and lithium chloride system with 4-dimethylaminopyridine as a catalyst.

Cellulose and hemicelluloses esterified with fatty acids have been coated on paper/board. The importance of those coatings were attributed to their unique properties from being hydrophobic with high moisture barrier characteristics. The best water and water vapor barrier was accomplished with the cellulose derivatives esterified with the longest fatty acid [93][94]. In the research of Freire and coworkers, the fatty acids (hexanoic (C6), dodecanoic (C12), octadecanoic (C18), and docosanoic (C22) acids) were used to esterify the native cellulose. Their results indicated that esterification of cellulose with fatty acids with the long R chain increases the hydrophobicity of cellulose, as observed in the increase in the water contact angle from 56^{o} of native cellulose to almost 94^{o} of cellulose esterified with octadecanoic (C18) acid [94] (Figure 16).

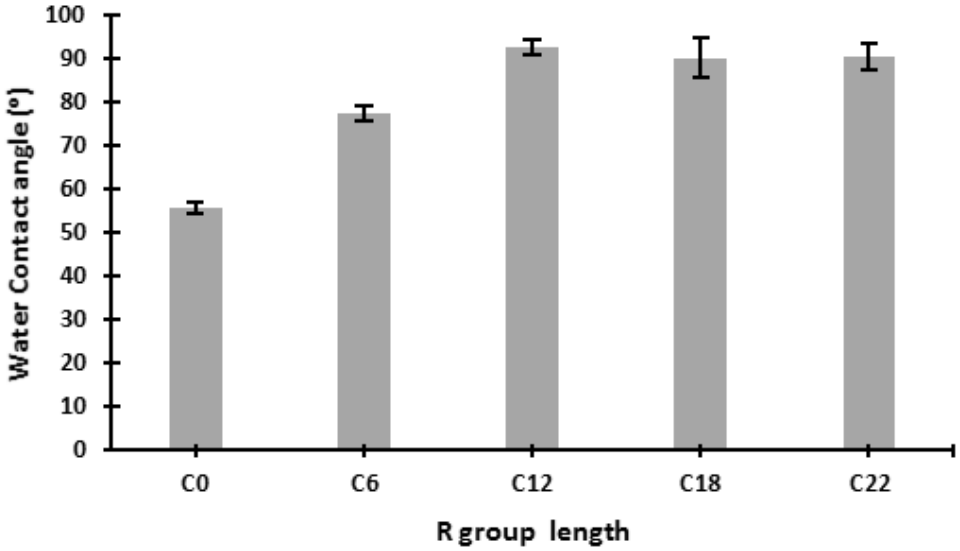

Figure 16. The contact angle of cellulose esters depends on the length of the fatty acid used for hemicellulose esterification. This figure is plotted from the data of the cited research [93]

The water vapor transmission rate (WVTR) of esterified cellulose was measured by Sebti and his group [93]; their results indicated that the incorporation of 15% of stearic acid (octadecanoic acid (C_{18})) to cellulose allowed a decrease of WVTR by ~60% relative to cellulosic films without hydrophobic compounds [93]. This observation is attributable to the apolar nature of stearic acid, which decreases the moisture affinity of films. Thus it might be beneficial for hydrophobicization to use oleoylated or octadecanoated hemicellulose in coating rather than acetylated hemicellulose. Oleoylation alters the solubility of hemicellulose and oleoylated hemicellulose is soluble in different organic solvents. For example it is completely soluble in pyridine and partially soluble in many other solvents including tetrahydrofuran (THF), toluene, and chloroform [92], indicating increases in their hydrophobic properties. Another study showed that the oleoylation of the sugarcane bagasse hemicelluloses with DS< 0.29 leads to a decrease in the hemicellulose thermal stability [91]. For instance, unmodified hemicellulose started to decompose at 200°C, whereas oleoylated polymer with DS of 0.04 started its thermal degradation at 187°C. The reduction in the thermal stability of hemicelluloses after its chemical modification might be due to the lack of the intermolecular interactions (mainly hydrogen bonding) between the polymeric chains in the unmodified material. Oleoylation increases the hydrophobicity and thus the water resistance of the esterified hemicellulose more significantly than acetylated hemicellulose at the same DS and may

be more efficient in the development of barrier films for the production of packaging materials for different food products.

4.1.3. Hemicellulose modification by fluorination

Fluorination is a technique used to provide polymers with unique chemical and surface properties. In addition to being super-hydrophobic, fluorinated polymeric materials exhibit the characteristics of good chemical resistance and thermal stability; it offers a strong barrier to gases and liquids, low coefficient of friction, and small dielectric constant values [95][96]. Those characteristics allow the fluorinated polymer to be employed in many applications including marine coatings, medical implants, protective clothing, and others [96].

The importance of hemicellulose fluorination is in converting it into a more hydrophobic polymer, mainly used in a plasticized film form (Figure 17).

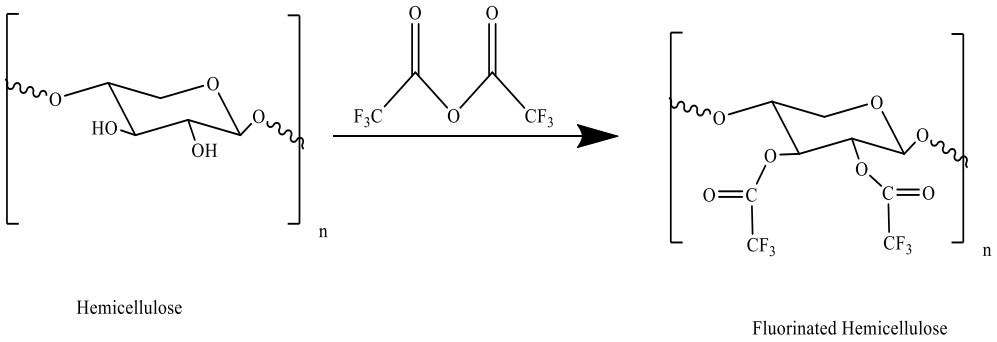

Figure 17. Fluorination of hemicelluloses

The fluorination of hemicellulose was carried out by the reaction of arabinoxylan with gaseous trifluoroacetic anhydride (TFAA) to yield hydrophobic films with potential as food packaging [97]. The attachment of the fluorinated moiety to the arabinoxylan was verified by FT-IR. This study showed that the contact angle of a water droplet with the fluorinated arabinoxylan surface was about 70º, compared to 30º for the unmodified surface [97]. Generally, if the water contact angle is higher than 90º, the corresponding material is conventionally defined as hydrophobic [53].

Also, Gröndahl *et al.* showed that the equilibrium moisture content dropped from 18% to 12% after fluorination of arabinoxylan. However, a limitation of the fluorination of hemicellulose may be partial hydrolysis of the trifluoroacetate groups upon contact with water, which might limit the applications using the trifluoroacetate groups with hemicellulose.

4.2. Etherification: Hemicellulose Structural Alteration

Polysaccharides reaction to form ethers is mostly used to regulate solubility, provide stability against microorganisms (biodegradability), or to produce film-forming ability. Etherification is a reaction between an alcohol and alkylating agent in the presence of a base. Typical alkylating agents include alkyl halides (chlorides, bromides, and iodides), alkyl sulfonates, and epoxides. The epoxides have an unstable 3-member ring containing oxygen that induce electron withdrawal from the adjacent carbon. This makes the epoxide relatively reactive with alcohol-containing molecules, including hemicellulose. Hemicellulose etherification has been carried out by many researchers [98][99][77]. The importance of the ether bond is that it is more stable than the ester bond, which is rather easily hydrolyzed, especially in alkaline conditions [100]. Ren and coworkers showed that the hemicellulose etherification using 2, 3-epoxypropyltrimethylammonium chloride as an alkylating agent resulted in the reduction of the thermal stability of hemicellulose. Indeed, native and etherified hemicelluloses showed a 50% weight losses, at 292^{o}C and 277^{o}C, respectively. Also it was observed that the average molecular weight of the native hemicelluloses decreased from 28,890 g/mol to 15,200 g/mol during the etherification of hemicellulose (DS 0.33) [99]. In contrast, the results of Fang indicated that hemicellulose methylation using methyl iodide as an alkylating agent increased thermal stability [98].

Hydroxyalkylated xylan has been prepared for coating applications [77]. In this study, Laine *et al*. obtained etherified xylan from the extracted non-dried xylan and directly from the birch pulp by reactive extraction. The results of this research revealed that the water vapor permeabilities of the xylan ether coatings were 50–100% of that measured for polyethylene terephthalate coating as commercial biopolymer coating. Furthermore, it was indicated that the oxygen permeability was one third of that for a commercial biopolymer coating. In addition, it has been shown that the surface strength of butylated and allylated xylan coating was close to that of the reference latex as

a binder in pigment coatings [77]. Benzyl ether derivatives from xylan have recently been prepared. These derivatives form hydrophobic and thermoplastic films [101][78]. The benzylation of hemicelluloses is the typical Williamson reaction (nucleophilic substitution) [78], which is shown in Figure 18.

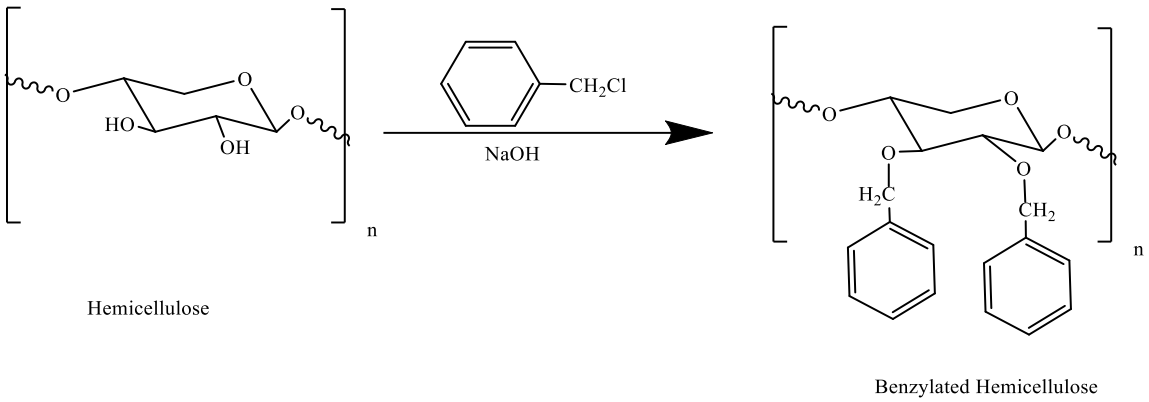

Figure 18. Benzylation of hemicellulose with benzyl chloride.

Hemicellulose from wheat straw was studied for its benzylation reaction [78]. Junli and coworkers subjected hemicellulose to benzylation with benzyl chloride under the presence of sodium hydroxide in an ethanol/water system. Depending on the experimental conditions, the DS of the benzylated hemicellulose varied between 0.09 to 0.35. The thermal stability increased after hemicellulose modification, in which the temperature at 50% weight loss of unmodified hemicellulose and benzylated hemicellulose was indicated to be 293 and 303^{o}C , respectively. Furthermore, the temperature at maximum degradation, T_{max} was shown to be 284 and 298^{o}C for native hemicelluloses and benyzlated hemicelluloses, respectively. The introduction of benzyl groups provides the hemicelluloses with hydrophobicity, which could be potentially applied in plastic industries.

Benzylation of AcGGM (acetylated galactoglucomannan) to create a strong, transparent, and flexible film was performed by Hartman and coworkers [102]. Blends of AcGGM with alginate were produced, as well as blends of AcGGM-CMC (carboxymethylcellulose) with a benzylated BnGGm film. Benzylation markedly increased the water resistance of the hemicellulose films. Blends of unmodified films dissolved rapidly when coming in contact with water; however, only less than 30% of the benzylated film was lost after extended immersion in water. The oxygen

permeability of the BnGGM film at both 50% and 83% relative humidity was higher than those found for the unmodified blend films.

4.3. Crosslinking: Hemicellulose resistance to harsh environments

Crosslinking of polymers can offer resistance to thermal degradation and improve resistance to cracking by liquids and other harsh environments. Crosslinking decreases solubility in liquids and thus improves its water resistance properties [103]. In addition, crosslinking can provide resistance to creep and cold flow [103]. The crosslinking of polymeric material can be done chemically, physically or by irradiation techniques. This will result in a covalently bonded thermosetting network that does not flow above its glass transition temperature. Hemicellulose cross-linking is mostly used to make hydrogels that have limited water solubility, despite their ability to swell in water [104].

The synthesis and characterization of a crosslinked hemicellulose citrate–chitosan gel as an absorbent foam material was prepared by Salam and his colleagues [105]. Chitosan is a polysaccharide abundant as a byproduct of the seafood industry, and it is well known to have anti-microbial properties. Ordinary polysaccharides with high carboxylic acid content are likely to have increased hydrophilic properties, such that they are useful in absorbent applications. The integration of carboxylic acid groups in hemicellulose can advance the chemical and physical functionality of these materials. In the cited work it was observed that the crosslinked hemicellulose citrate–chitosan foam is elastic at room temperature, and is very soft and highly porous with a finer pore structure compared to a non-crosslinked hemicellulose–chitosan material (Figure 19). Also it was indicated that the crosslinked hemicellulose citrate–chitosan foam has a higher water and saline absorption compared to the hemicellulose–chitosan material. Indeed the hemicellulose citrate–chitosan can absorb up to 100g of a saline solution per gram of material and up to 80g of water per gram of material [106].

Figure 19. Flexible foam material from hemicellulose citrate chitosan. From top left clockwise: unstressed foam, folded foam, localized impression, and flattened foam. After each of these deformations the unstressed shape of the foam returns. Reproduced from [105]

In another study performed by Karaaslan, pH-sensitive, semi-IPN (interpenetrating) hydrogels were created by crosslinking the hemicelluloses with chitosan using glutaraldehyde as the crosslinking agent (Figure 20). This hydrogel was developed as a drug carrier to control drug delivery into gastric fluid [107].

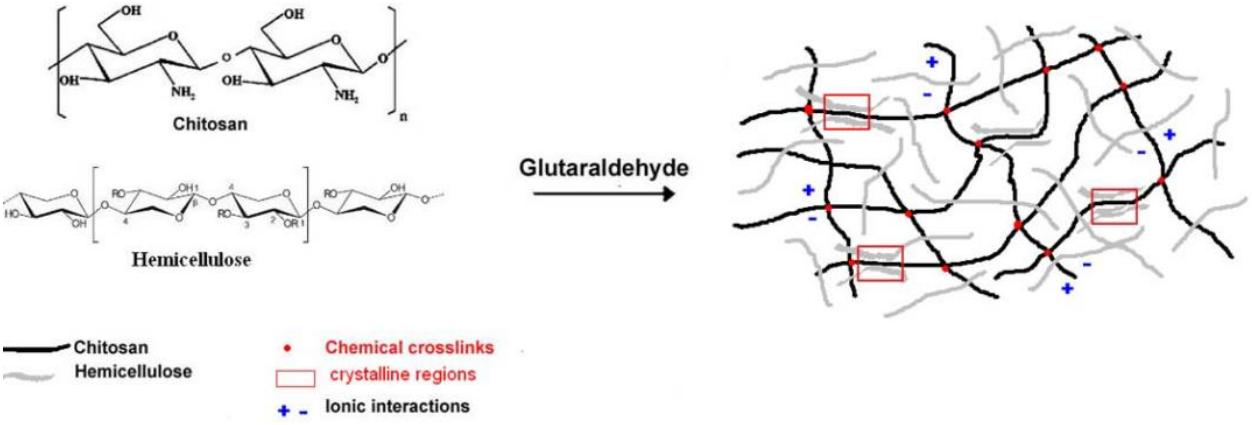

Figure 20. Semi-interpenetrating network of crosslinked chitosan and entrapped hemicellulose with weak interactions to chitosan [107].

Riboflavin was chosen as a model drug due to its different solubility at different pH ranges (it has a very low solubility at low pH) and minimal interference with the gel matrix. It was found that the higher the hemicellulose content, the higher the swelling ratios of the crosslinked gel. Also it was indicated that the swelling ratio of the hydrogel increases in acidic environment due to repulsion between similarly charged groups. An *in vitro* study revealed that the release of the riboflavin from semi-IPN hydrogels in acidic condition is favored, whereas at higher pH environments the gel matrix collapsed, not releasing the riboflavin. Based on such findings, these semi-IPNs could have potential for application as pH-sensitive controlled drug delivery vehicles in physiological environments, for example as a delivery of antibiotics or anti-ulcer drugs in the stomach.

Barrier films have been prepared from crosslinked galactoglucomannan [108]. In the cited study the crosslinking was catalyzed by the enzyme laccase, which is a class of copper-containing oxidase enzymes, found in fungi, plants, and microorganisms. Those enzymes are well-known for polymerizing and crosslinking phenolic structures; the reaction catalyzed by laccase is shown in Figure 21.

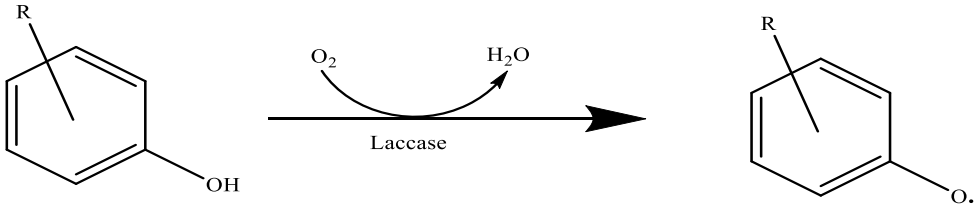

Figure 21. Laccase catalyzed reaction

Plants use laccases for lignin polymerization through monolignol oxidation [108]. The hemicelluloses used in the cited work contained lignin moieties, and those moieties were targeted by the laccase activity to generate crosslinked large molecules of hemicellulose bound to aromatic moieties. (Figure 22)

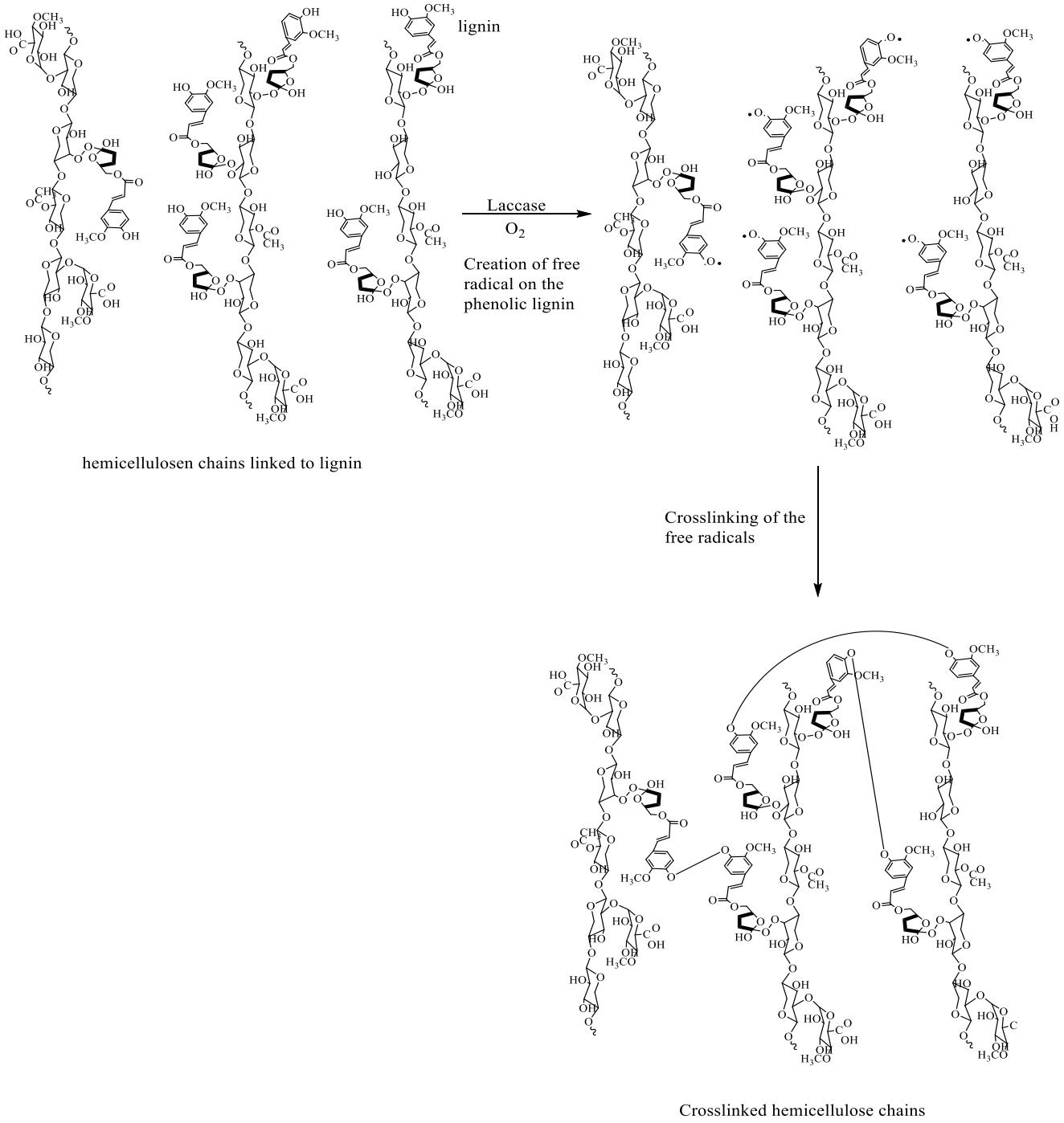

Figure 22. Mechanism of crosslinking of hemicellulose-lignin moieties by laccase activity

Oinonen and co-authors showed that laccase activity induces an increase in the average molecular weight of the hemicellulose. It was noticed that the increase in the molecular weight renders high mechanical properties of the films. Crosslinked hemicellulose film showed a four-fold increase in

the stress at maximum load compared to the un-crosslinked hemicellulose. Also, this film reduced the oxygen transmission, indicating that it was a good oxygen barrier [108].

Hemicelluloses have been also crosslinked by irradiation methods for several applications [104][109][110][111]. For instance, Peng and coworkers prepared an ionic hydrogel by free radical graft copolymerization of acrylic acid and bamboo hemicelluloses using N,N-methylene-bis-(acrylamide) as a cross-linker and ammonium persulfate/N,N,N′,N′-tetramethylethylenediamine as an initiator system (Figure 23) [104]. Their results revealed that the obtained hemicellulose-based hydrogel is sensitive to pH, ionic strength, media composition, and organic solvents.

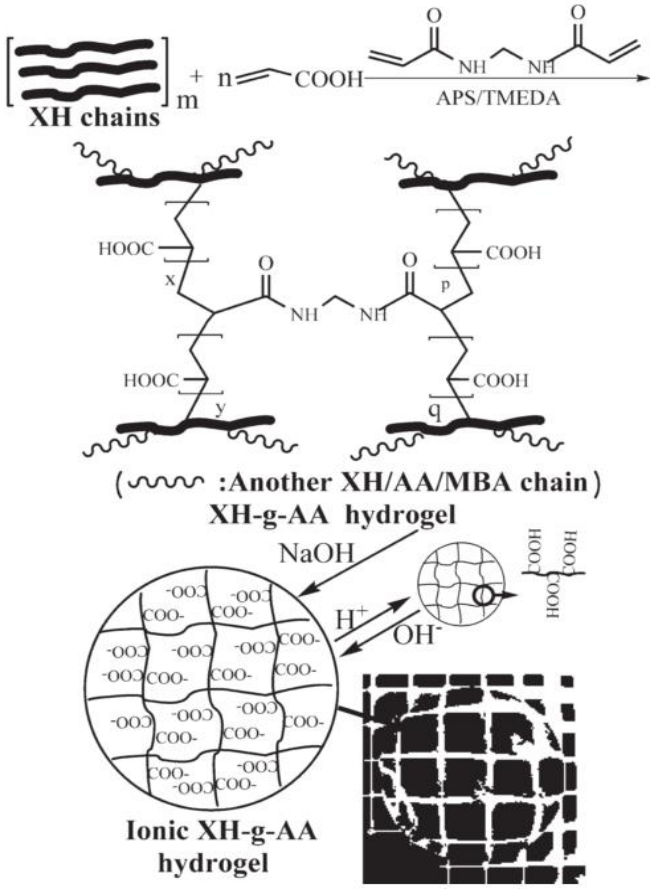

Figure 23. Proposed mechanistic pathway in the formation of xylan-rich hemicelluloses-graft-acrylic acid hydrogels (x, y, q, or p ≥ 1) [104].

In fact, it was indicated that the produced hydrogel shows an expanded network in water due to strong electrostatic repulsion among anion (COO^-) groups [104]. Furthermore, this network of hydrogel shows an increased expansion when immersed in solutions with high pH. Shrinkage occurred at lower pH, in salt solutions, and in organic solvents. In addition, hemicellulose-based hydrogels have the capability to perform a reversible on-off switching behavior in the following types of solutions: acidic-basic; water–ethanol; or acetone. Indeed those characteristics can provide such hydrogel with many applications that are useful in the market which include the removal of heavy metal ions from aqueous solutions and drug delivery systems.

Other novel methods have been used to generate crosslinked hemicellulose material. For instance, Ayoub and coworkers developed a new green process to produce crosslinked materials using reactive extrusion in one continuous process. These materials can be used for water treatment and as superabsorbent products [112].

5. Applications: Hemicellulose-based materials

Hemicelluloses show a high potential for utilization in remarkable applications. Its unique properties such as being a branched hetero-polymer with several structures based on the different sources, and its ability to be modified by several physical and chemical reactions, provides hemicelluloses with an ability to be used in the manufacturing of unique products.

5.1. Biomedical Field

Biomedical applications of hemicellulose have been reported and its modification to generate water-resistant materials have been shown to produce materials superior to non-modified hemicellulose.

Certain types of hemicelluloses have been used successfully to inhibit the growth of different tumors by inducing the activity of the host immune system [113][74]. It was indicated that arabinogalactan can stimulate natural killer (NK) cell cytotoxic activity, and thus activate the

immune system against tumor cells by inhibiting their metastasis to the liver [74]. One study showed that oxidized mannan as a bioactive material can be conjugated to the vaccine (MUC), giving a fusion protein (M-FP); this can be used as a target for cancer immunotherapy. The M-FP seemed to provide benefit to patients with an early stage breast tumor [114]. In the research of Apostolopoulos and his coworkers, oxidized mannan poly-L-lysine (OMPLL) and reduced mannan poly-l-lysine (RMPLL) have been prepared and used to target DNA vaccines to the antigen presenting cells, the dendertic cells (DC) [115].

Several polysaccharides have antimicrobial activities; chitosan is one example. When microorganisms initiate infectious diseases by attacking the host cells and tissues, adhesion is crucial for the pathogen to get better access into the source of nutrition and facilitate the delivery of their toxic agents into the cells of the host tissue [116]. Blocking the adhesion of the pathogens into the host cells is used for the prevention and treatment of microbial diseases. Zasshi and his group showed that mannan can inhibit the adherence of several *Candida albicans* strains to the plastic plates, and thus coating the medical equipment with the mannan type hemicellulose might be useful to prevent *C. albicans* adherence [117].

Sato *et al.* investigated mannan coating as an anti-adhesion on acrylic denture surfaces against *Candida albicans* and *Candida glabrata* microorganisms [118]. The research showed that mannan inhibits the adhesion of both *Candida* strains in a concentration-dependent manner. The application of 0.1 mg/mL of mannan coating overnight showed inhibitory effects on the adhesion of the hyphal form of *C. albicans*; however, in the case of *C. glabrata* the application of 10 mg/mL of mannan led to significantly higher anti-adhesive effects [118]. These results indicated that mannan coating inhibits the adhesion of *Candida* strains onto the plastic plates and denture surfaces and thus serve as a promising application as coating material for clinical applications, mainly clinical dentistry.

Hemicellulose has been used also as wound dressing [119][120][121]. An ideal wound dressing must have the ability to maintain a high moisture environment at the wound-dressing interface, get rid of exudate, allow the exchange of gases and vapor, be impermeable to microorganisms and water, reduce the pain caused by the wound, and be removable without causing trauma to the

wound [119][122]. A hemicellulose-based wound dressing has been developed and marketed under the name of Veloderm®.

Veloderm® is a biofilm with a polymeric structure based on hemicellulose microfibers. It is produced from sugarcane by a biotechnological process. Medestea Research & Production SpA, an Italian pharmaceutical company, has distributed Veloderm® into the market as a competitor with other wound dressings. This company describes Veloderm® as a wound dressing that is able to allow a selective permeability of gases and vapor and to prevent the permeability of water and microorganisms. They describe its ability to adhere to the wound and generate a sealing process that protects the wound externally from dirt and germs. They mentioned also that Veloderm® can reduce pain and creates an ideal environment for granulation and re-epithelialization which can promote a correct growth of fibroblasts and therefore a rapid and optimal healing of wounds. According to this company, a single application of Veloderm® is usually sufficient for a wound to heal, except in particular cases when it can be taken off and substituted by new dressing [121][119]. Melandri and his coworkers studied the healing capabilities of Veloderm® to the human skin and showed it to be effective and better than other types of dressings [121].

Another study by Ferreira and her colleagues, compared the effectiveness of a hemicellulose-based wound dressing (Veloderm®) with that of rayon dressing in the healing of split-thickness skin graft donor sites [119]. Rayon dressing was used as a control because the majority of the burn treatment units and plastic surgery services use rayon dressings to provide a favorable microenvironment for the regeneration of the epidermis. The cited results revealed that the hemicellulose dressing is as safe as the rayon dressing, and both types of treatment were found to be adequate and thus Veloderm® dressing can serve as a replacement for rayon dressing in the healing of the split-thickness skin graft donor site (Figure 24) [119]. All these data provide promising developments in the field of hemicellulose wound dressing as a biodegradable, green material in biomedical applications.

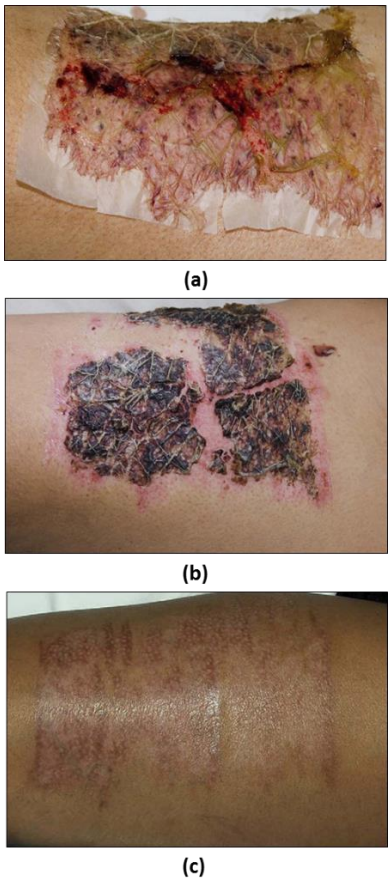

Figure 24. the effectivness of the hemicellulose-based wound dressing (Veloderm®). (a) Appearance of hemicellulose dressing after being wetted and placed on the skin graft donor site, (b) postoperative day 7, showing partial re-epithelialization, and (c) Final appearance of the donor site on postoperative day 60. Reproduced from [119]

On the other hand, interest in biopolymers as a drug delivery system has greatly increased in the last decades. Drug carriers have the ability to improve drug performance in terms of efficacy, safety, and patient compliance [123]. Xylan is well known to be degraded completely by the action of xylanases and ß-xylosidases enzymes secreted by the microflora of the colon in the human body [124][125]. Those enzymes can cleave the β-glycosidic linkage between the sugar units of the hemicellulose backbones. The presence of micro-organisms that secrete those enzymes in the colon will influence the utilization of hemicellulose as a drug carrier polymer for colon specific drug delivery.

Several forms of drug delivery systems have been described in the literature. These forms include: liposomes, microparticles (microcapsules and microspheres), nanoparticles, polymeric micelles, nanocrystals, and others [75]. Capsules have been used as drug delivery systems and as a protection of biologically active materials, for example, enzymes, drugs, and peptides [126]. A large variety of methods have been used for capsule fabrication, including layer-by-layer self-assembly, template polymerization, emulsion polymerization, phase separation, and interfacial reaction [126]. Nagashima and his colleagues developed a xylan microcapsule by means of interfacial crosslinking polymerization [123]. This method for microcapsule development requires two steps, the emulsification step plays a vital role in determining the particle size distribution and the aggregation arrangement of the microparticles, and the crosslinking step plays a crucial role in the stabilization of the capsule structure [75][126].

Galactoglucomannan-based microspheres with crosslinking as a drug delivery system has been developed by Edlund and coworkers [127]. In this research the microspheres incorporate either caffeine, which is a small hydrophilic substance, or a macromolecular model protein – the bovine serum albumin. It was shown that the release rate of the galactoglucomannan-based microspheres varied depending on several factors including the type of the encapsulated substance. In the research of Du *et al.,* glucomannans (GM)-based nanoparticles of a size range between 50 and 1200 nm were developed [128]. In this study the nanoparticles were formed by crosslinking the carboxymethylated-GM with chitosan by electrostatic interactions instead of chemical cross-linking, thus eliminating the toxicity associated with the crosslinking reagent. These nanoparticles have the ability to entrap and release bovine serum albumin (BSA).

In another study prepared by Alonso-Sande and other coworkers, nanoparticles were prepared from glucomannan and chitosan [129]. The nanoparticles had a high capacity to incorporate and release insulin and P1 protein. The addition of glucomannans into the nanoparticle facilitated the interaction of the nanoparticle with the intestinal epithelium both *in vitro* and *in vivo*. Despite the fact that pharmaceutical applications of hemicelluloises are still new, there has been substantial studies reported that conclude that hemicelluloses can incorporate diverse biomolecules, thus providing a promising structure for the preparation of new drug delivery systems.

5.2. Other Applications (Coating and Food Packaging)

Modified hemicelluloses, mainly the acetylated form have been reported and studied for added value applications. In the research of Shaikh *et al*., hemicellulose acetate was used as an internal plasticizer for cellulose acetate films [130]. It has been indicated that 5% of xylan acetate can reduce the T_g of the cellulose film from 148°C to 139°C. The 5% xylan acetate containing film shows tensile strengths of about 40 MPa, however those cellulose acetate films without xylan acetate could not be cut into notch-free specimens, hence they could not be tested without plasticizer. These samples showed a tensile strength of 14 MPa after addition of 15% plasticizer. This research indicated that acetylated hemicelluloses can function as an internal plasticizer by inducing a relatively good mechanical properties for the cellulose acetate film without addition of external plasticizer.

Many studies that deal with the coating applications of hemicelluloses have been reported [131][132][133]. In pulp and paper industry, paper coating plays a crucial role in the improvement of the paper quality such as the reduction in the ink absorbency. Coated papers gives much more clear and glossy results for printing, and it provides resistance to water and grease in packaging applications. In the food industry, coating is extremely important because it acts as a moisture barrier, therefore preventing food spoilage.

In the research of Anthony and co-workers, hemicellulose-based binders were used for paper coatings [134]. The hemicellulose-based binders were tested for paper coating formulation and these results were compared with the traditionally used polyvinyl alcohol (PVA). The results indicated that water absorption was reduced by 25% for both the hemicellulose-based binders and the PVA coatings from the base paper value. The water vapor transmission rate (WVTR) analysis for both the PVA and hemicellulose-based coatings was similar. Furthermore, there were no significant differences in the brightness, opacity, and color after coating in both materials. This research provides an important utilization of hemicelluloses as being a natural product for the replacement of synthetic coatings.

Péroval and co-authors developed an arabinoxylan film grafted with omega-3 fatty acid [52]. The omega-3 graft was induced to improve the water vapor barrier capability of the arabinoxylan-based film. Omega-3 fatty acids were obtained from fish and linseed oil. Grafting levels of 5.1-6.4% were obtained with the oils. The contact angle of the ungrafted film was 66.8°, however it reached 115° for that of 5.1% grafting level. The water vapor barrier properties were improved with grafting of omega-3 and significantly with linseed oil, where WVTR of 2.9×10^{-3} g m^{-2} s^{-1} and WVP of 1.1×10^{-10} g m^{-1} Pa^{-1} s^{-1} were found. Their results indicated that the surface hydrophobicity of the grafted arabinoxylan film with omega-3 fatty acids is higher than that of a waxy coating or a low-density polyethylene (LDPE) film. Furthermore, it was indicated that linseed oils provide better barrier properties and a higher surface hydrophibicity than oils extracted from marine oils [52] (Figure 25).

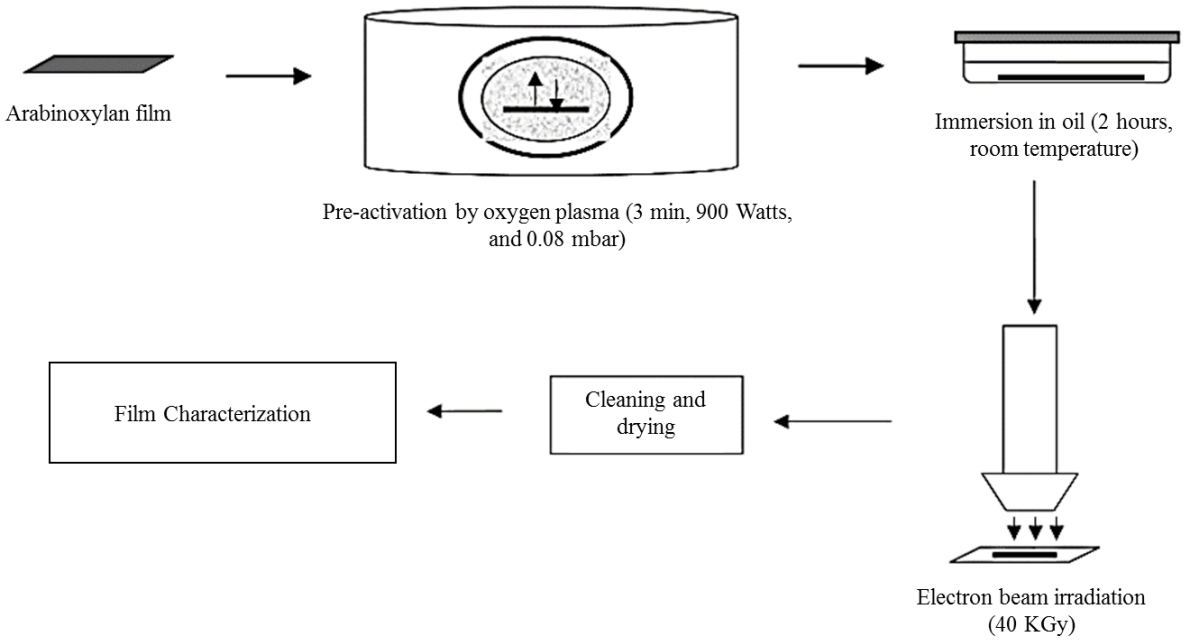

Figure 25. Experimental setup for grafting omega-3 fatty acids on arabinoxylan polymeric chains. Reproduced from [52].

In another study performed by Tatar and other colleagues, gum arabic (GA), gumarabic-hemicellulose (GA-HC) and hemicellulose (HC) emulsions were prepared to assess the effectiveness of hemicellulose as the coating material in fish oil microencapsulated by spray drying

[131]. Chemical and physical defense of food can be achieved through food packaging. Such measures can protect the food against spoiling. Modified hemicellulose, mainly hemicellulose acetate films have been used for food packaging. Those films have shown improvement in oxygen barrier capabilities compared to the unmodified hemicellulose films [89][135][136]. To facilitate the utilization of hemicellulose for coating applications, various sources of hemicelluloses need to be applied as coating material and also different combinations with other coating agents should be tested . From the reviewed data, it can be observed that hemicelluloses have been used in many applications, and further investigations would benefit this developing areas.

6. Concluding Remarks: Hemicellulose Modifications for Suitable Applications

Several modification methods have been used to alter the hemicellulose characteristics for suitable applications. Most of these modifications generates hemicelluloses with increased thermal and hydrophobic properties. As it was reported, the structure of the extracted hemicellulose varies depending on the raw materials and the extraction method used. Those structural variations in combination with the modification used, can have a strong effect on the properties of hemicelluloses and the targeted applications. In hardwood the major hemicellulose is the highly acetylated xylan form; those forms will lose their acetyl groups upon auto-hydrolysis or alkaline extraction, thus increasing the hydrophilic character of the retained hemicelluloses. Branched hemicellulose will be released if isolated from grasses or softwood; those extraction methods release oligomeric and polymeric hemicellulose, respectively. The high molecular weight hemicelluloses can be subjected to the chemical and/or physical modification to be utilized for its suitable applications. Furthermore the dilute acid pretreatment has been widely used for bioenergy application of hemicellulose in which it releases sugar residues of hemicelluloses [137].

Alkaline-extracted hemicellulose from hardwood Kraft pulp and wheat straw, showed an increased thermal stability and hydrophobicity upon acetylation; those acetylated hemicelluloses as well as the O-acetyl-galactoglucomannan (AcGGM) hemicellulose type can be used as films for food packaging [85][87][88]. Those films have a low oxygen transmittance, low sensitivity to water, and are biodegradable, making them useful barrier films for food products. In addition, acetylated hemicelluloses are a good polymeric option for the production of hydrogel-absorbent materials. A

new study has also used hemicellulose acetate as an internal plasticizer for cellulose acetate films [130]. To increase the hydrophobic character of the extracted hemicelluloses, esterification by a long fatty acid chain can be used. Those types of modifications including, esterification with omega-3 fatty acids and oleoylation, provide the hemicellulose with increased hydrophobicity. Even more significantly than acetylated hemicellulose at the same DS and this may be more efficient in the development of barrier films for the production of packaging materials for different food products [52][92].

On the other hand, due to its strong stability compared to the ester bond, etherification can be used to introduce hydrophobic groups into the hemicellulose chain [100]. Several alkylating groups can be used. Most importantly, etherification by benzylation provides the hemicellulose with extra thermal stability and hydrophobicity mainly due to the benzene ring introduced into the hemicellulose chain. The benzylated hemicellulose can be utilized in the production of hydrophobic films that can be used for food packaging and coating applications [101].

Crosslinking is another important modification that can significantly alter the physical properties of the extracted hemicelluloses. Crosslinking can be performed by several methods such as chemical crosslinking mainly by esterification reaction with citric acid or epichlorohydrin and enzyme-catalyzed crosslinking (the example provided in this review was laccase- and irradiation-induced crosslinking). Generally, crosslinking induces an increased water resistance and thermal stability to the modified hemicellulose [104]. Crosslinked hemicelluloses are mainly used for biomedical applications such as drug delivery systems and wound dressing [107][119][127]. However, the applications of crosslinked hemicelluloses are not limited to biomedical applications. Several other applications have been reported and those include films for food packaging, hydrogels as an absorbent material, and others [104][108]. A summary of the applications of hemicellulose reviewed herein is given in Figure 26.

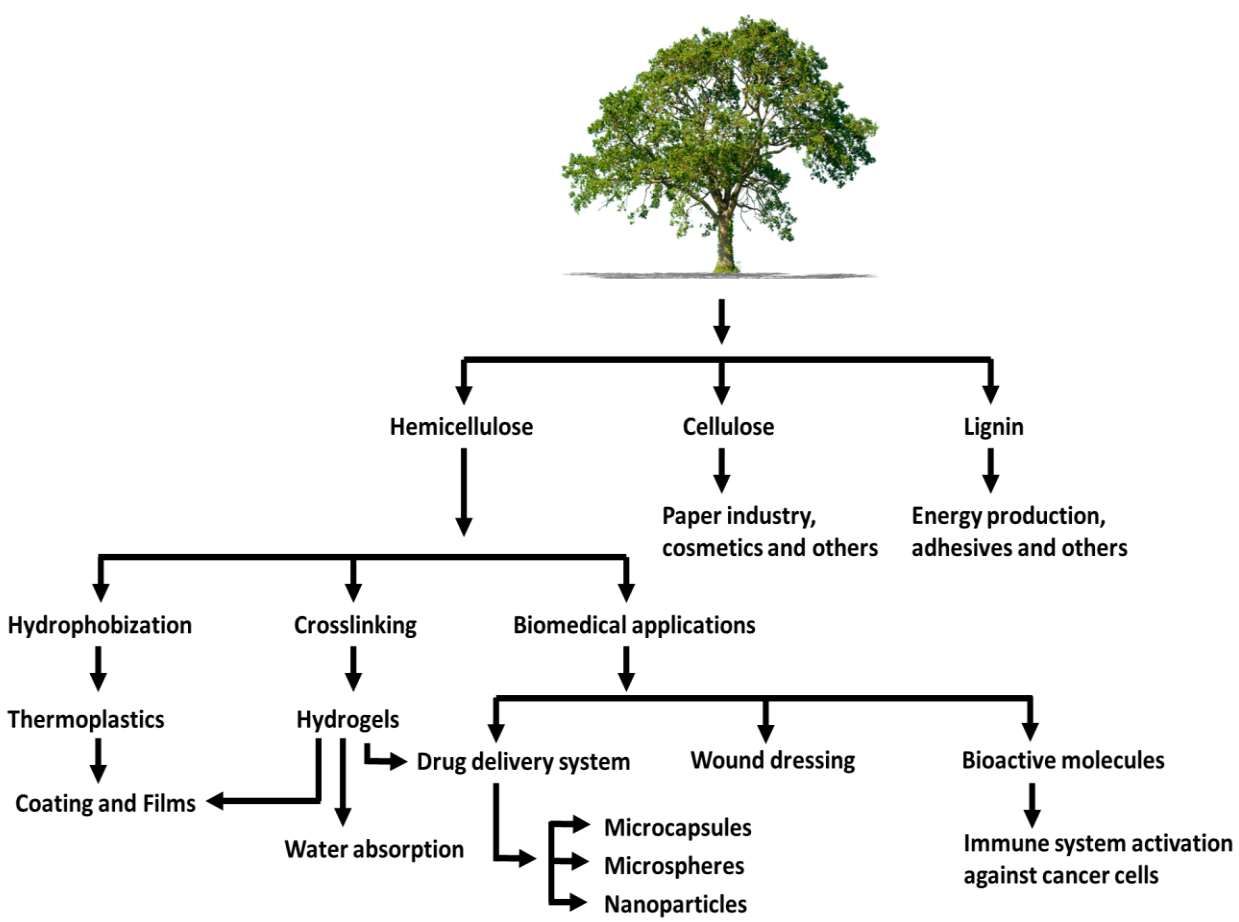

Figure 26. Illustration of the role of hemicellulose in a biomass refinery and its conversion into products for various applications.

Recent work, as cited in this work, has shown reactions that can be used to alter the hemicellulose structural featurs. Importantly, esterification improves hemicellulose miscibility and phase adhesion with commonly available thermo-plastic polymers. It has been reported that esterified hemicelluloses are hydrophobic with enhanced processability over native hemicellulose, which can allow their usage as thermoplastic films. For example, acetylated hemicellulose films have very good thermal and mechanical properties with a very low oxygen permeability. Those film properties facilitate its usage in food packaging. Because the ether bond is more stable than the ester bond, strategies based on etherification of hemicellulose have also been developed. Despite this stronger bond, depending on the alkylating agent, the etherified hemicellulose shows a higher or lower thermal stability compared to the native hemicellulose. Etherified hemicellulose films

have shown good mechanical properties in terms of high strength and flexibility.

In addition, hemicellulose crosslinking has been developed to create hydrogels used as drug delivery systems or as water absorption hydrogels. Recent research about hemicellulose-based hydrogels have combined the hemicellulose with chitosan to create a matrix capable to overcome acidic conditions. Moreover, despite the fact that pharmaceutical applications of hemicelluloses are relatively new, we can anticipate that hemicelluloses can incorporate diverse biomolecules, thus providing a promising structure for the preparation of new drug delivery systems. A focus on the green pathways using green solvents and reactants must be considered in the future applications.

References:

[1] M. M. Bugge, T. Hansen, and A. Klitkou, "What is the bioeconomy? A review of the literature," *Sustain.*, vol. 8, no. 7, 2016.

[2] L. Staffas, M. Gustavsson, and K. McCormick, "Strategies and policies for the bioeconomy and bio-based economy: An analysis of official national approaches," *Sustain.*, vol. 5, no. 6, pp. 2751–2769, 2013.

[3] Bioeconomy council of the German Government, "What is Bioeconomy?" 2017.

[4] J. Bjerg *et al.*, "Biomass 2020 : Opportunities, Challenges and Solutions," *Eurelectric*, p. 72, 2001.

[5] J. S. Golden, R. B. Handfield, J. Daystar, and T. E. McConnell, "An Economic Impact Analysis of the U.S. Biobased Products Industry: A Report to the Congress of the United States of America," p. 127, 2015.

[6] R. D. Perlack, L. L. Wright, A. F. Turhollow, R. L. Graham, B. J. Stokes, and D. C. Erbac, "Biomass as Feedstock for a Bioenergy and Bioproducts Industry: The Technical Feasibility of Billion-Ton Annual supply," 2005.

[7] Turyn yliopisto University of Turku, "Bioeconomy: Towards economically competitive and sustainable solutions to global challenges!" .

[8] P. McKendry, "Energy production from biomass (part 1): Overview of biomass," *Bioresour. Technol.*, vol. 83, no. 1, pp. 37–46, 2002.

[9] European Biomass Associtation, "Forest sustainability and carbon balance of EU importation of north american forest biomass for bioenergy production," no. September, p. 77, 2013.

[10] K. Löffler, N. Gillman, R. W. Van Leen, T. Schäfer, A. Faaij, and L. G. Plata, "the Future of Industrial Biorefineries," p. 40, 2010.

[11] IEA Bioenergy, "Bio-based Chemicals Value Added Products from Biorefinerie," 2012.

[12] S. Herrera, "Industrial biotechnology—a chance at redemption," *Nat. Biotechnol.*, vol. 22,

no. 6, pp. 671–675, 2004.

[13] C. Steiner, “Biochar Carbon Sequestration - Consulting.” .

[14] F. Cherubini, “The biorefinery concept: Using biomass instead of oil for producing energy and chemicals,” *Energy Convers. Manag.*, vol. 51, no. 7, pp. 1412–1421, 2010.

[15] A. Ilnicka and J. P. Lukaszewicz, “Discussion Remarks on the Role of Wood and Chitin Constituents during Carbonization,” *Front. Mater.*, vol. 2, no. March, pp. 1–6, 2015.

[16] L. Christopher, “Adding Value Prior to Pulping : Bioproducts from Hemicellulose,” *Glob. Perspect. Sustain. For. Manag.*, 2012.

[17] W. W. Al-Dajani and U. W. Tschirner, “Pre-extraction of hemicelluloses and subsequent kraft pulping Part I: Alkaline extraction,” *Tappi J.*, vol. 7, no. 6, pp. 3–8, 2008.

[18] E. O. Mária Fišerová, “Hemicelluloses Extraction From Beech Wood With Water and Alkaline Solutions,” vol. 57, no. 4, pp. 505–514, 2012.

[19] I. Gabrielii, P. Gatenholm, W. G. Glasser, R. K. Jain, and L. Kenne, “Separation, characterization and hydrogel-formation of hemicellulose from aspen wood,” *Carbohydr. Polym.*, vol. 43, no. 4, pp. 367–374, 2000.

[20] S. Marinkovic and B. Estrine, “Direct conversion of wheat bran hemicelluloses into n-decyl-pentosides,” *Green Chem.*, vol. 12, no. 11, pp. 1929–1932, 2010.

[21] E. E. Oliveira *et al.*, “Sustainable food-packaging materials based on future biorefinery products: Xylans and mannans,” *Bioresour. Technol.*, vol. 101, no. 14, pp. 5402–5406, 2010.

[22] T. Shahzadi *et al.*, “Advances in lignocellulosic biotechnology : A brief review on lignocellulosic biomass and cellulases,” *Adv. Biosci. Biotechnol.*, vol. 5, no. February, pp. 246–251, 2014.

[23] Z. Anwar, M. Gulfraz, and M. Irshad, “Agro-industrial lignocellulosic biomass a key to unlock the future bio-energy: A brief review,” *J. Radiat. Res. Appl. Sci.*, vol. 7, no. 2, pp. 163–173, 2014.

[24] A. Sunna and G. Antranikian, “Xylanolytic enzymes from fungi and bacteria.,” *Crit. Rev.*

Biotechnol., vol. 17, no. 1, pp. 39–67, 1997.

[25] N. G. V. Fundador, Y. Enomoto-Rogers, A. Takemura, and T. Iwata, "Acetylation and characterization of xylan from hardwood kraft pulp," *Carbohydr. Polym.*, vol. 87, no. 1, pp. 170–176, 2012.

[26] R. P. de Vries, J. Visser, P. Ronald, de Vries, R., and P., "Aspergillus Enzymes Involved in Degradation of Plant Cell Wall Polysaccharides," *Microbiol. Mol. Biol. Rev.*, vol. 65, no. 4, pp. 497–522, 2001.

[27] M. Edwards, C. Scott, M. J. Gidley, and J. S. G. Reid, "Control of mannose/galactose ratio during galactomannan formation in developing legume seeds," *Planta*, vol. 187, no. 1, pp. 67–74, 1992.

[28] B. T. Kusema *et al.*, "Acid hydrolysis of O-acetyl-galactoglucomannan," *Catal. Sci. Technol.*, vol. 3, no. 1, pp. 116–122, 2013.

[29] A. Ayoub, R. a. Venditti, J. J. Pawlak, H. Sadeghifar, and A. Salam, "Development of an acetylation reaction of switchgrass hemicellulose in ionic liquid without catalyst," *Ind. Crops Prod.*, vol. 44, pp. 306–314, 2013.

[30] A. R. Kulkarni, S. Pattathil, M. G. Hahn, W. S. York, and M. a. O'Neill, "Comparison of Arabinoxylan Structure in Bioenergy and Model Grasses," *Ind. Biotechnol.*, vol. 8, no. 4, pp. 222–229, 2012.

[31] G. Dervilly-Pinel, V. Tran, and L. Saulnier, "Investigation of the distribution of arabinose residues on the xylan backbone of water-soluble arabinoxylans from wheat flour," *Carbohydr. Polym.*, vol. 55, no. 2, pp. 171–177, 2004.

[32] G. Goma, *Advances in Biochemical Engineering*, vol. 61, no. 4. 1979.

[33] Q. a Nguyen, M. P. Tucker, F. a Keller, and F. P. Eddy, "Two-stage dilute-acid pretreatment of softwoods.," *Appl. Biochem. Biotechnol.*, vol. 84–86, pp. 561–576, 2000.

[34] D. Knappert, H. Grethlein, and A. Converse, "Partial acid hydrolysis of poplar wood as a pretreatment for enzymatic hydrolysis," *Biotechnol Bioengin Symp.* pp. 11–77, 1981.

[35] I. Egües, C. Sanchez, I. Mondragon, and J. Labidi, "Effect of alkaline and autohydrolysis

processes on the purity of obtained hemicelluloses from corn stalks," *Bioresour. Technol.*, vol. 103, no. 1, pp. 239–248, 2012.

[36] L. W. Doner and K. B. Hicks, "Isolation of hemicellulose from corn fiber by alkaline hydrogen peroxide extraction," *Cereal Chem.*, vol. 74, no. 2, pp. 176–181, 1997.

[37] I. Hasegawa, K. Tabata, O. Okuma, and K. Mae, "New Pretreatment Methods Combining a Hot Water Treatment and Water / Acetone Extraction for Thermo-Chemical Conversion of Biomass," vol. 45, no. 6, pp. 755–760, 2004.

[38] M. Saska and E. Ozer, "Aqueous extraction of sugarcane bagasse hemicellulose and production of Xylose syrup," *Biotechnol. Bioeng.*, vol. 45, no. 6, pp. 517–523, 1995.

[39] M. Palm and G. Zacchi, "Extraction of hemicellulosic oligosaccharides from spruce using microwave oven or steam treatment," *Biomacromolecules*, vol. 4, no. 3, pp. 617–623, 2003.

[40] S. Azhar, "Extraction of Polymeric Hemicelluloses from Spruce Wood," 2015.

[41] C. Froschauer, M. Hummel, M. Iakovlev, A. Roselli, H. Schottenberger, and H. Sixta, "Separation of hemicellulose and cellulose from wood pulp by means of ionic liquid/cosolvent systems," *Biomacromolecules*, vol. 14, no. 6, pp. 1741–1750, 2013.

[42] N. Mosier *et al.*, "Features of promising technologies for pretreatment of lignocellulosic biomass," *Bioresour. Technol.*, vol. 96, no. 6, pp. 673–686, 2005.

[43] H. Cheng, H. Zhan, S. Fu, and L. a. Lucia, "Alkali extraction of hemicellulose from depithed corn stover and effects on soda-AQ pulping," *BioResources*, vol. 6, no. 1, pp. 196–206, 2011.

[44] W. Al-Dajani, "Alkaline extraction of hemicelluloses from aspen chips and its impact on subsequent kraft pulping," *Tappi*, 2007.

[45] M. Balakshin, E. Capanema, H. Gracz, H. min Chang, and H. Jameel, "Quantification of lignin-carbohydrate linkages with high-resolution NMR spectroscopy," *Planta*, vol. 233, no. 6, pp. 1097–1110, 2011.

[46] M. F. S. Barbosa, M. B. de Medeiros, I. M. de Mancilha, H. Schneider, and H. Lee, "Screening of yeasts for production of xylitol from d-xylose and some factors which affect

xylitol yield in Candida guilliermondii," *J. Ind. Microbiol.*, vol. 3, no. 4, pp. 241–251, 1988.

[47] V. Meyrial, J. P. Delgenes, R. Moletta, and J. M. Navarro, "Xylitol production from D-xylose by Candida guillermondii: Fermentation behaviour," *Biotechnol. Lett.*, vol. 13, no. 4, pp. 281–286, 1991.

[48] J. M. Dominguez, C. S. Gong, and G. T. Tsao, "Pretreatment of sugar cane bagasse hemicellulose hydrolysate for xylitol production by yeast," *Appl. Biochem. Biotechnol.*, vol. 57–58, no. 1, pp. 49–56, 1996.

[49] A. P. F. Carlo N Hamelinck, Geertje van Hooijdonk, "Ethanol from lignocellulosic biomass : techno-economic performance in short- , middle- and long-term," vol. 28, pp. 384–410, 2005.

[50] F. Carvalheiro, L. C. Duarte, and F. M. G??rio, "Hemicellulose biorefineries: A review on biomass pretreatments," *J. Sci. Ind. Res. (India).*, vol. 67, no. 11, pp. 849–864, 2008.

[51] E. Fredon *et al.*, "Hydrophobic films from maize bran hemicelluloses," *Carbohydr. Polym.*, vol. 49, no. 1, pp. 1–12, 2002.

[52] C. Péroval, F. Debeaufort, A. M. Seuvre, B. Chevet, D. Despré, and A. Voilley, "Modified arabinoxylan-based films. Part B. Grafting of omega-3 fatty acids by oxygen plasma and electron beam irradiation," *J. Agric. Food Chem.*, vol. 51, no. 10, pp. 3120–3126, 2003.

[53] A. G. Cunha and A. Gandini, "Turning polysaccharides into hydrophobic materials: A critical review. Part 2. Hemicelluloses, chitin/chitosan, starch, pectin and alginates," *Cellulose*, vol. 17, no. 6, pp. 1045–1065, 2010.

[54] M. Rubio, J. F. Tortosa, J. Quesada, and D. Gómez, "Fractionation of lignocellulosics. Solubilization of corn stalk hemicelluloses by autohydrolysis in aqueous medium," *Biomass and Bioenergy*, vol. 15, no. 6, pp. 483–491, 1998.

[55] G. Garrote, H. Domınguez, and J. C. Parajo, "Mild autohydrolysis: An environmentally friendly technology for xylooligosaccharide production from wood," *J. Chem. Technol. Biotechnol.*, vol. 74, no. 11, pp. 1101–1109, 1999.

[56] D. Nabarlatz, D. Montane, A. Kardosova, S. Bekesova, V. Hribalova, and A. Ebringerova,

"Almond shell xylo-oligosaccharides exhibiting immunostimulatory activity," *Carbohydr. Res.*, vol. 342, no. 8, pp. 1122–1128, 2007.

[57] A. Moure, P. Gullón, H. Domínguez, and J. C. Parajó, "Advances in the manufacture, purification and applications of xylo-oligosaccharides as food additives and nutraceuticals," *Process Biochem.*, vol. 41, no. 9, pp. 1913–1923, 2006.

[58] J. Puls and B. Saake, "Industrially isolated hemicelluloses," *Hemicellul. Sci. Technol.*, vol. 864, pp. 24–37, 2004.

[59] F. Peng, P. Peng, F. Xu, and R. C. Sun, "Fractional purification and bioconversion of hemicelluloses," *Biotechnol. Adv.*, vol. 30, no. 4, pp. 879–903, 2012.

[60] J. Ogier, D. Ballerini, J. Leygue, and L. R. J. Pourquié, "Production d ' éthanol à partir de biomasse lignocellulosique," *Sci. Technol.*, vol. 54, no. 1, pp. 67–94, 1999.

[61] D. Vazquez, M. A. Lage, J. C. Parajo, and G. Vazquez, "Fractionation of Eucalyptus Wood in Acetic-Acid Media," *Bioresour. Technol.*, vol. 40, no. 2, pp. 131–136, 1992.

[62] Y. Sun and J. Cheng, "Hydrolysis of lignocellulosic materials for ethanol production : a review," *Bioresour. Technol.*, vol. 83, no. 1, pp. 1–11, 2002.

[63] S. Mazumder, P. Lerouge, C. Loutelier-Bourhis, A. Driouich, and B. Ray, "Structural characterisation of hemicellulosic polysaccharides from Benincasa hispida using specific enzyme hydrolysis, ion exchange chromatography and MALDI-TOF mass spectroscopy," *Carbohydr. Polym.*, vol. 59, no. 2, pp. 231–238, 2005.

[64] B. Ray, C. Loutelier-Bourhis, C. Lange, E. Condamine, A. Driouich, and P. Lerouge, "Structural investigation of hemicellulosic polysaccharides from Argania spinosa: Characterisation of a novel xyloglucan motif," *Carbohydr. Res.*, vol. 339, no. 2, pp. 201–208, 2004.

[65] W. Farhat *et al.*, "Hemicellulose extraction and characterization for applications in paper coatings and adhesives," *Ind. Crops Prod.*, vol. 107, no. April, pp. 370–377, 2017.

[66] Z. Sárossy, D. Plackett, and H. Egsgaard, "Carbohydrate analysis of hemicelluloses by gas chromatography-mass spectrometry of acetylated methyl glycosides," *Anal. Bioanal.*

Chem., vol. 403, no. 7, pp. 1923–1930, 2012.

[67] T. Hannuksela and C. H. Du Penhoat, "NMR structural determination of dissolved O-acetylated galactoglucomannan isolated from spruce thermomechanical pulp," *Carbohydr. Res.*, vol. 339, no. 2, pp. 301–312, 2004.

[68] a. Jacobs and O. Dahlman, "Characterization of the molar masses of hemicelluloses from wood and pulps employing size exclusion chromatography and matrix-assisted laser desorption lonization time-of-flight mass spectrometry," *Biomacromolecules*, vol. 2, no. 3, pp. 894–905, 2001.

[69] O. B. Dahlman, A. Jacobs, and M. Nordstrom, "Characterization of Hemicelluloses from Wood Employing Matrix-Assisted Laser Desorption / Ionization Time-of-Flight Mass Spectrometry," pp. 80–93, 2004.

[70] S. C. Fry *et al.*, "An unambiguous nomenclature for xyloglucan-derived oligosaccharides," *Physiol. Plant.*, vol. 89, no. 1, pp. 1–3, 1993.

[71] R. Sun, J. M. Lawther, and W. B. Banks, "Fractional and structural characterization of wheat straw hemicelluloses," *Carbohydr. Polym.*, vol. 29, no. 4, pp. 325–331, 1996.

[72] R. K. Jain, M. Sjöstedt, and W. G. Glasser, "Thermoplastic xylan derivatives with propylene oxide," *Cellulose*, vol. 7, no. 4, pp. 319–336, 2000.

[73] E. V Groman, P. M. Enriquez, C. Jung, and L. Josephson, "Arabinogalactan for hepatic drug delivery.," *Bioconjug. Chem.*, vol. 5, pp. 547–556, 1994.

[74] G. S. Kelly, "Larch arabinogalactan: Clinical relevance of a novel immune-enhancing polysaccharide," *Alternative Medicine Review*, vol. 4, no. 2. pp. 96–103, 1999.

[75] A. Eduardo da Silva, H. Rodrigues Marcelino, M. Christine Salgado Gomes, E. Eleamen Oliveira, T. Nagashima Jr, and E. Sócrates Tabosa Egito, "Xylan, a Promising Hemicellulose for Pharmaceutical Use," *Prod. Appl. Biopolym.*, p. 232, 2012.

[76] O. Gordobil, I. Egüés, I. Urruzola, and J. Labidi, "Xylan–cellulose films: Improvement of hydrophobicity, thermal and mechanical properties," *Carbohydr. Polym.*, vol. 112, pp. 56–62, 2014.

[77] C. Laine *et al.*, “Hydroxyalkylated xylans - Their synthesis and application in coatings for packaging and paper,” *Ind. Crops Prod.*, vol. 44, pp. 692–704, 2013.

[78] R. Junli, P. Xinwen, Z. Linxin, P. Feng, and S. Runcang, “Novel hydrophobic hemicelluloses: synthesis and characteristic.,” *Carbohydr. Polym.*, vol. 89, no. 1, pp. 152–7, 2012.

[79] R. Sun, J. M. Fang, J. Tomkinson, and C. A. S. Hill, “Esterification of hemicelluloses from poplar chips in homogeneous solution of N,N-dimethylformamide/lithium chloride,” *J. Wood Chem. Technol.*, vol. 19, no. 4, pp. 287–306, 1999.

[80] J. M. Fang, R. Sun, P. Fowler, J. Tomkinson, and C. A. S. Hill, “Esterification of wheat straw hemicelluloses in theN,N-dimethylformamide/lithium chloride homogeneous system,” *J. Appl. Polym. Sci.*, vol. 74, no. 9, pp. 2301–2311, 1999.

[81] F. Z. Belmokaddem, C. Pinel, P. Huber, M. Petit-Conil, and D. Da Silva Perez, “Green synthesis of xylan hemicellulose esters,” *Carbohydr. Res.*, vol. 346, no. 18, pp. 2896–2904, 2011.

[82] X.-W. Peng, J.-L. Ren, and R.-C. Sun, “Homogeneous esterification of xylan-rich hemicelluloses with maleic anhydride in ionic liquid.,” *Biomacromolecules*, vol. 11, no. 12, pp. 3519–24, 2010.

[83] J. L. Ren, R. C. Sun, C. F. Liu, Z. N. Cao, and W. Luo, “Acetylation of wheat straw hemicelluloses in ionic liquid using iodine as a catalyst,” *Carbohydr. Polym.*, vol. 70, no. 4, pp. 406–414, 2007.

[84] J. M. Fang, R. C. Sun, J. Tomkinson, and P. Fowler, “Acetylation of wheat straw hemicellulose B in a new non-aqueous swelling system,” *Carbohydr. Polym.*, vol. 41, no. 4, pp. 379–387, 2000.

[85] R. Sun, J. M. Fang, J. Tomkinson, and G. L. Jones, “Acetylation of wheat straw hemicelluloses in N,N-dimethylacetamide/LiCl solvent system,” *Ind. Crops Prod.*, vol. 10, no. 3, pp. 209–218, 1999.

[86] J. Aburto *et al.*, “Acid Esters of Amylose and Starch,” vol. 4628, no. February, pp. 1440–1451, 1999.

[87] J. Hartman, A. C. Albertsson, M. S. Lindblad, and J. Sjöberg, “Oxygen barrier materials from renewable sources: Material properties of softwood hemicellulose-based films,” *J. Appl. Polym. Sci.*, vol. 100, no. 4, pp. 2985–2991, 2006.

[88] P. G. Stepan, A. Hoije, H . Schols, “Arabinose Content of Arabinoxylans Contributes to Flexibility of Acetylated Arabinoxylan Films A.,” *Polym. Polym. Compos.*, vol. 21, no. 7, pp. 2348–2355, 2012.

[89] J. Zoldners and T. Kiseleva, “Modification of hemicelluloses with polycarboxylic acids,” *Holzforschung*, vol. 67, no. 5, pp. 567–571, 2013.

[90] A.-C. A. Jens Voepel, John Sjoberg, Michael Reif and U. G. Ulla-Karin Hultin, “Drug Diffusion in Neutral and Ionic Hydrogels Assembled from Acetylated Galactoglucomannan,” *J. Appl. Polym. Sci.*, vol. 21, no. 7, pp. 449–456, 2009.

[91] X. F. Sun, R. C. Sun, and J. X. Sun, “Oleoylation of sugarcane bagasse hemicelluloses using N-bromosuccinimide as a catalyst,” *J. Sci. Food Agric.*, vol. 84, no. 8, pp. 800–810, 2004.

[92] R. C. Sun, J. Tomkinson, J. . Liu, and Z. . Geng, “Oleoylation of Wheat Straw Hemicelluloses in New Homogeneous System.pdf,” *polymer journal*. p. pp 857_863, 1999.

[93] I. Sebti, F. Ham-Pichavant, and V. Coma, “Edible bioactive fatty acid-cellulosic derivative composites used in food-packaging applications,” *J. Agric. Food Chem.*, vol. 50, no. 15, pp. 4290–4294, 2002.

[94] C. S. R. Freire, A. J. D. Silvestre, C. P. Neto, M. N. Belgacem, and A. Gandini, “Controlled heterogeneous modification of cellulose fibers with fatty acids: Effect of reaction conditions on the extent of esterification and fiber properties,” *J. Appl. Polym. Sci.*, vol. 100, no. 2, pp. 1093–1102, 2006.

[95] A. Tressaud, E. Durand, C. Labrug??re, A. P. Kharitonov, and L. N. Kharitonova, “Modification of surface properties of carbon-based and polymeric materials through fluorination routes: From fundamental research to industrial applications,” *J. Fluor. Chem.*, vol. 128, no. 4, pp. 378–391, 2007.

[96] I. Woodward, W. C. E. Schofield, V. Roucoules, and J. P. S. Badyal, “Super-hydrophobic surfaces produced by plasma fluorination of polybutadiene films,” *Langmuir*, vol. 19, no.

8, pp. 3432–3438, 2003.

[97] M. Gröndahl, A. Gustafsson, and P. Gatenholm, “Gas-phase surface fluorination of arabinoxylan films,” *Macromolecules*, vol. 39, no. 7, pp. 2718–2721, 2006.

[98] J. M. Fang, P. Fowler, J. Tomkinson, and C. A. S. Hill, “Preparation and characterisation of methylated hemicelluloses from wheat straw,” *Carbohydr. Polym.*, vol. 47, no. 3, pp. 285–293, 2002.

[99] C.-F. L. Ren, Run-Cang Sun, “Etherification of hemicellulose from sugare bagasse,” *J. Appl. Polym. Sci.*, vol. 21, no. 7, pp. 449–456, 2007.

[100] J. Pourchez, A. Govin, P. Grosseau, R. Guyonnet, B. Guilhot, and B. Ruot, “Alkaline stability of cellulose ethers and impact of their degradation products on cement hydration,” *Cem. Concr. Res.*, vol. 36, no. 7, pp. 1252–1256, 2006.

[101] K. Talja, R., Shan, J., Vähä-Nissi, M., King, A. W. T., Kilpeläinen, I., & Poppius-Levlin, “A new birch xylan derivative by aqueous benzylation.” p. (pp. 16-18), 2010.

[102] J. Hartman, A. C. Albertsson, and J. Sjöberg, “Surface- and bulk-modified galatoglucomannan hemicellulose films and film laminates for versatile oxygen barriers,” *Biomacromolecules*, vol. 7, no. 6, pp. 1983–1989, 2006.

[103] S. W. Goodman, “Handbook of Thermoset Plastics, 2nd Ed.” p. 606, 1999.

[104] X. W. Peng, J. L. Ren, L. X. Zhong, F. Peng, and R. C. Sun, “Xylan-rich hemicelluloses-graft -acrylic acid ionic hydrogels with rapid responses to pH, salt, and organic solvents,” *J. Agric. Food Chem.*, vol. 59, no. 15, pp. 8208–8215, 2011.

[105] A. Salam, R. a. Venditti, J. J. Pawlak, and K. El-Tahlawy, “Crosslinked hemicellulose citrate-chitosan aerogel foams,” *Carbohydr. Polym.*, vol. 84, no. 4, pp. 1221–1229, 2011.

[106] A. Salam, J. J. Pawlak, R. A. Venditti, and K. El-tahlawy, “Incorporation of carboxyl groups into xylan for improved absorbency,” *Cellulose*, vol. 18, no. 4, pp. 1033–1041, 2011.

[107] A. M. Karaaslan, M. A. Tshabalala, and G. Buschle-Diller, “Wood hemicellulose/chitosan-based semi: Interpenetrating network hydrogels: Mechanical, swelling and controlled drug release properties,” *BioResources*, vol. 5, no. 2, pp. 1036–1054, 2010.

[108] P. Oinonen, D. Areskogh, and G. Henriksson, “Enzyme catalyzed cross-linking of spruce galactoglucomannan improves its applicability in barrier films,” *Carbohydr. Polym.*, vol. 95, no. 2, pp. 690–696, 2013.

[109] C. Péroval *et al.*, “Modified arabinoxylan-based films: Grafting of functional acrylates by oxygen plasma and electron beam irradiation,” *J. Memb. Sci.*, vol. 233, no. 1–2, pp. 129–139, 2004.

[110] A.-C. A. Jens Voepel, Ulrica Edlund, “Alkenyl-Functionalized Precursors for Renewable Hydrogels Design,” *J. Polym. Sci.*, vol. 49, no. 1, pp. 487–488, 2009.

[111] X. Cao, X. Peng, L. Zhong, and R. Sun, “Multiresponsive hydrogels based on xylan-type hemicelluloses and photoisomerized azobenzene copolymer as drug delivery carrier,” *J. Agric. Food Chem.*, vol. 62, no. 41, pp. 10000–10007, 2014.

[112] A. Ayoub, J. C. Bray, and R. N. CHAN, “Patent WO2015187631A1 - Modified biopolymers and methods of producing and using the same - Google Patents.” 2015.

[113] A. Ebringerov’a, Z. Hrom’adkov’a, and V. Hribalov’a, “Structure and mitogenic activities of corn cob heteroxylans,” *Int. J. Biol. Macromol.*, vol. 17, no. 6, pp. 327–331, 1995.

[114] V. Apostolopoulos *et al.*, “Pilot phase III immunotherapy study in early-stage breast cancer patients using oxidized mannan-MUC1 [ISRCTN71711835].,” *Breast Cancer Res.*, vol. 8, no. 3, p. R27, 2006.

[115] C. K. Tang, K. C. Sheng, S. E. Esparon, O. Proudfoot, V. Apostolopoulos, and G. A. Pietersz, “Molecular basis of improved immunogenicity in DNA vaccination mediated by a mannan based carrier,” *Biomaterials*, vol. 30, no. 7, pp. 1389–1400, 2009.

[116] N. Sharon, “Carbohydrates as future anti-adhesion drugs for infectious diseases,” *Biochim. Biophys. Acta - Gen. Subj.*, vol. 1760, no. 4, pp. 527–537, 2006.

[117] L. I. Wamoto, T. W. Atanabe, and A. O. Gasawara, “[Adherence of Can- dida albicans is inhibited by yeast mannan].,” vol. 126, no. 3, pp. 167–172, 2006.

[118] M. Sato, T. Ohshima, N. Maeda, and C. Ohkubo, “Inhibitory effect of coated mannan against the adhesion of Candida biofilms to denture base resin.,” *Dent. Mater. J.*, vol. 32,

no. 3, pp. 355–60, 2013.

[119] L. M. Ferreira *et al.*, “Hemicellulose dressing versus rayon dressing in the re-epithelialization of split-thickness skin graft donor sites: a multicenter study,” *J. Tissue Viability*, vol. 18, no. 3, pp. 88–94, 2009.

[120] L. M. Ferreira, C. S. Sobral, L. Blanes, M. Z. Ipolito, and E. K. Horibe, “Proliferation of fibroblasts cultured on a hemi-cellulose dressing,” *J. Plast. Reconstr. Aesthetic Surg.*, vol. 63, no. 5, pp. 865–869, 2010.

[121] D. Melandri *et al.*, “Use of a new hemicellulose dressing (Veloderm) for the treatment of split-thickness skin graft donor sites. A within-patient controlled study,” *Burns*, vol. 32, no. 8, pp. 964–972, 2006.

[122] C. K. Field and M. D. Kerstein, “Overview of wound healing in a moist environment,” *Am. J. Surg.*, vol. 167, no. 1 SUPPL., pp. 2–6, 1994.

[123] T. Nagashima *et al.*, “Influence of the lipophilic external phase composition on the preparation and characterization of xylan microcapsules--a technical note.,” *AAPS PharmSciTech*, vol. 9, no. 3, pp. 814–7, 2008.

[124] N. Kulkarni, A. Shendye, and M. Rao, “Molecular and biotechnological aspects of xylanases,” *FEMS Microbiol. Rev.*, vol. 23, no. 4, pp. 411–456, 1999.

[125] E. Schacht *et al.*, “Polymers for colon specific drug delivery,” *J. Control. Release*, vol. 39, no. 2–3, pp. 327–338, 1996.

[126] B. Jiang, L. Hu, C. Gao, and J. Shen, “Crosslinked polysaccharide nanocapsules: Preparation and drug release properties,” *Acta Biomater.*, vol. 2, no. 1, pp. 9–18, 2006.

[127] U. Edlund and a.-C. C. Albertsson, “A microspheric system: Hemicellulose-based hydrogels,” *J. Bioact. Compat. Polym.*, vol. 23, no. 2, pp. 171–186, 2008.

[128] J. Du *et al.*, “Novel polyelectrolyte carboxymethyl Konjac Glucomannan-Chitosan nanoparticles for drug delivery,” *Macromol. Rapid Commun.*, vol. 25, no. 9, pp. 954–958, 2004.

[129] M. Alonso-Sande, M. Cuña, C. Remuñán-López, D. Teijeiro-Osorio, J. L. Alonso-Lebrero,

and M. J. Alonso, “Formation of new Glucomannan - Chitosan nanoparticles and study of their ability to associate and deliver proteins,” *Macromolecules*, vol. 39, no. 12, pp. 4152–4158, 2006.

[130] H. M. Shaikh, K. V. Pandare, G. Nair, and A. J. Varma, “Utilization of sugarcane bagasse cellulose for producing cellulose acetates: Novel use of residual hemicellulose as plasticizer,” *Carbohydr. Polym.*, vol. 76, no. 1, pp. 23–29, 2009.

[131] F. Tatar, M. T. Tunç, M. Dervisoglu, D. Cekmecelioglu, and T. Kahyaoglu, “Evaluation of hemicellulose as a coating material with gum arabic for food microencapsulation,” *Food Res. Int.*, vol. 57, pp. 168–175, 2014.

[132] R. N. Antenucci, “Method of making a hemicellulose coated dietary fiber US 4927649 A,” 1990.

[133] V. Kisonen *et al.*, “O-acetyl galactoglucomannan esters for barrier coatings,” *Cellulose*, vol. 21, no. 6, pp. 4497–4509, 2014.

[134] R. Anthony, Z. Xiang, and T. Runge, “Paper coating performance of hemicellulose-rich natural polymer from distiller’s grains,” *Prog. Org. Coatings*, vol. 89, pp. 240–245, 2015.

[135] K. S. Mikkonen and M. Tenkanen, “Sustainable food-packaging materials based on future biorefinery products: Xylans and mannans,” *Trends Food Sci. Technol.*, vol. 28, no. 2, pp. 90–102, 2012.

[136] G.-G. Chen, X.-M. Qi, Y. Guan, F. Peng, C.-L. Yao, and R.-C. Sun, “High Strength Hemicellulose-Based Nanocomposite Film for Food Packaging Applications,” *ACS Sustain. Chem. Eng.*, vol. 4, no. 4, pp. 1985–1993, 2016.

[137] T. S. Jeong, B. H. Um, J. S. Kim, and K. K. Oh, “Optimizing dilute-acid pretreatment of rapeseed straw for extraction of hemicellulose,” *Appl. Biochem. Biotechnol.*, vol. 161, no. 1–8, pp. 22–33, 2010.

Chapter 2. Extraction optimization of hemicellulose from lab to pilot scale

1. Introduction

Currently, there is intense research activity targeted at the replacement of petroleum-based products with renewable lignocellulosic-biomass-based products in order to reduce the environmental impacts, provide new energy resources, and conserve petroleum resources. In addition, there is a great interest for the lignocellulosic biofuels industry to develop valuable co-products that can improve the overall economics of a biofuel production process.

Lignocellulosic biomass is a term referring to the woody and non-woody dry matter that is mainly composed of three polymers: cellulose, hemicellulose and lignin. Cellulose is a homogeneous polymer consisting of C6 glucose monomers, and hemicellulose is a heterogeneous polymer consisting of C5 and C6 monomeric residues [1]. Hemicellulose associates with lignin through covalent bonds known as lignin-carbohydrate complexes (LCC), of which comprise phenyl glycoside bonds, esters and benzyl ethers [2][3]. However the linkage between hemicellulose and cellulose has been assumed to be through H-bonding [4]. Hemicelluloses are carbohydrate polymers containing xylans (arabinoxylans and 4-O-methyl-glucuronoxylans), galactomannans, glucomannans, and xyloglucans (4-linked β-D-glucans with attached side chains). Upon acid hydrolysis, hemicelluloses are easily fragmented into their constitutional pyranoses and furanoses sugar units which include: xylose, mannose, arabinose, glucose, glucuronic acid and others [5]. Structural and compositional differences in hemicellulose exist between different biomasses [5].

During conventional Kraft pulping the majority of hemicelluloses are degraded into low molecular weight isosaccharinic acids which, along with lignin and other pulping chemicals, dissolve in the black liquor [6]. About 80% of the black liquor solids come from lignin and hemicellulose. The black liquor is usually burned to produce energy, however, since the heating value of hemicellulose (≈13.6 MJ/Kg) is much lower than that of lignin (≈27 MJ/Kg), its combustion represents an inefficient use of the feedstock resources [7]. Thus, it would be beneficial to pre-extract the hemicellulose prior to the pulping in order to develop a number of bioproducts such as biochemical and biomaterials to enhance the value extracted from woody and non-woody materials. Hemicelluloses can be used in value-added industrial applications including hydrogels, thermoplastics, couting and additives in papermaking, in cosmetics and in pharmaceutical applications such as drug carriers [8][9][10]. Hemicellulose is a green substitute for petroleum based polyols and is a non-food-based substitute for starch polyols.

Hemicellulose extraction from biomass is an essential step for the production of a wide range of fuels, biomaterials and chemicals [11]. Many different effective methods have been used to isolate hemicellulose from woody and non-woody tissues. Those methods include dilute acid pretreatments [12], alkaline extraction [13], alkaline peroxide extraction [14], liquid hot water extraction [15][16], steam treatment [17], microwave treatment [18], ionic liquid extraction [19] and others [20]. Alkaline extraction is well studied, and it is known as a strong and efficient method for hemicellulose extraction [21].

Hemicelluloses can be liberated by alkaline extraction since alkaline treatment can completely or partially cleave ester bonds between lignin and hemicellulose in the cell walls, resulting in the dissolution of hemicelluloses. Moreover, it is known that hydroxide ions cause swelling of cellulose, hydrolysis of ester linkage, and disruption of intermolecular hydrogen bonds between cellulose and hemicellulose, thereby bringing a portion of the hemicellulosic material into solution. Alkaline extraction is compatible chemically with the kraft pulping process, which is well established processing annually 100s of millions of tons of wood and its associated hemicellulose.

Extraction of hemicellulose from non-delignified biomass (lignocellulosic materials) yields polysaccharides that may be contaminated with high proportions of lignin, whereas its separation from bleached pulps results in a relatively pure hemicellulose [22].

This study identified an efficient alkaline extraction of hemicellulose from a woody and non-woody biomass source – bleached hardwood pulp (B-HWP) and partially delignified switchgrass (SWG) – using extraction conditions of 3, 7, 10, 13 and 17% NaOH w/w solutions at 50°C for 3 h. The physicochemical properties and the structural features of these hemicellulosic samples were investigated. The importance of this study are reflected in being the first report that investigated the differences between pure hemicelluloses and partially purified hemicelluloses. Also this is the first study that reports the possibility for lignin to have a role of plasticizer for hemicellulose. In addition, the technical and economic analysis for the extraction process was investigated. The analysis was performed to determine the economic feasibility of building a commercial biorefinery for the production of dissolving pulp and hemicellulose using bleached pulp as a starting raw material.

2. Experimental Section

2.1. Materials

Switchgrass (SWG) was harvested in August 2011 from Cherry Research Farm in Goldsboro, North Carolina, State Department of Agriculture, and bleached hardwood pulp (B-HWP), with an origin from the southeastern United States, was provided by International Paper. The materials were stored indoors and the moisture content allowed to equilibrate for 4 weeks prior to use. Moisture content of the air-dried materials was measured by oven drying at 105°C until constant moisture content was achieved.

2.2. Delignification of switchgrass

The SWG was processed into powder in a Wiley mill to pass through a 1-mm mesh size screen attached to the mill. The powder was sieved on a 60-mesh screen (250 um openings). SWG fractions were de-lignified by adding a solution consisting of 30% by weight of an aqueous NaOH solution (2% by weight of NaOH) and 70% anhydrous ethanol (96% by weight ethanol) at 75°C (40:1 liquid to solid ratio) and stirred for 2.5 h with a mechanical stirrer to solubilize some of the lignin. The suspension was allowed to cool to room temperature under ambient conditions before filtration with a house vacuum on Whatman Filter Paper (Whatman International Ltd., Maidstone,

England, Catalog Number 1004 150, quantitative number 4, 150 mm diameter). The obtained solid (partially delignified SWG) was used for downstream hemicellulose extraction

2.3. Hemicellulose extraction from partially delignified switchgrass and bleached hardwood pulp

Hemicellulose was isolated from partially delignified SWG and B-HWP by an alkaline extraction method. The partially delignified SWG were transferred to NaOH solution at concentration of 3, 7, 10, 13 and 17% by weight and stirred for 3 h at 50ºC to solubilize hemicellulose. However, after being processed by pulping it in a 200 gallon pilot plant hydrapulper, the B-HWP was subjected to hemicellulose extraction by 10% NaOH solution (based on optimum SWG results, see later) and stirred for 3 h at 50ºC same as the extraction conditions applied for hemicellulose extraction from SWG. At the end of the 3-h period, the suspension was filtered with a house vacuum on Whatman GF/A glass microfiber filter paper to remove the filtrate containing hemicellulose. The filtrate pH was adjusted to 5-6 by adding 25% acetic acid and then transferred to 96% ethanol (2x ethanol volume relative to the filtrate) at 4°C. The mixture was left for two days to allow the hemicellulose to precipitate (no stirring) and settle to the bottom. The clear liquid above the precipitate layer was carefully removed by vacuum suction. The hemicellulose precipitate was washed 3 times by 70% ethanol. The hemicellulose material was freeze-dried to yield hemicellulose powder. (Each extraction condition was repeated 4 times and the yield average and the standard deviation were calculated). The hemicelluloses are labeled as indicated in Table 1.

Table 1. Hemicellulose Extraction Conditions Nomenclature

Hemicellulose	Sodium hydroxide concentration (%)	Biomass
SWG-HC3	3	Switchgrass
SWG-HC7	7	Switchgrass
SWG-HC10	10	Switchgrass
SWG-HC13	13	Switchgrass
SWG-HC17	17	Switchgrass
HW-HC10	10	Bleached hardwood pulp

2.4. Sugar compositional analysis and lignin quantification

The sugar compositions of SWG and B-HWP, as well as hemicellulose extracted from both biomasses were determined by high performance liquid chromatography (HPLC) analysis of monomeric sugars (glucose, xylose, galactose, arabinose and mannose). Briefly, 0.3 g oven-dried, ground sample was taken and hydrolyzed by 72% (w/v) sulfuric acid followed by 4% (w/v), sulfuric acid hydrolysis [23]. The hydrolysate was then filtered to remove solids from the liquid (the filter paper were stored in the oven at 105°C for 2 days to quantify the acid insoluble lignin and ash content). The filtrate was neutralized by calcium carbonate. Sugars were quantified by the binary HPLC (Agilent Technologies 1200 Series, Palo Alto, CA, USA) system using a refractive index detector. Deionized water was used as the mobile phase. The cellulose and hemicellulose contents were calculated using equations (1) and (2), respectively. The correction coefficient for hydration is 0.9, where it is assumed that the predominant source of glucose is from cellulose and the hemicellulose released (g) is the summation of arabinose, galactose, xylose, and mannose [24].

$$Cellulose\ (\%) = \frac{\text{mass of glucose released x 0.9}}{Dry\ weight\ of\ the\ biomass} \text{ x } 100 \qquad (1)$$

$$Hemicellulose\ (\%) = \frac{\text{mass of (xylose+arabinose+mannose+galactose)}\ x\ 0.9}{Dry\ weight\ of\ the\ biomass} \text{ x } 100 \qquad (2)$$

Solids recovery was calculated as a percentage of the total component detected based on the initial sample dry weight. The total solids, acid-soluble lignin, and acid-insoluble lignin content were determined by the National Renewable Energy Laboratory's (NREL) Laboratory Analytical Procedures [23],[25].

Each sample was analyzed four separate times for its composition and an average and the standard deviation were calculated.

2.5. Molecular weight determination by viscosity

An Ubbelohde viscometer (No. S 66) was used to determine the viscosity; the extracted hemicelluloses were dissolved with 0.04 M cupriethylenediamine (CED); and the intrinsic viscosity of different hemicelluloses was determined at 25ºC for the measurement of the molecular weight. An amount of 7.2 mL of the solution was added to the viscometer by pipet. Vacuum was applied to force the solution into the bulb about 2 cm above the capillary tube, then the vacuum was removed and the solution was allowed to flow down through the tube by gravity. The time it took for the solution to flow through the capillary is the efflux time (the experiment was repeated 4 times for each sample and the average and standard deviation were calculated) [26].

Intrinsic viscosity [η] = K (t), where K is viscosity meter constant and (t) is the efflux time in second.

The Staudinger – Mark-Houwink equation of xylan in CED is:

$[\eta] = 2.2 \times 10^{-2} DP^{0.72}$, where DP is the degree of polymerization of hemicellulose

It was reported that a native hemicellulose with a degree of polymerization of 200 corresponds to a molecular weight of 32,800 g mol^{-1} [17].

2.6. Fourier transform infrared spectroscopy (FT-IR)

FTIR analyses were performed for the samples from 4000 to 650 cm^{-1}, with a spectral resolution of 4 cm^{-1}. The spectra were recorded on a single reflection attenuated total reflectance (ATR).

FTIR technique was performed by a Platinum ATR Alpha instrument. The spectra were obtained by an accumulation of 40 scans.

2.7. Thermal analysis

Thermogravimetric analysis was performed with a TGA Q500 (TA Inc., New Castle, DE) on 5-15 mg of sample for each experiment in a nitrogen atmosphere. The temperature range and heating rate were 30-800°C and 10°C/min, respectively. The analysis was repeated twice on different samples. Thermal transitions of the samples were studied using differential scanning calorimetry (DSC). The instrument used was a DSCQ2000 (TA Inc., New Castle, DE) with a hermetic pan (T 090127). Before analysis, the samples were dried at 50°C under vacuum overnight. The samples were heated from 40 to 205°C at a temperature ramp of 10°C/min. The samples were then cooled to 30°C and a second heating cycle was performed by heating the samples again to 205°C at 10°C/min. An empty pan was used as a reference.

2.8. NanoTA AFM Measurements

Two types of hemicelluloses (SWG-HC10 and HW-HC10) pressed into a pellet were analyzed using Nanothermal analysis (NanoTA) with AFM+ system (Anasys, Santa Barbara, USA). The measurement is based on bringing a probe that can be heated into contact with a sample surface. Then both nanoscale imaging and thermal analysis can be performed. Prior to measurements the thermal probe was calibrated with melting point standards of poly (caprolactone), poly (ethylene), and poly (ethyleneterepthalate). The measurements were performed as follows. The ThermaLever cantilever (APN-200) was used for capturing the height profile AFM image. Then, using the AFM image, the probe was targeted on an area of interest and a thermal ramp with heating rate between 15 to 25°C/min was performed. When applicable, following the thermal ramp, the film was again imaged to observe the thermal patterns on the films.

2.9. Solubility and film formation

A determined amount of SWG-HC10 or HW-HC10 was added to a known volume of the solvents (Dimethylsulfoxide (DMSO), 90% DMSO/10% H2O, Tetrahydrofuran (THF), 5% Hydrochloric acid (HCl), 5% sodium hydroxide (NaOH)) and mixed overnight separately at room temperature and 60°C. The mixture was then filtered and the amount dissolved was calculated. For film formation, the mixture was poured into a Petri-dish and the liquid was allowed to evaporate overnight in the oven.

2.10. Intrinsic viscosity

The intrinsic viscosity of the pulp was determined by a standard ISO 5351-1. The limiting viscosity number of cellulose is determined in dilute cupriethylenediamine (CED) solution.

2.11. Alkali resistance (R_{18})

The alkali resistance of the pulp R_{18} was determined according to ISO 699-1982.

3. Results and Discussion

3.1. Hemicelluloses extraction

The chemical composition of SWG, as well as B-HWP are listed in Figure 1. It has been indicated that the SWG delignification step reduces the lignin content from 20.3 to 12.7 %. It was shown also that the hemicellulose content in SWG (27.8%) is higher than that in B-HWP (13.9%). The chemical composition of SWG and B-HWP may depend on their variety, growing conditions, bleaching and storage conditions. Furthermore, the low hemicellulose content in the B-HWP compared with SWG is due to the pulping and bleaching processes which removes all of the lignin

in combination with some hemicellulose. Our results are close to other research results in which it was indicated that SWG is made up of 37% cellulose, 29% hemicellulose, 19% lignin and 6% ash [27].

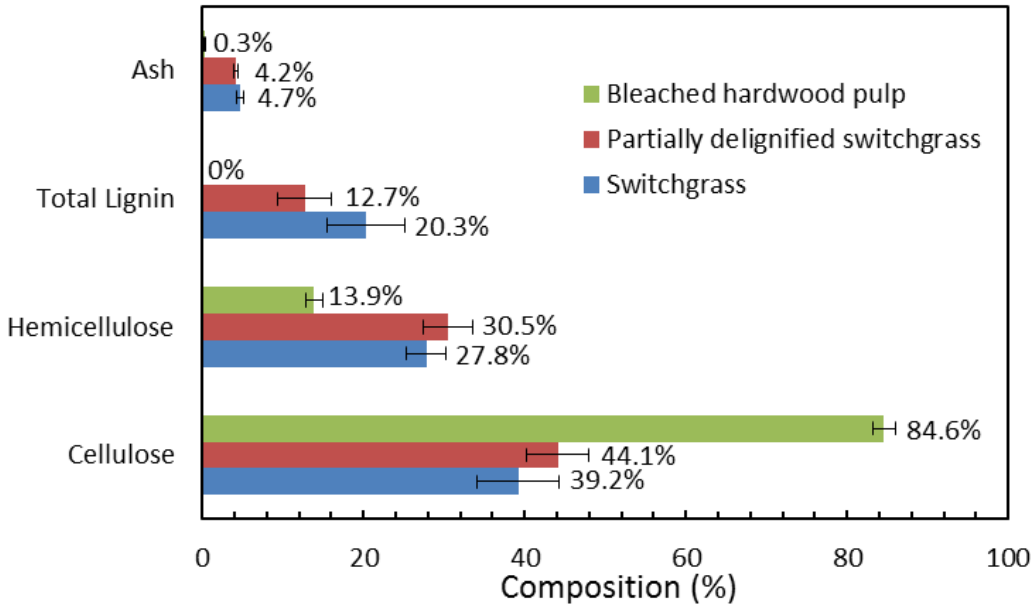

Figure 1. Compositional analysis of switchgrass and bleached hardwood pulp. Data is presented as means, the error bars indicate standard deviations (n=4)

Figure 2 shows the hemicellulose yields from B-HWP and partially delignified SWG. Hemicellulose extraction from B-HWP recovered 79.2% of the original hemicellulose in the original biomass. On the other hand, treatment of the partially delignified SWG recovered 40-72% of the original hemicellulose, with a maximum when 7-10% NaOH was used for extraction. This observation indicated that alkali solution favored hemicellulose release by the cleavage of the ester and/or ether bonds between lignin and hemicelluloses. Hemicellulose could be liberated by alkaline extraction since it is known that alkaline treatment can completely or partially cleave ester bonds between lignin and hemicellulose in the cell walls. Also, carboxylic moieties of hemicellulose and the phenolic groups of lignin can ionize in alkaline solution, becoming more soluble. Furthermore, upon alkaline treatment, the cellulose fibers will swell and decrease their crystallinity, enhancing release of the hemicelluloses and residual lignin, either by increasing the solubility of individual fragments or by inducing the swelling of the cell wall.

Our results indicated that at low alkaline concentration (3% NaOH), a very low yield of hemicellulose is obtained (about 40% yield on original hemicellulose). This observation can be attributed to the inability of the alkaline solution to solubilize the hemicellulose at this low concentration due to the hemicellulose still being bound to lignin. Increasing the concentration of NaOH to 7 and 10% increases the yield of extracted hemicellulose from partially delignified SWG to about 72% of the original hemicellulose (22% of the total biomass). The high solubility of hemicellulose at this alkaline concentration can be attributed probably to the cleavage of the ester-bond between ferulic acid and hemicelluloses by the dilute alkali. We also observed that increasing the concentration of NaOH to 13 and 17% reduced the yield of hemicellulose to 62.3 and 56%, respectively, of the original hemicellulose from partially delignified SWG. The reduction in the retained hemicellulose at high alkaline concentration was due to the degradation of hemicellulose. Indeed, it was reported that the increase in the alkali concentration can result in many variations in the polysaccharides [13],[14]. Alkali extractions have the drawback of eliminating acetyl functionalities. Also, a substantial quantity of hexuronic acid compartments in 4-O-methylglucuronoxylans are cleaved and alkaline degradation occurs at the reducing ends of the polysaccharides [13],[14].

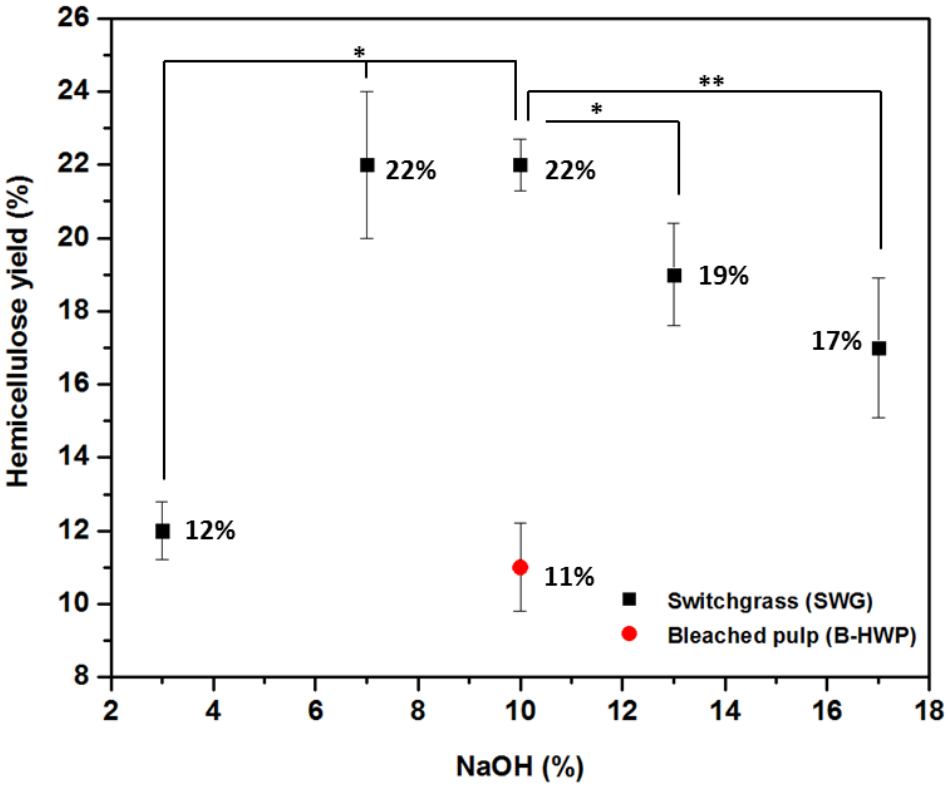

Figure 2: Average percent yield of hemicellulose based on the hemicellulose in the original biomass. The switchgrass used for extractions is the partially delignified switchgrass. Data is presented as means, the error bars indicate standard deviations (n=4).

3.2. Chemical characterization of Hemicellulose

Different hemicellulose composition, structure and amount could be obtained from different biomass sources. Hemicelluloses are a combination of different carbohydrate polymers, which primarily comprise different sugar residues including pentoses (β-D-xylose, α-L-arabinose), hexoses (β-D-mannose, β-D-glucose, α-D-galactose) and/or uronic acids (α-D-glucuronic, α-D-4-O-methylgalacturonic and α-D-galacturonic acids).

In hardwoods, the major hemicellulose component is O-acetyl-4-O-methyl-glucuronoxylan, in which one-tenth of the xylopyranose backbone units are substituted at C-2 with a (1→2)-linked 4-O-methyl-glucuronic acid residues, whereas a hydroxyl group is acetylated at C-2 or C-3 which occurs in about 70% of the xylopyranose backbone [28]. However, in grasses including SWG,

arabinoxylan is the predominant component of hemicellulose. The hemicellulose consists of β-(1→4) linked xylose units, with α-(1→2) and α-(1→3) linked arabinose units [29].

The compositional analysis of the different types of the extracted hemicelluloses is listed in Table 2. For the hemicellulose fractions extracted from SWG it can be clearly observed that with the increase in the NaOH concentration from 3% (SWG-HC3) to 17% (SWG-HC17) the xylose and glucose content increased from 72.2% and 2.4% to 81.7% and 3.9%, respectively. However, an opposite trend can be observed for galactose, arabinose and lignin in which they decreased as NaOH increased from 3% (SWG-HC3) to 17% (SWG-HC17). The structure of the major hemicellulose type in SWG (arabinoxylan) reveals that the arabinose/xylose ratio can provide a clear indication of the degree of linearity or branching of the hemicellulosic materials [30]. The increase in the xylose content and the decrease in the arabinose quantity with the increase in the alkali concentration is attributed to the cleavage of the arabinose branches and results in a more linear xylan polymer. This explanation is further confirmed with the decrease in the galactose content which is due to the cleavage of the galactose branches in other minor hemicellulose types found in SWG.

The slight increase in the glucose content can be explained as a minor degradation of the cellulose fibers as the alkaline concentration increased. Furthermore the reduction in the lignin quantity with the increase of the NaOH concentration is attributed to the increase in the frequency of ester linkage cleavage between hemicellulose and lignin and thus more lignin is removed. These data showed that the hemicellulosic portions obtained in the alkali solution of higher concentration had more linear structures. The relatively high xylose (89.5%) quantity obtained from the compositional analysis of HW-HC10 provide a clear indication that the major hemicellulose found in B-HWP is xylan. The purity of the hemicellulose from the B-HWP was determined to be the highest, as expected due to the extensive bleaching operations commonly used for kraft pulp.

Table 2. Analysis of the hemicellulose samples obtained by alkali extraction. Purity is the mass of Xylose, Galactose, Arabinose and Mannose relative to the total mass of the stream. Data is presented as means ± standard deviations (n=4). (N/D: Not determined)

	SWG-HC3	SWG-HC7	SWG-HC10	SWG-HC13	SWG-HC17	HW-HC10
Xylose (%)	72.2 ± 0.31	75.8 ± 0.26	77.4 ± 0.41	78.9 ± 0.34	81.7 ± 0.45	89.5 ± 0.32
Glucose (%)	2.4 ± 0.09	2.5 ± 0.11	2.8 ± 0.08	3.3 ± 0.16	3.9 ± 0.16	2.7 ± 0.09
Galactose (%)	3.1 ± 0.12	3.1 ± 0.20	2.8 ± 0.13	2.5 ± 0.15	2.3 ± 0.13	0.7 ± 0.06
Arabinose (%)	9.9 ± 0.42	6.3 ± 0.16	4.9 ± 0.17	4.1 ± 0.11	3.6 ± 0.15	0.4 ± 0.02
Mannose (%)	0.7 ± 0.03	0.6 ± 0.02	0.6 ± 0.01	0.8 ± 0.04	0.6 ± 0.02	0.8 ± 0.03
Total Lignin (%)	5.9 ± 0.13	5.1 ± 0.15	4.8 ± 0.15	3.9 ± 0.08	3.4 ± 0.09	0.0 ± 0.01
Ash (%)	1.8 ± 0.04	1.2 ± 0.04	1.5± 0.02	1.4 ± 0.05	1.2 ± 0.03	0.09 ± 0.01
Total (%)	96.0 ± 1.14	94.6 ± 0.94	94.8 ± 0.97	94.9 ± 0.93	96.7 ± 1.03	94.2 ± 0.54
Purity (%)	85.9 ± 0.77	85.8 ± 0.68	85.7 ± 0.74	86.3 ± 0.69	88.2 ± 0.73	91.4 ± 0.80
DP	291 ± 10	325 ± 15	392 ± 15	305 ± 30	215 ± 4	N/D

Furthermore, hemicelluloses are polymeric materials that are known to have a relatively low molecular weight (MW) compared with cellulose with a degree of polymerization (DP) that ranges between 80 and 425 monomeric residues [31]. The degree of polymerization (DP) of the different hemicellulosic materials are shown in Table 2. The results indicated that SWG-HC10, in which the hemicellulose fraction was extracted from SWG by 10% NaOH, had the highest MW of 64,288 g/mol (DP 392). This fraction had also the highest yield of biomass (22%). The discharge of relatively high MW hemicelluloses can be explained by the severe interruption of the macrostructure of the SWG holocellulose through the alkaline treatment.

The MW of the extracted hemicellulose from SWG increased from 47,700 to 64,300 g/mol as alkali concentration increased from 3 to 10% due to the increased dissolution of large molecular size hemicelluloses. Conversely, an increase in NaOH concentration from 10 to 17% decreased the MW of SWG extracted hemicellulose into 35,300g/mol. This indicates that a significant

amount of the solubilized hemicellulose was degraded during the extraction with high alkaline concentration.

Table 3 and Figure 3 represent the FT-IR spectra of all hemicelluloses. The spectra were examined in the frequency range of 650–4000 cm^{-1}. All hemicellulosic fractions appeared to be rather similar. Analysis indicated the absorbance at 3000–3640, 2889, 1483, 1416, 1045, 985 and 898 cm^{-1} that are associated with native hemicellulose [32].

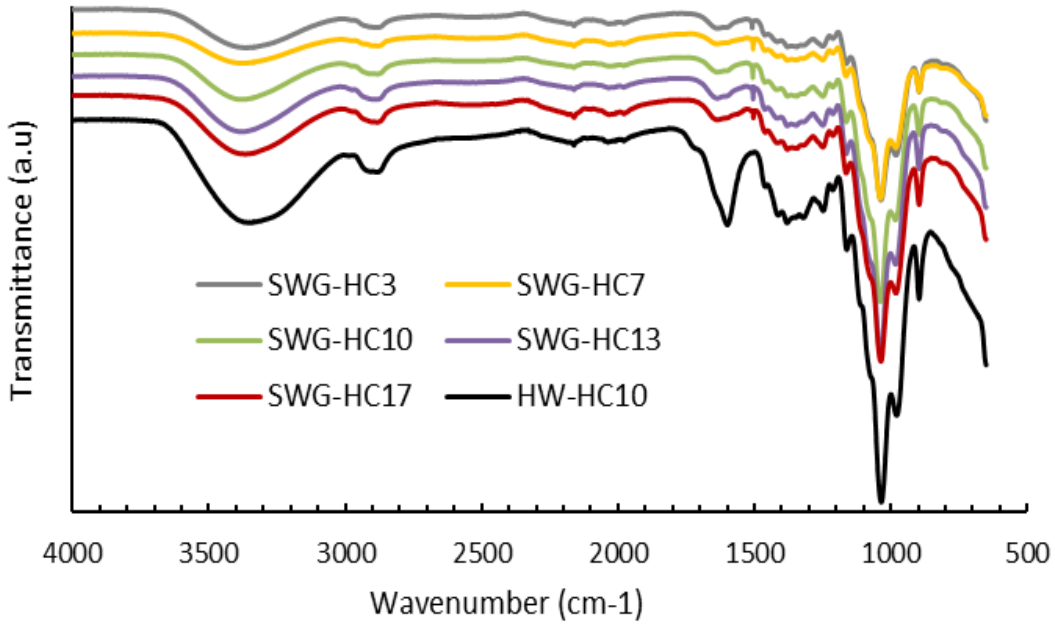

Figure 3. FT-IR spectra of hemicellulose samples

The 985 cm^{-1} band is attributed to C–O stretching, which is characteristic of carbohydrates structure. A sharp band at 898 cm^{-1} is characteristic of ß-glucosidic linkages between the sugars units [32]. In the carbonyl stretching region, the band around 1678-1598 cm^{-1} are probably due to the absorbed water. Hemicelluloses have a strong affinity for H_2O, and these carbohydrate polymers in the solid state may have disordered structures that can be easily hydrated [33]. A very small peak at around 1505 cm^{-1} can be observed in the spectrum of the SWG-HC samples; this is attributed to the aromatic skeletal vibrations, implying the occurrence of a small amount of the associated lignin. The absence of this band in HW-HC10 is also an indication of the absence of associated lignin in B-HWP. Furthermore, the absence of the band at around 1740-1710 cm^{-1}

relating to the carbonyl functionality, revealed that the acetyl group in xylan were removed in alkali solution.

Table 3. FT-IR absorption bands assigned to the hemicellulose samples

Peak Wavenumber (cm^{-1})	Assignment
3000–3640	Stretching vibration of O-H
2889	Symmetric and asymmetric vibration of C-H
1505	Aromatic skeletal vibrations
1483	CH_2 bending
1045	Asymmetric stretching of C–O–C bridge between the sugars units
985	C–O stretching characteristic of carbohydrates structure
898	Characteristic of ß-glucosidic linkages between the sugars units

3.3. Thermal behavior of the hemicellulosic materials

The thermal properties of the different hemicelluloses were studied by thermogravimetric analysis (TGA), differential scanning calorimetric (DSC) and NanoTA AFM measurements. The TGA results are shown in Table 4. The data are collected after a drying step to remove moisture for 10 min at 105ºC. The HW-HC10 primary decomposition was at 210–306ºC, whereas the SWG samples were at a higher temperature range of 258-301ºC. This may be due to lignin and its potential crosslinks in the SWG samples [34].

Table 4: Thermal analysis of hemicellulose samples. [(a)]Mass loss of 10% on the dry material

Sample	TGA-10%[a]	Residual at 800°C	T_g (°C)	ΔC_p (MJ/g)
SWG-HC3	267.1	19.0	136.2	0.1663
SWG-HC7	267.3	19.0	136.9	0.1704
SWG-HC10	267.3	19.3	137.3	0.1294
SWG-HC13	267.3	18.9	138.9	0.1355
SWG-HC17	267.2	15.6	139.5	0.1661
HW-HC10	222.8	26.6	144.3	0.1791

The HW-HC10 showed a significantly higher residual mass remaining (26.6%) after heating to 800ºC compared with all SWG-HC fractions (≈19%). SWG-HC17, which has the lowest molecular weight (DP 215), shows the lowest residual at 800ºC of about 15.6%, much lower than the 19.3% of SWG-HC10 which has the highest MW (DP 392). This suggests that the thermal stability of the hemicelluloses decrease with reduced molecular weight in agreement with other observations in the literature [35].

The glass transition temperatures (T_g) of the hemicellulose materials, as well as the ΔC_p are reported in Table 4. The T_g is identified as the midpoint temperature of the transition region of the DSC curves. The results indicate that HW-HC10 has a higher T_g (144.3°C) compared with all SWG-HC samples (136.2-139.5°C) (Table 4).

To further evaluate the glass transition, a Nano-TA Atomic Force Microscopy (AFM+) was used. With the AFM+ system the thermal response of nano-regions of the material is measured as the cantilever (holding the probe) deflection is determined as a function of rapidly ramping temperature. When the temperature of the probe is increased it will heat the nano-region of the sample at the contact point. An increasing deflection reflects thermal expansion of the material. A drop in deflection indicates penetration of the probe into the material revealing a softening or melting point. This change typically occurs at the glass or melt transition of the sample.

Representative thermal ramps are presented in Figure 4. For example, thermal analysis with the nano-TA of the HW-HC10 and SWG-HW10 systems, appeared to have softening points around

147 and 132°C, respectively (Figure 4) which are near the DSC measured value. It is not expected that the softening points from nano-TA and DSC are the same since the heating rate and other experimental conditions are different. However, both the DSC T_g and the nano-TA softening points are higher for the HW-HC10 and SWG-HW10 samples. The analysis of the distribution of results from nano-regions showed that these materials are homogeneous. The standard deviation of the softening points were 3 and 4°C for HW-HW10 and SWG-HW10, respectively.

The Nano-TA results are in agreement with the DSC results regarding the higher T_g of the pure hemicellulose compared with the lignin containing hemicelluloses. This in combination with the T_g results of the series of switchgrass extracted hemicelluloses provides an indication that lignin is probably acting as a plasticizer between the hemicellulose polymeric chains

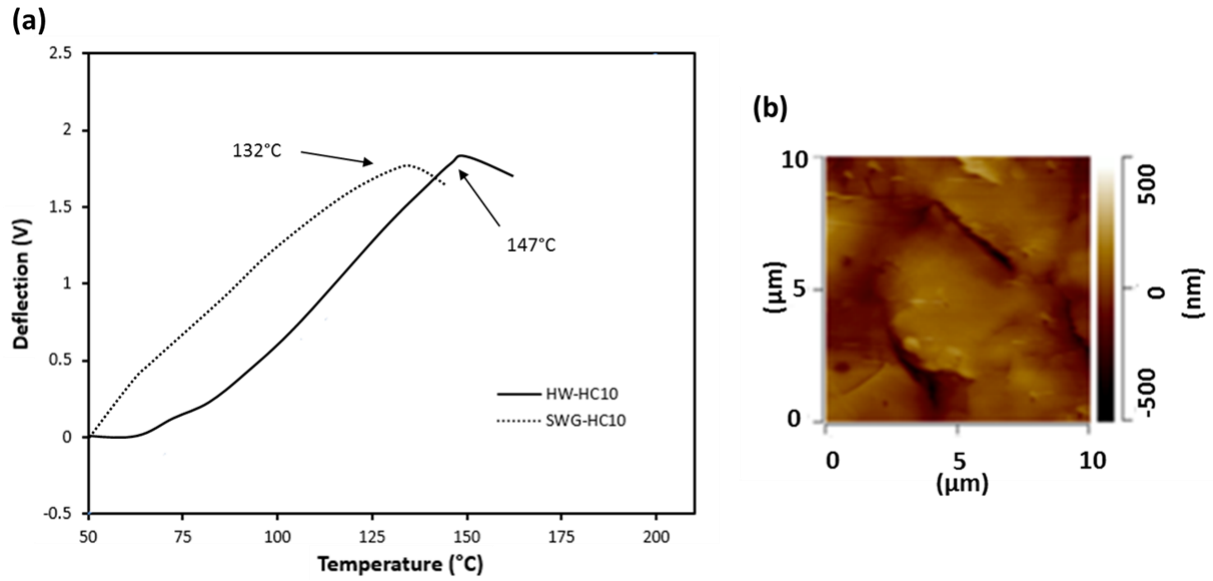

Figure 4: Thermal analysis of the hemicellulose samples. (a) Thermal ramp of two types of hemicelluloses extracted with 10% NaOH. The plots show a representative scan for each sample. (b) One AFM topography surface of HW-HC10

Also, Figure 5 indicated that the hemicellulosic preparations obtained by the extraction of SWG and B-HWP showed that the increase in the lignin content possibly leads to a significant decrease in the T_g of the extracted hemicelluloses. The B-HWP that has a zero lignin content and has the highest T_g value (144.3°C). However, the increase in the lignin content in the extracted hemicellulose from the partially delignified SWG, induces a reduction in the T_g of the extracted

hemicellulose that reaches 136.2°C for the SWG-HC3 that contains about 6% lignin. These findings indicate the possibility for lignin to act as a plasticizer for the hemicellulose chains by spacing them apart and creating additional free volume in the system.

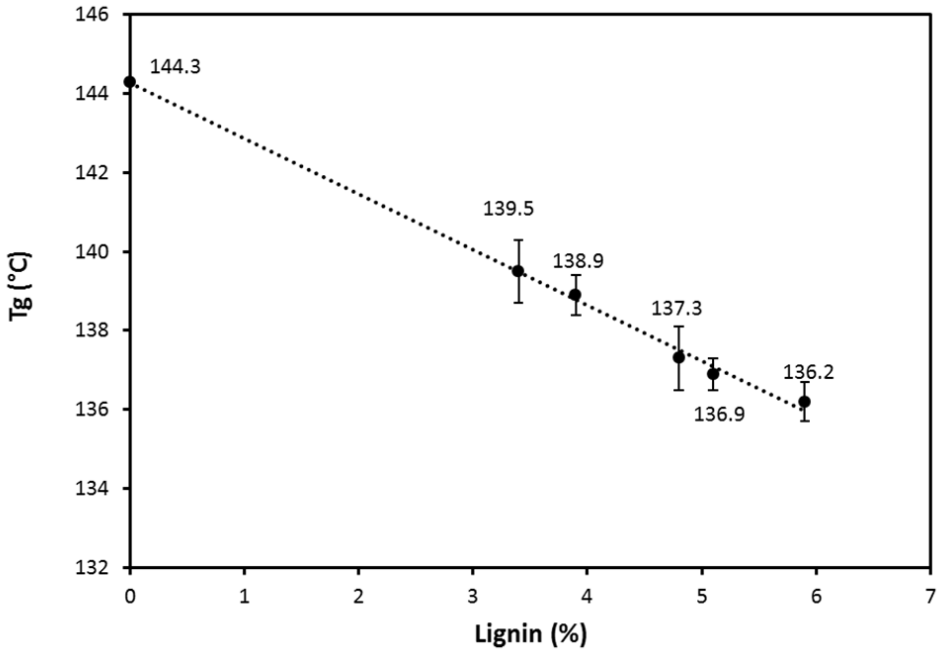

Figure 5: The effect of lignin on the T_g of the extracted hemicellulose samples

3.4. Hemicellulose solubility and film formation

The solubility and film formation capability of the SWG-HC10 was investigated in different solvents and the results are indicated in Table 5.

It is observed in Table 5 that SWG-HC10 has a very poor solubility in THF at either room temperature or at 60°C. However, this hemicellulose fraction shows very good solubility in both 5%NaOH and 5% HCl solutions at both temperatures. The solution 90% DMSO/10% water appears to be a better solvent than DMSO 100%. Indeed, the isolated polysaccharide is soluble in DMSO as a double stranded complex [36]. However, over time clusters aggregate, due to H-bonding, to form very large clusters (hundreds of strands in each cluster). DMSO is not capable of disrupting these large clusters, and so, for this reason, it needs water (10%) to compete with the

H-bonds that are formed between the polymeric chains of hemicellulose [36]. The high solubility of SWG-HC10 hemicellulose in the solvents listed in Table 5 leads to a potential use of this hemicellulose fraction in the production of films and membranes from the mixture by allowing the solvent to evaporate.

Table 5: Solubility and film formation of SWG-HC10. (+): Film formation and (-): No film formation

	Solubility at room temperature (g/ml)	Solubility at 60°C (g/ml)	Film formation	
			RT	60°C
Dimethylsulfoxide (DMSO)	0.019	0.031	-	+
90% DMSO/10% H_2O	0.033	0.042	+	+
Tetrahydrofuran (THF)	0.002	0.003	-	-
5% Hydrochloric acid (HCl)	0.048	0.049	+	+
5% sodium hydroxide (NaOH)	0.049	0.05	+	+

The films produced herein were semi-flexible, yellowish and opaque. HW-HC10 was also studied for its solubility and film formation capability. In fact, HW-HC10 showed similar solubility to that of SWG-HC10 but dried material was very brittle and did not form continuous films. The HW-HC10 and SWG-HC10 both have xylose as the major sugar unit. It appears that the lignin present in SWG-HC10 improves the flexibility of the films, in agreement with the depression of T_g of the system induced by lignin as seen in Figure 5.

3.5. Techno-economic Analysis for the Production of Hemicellulose using Bleached Market Pulp as Raw Materials

Based on our experimental results, hemicellulose extraction from non-delignified biomass results in hemicellulosic materials that are contaminated with a remarkable proportions of lignin, whereas its separation from bleached pulp results in a relatively pure hemicellulose. Removal of hemicellulose from the bleached pulp will obviously results in production of dissolving pulp which

can be used as raw material for different applications such as starting material for Viscose and LyoCell as well as for production of cellulose derivatives including Carboxymethyl Cellulose (CMC) which can be used as a thickening and dispersion agent in food and cosmetic products. Our results indicated that the extraction of hemicellulose from bleached pulp release a relatively pure cellulose fibers. After extraction, the viscosity of the pulp increases slightly (from 740 into 765 ml/g) probably due to the removal of the short polymeric chain hemicelluloses and leaving the high molecular weight cellulose fibers. The purity of the pulp was remarkable, with R_{18}-value of 96.7%. In addition, dissolving pulp shows a higher thermal stability (TGA_{max} 338°C) than both the bleached pulp (TGA_{max} 323°C) and the extracted hemicellulose (TGA_{max} 245°C). Indeed, hemicelluloses are known to degrade at a lower temperature than cellulose because it contain somewhat random, amorphous structure, rich of branches which are very easy to degrade to volatiles evolving CO, CO_2 and some hydrocarbons.

The word wide demand for dissolving pulp is growing by 10% annually and many factories are being built or converted to meet this new demand [37]. These pulps have high cellulose content, over 90%, and low levels of hemicelluloses (2–4%) [38]. Recent studies indicated an increasing trend in the demand of dissolving pulp for its industrial applications [39]. Dissolving pulp is not used for paper manufacture, rather they are dissolved to make highly pure cellulose and cellulose derivatives (cellulose nitrate, cellulose acetate, and cellulose ethers). The global production of dissolving pulp increased significantly form 2.67 MT in 2001 to 6.68 MT in 2014 [40]. This increased production is attributed to the elevated consumption of cellulose based products including textile fibers, coatings, paints and others. Also it can be attributed to the increased cotton price and the advances in the environmental issues for dissolving pulp production. For example, it was proposed that the annual per capita consumption of cellulosic fibers will increase from its present 3.7–5.4 kg in 2030 [39].

On the other hand, the interest in hemicellulose applications is relatively growing, this interest can be reflected by the increased research done on the hemicellulose and is applications as discussed in chapter 1. Despite the increased interest in hemicellulose for its industrial utilization, there is a very limited data that concern with the cost evaluation and energy required to isolate the hemicellulose at industrial scale. To the best of our knowledge, there is no commercial hemicellulose extraction processes described in literature.

This part is aimed to study the economical feasibility to build a bio-refinery for the coproduction of dissolving pulp and hemicellulose by alkaline extraction technology using the market bleached pulp as starting material. In this study, we aimed to provide a preliminary techno-economic analysis for hemicellulose and dissolving pulp production, identify the most important cost and revenue drivers, and evaluate alternatives to improve economics.

In Figure 6, we represent the overall laboratory scale procedure to extract the hemicellulose from bleached pulp. The pulp was exposed to hemicellulose extraction by NaOH solution. The suspension was filtered to separate the filtrate (hemicellulose rich fraction) from the solid (cellulose rich fraction). The filtrate was then neutralized by adding acetic acid and the hemicellulose was precipitated using ethanol. Then the obtained hemicellulose is washed with ethanol and dried to obtain pure and dry hemicellulose fraction. On the other hand, the cellulose rich fraction was directly watched with water and then dried to obtain the dissolving pulp.

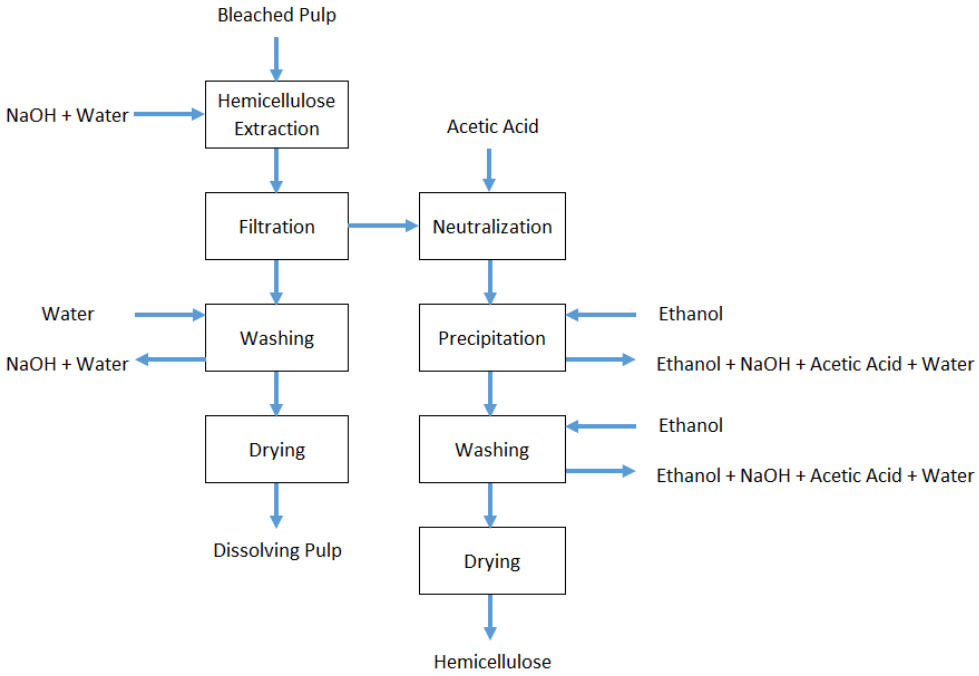

Figure 6: The laboratory scale extraction process of hemicellulose from bleached pulp

In reality, the industrial level differs from the laboratory scale and several factors must be considered. In the current research, we simulated the process based on the production of 10 OD tons/day of hemicellulose plant capacity. The overall conceptual biorefinery process is shown Figure 7. In this process, the fibers in the bleached pulp will be disintegrated in the hydropulper. Disintegrated fibers will be subjected to

hemicellulose extraction by 10% sodium hydroxide solution at 50°C using LP steam. The extracted solution will be filtered to separate the liquid hemicellulose rich phase from the solid cellulose rich phase. The solid phase will be washed with water, which intern will be filtered and sent to the pulp machine to get dissolving pulp sheets. The filtrate will go to sodium acetate recovery.

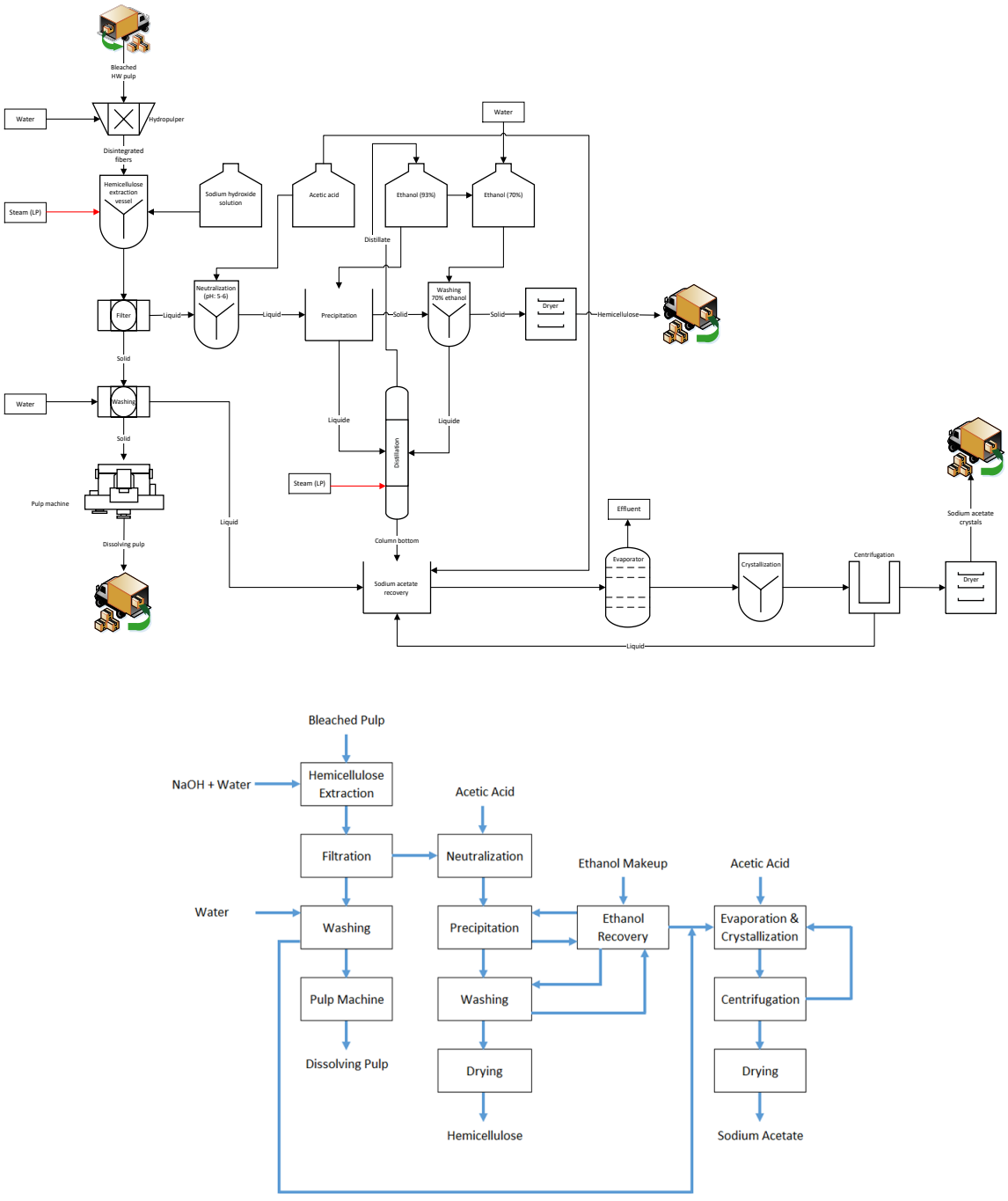

Figure 7. Schematic representation of the bio-refining pathways for the production of dissolving pulp and hemicellulose

The liquid phase will go to neutralization step with acetic acid solution. The neutralized liquid will be precipitated with 93% ethanol (2:1 of E:L ratio). Precipitated hemicellulose is washed by 70% ethanol solution. Actually, the quantity of ethanol required to precipitate and wash the hemicellulose is very high; however, this ethanol will be recycled by distillation. During distillation the ethanol will be recycled and the liquid in the bottom of the distillator will go to sodium acetate recovery. Due to ethanol recycling, a low amount of ethanol makeup will be required as reported in Figure 8. After washing, the hemicellulose will be filtered, dried and grinded to have a fine particles hemicellulose.

Sodium acetate will be produced during the neutralization step in which the acetic acid react with sodium hydroxide to produce the sodium acetate salt; however, since there is an un-neutralized stream coming to sodium acetate recovery from the filtration of the dissolving pulp which means that the sodium hydroxide is in excess to acetic acid, this requires more acetic acid to achieve equilibrium during the reaction and to have only sodium acetate. The recovered sodium acetate will be considered as an extra incomes for the dissolving pulp-hemicellulose biorefinery.

The process simulation was done using WinGems software and the techeno-economic analysis was performed using excel sheet. The inputs and outputs are shown in Figure 8. Based on our simulation, the designed refinery requires 101 tonne/day bleached pulp, 268 tonne/day acetic acid, and 37 tonne/day makeup ethanol to produce 88 tonne/day dissolving pulp, 10 tonne/day hemicellulose, and 376 tonne/day sodium acetate (Figure 8). A lot of sodium acetate is recovered by this method.

The techno-economic study was performed based on the cost of the row materials in October 2016. The capital investment, that is the money that will be used to build this industry, is reported in Figure 9. The Total Capex is MU$ 184.6. The production of sodium acetate costs $ 52.8, which represent about 28.6% of the total investment. However, the cost of the production of hemicellulose (extraction and purification) is $ 10.4, which represent 5.6% of the total investment.

Based on our results, the major product of the designed industry is sodium acetate and not hemicellulose and/or dissolving pulp. The produced sodium hydroxide will actually have a significant effect on the project economics as observed by sensitivity analysis (Figure 10). Sensitivity analysis is a common tool that is used to determine the risk of a model, while identifying the critical input parameters. It is used to evaluate the stability of a project's economics by determining the impact of certain key input parameters on the output.

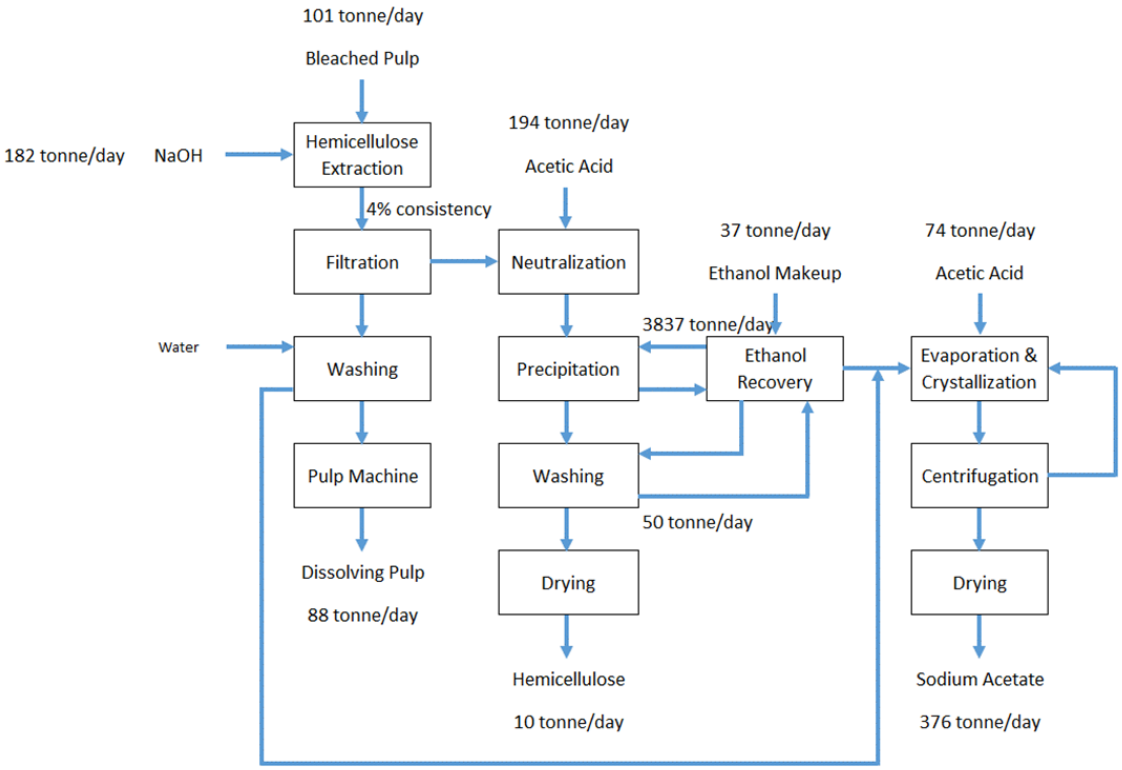

Figure 8. Process simulation: Inputes-outputs diagram.

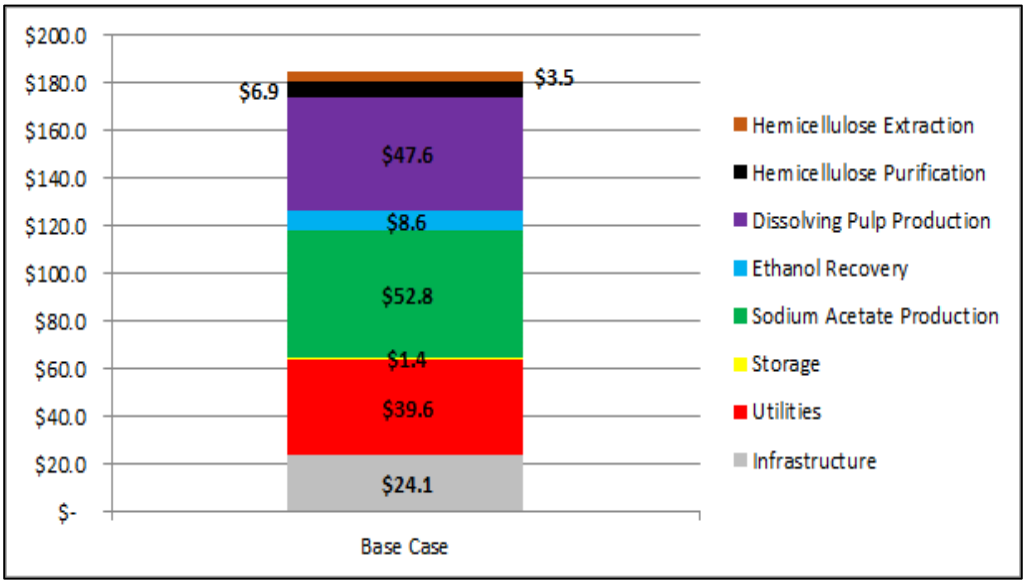

Figure 9. Capital investment: Hemicellulose-dissolving pulp production

In fact, the sensitivity study indicated that, sodium acetate price, dissolving pulp price and hemicellulose price, all contribute positively to the base case project net present value (NPV MU$) on the positive range, while an increase in inputs price (e.g. acetic acid, bleached pulp, and others) will negatively affect the project economics. More important, is the rate at which these inputs change the project's NPV. The price of sodium acetate is seen to have the largest overall impact on project economics and the largest positive affect on NPV when it increases. However, a much lower contribution of the hemicellulose and dissolving pulp price is observed. The combined analysis reveals that by this, we are actually building a sodium acetate plant and not hemicellulose-dissolving pulp plant.

In order to improve the outcomes of this plant, an alternative methods should be investigated. For example, the alkaline solution used to extract the hemicellulose can be used for several extraction sets. This will reduce the amount of the generated sodium acetate; however, a further analyses and investigations are required to check the efficiency of the alkaline solution to extract the hemicellulose if used several times and what will be the maximum sets to reuse this solution.

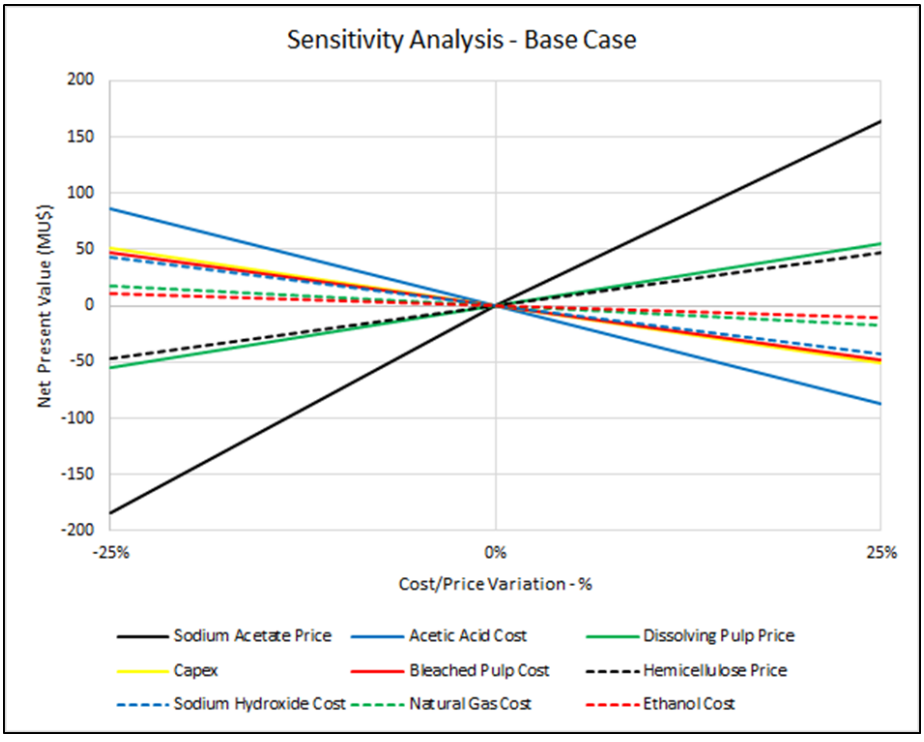

Figure 10. Sensitivity analysis: Hemicellulose-dissolving pulp production

4. Conclusion

In this research an alkaline treatment was optimized for extraction of polymeric hemicellulose from fully bleached hardwood pulp (B-HWP) and partially delignified switchgrass (SWG). The hemicellulose extracted from B-HWP was relatively pure with zero percent lignin and 89.5% xylose content whereas the partially delignified SWG hemicellulose contained about 6-3% lignin and 72-82% xylose, depending on the NaOH concentration during extraction (3-17% NaOH solution). The presence of lignin reduces the T_g of the hemicellulose in a concentration dependent manner. The hemicellulose from 10% NaOH extraction conditions have the highest yields of about 80% of the initial biomass hemicellulose relative to higher and lower sodium hydroxide concentrations in the extraction. In addition, the technical and economical analysis for this extraction process was investigated to provide a preliminery results about the feasibilityof commercial biorefinery for the production of dissolving pulp and hemicellulose using bleached pulp as a starting raw material. Our results indicated that the scaled-up extraction is an inefficient strategy. In fact, we obtained a high capital investment for sodium acetate production (29%) and utilities (21%) and a low capital investment for the production of hemicellulose (5.6%). Furthermore, economics are very sensitive to sodium acetate price, acetic acid cost, dissolving pulp price and capex. Alternatives to this strategy can be suggested. For instance, co-location of this industry in a pulp and paper mill will reduce the cost of the utilities and enhance the incomes.

References

[1] Z. Anwar, M. Gulfraz, and M. Irshad, "Agro-industrial lignocellulosic biomass a key to unlock the future bio-energy: A brief review," *J. Radiat. Res. Appl. Sci.*, vol. 7, no. 2, pp. 163–173, 2014.

[2] M. Balakshin, E. Capanema, H. Gracz, H. min Chang, and H. Jameel, "Quantification of lignin-carbohydrate linkages with high-resolution NMR spectroscopy," *Planta*, vol. 233, no. 6, pp. 1097–1110, 2011.

[3] L. Christopher, "Adding Value Prior to Pulping : Bioproducts from Hemicellulose," *Glob. Perspect. Sustain. For. Manag.*, 2012.

[4] et al Lodish H, Berk A, Zipursky SL, "The Dynamic Plant Cell Wall - Molecular Cell Biology . 4th edition." 2000.

[5] E. Sjöström, "Wood Chemistry_ Fundamentals and Applications." 1993.

[6] W. W. Al-Dajani and U. W. Tschirner, "Pre-extraction of hemicelluloses and subsequent kraft pulping Part I: Alkaline extraction," *Tappi J.*, vol. 7, no. 6, pp. 3–8, 2008.

[7] L. Kang, Y. Y. Lee, S. Yoon, A. J. Smith, and G. a Krishnagopalan, "Ethanol production from the mixture of hemicellulose prehydolysate and paper sludge," *BioResources*, vol. 7, pp. 3607–3626, 2012.

[8] I. Gabrielii, P. Gatenholm, W. G. Glasser, R. K. Jain, and L. Kenne, "Separation, characterization and hydrogel-formation of hemicellulose from aspen wood," *Carbohydr. Polym.*, vol. 43, no. 4, pp. 367–374, 2000.

[9] R. K. Jain, M. Sjöstedt, and W. G. Glasser, "Thermoplastic xylan derivatives with propylene oxide," *Cellulose*, vol. 7, no. 4, pp. 319–336, 2000.

[10] E. Fredon *et al.*, "Hydrophobic films from maize bran hemicelluloses," *Carbohydr. Polym.*, vol. 49, no. 1, pp. 1–12, 2002.

[11] W. Farhat, R. A. Venditti, M. Hubbe, M. Taha, F. Becquart, and A. Ayoub, "A Review of Water-Resistant Hemicellulose-Based Materials: Processing and Applications,"

ChemSusChem, vol. 10, no. 2, pp. 305–323, 2017.

[12] D. Knappert, H. Grethlein, and A. Converse, "Partial acid hydrolysis of poplar wood as a pretreatment for enzymatic hydrolysis," *Biotechnol Bioengin Symp.* pp. 11–77, 1981.

[13] I. Egües, C. Sanchez, I. Mondragon, and J. Labidi, "Effect of alkaline and autohydrolysis processes on the purity of obtained hemicelluloses from corn stalks," *Bioresour. Technol.*, vol. 103, no. 1, pp. 239–248, 2012.

[14] L. W. Doner and K. B. Hicks, "Isolation of hemicellulose from corn fiber by alkaline hydrogen peroxide extraction," *Cereal Chem.*, vol. 74, no. 2, pp. 176–181, 1997.

[15] I. Hasegawa, K. Tabata, O. Okuma, and K. Mae, "New Pretreatment Methods Combining a Hot Water Treatment and Water / Acetone Extraction for Thermo-Chemical Conversion of Biomass," vol. 45, no. 6, pp. 755–760, 2004.

[16] M. Saska and E. Ozer, "Aqueous extraction of sugarcane bagasse hemicellulose and production of Xylose syrup," *Biotechnol. Bioeng.*, vol. 45, no. 6, pp. 517–523, 1995.

[17] M. Palm and G. Zacchi, "Extraction of hemicellulosic oligosaccharides from spruce using microwave oven or steam treatment," *Biomacromolecules*, vol. 4, no. 3, pp. 617–623, 2003.

[18] S. Azhar, "Extraction of Polymeric Hemicelluloses from Spruce Wood," 2015.

[19] C. Froschauer, M. Hummel, M. Iakovlev, A. Roselli, H. Schottenberger, and H. Sixta, "Separation of hemicellulose and cellulose from wood pulp by means of ionic liquid/cosolvent systems," *Biomacromolecules*, vol. 14, no. 6, pp. 1741–1750, 2013.

[20] N. Mosier *et al.*, "Features of promising technologies for pretreatment of lignocellulosic biomass," *Bioresour. Technol.*, vol. 96, no. 6, pp. 673–686, 2005.

[21] H. Cheng, H. Zhan, S. Fu, and L. a. Lucia, "Alkali extraction of hemicellulose from depithed corn stover and effects on soda-AQ pulping," *BioResources*, vol. 6, no. 1, pp. 196–206, 2011.

[22] J. Puls and B. Saake, "Industrially isolated hemicelluloses," *Hemicellul. Sci. Technol.*, vol. 864, pp. 24–37, 2004.

[23] T. Ehrman, "Determination of acid-soluble lignin in biomass," *Natl. Renew. Energy Lab.*

Tech. Rep. NREL-LAP-004, Golden, CO., 1996.

[24] J. M. Lee, J. Shi, R. A. Venditti, and H. Jameel, "Autohydrolysis pretreatment of Coastal Bermuda grass for increased enzyme hydrolysis," *Bioresour. Technol.*, vol. 100, no. 24, pp. 6434–6441, 2009.

[25] T. Ehrman, "Method for determination of total solids in biomass.," *Lab. Anal. Proced. 001*, 1994.

[26] T. Koshijima, "Weight of Native Hardwood Xylans," vol. 279, no. 11, pp. 265–279, 1965.

[27] D. Lee, V. N. Owens, A. Boe, and P. Jeranyama, "Composition of herbaceous biomass feedstocks," *Cellulose*, no. June, p. 16, 2007.

[28] A. Sunna and G. Antranikian, "Xylanolytic enzymes from fungi and bacteria.," *Crit. Rev. Biotechnol.*, vol. 17, no. 1, pp. 39–67, 1997.

[29] G. Dervilly-Pinel, V. Tran, and L. Saulnier, "Investigation of the distribution of arabinose residues on the xylan backbone of water-soluble arabinoxylans from wheat flour," *Carbohydr. Polym.*, vol. 55, no. 2, pp. 171–177, 2004.

[30] S. N. Sun, T. Q. Yuan, M. F. Li, X. F. Cao, F. Xu, and Q. Y. Liu, "Structural Characterization of Hemicelluloses From Bamboo Culms (Neosinocalamus Affinis)," *Cellul. Chem. Technol. Cellul. Chem. Technol*, vol. 46, pp. 3–4, 2012.

[31] L. Bai, H. Hu, and J. Xu, "Influences of configuration and molecular weight of hemicelluloses on their paper-strengthening effects," *Carbohydr. Polym.*, vol. 88, no. 4, pp. 1258–1263, 2012.

[32] R. Sun, J. M. Lawther, and W. B. Banks, "Fractional and structural characterization of wheat straw hemicelluloses," *Carbohydr. Polym.*, vol. 29, no. 4, pp. 325–331, 1996.

[33] R. C. Sun, J. Tomkinson, P. L. Ma, and S. F. Liang, "Comparative study of hemicelluloses from rice straw by alkali and hydrogen peroxide treatments," *Carbohydr. Polym.*, vol. 42, no. 2, pp. 111–122, 2000.

[34] B. Xiao, X. F. Sun, and R. Sun, "Chemical, structural, and thermal characterizations of alkali-soluble lignins and hemicelluloses, and cellulose from maize stems, rye straw, and

rice straw," *Polym. Degrad. Stab.*, vol. 74, no. 2, pp. 307–319, 2001.

[35] R. C. Sun and J. Tomkinson, "Characterization of hemicelluloses obtained by classical and ultrasonically assisted extractions from wheat straw," *Carbohydr. Polym.*, vol. 50, no. 3, pp. 263–271, 2002.

[36] E. Haimer, M. Wendland, A. Potthast, U. Henniges, T. Rosenau, and F. Liebner, "Controlled precipitation and purification of hemicellulose from DMSO and DMSO/water mixtures by carbon dioxide as anti-solvent," *J. Supercrit. Fluids*, vol. 53, no. 1–3, pp. 121–130, 2010.

[37] L. JON Bood; Nilsson, "Energy Analysis of Hemicellulose Extraction at a Softwood Kraft Pulp Mill," 2013.

[38] Sixta, "Pulp Properties and Applications, Handbook of Pulp, 2, Wiley-VCH." pp. 1022–1067, 2006.

[39] H. Sixta *et al.*, "Novel concepts of dissolving pulp production," *Cellulose*, vol. 20, no. 4, pp. 1547–1561, 2013.

[40] Y. Liu, L. Shi, D. Cheng, and Z. He, "Dissolving Pulp Market and Technologies: Chinese Prospective - A Mini-Review," *BioResources*, vol. 11, no. 3, pp. 1–15, 2016.

Chapter 3. Innovations in the development of hemicellulose coatings and the enhancement of the barrier properties

1. Introduction

Coatings are generally a thin films that are placed on some supplies and materials to improve particular properties such as corrosion resistance, water resistance, and conductivity. These products engineered specifically for their protective and functional properties [1]. Coating materials are used to coat and cover distinct parts, finished assemblies (automobiles, aircraft, and vessels), tanks, piping, metal sheet, pharmaceuticals, wood panels, paper, and paper board. But while protection is their underlying goal, they also can be aesthetic [2][3]. Coatings make up a large market, with hundreds of millions of gallons sold to customer industries per year – calculating to billions of dollars [3]. In fact, the coatings industry in the United State and Western Europe is well established and correlates with the health of the economy, mainly housing, construction, and transportation. Total demand from 2016 to 2021 will increase at average annual rates of 3% in the United States and 2% in Western Europe [4].

The rapid evolution in human civilization and the sharp exhaustion in natural resources are the vital factors driving sustainable and renewable development. Coating industrial sector is invigorated and facilitated from the stages occupied by academia in training the following generation of scientists and engineers towards sustainable evolution and the development of new strategies and technologies. According to the market research report, the worldwide market of environment-friendly coatings in 2012 was estimated at about USD $84 billion and is anticipated to reach USD $117 billion in 2018 [5].

Paper coating resources are numerous compounds that are used to coat the paper in order to improve its glossy appearance, brightness, opacity, ink absorption, and water and grease resistance. Coatings contribute about 10% of the total cost of paper production of which, the binder is the highest cost component in the formulation [6]. Actually, paper coated with waxes, polyolefins and other synthetic materials are difficult to recycle or compost. Natural and biobased polymers have received a great attention in edible coatings for food applications; however, their usage as coatings and films in paper and packaging is relatively recent [7].

The chief types of sustainable binders used today for paper coatings are starch, casein, and soy protein. Of these, the relative consumption on a dry basis circa 2010 was 120 million pounds of starch, 35 million pounds of casein, and approximately 20 million pounds of lattices of all types [8]. Starch was crosslinked to form an efficient paper coating material and a patent was issued in 1970 [9]. Since hemicelluloses are short chain carbohydrate polymers bearing many hydroxyl groups which show a tendency to associate with hydrophilic solvents such as water, hemicelluloses have potential to supply raw materials for the coating industry.

In the current research, a simplified coating composition of hemicellulose as a coating binder material, water and a water-soluble ammonium zirconium (IV) carbonate (AZC) salt was evaluated. The salt is capable of forming coordinate covalent bonds with the free electron pairs of the oxygen atoms of the hemicellulose hydroxyl groups. The zirconium coordinates with the hemicellulose to form gels and upon subsequent drying will be somewhat water resistant. Our results showed that the loading stress required to break an adhesive connection between two paper surfaces was 0.89, 2.02, 2.75, 3.46, and 3.11 (MPa) for 2, 4, 6, 8 and 10 % AZC samples, indicating that up to about 8% AZC crosslinker in the hemicellulose increases the adhesive behavior of the material. In addition, of the use of the material as an adhesive for paper and board is also demonstrated herein. Some other applications may be for coating of lithographic and offset printing labels, wallpaper and board posters, as a strength enhancement in paper, and as adhesives for containers and folding cartons, all of which require a degree of in-solubilization not demonstrated by unmodified polysaccharides.

2. Experimental part

2.1. Preparation of hemicellulose adhesive

Hemicellulose (SWG-HC10, described in chapter 2) and water were added to a round bottom flask at specific ratios to create 3-50 % concentrations of hemicellulose. The mixture was treated with ammonium zirconium (IV) carbonate (AZC, Catalog # 464597, Sigma-Aldrich) at room temperature for 30 min under continuous agitation to perform crosslinking. The percentage of AZC to hemicellulose ranged from 0-20% wt/wt basis of solids. The pH of the prepared solution was about 8-9. This procedure produced a viscous hydrogel with a slight yellow color, somewhat clear at low concentrations and opaque at the higher concentrations of hemicellulose.

2.2. Coated paper testing

To test the coating performance, the gel/paste was smoothed over the wire side of an uncoated free sheet (Bristol office paper, basis weight of 150 g/m^2) with a manual coating rod. A number 24 wire wound coating rod (wire diameter of 0.61 mm) was used to produce a wet coating film of approximately 61 microns expected thickness. The coating formulation was manually metered onto the wire side of the sheet and then coated with the rod. The coating formulations included different combinations of hemicellulose crosslinked and uncrosslinked with different levels of AZC and water. After coating the samples were allowed to air dry overnight.

The gloss that represent the optical property of specular reflection from the surface was tested according to Tappi Method T480, 75 degrees

Parker Print Surface roughness which measures the average surface roughness based on air leakage at the surface pressed against a metal cylinder (PPS, 1.0 MPa) were tested according to TAPPI procedures prior to performing the Hercules Size Test (HST) (Hercules Size Test indicating the water resistance of a paper substrate).

The viscosity of the hemicellulose material was measured using a Brookfield cone-plate viscometer; model LVT, spindle#2 at 30 rpm, 25°C (ASTM Method D 2196-81).

3. Results and discussion

As a crosslinking agent, ammonium zirconium (IV) carbonate (AZC) can react with polymers containing hydroxyl groups and carboxylic groups (Figure 1). Similarly, with relatively large number of hydroxyl groups in its molecule, self-assembly of AZC molecules can also occur. Therefore, in a one-component system of AZC solutions, AZC self-crosslinking can occur. In a two-component system of AZC hemicellulose blends, both AZC self-crosslinking and AZC-hemicellulose co-crosslinking exist and may compete with each other.

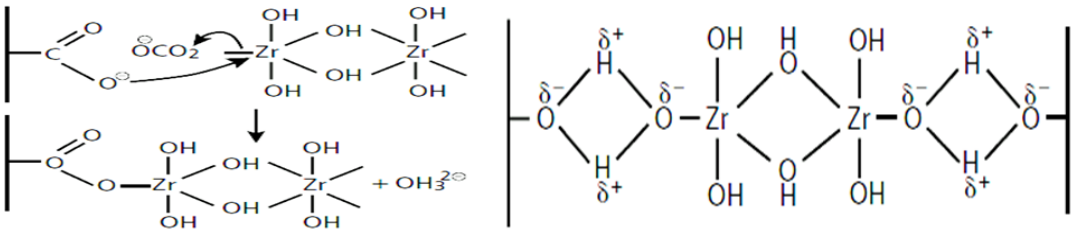

Figure 1. Interaction between zirconium and the carboxylic and free hydroxyl groups of hemicellulose

Figure 2 shows different samples of the hemicellulose-zirconium in inverted vials all with 23% total solids level. It can be clearly observed the formation of continuous film with 5-10% AZC which can be used as coating material. The AZC significantly causes a gel to form and increases the viscosity of the material. The hemicellulose viscosity of the coating formulation increased with the increase in the concentration AZC in the range of 0 to 10% AZC levels, Table 1. The measured viscosity was lower at 20% AZC, probably due to the agglomeration of the material interfering with the viscosity measurement. The increased viscosity at 5 and 10% AZC also endowed the coating formulation with better shear flow characteristics during the lab based rod coating, producing a smoother well distributed coating surface. The material at 20% AZC did not form a continuous film but formed an irregular suspension of solid granules that could not be used as a coating material, Figure 2.

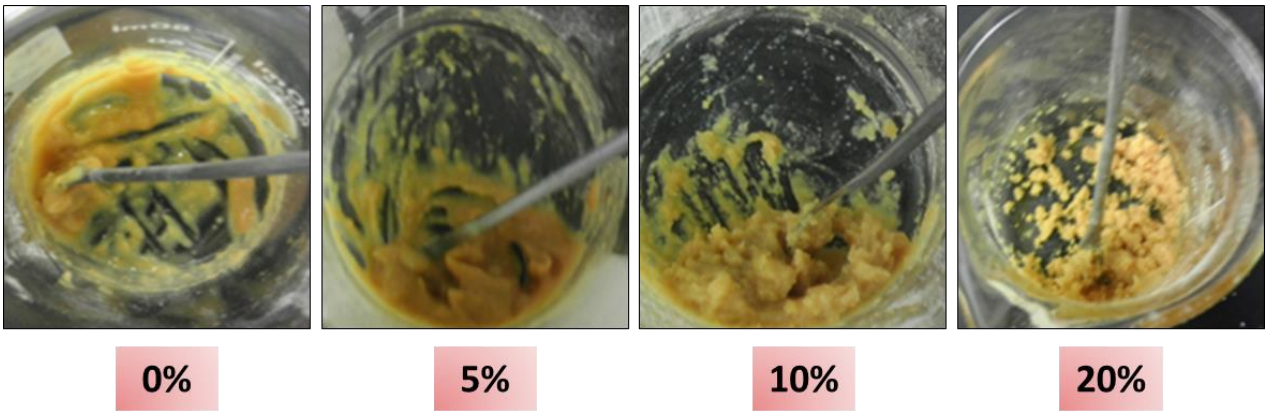

Figure 2. Hemicellulose-AZC materials at different AZC levels (indicated under the image) with a total solids level of 23% in all cases. At the AZC level of 20% the materials becomes unsuitable as a coating due to the formation of elastic agglomerates.

Several % solids levels of the hemicellulose-AZC were evaluated with manual coating trials. A quantity of about 23% solids content was determined to be optimal for spreading the gel onto the surface of the paper. The addition of hemicellulose with no AZC cross-linker was shown to increase the gloss, smoothness, and water resistance of the paper surface relative to the uncoated sheet, Table 5. The presence of AZC in the coating improved the paper gloss, smoothness and liquid resistance at the 5% and 10% AZC levels relative to the uncoated sheet. The 10% AZC level did not appreciably improve the coating properties over the 5% level. As stated above the coating distribution and properties of the 20% AZC material were very poor.

Table 1. Properties of hemicellulose gels and the resulting coatings. HST stands for Hercules Size Test with larger numbers indicating more water resistance. (*) Lower viscosity attributed to agglomeration and poor dispersion of the gel. (n/d) not determined.

	Uncoated Sheet	0% AZC	5% AZC	10% AZC	20% AZC
Viscosity (MPa.s)	n/d	n/d	1000	1270	620*
Gloss (%)	9.0	21.1	30.6	15.2	n/d
PPS roughness (um)	18.0	8.6	7.5	11.0	n/d
HST (seconds)	1950	2260	2680	2810	n/d

Adhesive strength was measured by applying the hemicellulose-zirconium materials in gel form to a 1 cm^2 area of a linerboard strip and then placing another strip on top of the coated area. The strips were manually pressed and then dried overnight. The loading stress required to break the adhesive connection was 0.89, 2.02, 2.75, 3.46, and 3.11 (MPa) for 2, 4, 6, 8 and 10 % AZC samples, indicating that up to about 8% AZC increases the adhesive behavior of the material. There is a need to further quantify and optimize the adhesive properties of the hemicellulose-AZC material.

4. Conclusion

A new hemicellulose based coating/adhesive was prepared by mixing hemicelluloses, ammonium zirconium carbonate and water. The prepared crosslinked hemicelluloses coating/adhesive showed a significantly improved coating/binder effect when the ammonium zirconium carbonate gel was about 5-10 % by weight of the hemicellulose. Also, the loading stress required to break an adhesive connection between two paper surfaces was 0.89, 2.02, 2.75, 3.46, and 3.11 (MPa) for 2, 4, 6, 8 and 10 % AZC samples, indicating that up to about 8% AZC crosslinker in the hemicellulose increases the adhesive behavior of the material. The modified hemicellulose coating improved the paper surface in terms of smoothness, gloss, and liquid penetration resistance. The hemicellulose crosslinked with the ammonium zirconium carbonate has a good potential for coating and adhesive applications and may be an important higher valued byproduct for the paper or biofuel industries.

References

[1] P. a. Schweitzer, *Paint and Coatings: Applications and Corrosion Resistance*. 2006.

[2] G. Banker, “Film coating theory and practice,” *J. Pharm. Sci.*, vol. 12, pp. 325–334, 1966.

[3] D. K. Chattopadhyay and K. V. S. N. Raju, “Structural engineering of polyurethane coatings for high performance applications,” *Prog. Polym. Sci.*, vol. 32, no. 3, pp. 352–418, 2007.

[4] IHS Markit, “Paint and Coatings Industry Overview - Chemical Economics Handbook (CEH) | IHS.” 2017.

[5] A. Tiwari, “Anticorrosion Coating Industry Transitioning to Sustainable Development.” 2017.

[6] R. Anthony, Z. Xiang, and T. Runge, “Paper coating performance of hemicellulose-rich natural polymer from distiller’s grains,” *Prog. Org. Coatings*, vol. 89, pp. 240–245, 2015.

[7] C. Aulin and L. Tom, *Biopolymer Coatings for Paper and Paperboard*. 2011.

[8] H. H. Murray and J. E. Kogel, “Engineered clay products for the paper industry,” *Appl. Clay Sci.*, vol. 29, no. 3–4, pp. 199–206, 2005.

[9] D. L. Wilhelm, “Amylose starch-based corrugating adhesive." U.S. Patent No. 3,532,648.,” no. 1, 1970.

Chapter 4. A green technology for hemicellulose processing: Bio-based hydrogels produced by reactive extrusion process.

1. Introduction

There is an increasing trend towards the utilization of sustainable and renewable resources. [1][2]. Biomass, has been widely used in many disciplines, and converted into a wide range of marketable products such as fuel, chemicals, paper, plastics, and pharmaceutical products [3][4]. Biomass is divided into two categories, first and second generation. In the former, they are edible biomass based-products mostly composed of starch-rich plants [6]. Starch is a food based product and its wide industrial applications may lead to issues including food shortages and increased pressure on the current crops growth with possible food price increases. Societies increased demands on food systems has caused many to look for non food replacements for starch, such as second–generation biomass, which consists of residual non-food parts of the current crops or other non-food sources such as forest resources. These materials include cellulose, hemicelluloses and lignin [6], available in massive quantities.

One application of natural polymers are as hydrogels which are crosslinked polymeric networks that are capable of absorbing large volumes of water or biological fluids in a short time and can retain the absorbed fluid even under heating or some pressure [7]. The presence of hydrophilic groups such as –OH, –CONH–, –COOH, $–CONH_2$, and $–SO_3H$ in polymers forming hydrogels stems from their affinity to absorb water [8]. In 1926, Dorothy Jordan Lloyd have defined hydrogel as “the colloidal condition, the gel, is one which is easier to recognize than to define”[9]. This definition was raised because hydrogels owes certain solids and liquids properties. Indeed, as solids they don’t flow and as liquids they allow the diffusion of small molecules.

However, nowadays, hydrogels are viewed as a smart and stimulus responsive materials that changes their swelling property in response to environmental changes (pH, temperature and ionic strength)[10]. For instance, the presence of solutes depresses the thermodynamic activity of water which is linked to polymer swelling [11][12].

Hydrogels have been used in several applications that include; hygiene (disposable diapers and feminine care products), agriculture (water retention, and pesticide delivery), biomedical materials (drug carriers, wound dressings, and tissue engineering scaffolds), biosensors and others [13]. The hydrogels used in drug delivery systems are of great interest because they are able to alter their volume in response to environmental stimuli expeditiously [14][15]. Biopolymers, including starch, proteins, gelatin, hemicelluloses, lignin, cellulose, and their derivatives have been copolymerized or blended with other synthetic polymers to create composites that can be used to manufacture bio-polymer based hydrogels [16][17][18].

Reactive extrusion is a technique known to be exploited by plastics industry to mix polymer formulations to obtain thermoplastic materials. It is known to be suitable for many reactions, including polymerization and grafting as a continuous and solvent-free process. This technique allows the material processing to be performed at a flexible scale without the need for solvents. Native bio-polymers typically cannot be processed by the reactive extrusion due to the strong hydrogen bonds between the polymeric chains at the inter and intra molecular levels [19]. Several substances have been used as a plasticizer for bio-based polymers including: citric acid, glycerol, sorbitol, urea and others [19][20]. The presence of plasticizer can facilitate the reactive extrusion processes and thus, enables the biomass processing and modification with great advantages in scalability.

For instance, citric acid (CA) is a multi-carboxylic structure with three carboxyl and one hydroxyl groups. CA is produced mainly by the fermentation of some carbohydrates and is generated as a nontoxic metabolic product of the body in all living cells that use oxygen as part of cellular respiration. The carboxylic groups of CA can esterify the hydroxyl groups of biopolymers and at the same time crosslink the polymers [21]. According to several studies, the structure of CA dictates its functions: as a plasticizer, crosslinking agent, and/or hydrolytic agent [21][22]. Although the crosslinking reaction of a biopolymer with CA can take place at high temperature,

the presence of a catalyst, an example being sodium hypophosphite (SHP), is essential for the reaction to proceed rapidly to achieve a highly esterified crosslinked material [23][24].

In this research, we have developed biodegradable hydrogels based on the biological macromolecules, starch, lignin and hemicellulose by reactive extrusion. To our knowledge, this is the first report of the development of drug delivery hydrogels by reactive extrusion from these macromolecules. The natural polymers were plasticized and crosslinked by CA in the presence and absence of SHP as a catalyst. The present investigation was aimed to focus on the basic differences between the first and second generation biomasses as a drug delivery system. The bio-based hydrogels were characterized for their processing conditions and the influence of CA on the polymer forming hydrogels during the reaction was determined. The dynamic swelling of the resulting gels were studied at different pH in buffer solutions and the types of water-transport mechanisms were analyzed. Also, the hydrogel degradation at physiological condition was determined over a period of 15 days and the effect of the degradation on the mechanical properties were examined. Interesting hydrogels were produced from all three biopolymers with good potential as drug delivery systems.

2. Experimental part

2.1. Materials

Commercially available unmodified corn starch was provided from Cargill, USA (CAS: 9005-25-8), Kraft lignin (SWKL - Indulin AT™, Westvaco), hemicellulose extracted from bleached hardwood pulp (HW-HC10) as described in chapter 2 , citric acid monohydrate granular was obtained from Mallinckrodt chemicals (CAS 5949-29-1) and sodium hypophosphite monohydrate (CAS 10039-56-2) was obtained from Sigma-Aldrich.

2.2.Hydrogel preparation by reactive extrusion

Hydrogels were synthesized based on the three different natural polymers, starch, lignin, and hemicellulose. The hydrogels were prepared using a micro-extruder (Xplore, Micro 15cc Twin Screw Compounder). The extruder feed is open to atmosphere and the outlet pressure is not measured; there is a recirculation line in the extruder. Several formulations were prepared by varying the CA contents from 20 to 200% (wt CA:wt polymer). Also SHP was included in some formulations, when included it was 20% relative to CA content in the desired formulation (wt SHP:wt CA). The residence time in the extruder was either 2 or 5 min of recirculation, and a screw rotation speed of 120 rpm was used. The twin-screw extruder was maintained at a temperature of 120°C. (Thermogravimetric analysis showed no degradation of the carbohydrates and lignin at 120°C.) The formulations are listed in Table 1 and the extrusion process is illustrated in Figure 1.

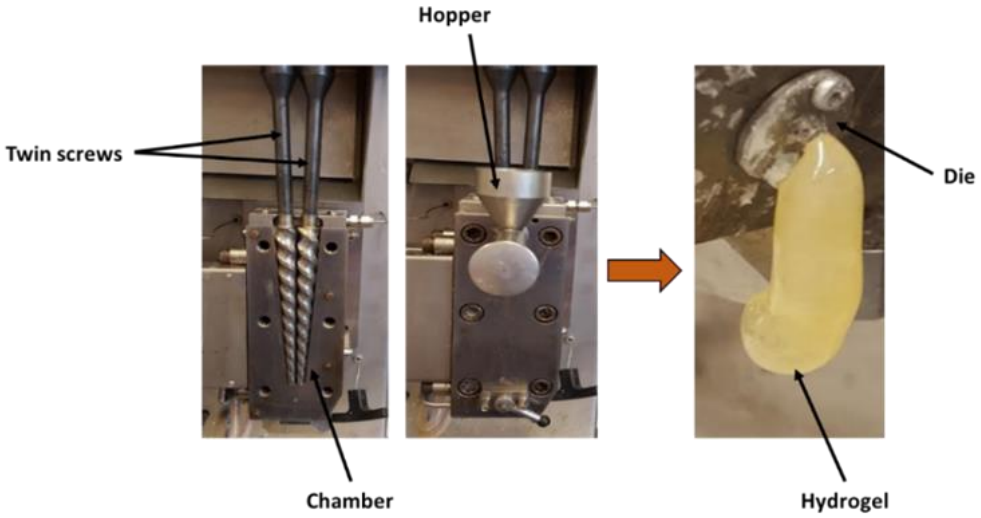

Figure 1. Illustration of the extrusion process. The inset images show the cross-section and assembled views of micro-scale twin-extruder

Table 1: Parameters used to optimize the extrusion and formulation of biopolymer-citric acid materials. (n/a) not applicable and (+[a]) presence of SHP in 20% by weight of CA. ([b])Weight percentage relative to starch, lignin and hemicellulose. (√) the material extruded and (x) the material did not extrude.

Sample	Starch (g)	Lignin (g)	Hemicellulose (g)	Citric acid (wt%)[b]	SHP (wt%)	Residence time (min)	Torque (N)	Extrude
S-CA20-2	50	n/a	n/a	20	n/a	2	5300	x
S-CA40-2	50	n/a	n/a	40	n/a	2	1000	✓
S-CA40-5	50	n/a	n/a	40	n/a	5	1290	✓
S-CA60-2	50	n/a	n/a	60	n/a	2	190	✓
S-CA60-5	50	n/a	n/a	60	n/a	5	580	✓
S-CA80-2	50	n/a	n/a	80	n/a	2	80	✓
S-CA80-5	50	n/a	n/a	80	n/a	5	310	✓
S-CA100-2	50	n/a	n/a	100	n/a	2	55	✓
S-CA100-5	50	n/a	n/a	100	n/a	5	190	✓
S-CA40-s-2	50	n/a	n/a	40	+[a]	2	2170	✓
S-CA40-s-5	50	n/a	n/a	40	+[a]	5	2200	✓
S-CA60-s-2	50	n/a	n/a	60	+[a]	2	620	✓
S-CA60-s-5	50	n/a	n/a	60	+[a]	5	1000	✓
S-CA80-s-2	50	n/a	n/a	80	+[a]	2	550	✓
S-CA80-s-5	50	n/a	n/a	80	+[a]	5	760	✓
S-CA100-s-2	50	n/a	n/a	100	+[a]	2	110	✓
S-CA100-s-5	50	n/a	n/a	100	+[a]	5	110	✓
L-CA20-2	n/a	50	n/a	20	n/a	2	5800	x
L-CA40-2	n/a	50	n/a	40	n/a	2	4700	x
L-CA60-2	n/a	50	n/a	60	n/a	2	3200	✓
L-CA60-5	n/a	50	n/a	60	n/a	5	3900	✓
L-CA80-2	n/a	50	n/a	80	n/a	2	1700	✓
L-CA80-5	n/a	50	n/a	80	n/a	5	2450	✓
L-CA100-2	n/a	50	n/a	100	n/a	2	1400	✓
L-CA100-5	n/a	50	n/a	100	n/a	5	1670	✓
L-CA60-s-s	n/a	50	n/a	60	+[a]	2	5450	x
L-CA80-s-2	n/a	50	n/a	80	+[a]	2	5100	x
L-CA100-s-2	n/a	50	n/a	100	+[a]	2	4920	x
HC-CA20-2	n/a	n/a	50	20	n/a	2	7500	x
HC-CA-40-2	n/a	n/a	50	40	n/a	2	7400	x
HC-CA60-2	n/a	n/a	50	60	n/a	2	6950	x
HC-CA80-2	n/a	n/a	50	80	n/a	2	6950	x
HC-CA100-2	n/a	n/a	50	100	n/a	2	6600	x
HC-CA150-2	n/a	n/a	50	150	n/a	2	3800	✓
HC-CA150-5	n/a	n/a	50	150	n/a	5	4800	x
HC-CA200-2	n/a	n/a	50	200	n/a	2	2100	✓
HC-CA200-5	n/a	n/a	50	200	n/a	5	3000	✓
HC-CA200-s-2	n/a	n/a	50	200	+[a]	2	3600	✓
HC-CA200-s-5	n/a	n/a	50	200	+[a]	5	4860	x

2.3.Characterization

FTIR analysis were performed on the samples from 4000 to 650 cm^{-1}, with a spectral resolution of 4 cm^{-1}. The spectra were recorded on a single reflection attenuated total reflectance (ATR) FTIR technique performed by a Platinum ATR Alpha instrument with 40 scans. The samples were washed with copious amounts of water to remove unreacted citric acid and SHP prior to FTIR analysis.

The carboxyl content can be determined after excessive washing of the material with water to remove unreacted citric acid and SHP. Acid–base titrations were used to determine the carboxyl content of the absorbent materials, a known amount of synthesized product was dissolved in excess 0.1 N NaOH (pH 12.5) and was allowed to react with the sample for 1 h. The remaining excess amount of NaOH was determined by titration with 0.1 N HCl using phenolphthalein as an indicator. The carboxyl content in milliequivalents of acidity per 100 g is calculated as:

$$\text{Carboxyl Content} = \frac{(\mathrm{V}_b - \mathrm{V}_a) \times N}{\mathrm{W}} \times 100$$

Where, N is the HCL normality (eq/L), V_b = Volume of HCL without sample (mL), V_a = Volume of HCl in the presence of sample (mL), W = Weight of sample (g)

The degree of esterification and degree of substitution were determined by first dissolving the product in DMSO in a conical flask for 12 h, and then adding an excess of 0.3 N NaOH to the solution to saponify the ester for 2 h. The excess NaOH was determined by titration with calibrated HCL to determine the percent esterification and the degree of substitution [25].

$$\text{Degree of esterification} = \frac{6.005(V_b - \mathrm{V}_a) \times H}{\mathrm{W}} \times 100$$

Where, H = Normality of HCL (eq/L), V_b = Volume of HCL without sample (mL), V_a = Volume of HCl in presence of sample (mL), W = Weight of sample (g).

$$\text{Degree of substitution} = \frac{162 \times E(\%)}{(100 \times \text{M}) - [(\text{M} - 1) \times E(\%)]}$$

Where, E (%) = Degree of Esterification, M = Molecular weight of crosslinking agent (Citric acid 192.124 g/mole)

2.4.Swelling behavior

Dried hydrogels were left to swell within a permeable plastic fine mesh specimen holder in 10 ml buffer solutions (Titrisol, Merck) of different pH: 4, 6, 7.4, 8 and 9 at 37°C. Swollen gels inside the specimen holder were removed from the buffer solution at regular intervals blotted on filter paper, weighed and then replaced in the solution. Measurements were taken until equilibrium hydration degree was reached. The percentage swelling at time (t), W_t (%) and at equilibrium, W_{eq} (%), was calculated from the following equation:

$$W_t(\%) = \frac{M_t - M_0}{M_0} \times 100$$

$$W_{eq}(\%) = \frac{M_f - M_0}{M_0} \times 100$$

Where M_0 is the mass of the dry sample, M_t is the mass of the swollen gel at time (t) and M_f is the final mass of the swollen gel at equilibrium of the immersion.

2.5.Hydrogels degradation study

The degradation of the materials was studied by immersing about 3 g of the sample within a permeable plastic fine mesh specimen holder in 100 ml of physiological isotonic solution (0.154 M NaCl aqueous solution at pH 7.4) and mass loss versus time determined. Prior to the immersion the materials were conditioned to the minimum weight at 37°C in an oven with desiccant. Samples were removed at regular intervals, 1, 3, 5, 8, 12 and 15 days, being taken out of the solution, blotted on filter paper to remove excess solution on the surface, weighed and then dried in an oven to 60°C to constant weight in order to determine weight loss, taking an average of three readings. The weight loss of the material in water and saline solution was determined according to the following:

$$\%\, Weight\ Loss = \frac{W_i - W_f}{W_i} \times 100$$

Where W_f is the final dry sample weight and W_i is the initial dry sample weight

2.5. Dynamic Mechanical Analysis (DMA)

The DMA was used for characterizing the mechanical properties of the materials in wet conditions. Compression tests were performed on the hydrogels at 37°C with DMA Model 2980 (TA, Inc., New Castle, DE, U.S.A.). Cylindrical disks with a radius of 5 mm and thickness of 8 mm were cut from the gel layers. The hydrated samples were placed in between two metal, parallel plates and lubricated with dodecane to prevent drying and barreling. Each sample was preloaded to 0.005 N, which was followed by a strain sweep. Dynamic mechanical analysis was carried out at nominal compressive strain amplitudes ranging from 1% to 12% and at a frequency of 1 Hz.

3. Results and discussion

3.1. Hydrogels formation and extrusion process

Evaluation of the different compositions was performed by monitoring the extrusion process, with the extrusion torque reading reflecting the extrudability of the starch, lignin and hemicellulose materials in the presence of CA and with and without catalyst, Table 1 and Figure 2. Citric acid has been reported to have a glass transition temperature of 11°C [28], which we have confirmed using DSC for the CA used in this study (data not shown), much lower than the glass transition temperature of lignin (185°C), starch (190°C), and hemicellulose (144°C). Thus, when mixed, the system T_g of CA and the biopolymers is expected to be lower than that of the biopolymer. In fact, DSC experiments on simple mixtures of CA with biopolymers showed a reduction in the T_g of the biopolymer with increased amounts of CA.

Samples without CA would not extrude, reflected by a high torque above 6500 N. This behavior is due to the excessive H-bonding between the entangled polymeric chains. The increase in CA concentration induces a reduction in the extrusion torque for the three natural polymers. This decrease in the extruder torque varies between the biopolymers mainly due to structural and molecular weight differences between the biopolymers. Actually, starch shows the best processing with the increase of CA concentration to reach 50 N when the CA concentration was 100% compared to 1300 N for lignin and 6550 N for hemicellulose at the same CA concentration. However, hemicellulose was not able to be extruded until the CA concentration reached 150% and above.

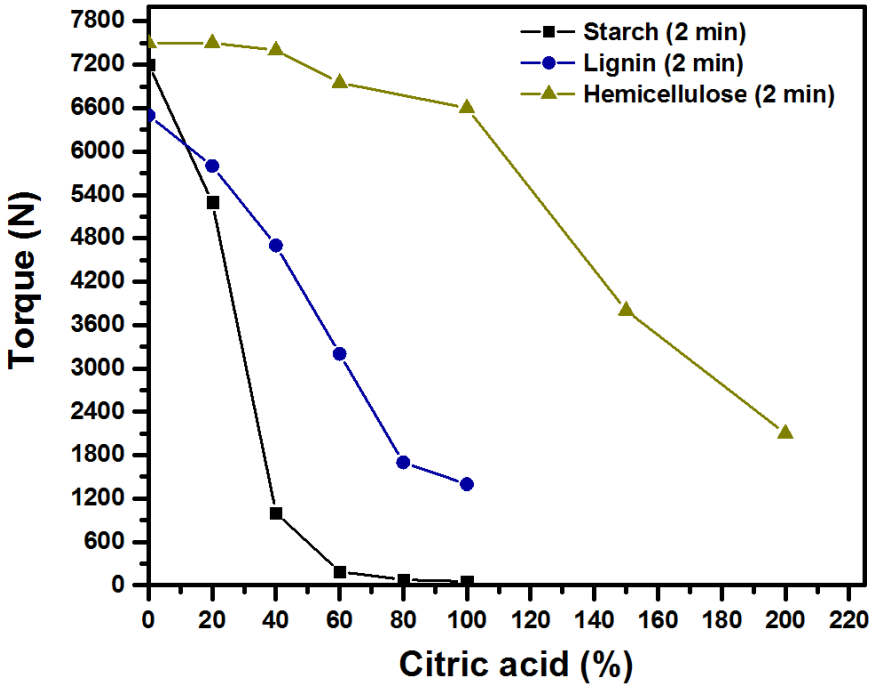

Figure 2. Effect of plasticizer concentration on the torque required in a twin screw extruder at 120 RPM after 2 minutes at 120 ºC.

The ease of starch extrusion compared to lignin and hemicelluloses arises from being a semi-crystalline polymer with a fraction of crystalline regions not disrupted during extrusion. In contrast, branched, highly crosslinked lignin and branched amorphous hemicellulose had no crystalline regions and had higher viscosity.

Furthermore, as it is indicated in Table 1, not only does the CA concentration determine the feasibility of the extrusion, but also the residence time of the macromolecules in the extruder and the presence of SHP catalyst have a significant effect. The increase in the residence time from 2 to 5 min as well as the presence of SHP may increase the crosslinking yield in the extruder and thus crosslinking will increase the viscosity and generate a thermosetting material that cannot be processed in the extruder (Table 1).

As depicted in Figure 3, heating of CA triggers the formation of reactive anhydride with the release of one water molecule. This anhydride can react with the hydroxyl group of the biopolymer resulting in the formation of monoester polymer with citric acid grafted on the biopolymer. With further heating, another water molecule will be released to form a polymer grafted anhydride. This

can react with another biopolymer to generate a crosslink between polymeric chains. Other research has proposed that SHP can serve as a catalyst for the reaction of biopolymers and citric acid [29][30]. According to that research, in addition to being a catalyst, SHP can be considered an electrophilic agent, making a bridge between one molecule of biopolymer citrate and another molecule of native polymer, making crosslinks. In this case, SHP is considered to be a reactant, not a catalyst (Figure 3) [29][30].

In fact, the extruded materials were referred herein as crosslinked hydrogels. It is understood that some materials that behave like rubbers, without evident flowing at room temperature, are also known as crosslinked materials. All the materials synthesized by reactive extrusion herein were flowing in the extruder. Consequently, all the polymer chains were not chemically crosslinked. By both the chosen strategy and processing, CA first acts as a plasticizer and then as a crosslinking agent by its functionality. To be compatible with the extrusion process, the rates of reaction by the trifunctional CA must not reach the gelation as defined by the Flory and Stockmeyer theory. The reaction was stopped with possible microgels formation but prior the gelation. Despite that, the materials behave globally like gels at room temperature. One very possible reason for this is the presence of strong inter-chain hydrogen bonds at room temperature that can exist after the chemical modification, which are strong enough to produce this gel behavior with physical interactions well described in colloids with hydroxylated polymers but are not by a chemical crosslinking that could be expected with high CA conversion rates.

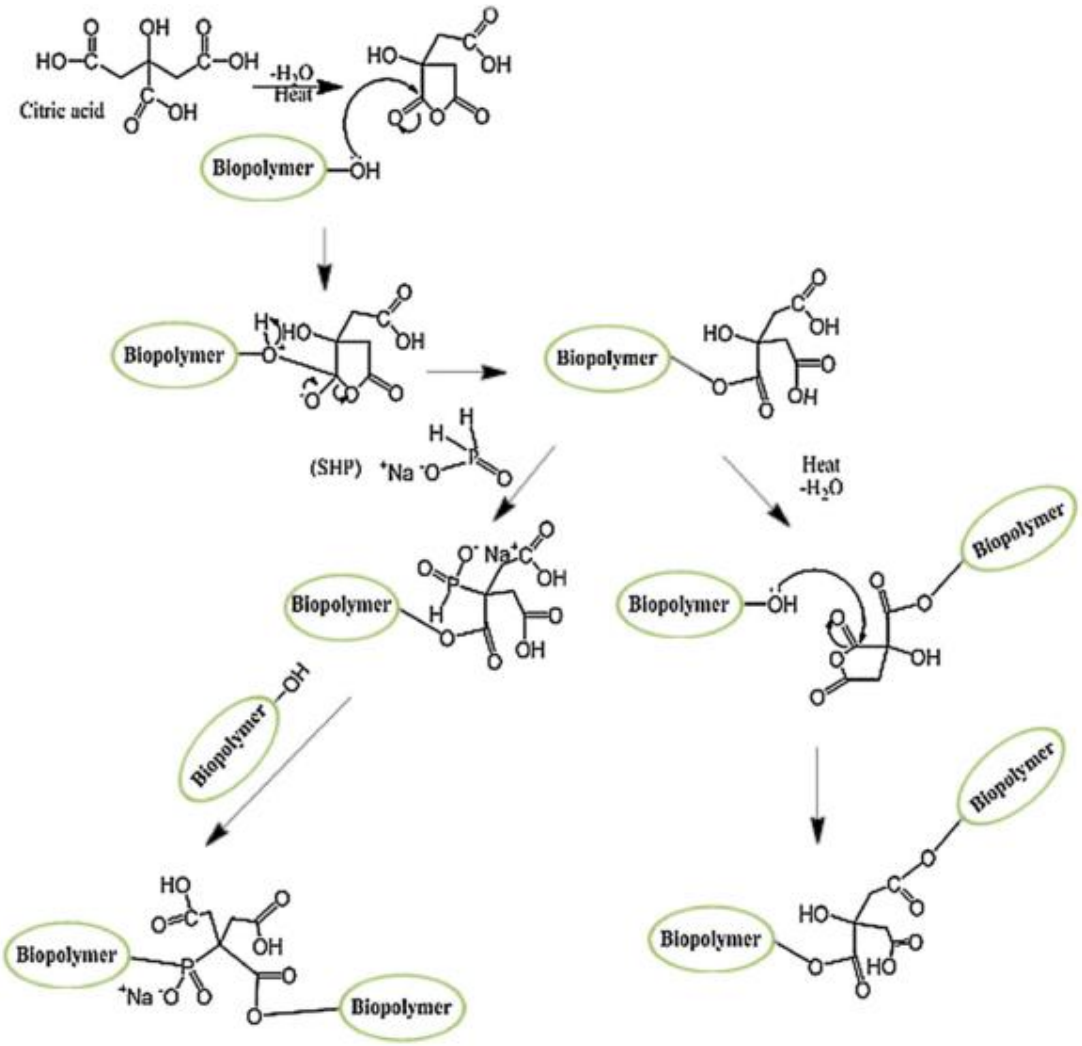

Figure 3. Schematic representation of the reaction of biopolymer with citric acid in the presence and absence of SHP.

3.2. Hydrogels characterization

In order to investigate the occurrence of those reactions, FT-IR analysis for the different materials was performed and shown in Figure 4. The FT-IR analysis indicated the same peaks between thoroughly washed control samples and the extruded materials, except for an additional peak at around 1718 cm^{-1} attributed to the stretching band of the carboxyl and ester carbonyl bands [24], indicative of a reaction of citric acid with the biopolymer. All samples have a broad band at about

3100–3500 cm^{-1} which is attributed to a stretching vibration of OH. The absorption peaks at 1145 cm^{-1} are attributed to asymmetric stretching of C–O–C bridge and the 995 cm^{-1}attributed to C–O stretching. Aromatic ring bands and C-H deformation of lignin and lignin based hydrogels are between 1506 and 1450 cm^{-1}. The carbonyl at 1718 cm^{-1} peak intensity increased qualitatively when SHP was added, indicating more carbonyl groups are formed. Indeed it can be observed that the peak at 3350cm^{-1} decreases qualitatively in the presence of CA and SHP compared to the natural polymers, indicating the conversion of hydroxyl to esters.

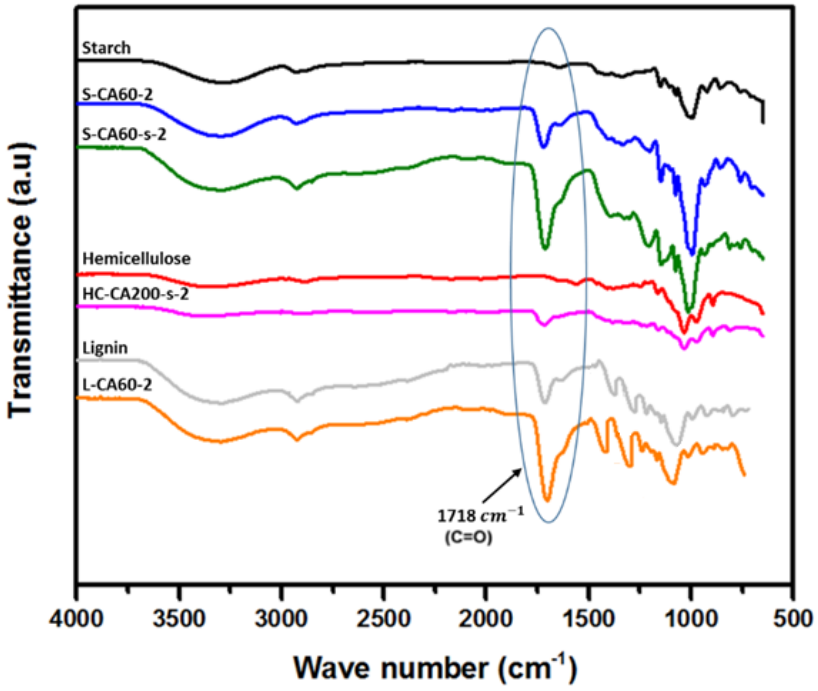

Figure 4. FTIR spectra of the extruded samples

Furthermore, CA increases the carboxyl content, degree of esterification and degree of substitution of the extruded materials compared to the native biopolymers (Table 2). The carboxyl content and degree of substitution was further increased with the presence of SHP and with the increase in the residence time in the extruder.

Table 2: Characteristics of the Extruded Hydrogels

Sample	Sample Color	Carboxyl Content (meq/100g)	Degree of esterification	Degree of substitution
Starch	White	n/a	n/a	n/a
S-CA40-2	White	410	38.3	0.52
S-CA40-5	Yellow	435	39.0	0.54
S-CA60-2	White	580	39.5	0.55
S-CA60-5	Yellow	607	42.6	0.62
S-CA80-2	Yellow	600	43.4	0.64
S-CA80-5	Yellow	655	46	0.72
S-CA100-2	Yellow	692	46.7	0.74
S-CA100-5	Yellow	740	47.8	0.77
S-CA40-s-2	Yellow	525	42	0.61
S-CA40-s-5	Yellow	570	45.3	0.70
S-CA60-s-2	Yellow	746	48.7	0.80
S-CA60-s-5	Yellow	825	49.9	0.84
S-CA80-s-2	Yellow	838	50.6	0.86
S-CA80-s-5	Yellow	864	52.2	0.92
S-CA100-s-2	Yellow	916	52.8	0.94
S-CA100-s-5	Yellow	995	54.2	0.99
Lignin	Dark Brown	20	n/a	n/a
L-CA60-2	Dark Brown	302	26	0.30
L-CA60-5	Dark Brown	355	28	0.33
L-CA80-2	Dark Brown	340	27.5	0.32
L-CA80-5	Dark Brown	400	30.2	0.36
L-CA100-2	Dark Brown	384	30.2	0.36
L-CA100-5	Dark Brown	432	30.9	0.38
Hemicellulose	White	220	n/a	n/a
HC-CA150-2	Orange	470	45.4	0.70
HC-CA200-2	Orange	506	46.8	0.74
HC-CA200-5	Orange	580	48.5	0.79
HC-CA200-s-2	Orange	594	49.2	0.81

The extruded materials had a darker color than the native carbohydrates. This is expected since crystals of citric acid change from white to orange upon heating to 120 ºC. CA can react with all three hydroxyl groups in the anhydroglucose monomer of starch and with two hydroxyl groups in the xylose monomer of hemicellulose. However, due to its complex structure the reaction of CA with lignin varies depending on the mono-lignol residues of the lignin. The esterification reaction between the biopolymers and CA could result in CA mono-, di-, and tri-esters in case of starch, mono- and di-esters in case of hemicelluloses. Lignin has a rich quantity of –OH and is known to

have about 0.8–11 µmol/mg of reactive functional groups [31]. As shown in Table 2 and Figure 5 the carboxyl content increases with the increase of CA concentration. The carboxyl content increases from 410 to 692 mequ/100g for 40% charge of CA (S-CA40-2) and 100% charge of CA (S-CA100-2), respectively. The presence of SHP induces an increase in the carboxyl content compared to CA alone, for example, the 692 mequ/100g the in case of S-CA100-2 increases to 916 mequ/100g in the case of S-CA100-s-2 due to SHP present in the latter sample.

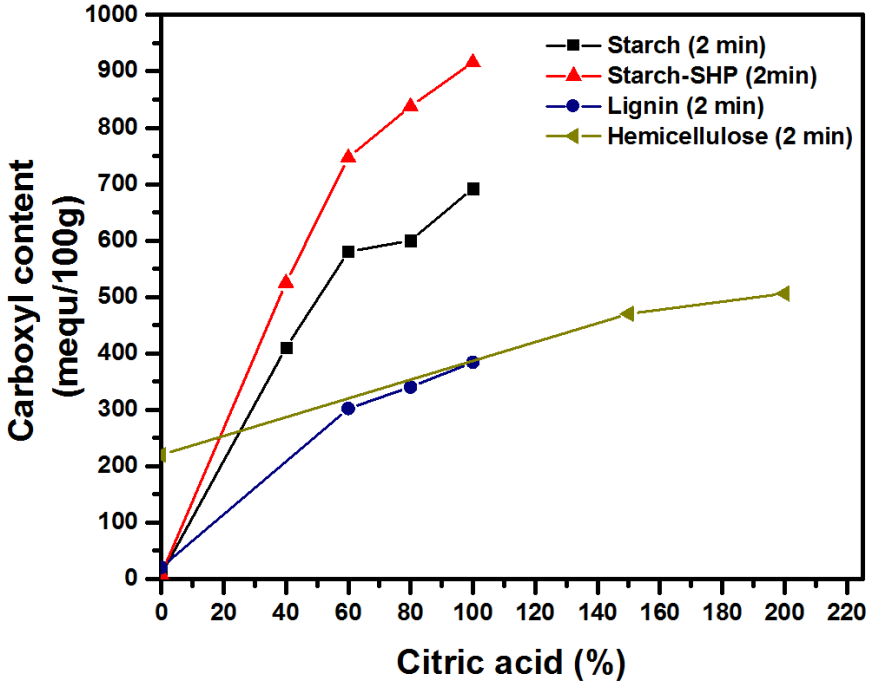

Figure 5. The effect of CA concentration and SHP on the carboxyl content as measured by titration of the three extruded biopolymers

In addition, the residence time induces a significant increase in the carboxyl content, Table 2. The starch carboxyl content shows a higher increase than hemicellulose, presumably due to its tri-functional repeat unit (versus di-functional hemicellulose) and the increasing amount of starch that is swollen and solubilized in the reaction media with time. Hemicellulose, as a non-crystalline lower molecular weight material is not expected to increase its solubility over extrusion time.

Moreover, Table 2 and Figure 6 indicated that the degree of esterification as well as the degree of substitution as measured with titrations, increase with the same trend as the carboxyl content for the three biological macromolecules.

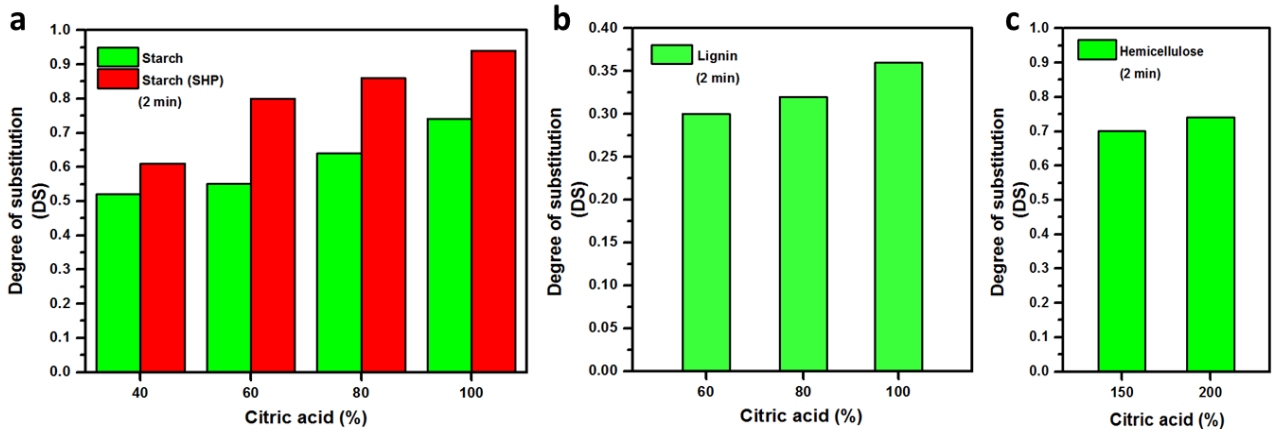

Figure 6. The effect of CA concentration and SHP on the degree of substitution of the three extruded biopolymers. (a) The increase in CA (%) and the presence of SHP increases the DS of starch, (b) and (c) the increase in CA (%) increases the DS of lignin and hemicellulose, respectively.

3.3. Swelling behaviors of the hydrogels

The swelling behavior is a very important characteristic for polymeric systems in biomedical applications as a device for drug release. The swelling capability is a vital indicator of the hydrogel crosslinking density and its internal structure, indicating the quantity of absorbed water in the hydrogel system. The water uptake of the hydrogels was determined for a pH range from 4 to 9 and temperature of 37°C, similar to physiological conditions. The majority of the samples attained the equilibrium hydration degree in 5 h post immersion at the studied pH ranges (Figure 7 indicates the swelling vs time at pH 9).

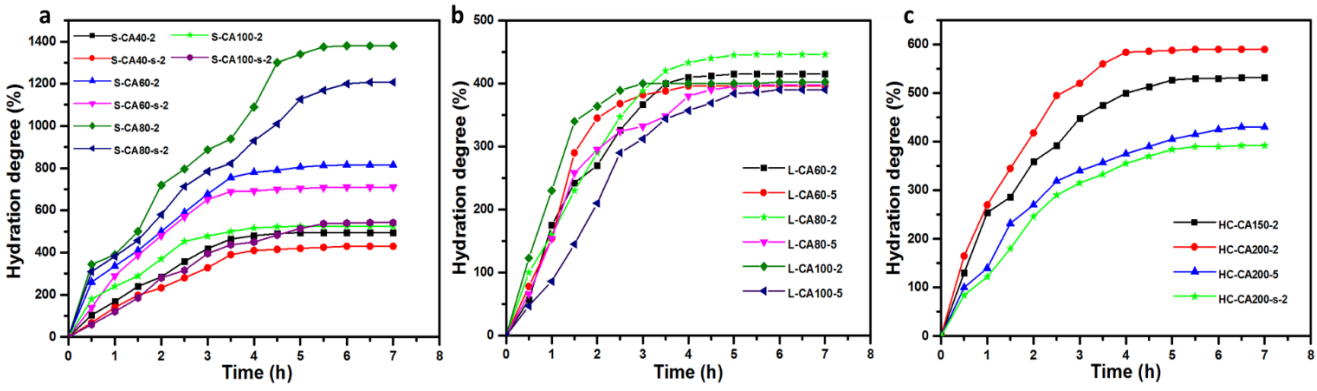

Figure 7. Swelling behavior of the prepared hydrogels 37°C and pH 9: (a) Starch based hydrogels (b) Lignin based hydrogels and (c) Hemicellulose based hydrogels

The equilibrium hydration degree (W_{eq}) of all materials was determined after immersion time of 7 h which showed the equilibrium water uptake. It has been indicated in Figure 8 as well as in Table 3 that the increase in the pH from 4 to 9 significantly increases the hydration degree of all obtained hydrogels. For example S-CA80-2 shows the highest hydration degree of starch based hydrogels of 1380% at pH 9 compared to 345% at pH 4. The highest W_{eq} for lignin was 446% and for hemicellulose was 590% at pH 9, significantly higher than at pH 4. The higher W_{eq} of starch hydrogels relative to lignin and hemicellulose hydrogels is due to its higher molecular weight and more carboxyl incorporation of starch compared to the others hydrogel in accordance with other literature results [34].

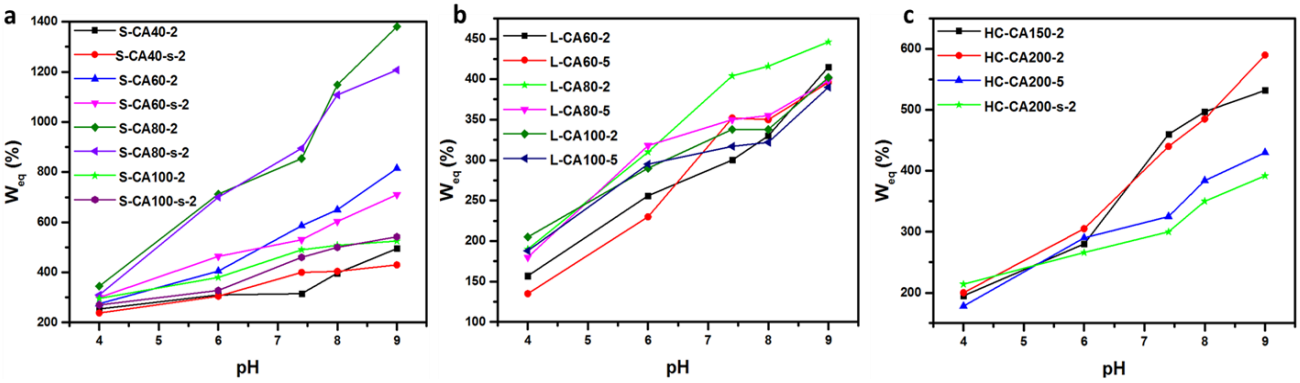

Figure 8. Equilibrium hydration degree (Weq %) versus pH: (a) Starch based hydrogels (b) Lignin based hydrogels and (c) Hemicellulose based hydrogels

The sensitivity of the hydrogels to the pH can be explained by the fact that the carboxyl group of CA in the hydrogels ionizes with increased pH. If the pH value of the contiguous medium rises above its pKa, the ionized form will induce an extraordinary increase in the electrostatic repulsion between $-COO^-$. The first, second and third dissociation constants of CA are $pKa_1 = 2.94$, $pKa_2 = 4.14$ and $pKa_3 = 5.82$ [35]. This repulsion results in the formation of a very loose structure capable of absorbing a relatively high amounts of water. Moreover, under more basic media, the unreacted hydroxyl groups of the biopolymers are capable also of deprotonation which will induce an extra swelling in the hydrogel.

Table 3. Equilibrium hydration degree, Weq (%) of polymeric hydrogels at 37°C as function of pH

Sample	pH				
	4	6	7.4	8	9
S-CA40-2	254	310	315	397	495
S-CA40-5	239	288	325	414	470
S-CA60-2	275	405	586	650	815
S-CA60-5	288	493	536	540	793
S-CA80-2	345	712	854	1148	1380
S-CA80-5	340	716	825	784	1118
S-CA100-2	296	380	490	508	528
S-CA100-5	280	306	400	510	495
S-CA40-s-2	238	305	400	404	430
S-CA40-s-5	190	310	294	390	445
S-CA60-s-2	300	464	530	603	710
S-CA60-s-5	320	488	523	581	603
S-CA80-s-2	310	700	895	1108	1207
S-CA80-s-5	300	715	780	845	945
S-CA100-s-2	270	328	460	500	542
S-CA100-s-5	274	312	410	420	555
L-CA60-2	157	256	300	330	415
L-CA60-5	135	230	352	350	396
L-CA80-2	190	310	404	416	446
L-CA80-5	180	318	350	355	398
L-CA100-2	205	290	338	338	402
L-CA100-5	188	295	317	322	390
HC-CA150-2	195	280	460	497	532
HC-CA200-2	200	305	440	485	590
HC-CA200-5	178	290	325	384	430
HC-CA200-s-2	214	266	300	350	392

At low pH the carboxylic acid groups of the grafted CA are in the protonated form and thus, the hydrogels exhibit the lowest swelling capability (W_{eq}) for pH 4 [36][37] (Figure 9). Furthermore, increases in the grafted CA concentration should increase the carboxylic acid content. However, highly crosslinked hydrogels have a W_{eq} significantly lower than those with a lower degree of crosslinking. This is attributed to the lower ability of the polymer chains to extend and swell. This phenomena can be observed upon comparing the SHP containing hydrogels with those without SHP of similar formulation. For example, the W_{eq} at pH 9 of S-CA80-2 is 1380% but is 1207% for the same conditions but with SHP (S-CA80-s-2). The same observation of lower W_{eq} can be made for a majority of the samples that have higher crosslinking at 5 min than 2 min.

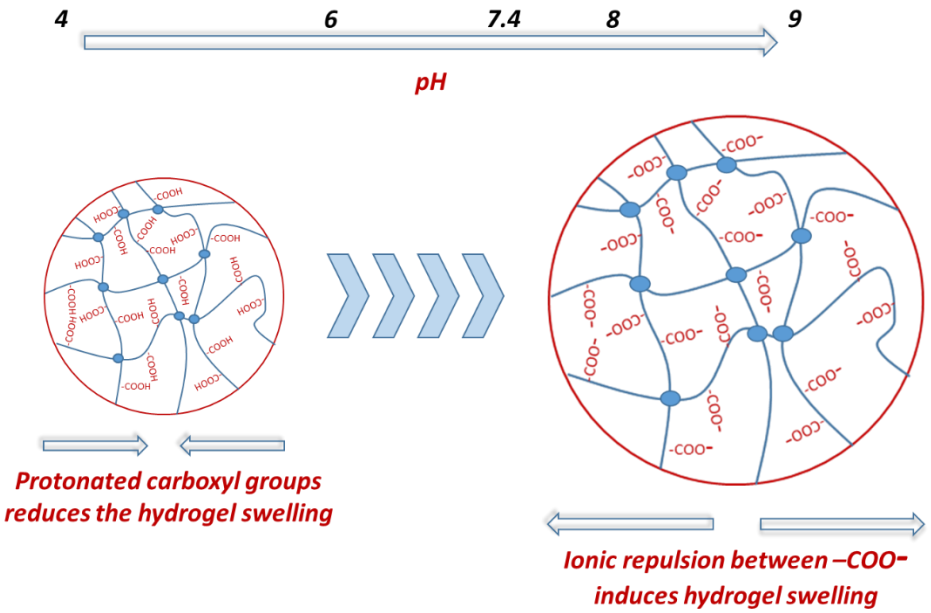

Figure 9. Schematic representation of the pH controlled swelling of the extruded bio-based hydrogels

The diffusion mechanism of small molecules through a gel structure is classified according to the diffusional coefficient, (n) [37][38]. The initial swelling data were fitted using the following equation:

$$\frac{M_t}{M_{eq}} = Kt^n$$

Where M_t and M_{eq} are the masses of water absorbed at a given time t and at equilibrium condition, respectively, k and n are constants [37][38]. Drug delivery systems can be classified based on the release profile of the bioactive agent from the system. The classification includes a Fickian system (n = 0.5) where the transport of molecules through matrix without any specific interactions between liquid molecule and matrix take place, anomalous transport system (n = 0.5–1) where both diffusion and polymer relaxation simultaneously control the overall rate of water uptake, case II transport systems (n = 1) that considers interaction between penetrant molecule and polymer matrix and finally, super case II transport systems (n>1) that represents plasticization at the gel

layer, in which the transport is faster than in the Case II Diffusion.

The slope of $\ln(M_t/M_{eq})$ plotted versus ln(time) corresponds to n. The values of the diffusion exponent (n) are presented in Table 4. The R^2 value of the fits was $R^2 > 0.96$. The majority of the prepared hydrogels shown values in the range between 0.5 and 1 show anomalous transport behavior. Some samples have (n) value above one indicating a super case II transport behavior which corresponds to the most desirable kinetic behavior for a swelling controlled release material [37][38].

Table 4. Diffusional exponent n for water transport of polymeric hydrogels as function of pH

Sample	pH				
	4	6	7.4	8	9
S-CA40-2	0.63	0.55	0.81	0.75	0.54
S-CA40-5	0.61	0.64	0.78	0.83	0.66
S-CA60-2	0.79	0.92	0.87	0.44	0.96
S-CA60-5	0.95	0.65	0.73	0.52	1.01
S-CA80-2	0.82	0.68	0.75	0.81	1.04
S-CA80-5	0.76	0.73	0.62	0.92	0.87
S-CA100-2	0.66	1.09	0.99	0.64	0.67
S-CA100-5	0.47	0.82	0.56	0.51	0.74
S-CA40-s-2	0.71	0.65	0.76	0.84	0.64
S-CA40-s-5	0.58	0.74	0.96	0.94	0.59
S-CA60-s-2	0.91	0.83	0.77	0.56	0.96
S-CA60-s-5	0.88	0.62	0.84	0.62	1.14
S-CA80-s-2	0.65	0.69	1.05	0.64	1.16
S-CA80-s-5	0.77	0.73	0.79	0.88	0.96
S-CA100-s-2	0.42	1.04	1.12	0.94	0.75
S-CA100-s-5	0.51	0.82	0.66	0.55	0.72
L-CA60-2	0.88	1.11	0.46	0.65	0.45
L-CA60-5	0.88	0.95	0.63	0.72	0.96
L-CA80-2	0.59	0.99	0.67	0.68	0.69
L-CA80-5	0.56	1.03	0.82	0.55	0.83
L-CA100-2	0.65	0.76	0.78	0.85	0.73
L-CA100-5	0.78	0.84	1.04	0.86	0.99
HC-CA150-2	0.69	0.78	0.72	0.97	0.52
HC-CA200-2	0.73	0.88	0.48	0.85	0.94
HC-CA200-5	0.78	0.82	0.55	0.95	0.99
HC-CA200-s-2	0.81	0.96	0.71	0.83	1.02

It was observed from the pH controlled swelling of the obtained hydrogel, that the highest drug release can be obtained in alkaline medium, based on the diffusion of water into the gel data, whereas the lowest release can be achieved at acidic medium. The controlled drug release rate depends on which part of the body the material is targeting, such as the duodenal glands (pH 8-9), pancreas (pH 8-8.3), small and large intestine (pH 7.5-8), or stomach (pH 1-3).

3.4. Dynamic degradation behavior of the hydrogels:

The degradation as determined by mass loss versus time in simulated physiological solution (pH 7.4) is shown in Figure 10. For all the studied samples, an extremely high weight loss rate was obtained after the first day of immersion in water. This trend is reduced after day 2 until a stabilization in the weight loss is achieved after day 12. One study reported that the degradation of biopolymers when immersed in water is related to: (a) an initial step of leaching of the plasticizers (it is required in the sample formulation to allow material to be processed in the reactive extruder); (b) elimination of lower molecular weight chains generated from the thermal degradation that occurred in previous processing stages; and (c) chemical degradation [39].

In starch based hydrogels, the highest initial weight loss was observed in S-CA100-2 (25%) which contained the highest amount of CA in this group. This effect can be attributed primarily to the plasticizing effect of CA. The excess unreacted CA is free in the hydrogel matrix and can leach easily from the system. However this sample shows a significantly lower weight loss (37%) after 15 days of immersion compared to S-CA60-2 and S-CA40-2 which shows 38 and 51% weight loss, respectively. This observation is attributed to the increased crosslinking density for the higher CA reaction charge, which stabilizes the hydrogel structure by developing more crosslinks. This effect of lower ultimate degradation with increased crosslink was further boosted with the addition of SHP and the increase in the residence time. The lowest degradation was observed in S-CA80-s-2 and S-CA80-2 which have a 23 and 26% weight loss after 15 days of immersion at 37°C, respectively. Those samples show the highest swelling as well as the lowest degradation and this is due to the extremely high carboxyl content and high degree of crosslinking.

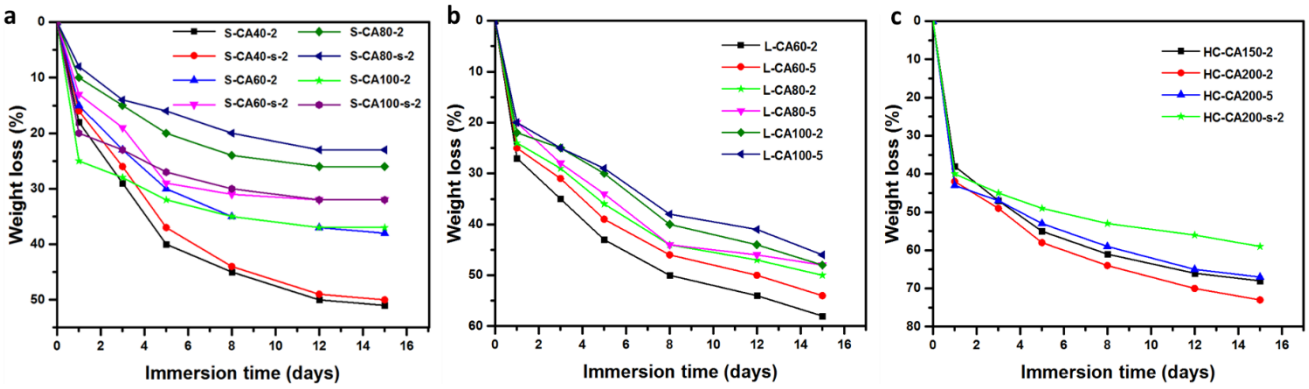

Figure 10. Weight loss as a function of immersion time in physiological solution (pH 7.4) over a period of 15 days at 37°C: (a) Starch based hydrogels (b) Lignin based hydrogels and (c) Hemicellulose based hydrogels

On the other hand, both lignin and hemicellulose based hydrogels show a higher weight loss than starch based hydrogels after 15 days of immersion. This is mainly due the lower molecular weight of lignin and hemicellulose relative to starch. Indeed, the lowest weight loss in the lignin and hemicellulose based hydrogels was 46 and 59%, respectively. An important observation in the hemicellulose based hydrogels is that about 38-43% of the initial weight depending on the formulation of the sample was lost after the first day of immersion. This is due to the extremely high CA content compared to starch and lignin based hydrogels, this CA as discussed above can leach easily from the system.

In all cases, increased hydrogel crosslinking reduces the weight loss after 15 days of immersion. However, the main weight loss inducer during the first day of immersion is primarily attributed to the free unreacted CA plasticizer which can leach easily from the hydrogel matrix. Furthermore, due to enzymatic activity, those hydrogels will probably degrade quicker when applied for *in vivo* applications.

3.5. Changes in the Mechanical Properties of the Hydrogels with Immersion Time

In order to determine the correlation between the mechanical property changes and the degradation of hydrogels, constant frequency compression tests for different dynamic strains were performed on some selected hydrogels during degradation. Figure 11 shows the stress–strain curves of S-

CA80-2, L-CA100-2 and HC-CA200-2 hydrogels during the degradation study. Those samples were selected for this study for the reason that they have the highest swelling and a low degradation extent in their group.

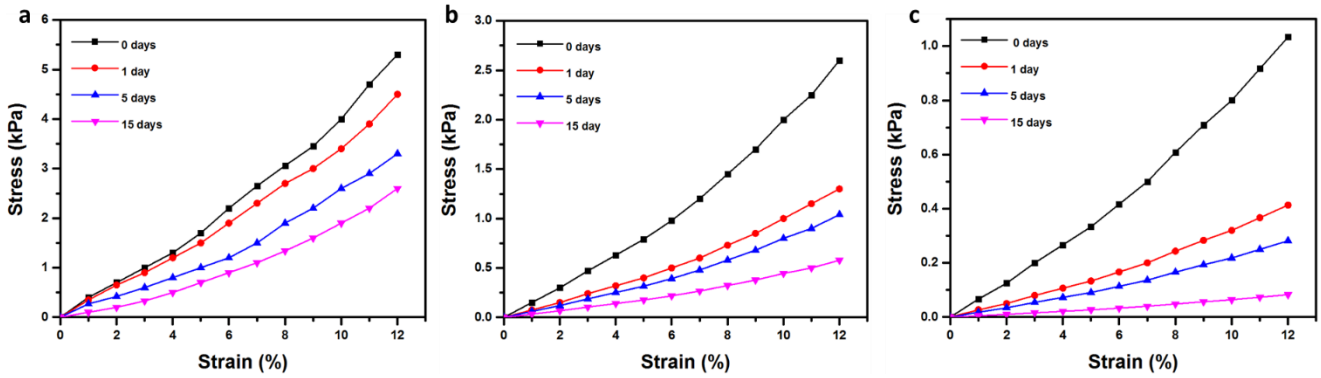

Figure 11. Stress–strain curves in compression representing the correlation between mechanical property change and degradation of selected hydrogels, (a) S-CA80-2 formulation, (b) L-CA100-2 formulation and (c) HC-CA200-2 formulation

The dynamic compression modulus is the ratio of stress to strain, and it is an important parameter of compressive deformation. Figure 12 shows the compression modulus of the hydrogel at the strain of 12%. A greater value of compression modulus indicates more stiffness of the hydrogel, and a lesser value indicates that the hydrogels are more compliant and easy to compress. The compression modulus of the samples decreases with immersion time presumably due to a combination of the degradation of the gel structure and the increased swollen nature of the gel with the aqueous fluid.

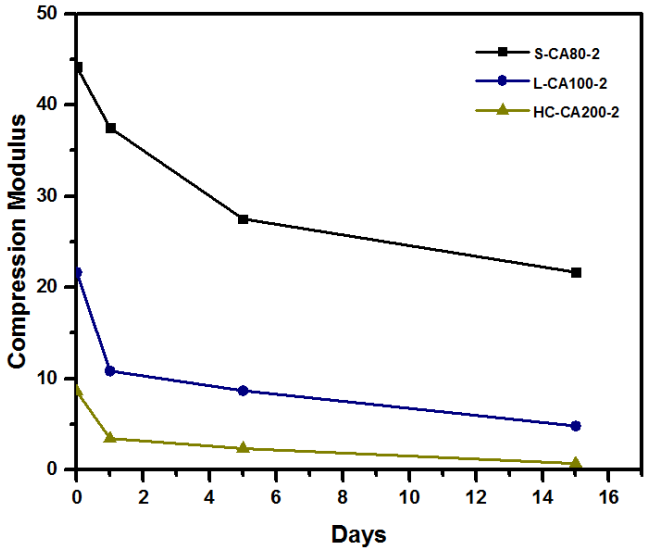

Figure 12. Compression modulus, of S-CA80-2, L-CA100-2 and HC-CA200-2 hydrogels during the degradation study

4. Conclusion

This research describes the development of drug delivery hydrogels from natural polymers, starch, hemicellulose, and lignin using reactive extrusion in the presence of citric acid with and without SHP catalyst. Equilibrium swelling of the hydrogels was as high as 1380%. Based on the material formulation, as well as the pH of the medium, the produced hydrogels may show extreme differences in swelling behavior. Hydrogels swelling degree increased at high pH values due to electrostatic repulsion generated by the ionized citric acid moieties grafted to the polymer. Furthermore, the weight loss of such a system in physiological solution is highly dependent on the concentration of CA during the reactive extrusion process and also dependent on the molecular weight of the polymeric material. The combination of the properties of the developed hydrogels might allow for the application of these renewable plant based biopolymers in a wide range of biomedical applications. This study demonstrates the characteristics and potential of natural polymers as a drug release system.

References

[1] T. S. Khoo, M. M. Ratnam, S. a. B. Shahnaz, and H. P. S. Abdul Khalil, "Wood Filler-recycled Polypropylene (WF-RPP) Composite Pallet: Study of Fastening Method," *J. Reinf. Plast. Compos.*, vol. 27, no. 16–17, pp. 1723–1731, 2008.

[2] Stockholm Environment Institute, "Biomass in a Low-Carbon Economy : Resource Scarcity , Climate Change , and Business in a Finite World," 2012.

[3] IEA Bioenergy, "Bio-based Chemicals Value Added Products from Biorefinerie," 2012.

[4] S. Herrera, "Industrial biotechnology—a chance at redemption," *Nat. Biotechnol.*, vol. 22, no. 6, pp. 671–675, 2004.

[5] W. Farhat, R. A. Venditti, M. Hubbe, M. Taha, F. Becquart, and A. Ayoub, "A Review of Water-Resistant Hemicellulose-Based Materials: Processing and Applications," *ChemSusChem*, vol. 10, no. 2, pp. 305–323, 2017.

[6] K. Löffler, N. Gillman, R. W. Van Leen, T. Schäfer, A. Faaij, and L. G. Plata, "the Future of Industrial Biorefineries," p. 40, 2010.

[7] D. History, "Superabsorbent materials 1.," no. 52, 1979.

[8] M. Hamidi, A. Azadi, and P. Rafiei, "Hydrogel nanoparticles in drug delivery," *Adv. Drug Deliv. Rev.*, vol. 60, no. 15, pp. 1638–1649, 2008.

[9] S. Kasapis, I. T. Norton, and J. B. Ubbink, "Modern Biopolymer Science: Bridging the Divide between Fundamental Treatise and Industrial Application." p. 640, 2009.

[10] S. Atta *et al.*, "Injectable biopolymer based hydrogels for drug delivery applications," *Int. J. Biol. Macromol.*, vol. 80, pp. 240–245, 2015.

[11] G. Gerlach, M. Guenther, J. Sorber, G. Suchaneck, K. F. Arndt, and A. Richter, "Chemical and pH sensors based on the swelling behavior of hydrogels," *Sensors Actuators, B Chem.*, vol. 111–112, no. SUPPL., pp. 555–561, 2005.

[12] N. A. Peppas, J. Z. Hilt, A. Khademhosseini, and R. Langer, "Hydrogels in biology and medicine: From molecular principles to bionanotechnology," *Adv. Mater.*, vol. 18, no. 11,

pp. 1345–1360, 2006.

[13] X. Shen, J. L. Shamshina, P. Berton, G. Gurau, and R. D. Rogers, “Hydrogels Based on Cellulose and Chitin: Fabrication, Properties, and Applications,” *Green Chem.*, no. Mc, pp. 53–75, 2015.

[14] D. Dhara, C. K. Nisha, and P. R. Chatterji, “Super absorbent hydrogels: interpenetrating networks of poly(acrylamide-co-acrylic acid) and poly (vinyl alcohol): swelling behavioe and structural parameters,” *J. Macromol. Sci. Part A*, vol. 36, no. 2, pp. 197–210, 1999.

[15] Y. Luo, K. Zhang, Q. Wei, Z. Liu, and Y. Chen, “Poly(MAA-co-AN) hydrogels with improved mechanical properties for theophylline controlled delivery,” *Acta Biomater.*, vol. 5, no. 1, pp. 316–327, 2009.

[16] A. Salam, J. J. Pawlak, R. A. Venditti, and K. El-Tahlawy, “Synthesis and characterization of starch citrate-chitosan foam with superior water and saline absorbance properties,” *Biomacromolecules*, vol. 11, no. 6, pp. 1453–1459, 2010.

[17] A. Salam, R. a. Venditti, J. J. Pawlak, and K. El-Tahlawy, “Crosslinked hemicellulose citrate-chitosan aerogel foams,” *Carbohydr. Polym.*, vol. 84, no. 4, pp. 1221–1229, 2011.

[18] E. S. Stevens, A. Klamczynski, and G. M. Glenn, “Starch-lignin foams,” *Express Polym. Lett.*, vol. 4, no. 5, pp. 311–320, 2010.

[19] W. Ning, Y. Jiugao, M. Xiaofei, and W. Ying, “The influence of citric acid on the properties of thermoplastic starch/linear low-density polyethylene blends,” *Carbohydr. Polym.*, vol. 67, no. 3, pp. 446–453, 2007.

[20] J. B. Olivato, M. V. E. Grossmann, A. P. Bilck, and F. Yamashita, “Effect of organic acids as additives on the performance of thermoplastic starch/polyester blown films,” *Carbohydr. Polym.*, vol. 90, no. 1, pp. 159–164, 2012.

[21] B. Ghanbarzadeh, H. Almasi, and A. A. Entezami, “Improving the barrier and mechanical properties of corn starch-based edible films: Effect of citric acid and carboxymethyl cellulose,” *Ind. Crops Prod.*, vol. 33, no. 1, pp. 229–235, 2011.

[22] P. S. Garcia, M. V. Eiras Grossmann, F. Yamashita, S. Mali, L. H. Dall’Antonia, and W. J.

Barreto, “Citric acid as multifunctional agent in blowing films of starch/PBAT,” *Quim. Nova*, vol. 34, no. 9, pp. 1507–1510, 2011.

[23] A. Lehmann and B. Volkert, “Preparing esters from high-amylose starch using ionic liquids as catalysts,” *Carbohydr. Polym.*, vol. 83, no. 4, pp. 1529–1533, 2011.

[24] N. Reddy and Y. Yang, “Citric acid cross-linking of starch films,” *Food Chem.*, vol. 118, no. 3, pp. 702–711, 2010.

[25] A. Salam, J. J. Pawlak, R. A. Venditti, and K. El-tahlawy, “Incorporation of carboxyl groups into xylan for improved absorbency,” *Cellulose*, vol. 18, no. 4, pp. 1033–1041, 2011.

[26] M. Palm and G. Zacchi, “Extraction of hemicellulosic oligosaccharides from spruce using microwave oven or steam treatment,” *Biomacromolecules*, vol. 4, no. 3, pp. 617–623, 2003.

[27] O. S. Adeyefa, “Biogradable Starch Film from Cassava , Corn , Potato and Yam,” *Chem. Mater. Res.*, vol. 7, no. 12, pp. 15–24, 2015.

[28] Q. Lu and G. Zografi, “Properties of citric acid at the glass transition,” *Journal of Pharmaceutical Sciences*, vol. 86, no. 12. pp. 1374–1378, 1997.

[29] A. M. Abdel-Mohsen, A. S. Aly, R. Hrdina, A. S. Montaser, and A. Hebeish, “Biomedical Textiles Through Multifunctioalization of Cotton Fabrics Using Innovative Methoxypolyethylene Glycol-N-Chitosan Graft Copolymer,” *J. Polym. Environ.*, vol. 20, no. 1, pp. 104–116, 2012.

[30] P. S. Garcia *et al.*, “Improving action of citric acid as compatibiliser in starch/polyester blown films,” *Ind. Crops Prod.*, vol. 52, no. JANUARY, pp. 305–312, 2014.

[31] J. Zhang, E. Fleury, and M. A. Brook, “Foamed lignin–silicone bio-composites by extrusion and then compression molding,” *Green Chem.*, vol. 17, no. 9, pp. 4647–4656, 2015.

[32] C. Menzel *et al.*, “Molecular structure of citric acid cross-linked starch films,” *Carbohydr. Polym.*, vol. 96, no. 1, pp. 270–276, 2013.

[33] (2001). doi:10.1016/j.carbpol.2013.02.006.erian Dumitriu, Sev[1] S. Dumitriu, Influence of citric acid and curing on moisture sorption, diffusion and permeability of starch films, “Influence of citric acid and curing on moisture sorption, diffusion and permeability of

starch films," 2001.

[34] S. Dumitriu, "Polymeric Biomaterials, Second Edition, Revised and Expanded," vol. 29. p. 1168, 2001.

[35] T. Caykara, C. Ozyurek, O. KantoGlu, and O. Guven, "Equilibrium swelling behavior of pH- and temperature-sensitive poly(N-vinyl 2-pyrrolidone-g-citric acid) polyelectrolyte hydrogels," *J. Polym. Sci. Part B Polym. Phys.*, vol. 38, no. 15, pp. 2063–2071, 2000.

[36] D. S. Franklin and S. Guhanathan, "Synthesis and characterization of citric acid-based pH-sensitive biopolymeric hydrogels," *Polym. Bull.*, vol. 71, no. 1, pp. 93–110, 2014.

[37] V. B. Bueno, R. Bentini, L. H. Catalani, and D. F. S. Petri, "Synthesis and swelling behavior of xanthan-based hydrogels," *Carbohydr. Polym.*, vol. 92, no. 2, pp. 1091–1099, 2013.

[38] K. Pal, A. Banthia, and D. Majumdar, "Polymeric hydrogels: characterization and biomedical applications," *Des. monomers …*, vol. 12, no. July, pp. 197–220, 2009.

[39] D. Demirgöz, C. Elvira, J. F. Mano, A. M. Cunha, E. Piskin, and R. L. Reis, "Chemical modification of starch based biodegradable polymeric blends: Effects on water uptake, degradation behaviour and mechanical properties," *Polym. Degrad. Stab.*, vol. 70, no. 2, pp. 161–170, 2000.

Chapter 5. Ring opening graft polymerization of ε-caprolactone onto Hemicellulose: Synthesis and Characterization

1. Introduction

Bio-based economy or "*bioeconomy*" is a strategy adopted to reduce the environmental hazards the world is facing today [1]. The European Commission has arranged a strategy to shift the European economy towards a superior and more sustainable consumption of renewable resources [2]. In addition, according to the U.S. Department of Agriculture (USDA), the biobased products already contribute $369 billion to the U.S. economy each year and employment of four million workers [3].

In fact, current research activity targets the replacement of petroleum-based products (products of petrorefinery) with renewable and sustainable materials (biorefinery products) in order to reduce the environmental impacts, provide new energy resources, and conserve petroleum resources [4][5]. According to EA Bioenergy Task 42 Biorefinerie, "Biorefining is the sustainable processing of biomass into a spectrum of marketable products and energy [6]. Biorefinery systems work by processing the input (biomass, that is all plants and plants derivatives) to generate an output (fuel, chemicals, heat, and materials) [7]. The ideal outcome would be to accomplish all of these objectives with the least impact on wildlife, water, soil, or air quality.

The leading polysaccharides that are found in biomass are starch, cellulose, chitin, and hemicelluloses. Hemicellulose (HC) is one of the most common polysaccharides next to cellulose

and chitin, representing about 20-35% of lignocellulosic biomass, and has not yet found broad industrial applications as does cellulose [8]. Actually, hemicellulose not incorporated into paper products is not utilized for value-added applications, rather it is primarily incinerated to produce energy. In the paper industry, much of the hemicellulose remains in the fibers, which provides a strength benefit to the paper product. Moreover, another portion of hemicellulose is discarded as a waste material during pulping, bleaching and other operations or used for energy [8][9][10]. However, in order to improve the "*bioeconomic value*" extracted from biomass, it would be beneficial to pre-extract hemicellulose prior to the pulping process and develop a number of bioproducts such as biochemicals and biomaterials. This could be an important part of a forest-based biorefinery that offers technologies enabling the conversion of biomass into a wide range of marketable products such as fuel, chemicals, food, and materials.

Hemicelluloses are heterogeneous, low molecular weight and branched polysaccharides made up of C6 and C5 sugar units [11]. The most commonly existing sugars that constitute hemicellulose are D-xylose, D-glucose, D-mannose, D-glucuronic acid, 4-O-methyl-D-glucuronic acid, and others. The main hemicellulose type is xylan, which is estimated to count for one-third of all renewable organic carbon available on earth [12]. Hemicellulose is known to be biodegradable, biocompatible and a good candidate for varieties of biomedical applications, that include wound dressing, drug delivery hydrogel, and scaffold system in tissue engineering [13][14][15][16].

Over the last several decades, significant research was done on the possibility of utilizing hemicellulose for applications in the plastic industry as an alternative to polyol synthetic polymers and food-based polyols (starch) [17][18][19][20]. Hemicellulose is not actually thermoplastic [21]. However, its properties can be altered by incorporating certain functions into its backbone hence, facilitating its processability for value-added applications. Graft polymerization has been one of the commonly used approaches for the derivatization of hemicelluloses and other natural polymers [21][22]. Hemicellulose modification by graft polymerization can diminish the formation of a hydrogen bond network. This can lead to an increase in their hydrophobicity and solubility in organic solvents. Similarly, the alteration in its structure can also influence the thermal and the mechanical properties of hemicellulose based materials.

The graft polymerization of hemicellulose by grafting small poly-(ε-caprolactone) (PCL) chains onto the backbone can enhance both the processability and the thermomechanical properties. PCL

grafting onto hydroxylated polymers can modify the material properties influenced by the reduction of hydrogen bonds. Polycaprolactone (PCL) is a hydrophobic, semi-crystalline and biodegradable polyester commonly prepared by ring-opening polymerization of ε-caprolactone in the presence of catalysts or by free radical ring-opening polymerization of 2-methylene-1-3-dioxepane [23]. It can be degraded by hydrolysis of the ester linkages and has thus attracted significant attention for applications as implantable hydrogels [24].

In fact, PCL was approved by the FDA for biomedical applications such as drug delivery systems and scaffolds in tissue engineering [25]. PCL has been a very attractive biomedical starting materials for copolymerization and blending to develop medical devices with favorable mechanical properties and degradation kinetics [26]. Chang *et al*. reported the synthesis of starch-graft-polycaprolactone copolymer by ring-open polymerization of caprolactone monomer onto starch under microwave irradiation [27]. Grafting of PCL induces a significant thermoplastic and hydrophobic alteration of the grafted starch material.

In the present study, a series of hemicellulose-grafted-PCL (HC_gPCL) were prepared in solution by the homogenous ring-opening graft polymerization of caprolactone onto hemicellulose. The molar ratio of caprolactone to hemicellulose was varied in the different grafting reactions. The structural features of the products obtained by FT-IR and NMR analyses are presented. The molecular weights, thermal, hydrophobic, mechanical and biodegradable properties of the materials were examined and compared. The grafted materials exhibit interesting *"thermoplastic features"*.

2. Experimental part:

2.1.Hemicellulose extraction and characterization

Xylan type hemicellulose was isolated from bleached hardwood pulp by an alkaline extraction technology as described in our previous research [28]. Briefly; hardwood pulp was subjected to 10% NaOH treatment to recover a pure xylan type hemicellulose with 11% average percent yield based on the original biomass. This material showed a high thermal stability as investigated by TGA and a high T_g (144.9°C) as determined by DSC. A detailed analysis of the structural features

and the physicochemical properties of the extracted hemicellulose were considered in our previous research [28].

2.2.Grafting reaction

The grafting reactions were performed according to the conditions listed in Table 1, briefly: oven-dried hemicellulose (5.00 g, 0.076 mol of hydroxyl group in the hemicellulose) was poured into a 300 ml glass reactor (60 mm diameter, with a 3-necked steel cover, the steel cover anchor stirrer operating with IKA motor) containing 10 ml of DMSO solvent with silicon oil bath at 80°C. DMSO was selected because it is a good solvent for hemicellulose and compatible with Cl grafting reaction [29]. The mixture was agitated at 60 rpm until a homogeneous viscous solution was obtained. The silicon oil bath temperature was then increased to 110°C and the **ε**-caprolactone monomer was introduced into the hemicellulose solution and mixed for 30 min. Then 1,5,7-triazabicyclodecene [4.4.0] catalyst (TBD, 1% of the total mass of the reactants) was introduced into the reaction mixture and the reaction was kept for about 4 h under the flow of nitrogen gas. TBD was used herein because it is known to be one of the most efficient catalysts for ring-opening graft polymerization [30]. The solution was cooled at room temperature and precipitated 3 times in an excess volume of diethyl ether in an ice bath. The obtained materials were poured into an aluminum pan and dried under vacuum (0.2 mbar) at 60°C for 2 days.

The average degree of polymerization (DP) of the grafted PCL sidechains was determined by ^{1}H NMR according to the following equation:

$$DP = \frac{CL_{(Total)}}{CL_{(Terminal)}}$$

Where, $CL_{(Terminal)}$ is the PCL end unit, $CL_{(Total)}$ is the PCL total units.

2.3.Fourier transform infrared spectroscopy (FT-IR)

FT-IR analyses were performed for the samples from 4000 to 700 cm^{-1}, with a spectral resolution of 4 cm^{-1}. The spectra were recorded on a single reflection attenuated total reflectance (ATR). FT-IR technique was performed by a Nicolet Nexus spectrometer. The spectra were obtained by an accumulation of 60 scans.

2.4.Nuclear magnetic resonance (NMR) analysis

NMR analyses (^{1}H, ^{13}C, homonuclear correlation spectroscopy (COSY), and Heteronuclear Single-Quantum Correlation (HSQC)) were recorded using Bruker Avance III 400 MHz spectrometer, equipped with a 5mm multinuclear broad band probe (BBFO+) and z-gradient coil. The samples (30 mg) were dissolved in d6-DMSO (1 ml) and the spectra were recorded at 60°C (333ºK) and with 128 scans for 1D ^{1}H, 32 scans and 128 increments for 2D ^{1}H-^{1}H COSY and 16 scans and 256 increments for 2D ^{1}H-^{13}C HSQC. Chemical shifts (in ppm) were expressed relative to the resonance of tetramethylsilane TMS ($\delta = 0$ ppm).

2.5.Gel Permeation Chromatographic (GPC) analysis

The molecular weights of hemicellulose and its derivatives were determined by GPC analysis. The analyses were performed on a Malvern Viscotek HT GPC 350 system equipped with refractive index (RI) and viscometer detectors. PSS-GRAM columns with a range of 100–1,000,000 g/mol were used and the samples were eluted by DMSO at 80 °C. Molecular weights were calculated referring to a universal calibration with pullulan polysaccharide standards.

2.6.Differential Scanning Calorimetry (DSC), T_g analysis

Thermal transitions of the samples were determined using differential scanning calorimetry (DSC). The instrument used was a DSCQ10 (TA Inc., New Castle, DE) with a hermetic pan (T 090127). Before analysis, the samples were dried at 50 °C under vacuum overnight. The samples were heated from 25 to 165 °C at a temperature ramp of 10 °C/min. The samples were then cooled to 15°C and a second heating cycle was performed by heating the samples again to 165 °C at 10

°C/min. An empty pan was used as a reference. The glass transition temperatures (T_g) were determined from the second heating ramp by identifying the inflection points.

2.7.Thermal properties and FT-IR gas analysis

Thermogravimetric analysis was performed with a TGA Mettler-Toledo (TGA/DSC 1 STARe System) on 5–15 mg of a sample for each experiment in a nitrogen atmosphere (gas flow rate 85 ml/min). The temperature range and heating rate were 30–500 °C and 10 °C/min, respectively. Temperature resolved compositions of gases produced during heating of the different samples were characterized using an FT-IR spectrometer (Thermo Scientific™, Nicolet™, ™50 FT-IR, deuterated triglycine sulfate (DTGS) detector) coupled to the TGA instrument. The temperatures of the sampling line and the gas cell were set to 250 °C. FT-IR analyses were performed from 4000 to 650 cm^{-1} with a 4 cm^{-1} resolution.

2.8.Film preparation

The different films were prepared using a hydraulic manual press compression mold. The materials (2 g) were loaded into a square Teflon board and subsequently compression molded under 100 bar for 2 min and then under 200 bar for 5 min at the molding temperatures of 100°C. After molding, the specimens were allowed to cool and stored at room temperature. The thickness of the obtained films was determined by an electronic caliper and was in the range of 0.2–0.4 mm. Measurements of the thickness of the designed films did not shows any significant difference.

2.9.Mechanical properties

Mechanical tensile testing of the films (35×4×0.3mm) was conducted at room temperature using a Shimadzu Autograph AG-500A (Shimadzu Corporation, Kyoto, Japan). Dog-bone shaped sample specimens were prepared according to ISO ½ standard (1BA, ISO 527.2). A crosshead speed of 10 mm/min and a 12 mm distance between grips were used. The ultimate strength, Young's modulus, and elongation at break were calculated from five independent measurements.

2.10. Water contact angle

The water contact angle measurements were conducted with an NRL Contact Angle Goniometer by Rame-Hart (model 100–00) at room temperature and ambient humidity. A drop of deionized water was placed on the top of a flat surface of HC_gPCL copolymer film (1×1cm). The contact angles on two sides of the drop were measured immediately and the average reported. The contact angle was then measured as a function of time. Eight independent measurements were collected and the average was reported.

2.11. Aerobic biodegradation test

Biodegradability test was performed based on ISO 14851 standard (Biochemical Oxygen Demand (BOD) measurement) measuring the biological oxygen demand required for degradation of materials by microorganisms under aerobic conditions in a closed respirometer bottles (OxiTop® Control, WTW GmbH, Weilheim, Germany). The OxiTop system includes glass reactors with a carbon dioxide snare in the headspace and a cover containing an electronic pressure indicator. The aqueous medium was prepared as described in the ISO 14851 standard (and mixed with activated sludge sampled in a municipal wastewater treatment station (Monistrol, France)). Between 15-20 mg of samples were mixed in the aqueous medium and stirred at 23 °C for 28 days. The biodegradability of each sample was investigated in duplicate and the average was reported. The ultimate biodegradability was then calculated by the following equation:

$$D_T\ (\%) = \frac{BOD_{test} - BOD_{blank}}{C \times DthO_{test}} \quad (1)$$

Where D_T is the biodegradability (%), BOD_{test} and BOD_{blank} are the biological oxygen demand of the sample and blank (activated sludge), respectively. C ($g.L^{-1}$) is the concentration of the sample in the aqueous medium and $DthO_{test}$ ($mg.g^{-1}$) is the theoretical BOD of the sample [31].

3. Results and discussion:

3.1. Grafting reaction and mechanism

In our previous research [28], we have extracted and characterized xylan type hemicellulose from bleached hardwood pulp by an optimized alkaline extraction technology [28]. The extracted xylan displays high purity with a predominant xylose content (90%). HC$_g$PCL copolymers with various graft lengths were synthesized by adjusting the molar ratio of ε-caprolactone monomers to the anhydroxylose (Xylopyranose, *XylP*) residues (Table 1). The other conditions including the amount of catalyst, reaction time and reaction temperature were kept constant within the series of grafting reactions.

Table 1. Characteristics and structural features of the grafted materials. DP represents the degree of polymerization of grafted PCL, SR is the substitution ratio (SR_T, SR_2, and SR_3 indicate the SR at C_2+C_3, C_2, and C_3 of anhydroxlose units, respectively), CY: is the conversion yield representing the amount of the materials obtained based on the starting materials. (a) represent the CY established on the bases on real masses and (b) represent the CY calculated based on the NMR analysis.

Sample	XylP:Cl	DP	SR_T	SR_2	SR_3	CY (%)[a]	CY (%)[b]
HC$_g$PCL-1	1:1.1	1.82	0.51	0.26	0.76	63.2	60.5
HC$_g$PCL-2	1:1.8	3.35	0.62	0.34	0.90	71.5	74.2
HC$_g$PCL-3	1:2.6	4.26	0.69	0.45	0.93	75.1	75.5
HC$_g$PCL-4	1:6.5	3.11	0.50	0.29	0.71	59.6	58.1

The expected mechanism of the grafting reaction is illustrated in Figure 1. TBD is known to be an efficient catalyst for the ring-opening graft polymerizations of cyclic esters [32]. The amidine imine nitrogen (TBD catalyst) will first induce a nucleophilic attack to the ester carbonyl (CL monomer) generating an activated intermediate where the adjacent protonated nitrogen is typically suitable for proton transfer to the incipient alkoxide to generate the TBD amide. H-bond activation of the incoming hemicellulose should facilitate the esterification, releasing a grafted polysaccharide and regenerating TBD [33]. Herein, the hydroxyl groups on hemicellulose act as initiators of CL graft polymerization so that the PCL will be covalently linked to hemicellulose.

It is also expected that the hydroxyl terminal of the grafted PCL will interact with another TBD amide intermediate. Hence, stimulating a further increase in the length of the PCL tail (DP).

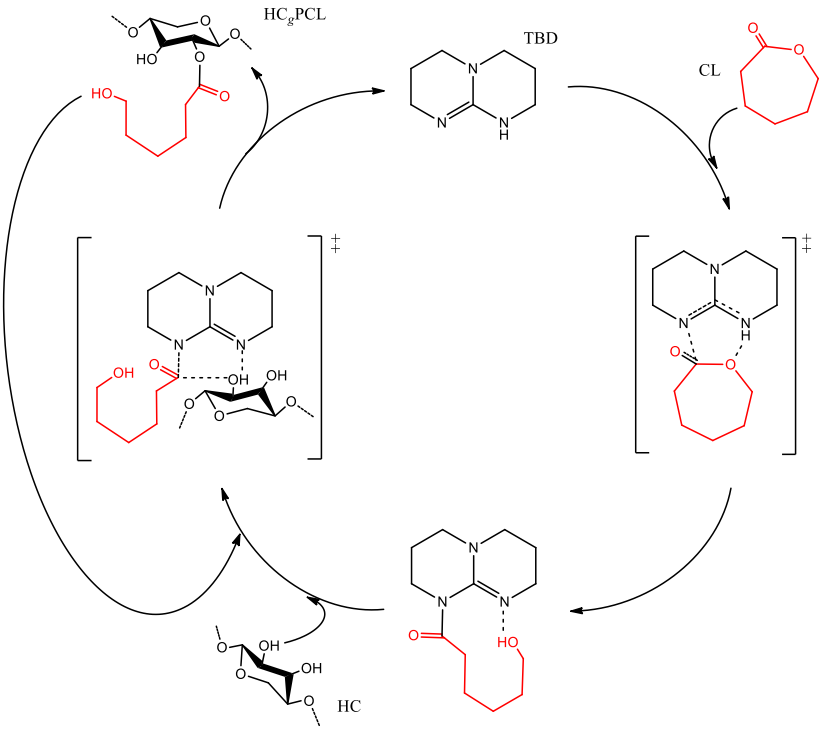

Figure 1. Expected mechanism of the ring-opening graft polymerization of PCL onto hemicelluloses in the presence of TBD catalyst.

Actually, both the hydroxyl groups of the un-grafted anhydroxylose residues and the hydroxyl terminal of PCL sidechains will compete with each other to interact with TBD amide intermediate and thereby, stimulating both the increase in the substitution ratio (SR) and the DP. The reactivity of the different hydroxyl groups will determine whether the reaction will favor the growing and propagation of PCL sidechains or the increase in the SR. In fact, others have shown that primary alcohols (–OH terminal of PCL sidechains) are more reactive toward ring-opening graft polymerization than secondary and strictly hindered alcohols [34]. Thus, at a certain point, the PCL sidechains will interfere with the ability of un-grafted anhydroxylose hydroxyl groups to interact with TBD amide intermediate, prohibiting the further increase in the SR and stimulates the increased propagation of the PCL tail.

Figure 2 shows the materials obtained after drying. In fact, each xylose repeating unit of the hemicellulose has two hydroxyl groups available to stimulate the ring-opening graft polymerization of ε-caprolactone onto the hemicellulose main chain.

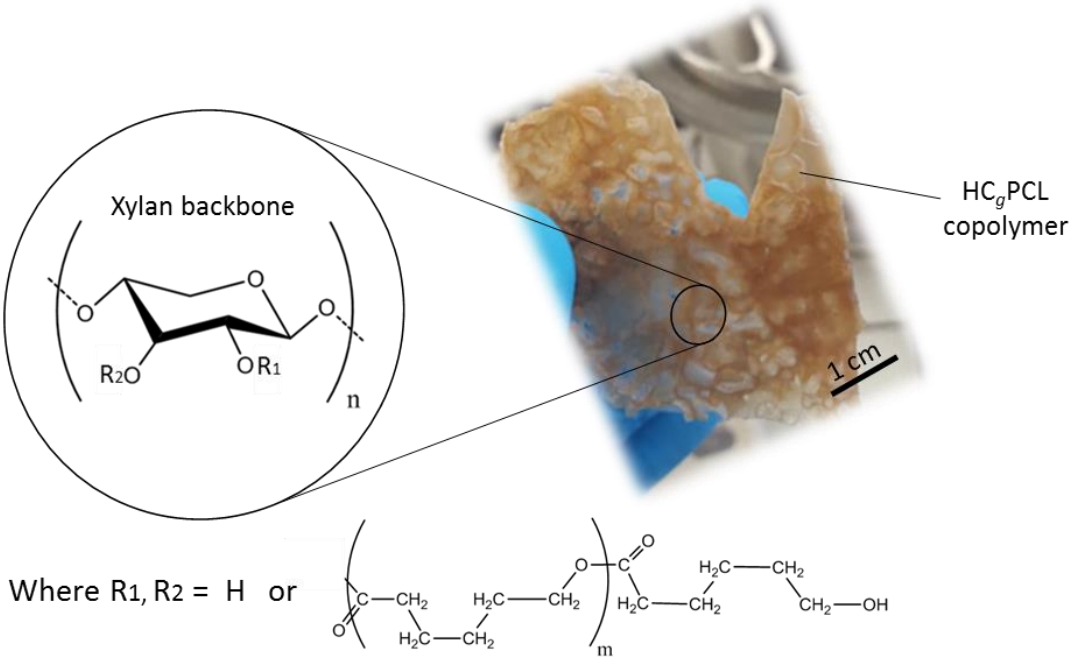

Figure 2 Schematic illustration of (molecular and macroscopic) HC_gPCL copolymers.

The existence of PCL grafts was first examined by FT-IR (Figure 3) in the frequency range of 4000–700 cm^{-1}. Analysis indicated that the absorbance at 3000–3640, 2889, 1483, 1416, 1045, 985 and 898 cm^{-1} are associated with the hemicellulose [35]. The spectrum of HC_gPCL-1 revealed intense absorption peaks at around 2906 and 1738 cm^{-1} attributed to the stretching bands of CH_2 and carbonyl ester (C=O) bands, respectively [22], indicative of the occurrence of the grafting reaction. The intensity of the peak at 3000–3640cm^{-1} for hydroxyl stretching reduces significantly probably due to the decrease of H-bonded hydroxyl groups in the hemicellulose. The hydroxyl stretching was shifted to a higher wavenumber region, explained also by the diminished H-bonding force in hemicellulose after PCL grafting [36].

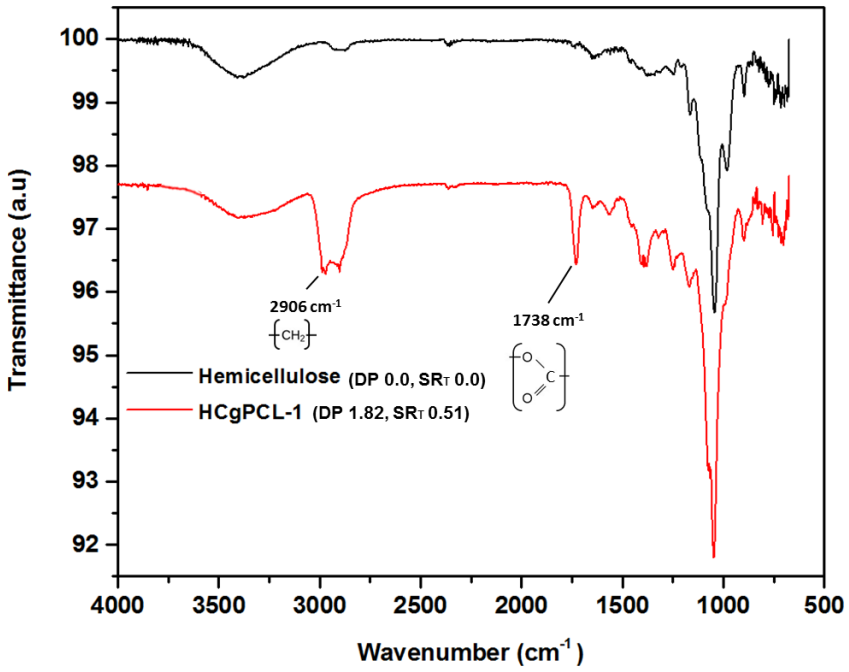

Figure 3. FT-IR spectra of pure hemicellulose and PCL grafted hemicellulose

3.2. NMR analysis

The characteristics and the chemical structures of hemicellulose and HC$_g$PCL copolymers were also investigated by NMR analyses (Figure 4). As illustrated, the hemicellulose used herein is xylan type hemicellulose [confirmed also by the NMR analyses (Figure 4a)]. The β-(1→4) linked D-*XylP* residues are assigned to resonances at 3.05, 3.15, 3.25, 3.5, 3.9 and 4.25 ppm which correspond to H-2, H-5'(represent the axial proton), H-3, H-4, H-5 (represent the equatorial proton) and H-1, respectively [37]. The signals at 5.05 and 5.15 ppm are assigned to protons from the hydroxyl groups at C_2 and C_3 of *XylP* residues.

In the ^{1}H NMR spectra of the HC$_g$PCL-1 copolymer (Figure 4b), the proton signals of hemicellulose were clearly evident. The signals between 1.2 and 1.7 ppm correspond to β, β', γ, γ', δ, and δ' of PCL sidechains [38]. The chemical shifts at 2.25 and 4.0 ppm corresponds to α+α' and ε, respectively. The proton signal of ε' is overlapped with protons of *XylP* residues between 2.8 and 3.7 ppm. Furthermore, the signal at 2.85 ppm is assigned to the proton at substituted C_2 (H_{2g}). The signal of H_{3g} that corresponds to the proton at substituted C_3 is overlapped with other

protons in the area between 2.95 and 3.7 ppm. The signal of H_{5g} (equivalent to $2(H_{2g} + H_{3g})$) can be assigned to the chemical shift at 4.80 ppm. Our results confirmed the successful PCL grafting onto hemicellulose).

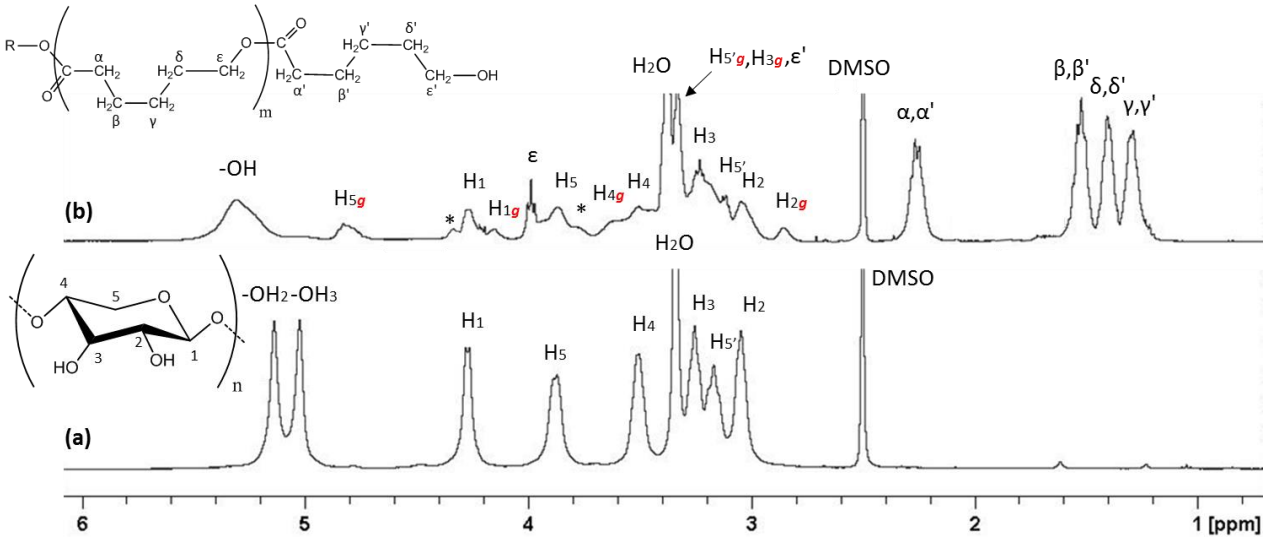

Figure 4. ^{1}H NMR spectra of pure hemicellulose (a) and HC$_g$PCL-1 (DP 1.82, SR$_T$ 0.51) (b)

These assignments were also confirmed by ^{1}H-^{1}H COSY and ^{1}H-^{13}C HSQC spectrum as powerful and effective techniques for quantitative and qualitative analyses of chemical structures (Figure 5).

The degree of polymerization (DP) representing the number average length of the PCL tails can be estimated based on the peak intensity of the corresponding signals according to the following equation:

$$DP = \frac{CL_{(Total)}}{CL_{(Terminal)}} = \frac{I(\alpha + \alpha')}{I(\alpha')} = \frac{I(\varepsilon + \varepsilon')}{I(\varepsilon')} \quad (2)$$

Where, CL $_{(Terminal)}$ is the end unit of PCL, CL $_{(Total)}$ is the total units of PCL and (I) is the integral (area) of the selected proton.

Actually, for the ease of attribution and calculation, the DP can be also presented as follows:

$$DP = \frac{I(\alpha + \alpha')}{I(\varepsilon')} = \frac{I(\alpha + \alpha')}{I[(\alpha + \alpha') - \varepsilon]} \quad (3)$$

The substitution ratio (SR) can be investigated also by the peaks intensity of the corresponding signals. SR is defined as the fraction of hemicellulose hydroxyl groups bearing PCL grafts hence, reflecting the grafting efficiency. The SR can be established according to the following equation:

$$SR_T = \frac{XylP_{(Grafted)}}{XylP_{(Total)}} = \frac{I(H_{2g} + H_{3g})}{I(H_{2g} + H_{3g} + H_2 + H_3)} \quad (4)$$

Alternatively, the SR_T could be also expressed as follows:

$$SR_T = \frac{I(H_{2g} + H_{3g})}{2 \times I(H_1 + H_{5g})} = \frac{2 \times I(H_{5g})}{2 \times I(H_1 + H_{5g})} = \frac{I(H_{5g})}{I(H_1 + H_{5g})} \quad (5)$$

Where, SR_T is the total substitution ratio (representing the grafting at both C_2 and C_3 of *XylP*), *XylP* (Total) is the total xylose residues (grafted and un-grafted), and $XylP_{(Grafted)}$ represents the grafted fraction of xylose repeating units.

On the contrary, in order to investigate the SR at C_2 and C_3 separately, equations (6) and (7) can be used:

$$SR_2 = \frac{I(H_{2g})}{I(H_2 + H_{2g})} \quad (6)$$

$$SR_3 = \frac{I(H_{3g})}{I(H_3 + H_{3g})} \quad (7)$$

However, since the protons H_3 and H_{3g} are overlapped with other protons, the SR_3 could be presented as follows:

$$SR_3 = 2SR_T - SR_2 \quad (8)$$

Where, SR_2 and SR_3 are the substitution ratio at C_2 and C_3, respectively.

The conversion yield (CY) representing the efficiency of the grafting reaction indicated by the percentage converted into the copolymers, can be established as follows:

$$CY(\%) = \frac{MF_{(Relative)}}{MF_{(Expected)}} \times 100 \quad (9)$$

Actually, MF is the mole fraction, defined as:

$$MF_{(Relative)} = \frac{m_{1(Relative)}}{m_{2(Relative)}} \quad (10)$$

$$m_{1(Relative)} = \frac{I(\alpha + \alpha')}{2} \quad (11)$$

$$m_{2(Relative)} = I\left(H_1 + H_{1g}\right) \quad (12)$$

Where, m_1 is the relative mole number of Cl monomers, and m_2 is the relative mole number of xylose repeating units in hemicellulose chain.

The DP, SR_T, SR_2, SR_3, and CY were indicated in Table 1. The increase in the molar ratio of CL relative to *XylP* from 1.1 to 2.6 induces a significant increase in the DP (from 1.82 to 4.26), SR_T (0.51 to 0.69, with higher substitution at C_3 to that of C_2) and CY(63.2 to 75.1%). This can be attributed probably to the increase in the compatibility of the reaction components and the mobility of the reactants. Indeed, the higher concentration of grafting agent will provide a greater availability of caprolactone molecules at the proximity of the hemicellulose chains. The hydroxyl

groups of the hemicellulose molecules are immobile and their reaction with caprolactone depends on the availability of the grafting agent in the vicinity of the hydroxyl groups [39].

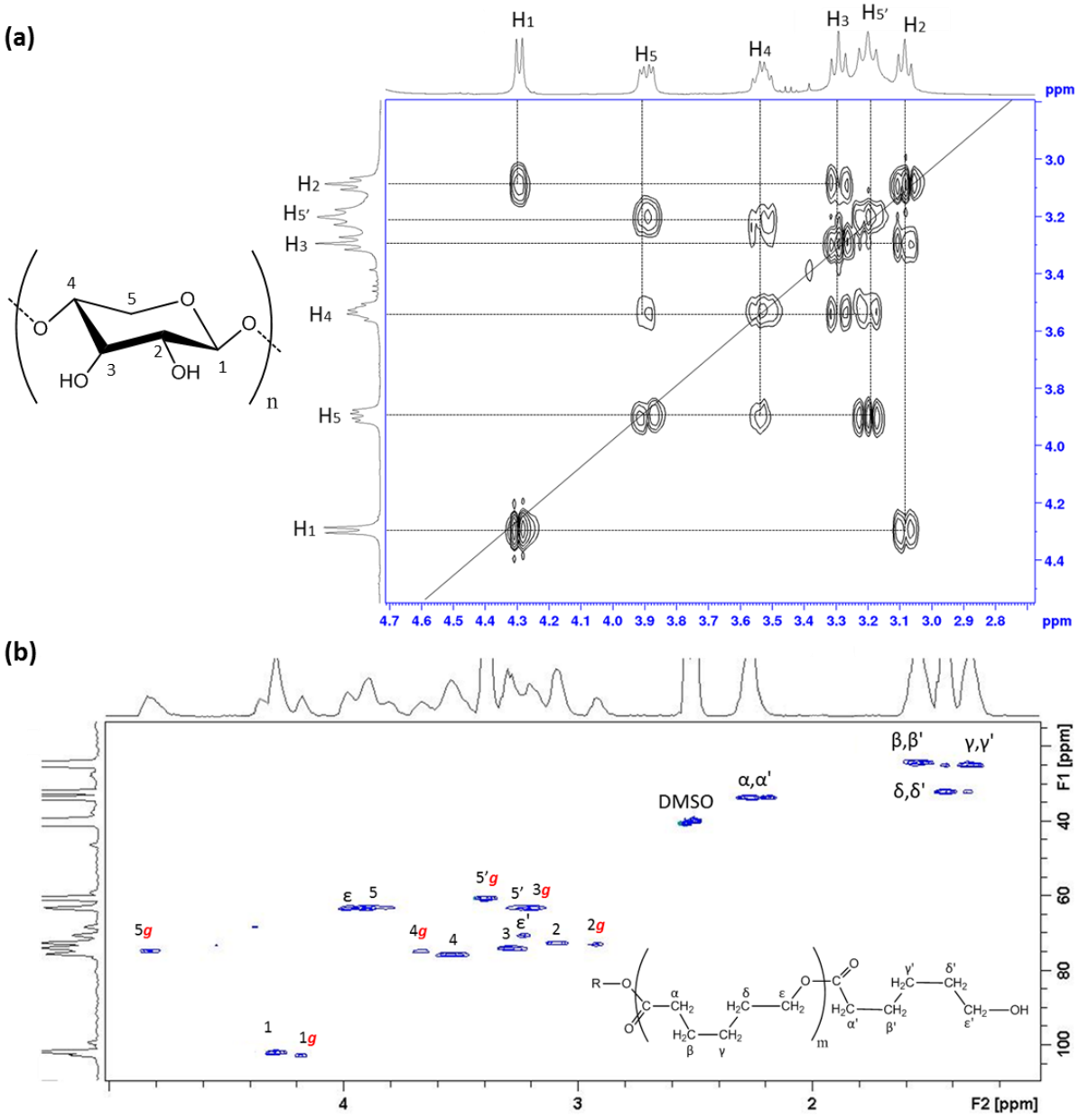

Figure 5. 2D NMR spectra. (a) ^{1}H-^{1}H COSY spectrum of pure hemicellulose, (b) ^{1}H-^{13}C HSQC spectrum of HCgPCL-2 (DP 3.35, SR_T 0.62) copolymer

These results show that the graft efficiency is sensitive to reaction conditions (molar ratios of the reactants). Our results are significantly higher than the findings of Zhang *et al.* [40] in which he reported the grafting of caprolactone onto xylan in dual polar aprotic solvents (N,N-

dimethylformamide/lithium chloride (DMF/LiCl), N,N-dimethylacetamide/LiCl (DMAc/LiCl), and 1-methyl-2-pyrrolidinone/LiCl (NMP/LiCl)). In that research, the PCL grafted hemicelluloses show a low SR (0.01–0.55) and a low DP (1.00–1.54) [39].

In contrast, the additional increase of the molar ratio from 2.6 to 6.5 results in a reduction of DP, SR_T, and CY. This reduction was probably due to a fast homo-polymerization of PCL compared with graft polymerization onto the hemicellulose under the high molar ratio. Furthermore, the differences in the CY among the series of grafts can be also attributed to experimental errors such as product loss during washing or incomplete precipitation. In fact, since the grafting reaction did not proceed to give a relatively high SR, then unreacted or partially grafted hemicelluloses were obtained [41]. Moreover, the SR at C_2 (SR_2) is significantly lower than that of SR at C_3 (SR_3), suggesting that the reactivity of C_3 hydroxyl groups in the xylan type hemicellulose toward ring-opining graft polymerization is higher than that of C_2 hydroxyl group. Our results are in agreement with Zhang *et al.* [40] findings in which C_2 hydroxyl group exhibited a lower PCL content than C_3.

3.4. Molecular weights

The molecular weights (M_n) of hemicellulose and its derivatives were determined by GPC (Table 2). Our results indicated that the M_n is influenced by the DP and the SR of the grafts. The M_n of the extracted unmodified hemicellulose is 9,200 g/mol. Grafting of PCL onto hemicellulose shows a significant increase of the M_n that is proportional to the increase in the DS and SR hence, providing a further indication of the success of the grafting reaction. The M_n of HC_gPCL-1 (DS 1.82, SR_T 0.51) is 17,500 g/mol increases to 30,000 g/mol in case of HC_gPCL-3 (DS 4.26, SR_T 0.69). In contrast, HC_gPCL-4 shows a reduction in the M_n (M_n 20,900 g/mol) compared to the other grafted materials, influenced by a reduction in the DP (DP3.11) and SR_T (SR_T 0.50). The single elution peak revealed a complete removal of PCL homopolymer.

All of the M_n of grafted materials that were produced were lower than the expected M_n based on the original hemicellulose molecular weight and the independently measured DP and SR_T. Table 2 shows the estimated and actual measured results. Note that the GPC measured molecular weight

is confounded since GPC is most sensitive to the radius of gyration of the polymer; grafting adds weight to the molecule but does not necessarily increase radius of gyration as would increase the length of the backbone of the polymer.

Table 2. Estimated and actual measured molecular weight results. n.a: not applicable

	Hemicellulose (DP 0.0)	HC_gPCL-1 (DP 1.82)	HC_gPCL-2 (DP 3.35)	HC_gPCL-3 (DP 4.26)	HC_gPCL-4 (DP 3.11)
$M_{n(expected)}$ (g/mol)	n.a	24,200	42,500	56,000	34,000
$M_{n(measured)}$ (g/mol)	9,200	17,500	22,100	30,000	20,900

Another possibility is that thermal degradation may have occurred during the grafting reaction at 110°C. Actually, others have reported that the continuous heating of hemicellulose may lead to its disaggregation, thus reducing its molecular weight [42]. Our results indicated that the continuous heating of the native hemicellulose (without any reactant) in solution at 110°C for 4h reduces its molecular weight from 9,200 to 7,000 g/mol.

3.5. Glass transition temperature (T_g)

The glass transition temperatures (T_g) of the hemicellulose and its derivatives (HC_gPCL copolymers) are reported in Figure 6 of the supporting information. The T_g is identified as the midpoint temperature of the transition region of the DSC curves. The results indicate that the un-grafted hemicellulose has a T_g of 144.9°C.

Grafting of PCL onto the hemicellulose molecule reduces the T_g of the system to 84.1°C (HC_gPCL-3). The reduction in the T_g was influenced by the DP and SR of the system. Indeed, hemicellulose is known to have numerous and strong inter and intramolecular hydrogen bonds that are created during the drying and the storage process of the isolated polysaccharide [43]. These hydrogen bonds induce the formation of crosslinks between the hemicellulose chains which in turn reduce

the chain mobility, forming stiffer chains which need higher energy to attain the molecular motion necessary for the glass transition and thus show a higher T_g [44].

Grafting of PCL with increasing SR and DP (longer grafted PCL chains), shows a lower T_g. PCL has been reported to have a T_g of -50°C [45]. Thus, when grafted onto hemicellulose (T_g 144.9°C), the system T_g is expected to be lower than that of pure hemicellulose as already governed by the Fox Law [46]. Furthermore, the more entanglements and ordered arrangement of PCL tails (with higher DP) will diminish the capability of hydrogen bonds formation and thereby reduce the system T_g. In this case, the grafted PCL tails seem to act as an "*internal plasticizer*" to the hemicellulose, forming a thermoplastic material [27]. The T_g values of the HC$_g$PCL copolymers revealed the possibility of subsequent melt-processing of these copolymers under mild conditions into bio-based plastic materials with suitable thermal tolerance.

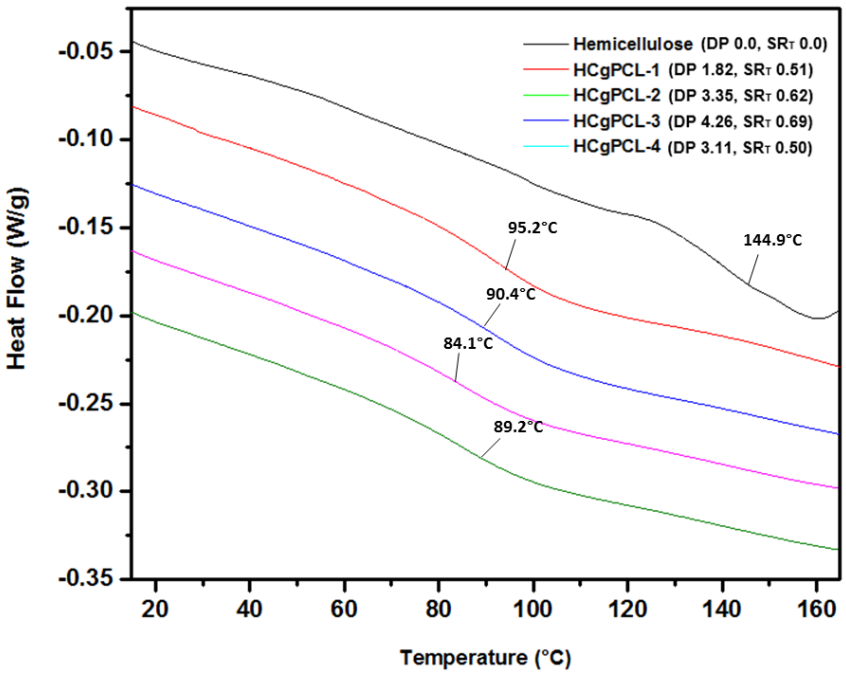

Figure 6. DSC curves of hemicellulose and its derivatives (10 ºC/min). Each curve has been shifted for clarity of presentation.

3.6. Thermal stability and decomposition analysis

The thermal stability of hemicellulose and its derivatives were evaluated by thermogravimetric analysis (TGA) and derivative thermogravimetry (DTG) in a temperature range from 30 to 500 °C under nitrogen atmosphere. The TGA/DTG curves are shown in Figure 2. The weight loss could be divided into three stages. In the first stage, a minor weight loss below 120 °C is explained by water loss. This represents about 11% (hemicellulose), 10% (HC$_g$PCL-1), 6% (HC$_g$PCL-2), 4% (HC$_g$PCL-3), and 4% (HC$_g$PCL-4) of the initial weight of the materials, respectively. These results confirm the increase in the hydrophobic properties of the PCL grafted hemicellulose. In the second stage, substantial weight loss occurs as a result of the material degradation. The materials start their thermal degradation (T_{onset}) at 220°C for hemicellulose, and 170°C for HC$_g$PCL copolymers (Figure 7a).

In addition, the maximum degradation rate temperature (T_{max}) was determined to be 315, 280, 300, 290, and 280°C of hemicellulose, HC$_g$PCL-1, HC$_g$PCL-2, HC$_g$PCL-3, and HC$_g$PCL-4, respectively. In fact, T_{max} of the hemicellulose seems to be reduced after PCL grafting. The T_{max} decreases with respect to DP and SR. In the last stage, the subsequent marginal weight loss at high temperature, indicating the pyrolysis residues at 500 °C was 23, 20, 17, 23, and 18% for hemicellulose, HC$_g$PCL-1, HC$_g$PCL-2, HC$_g$PCL-3, and HC$_g$PCL-4, respectively.

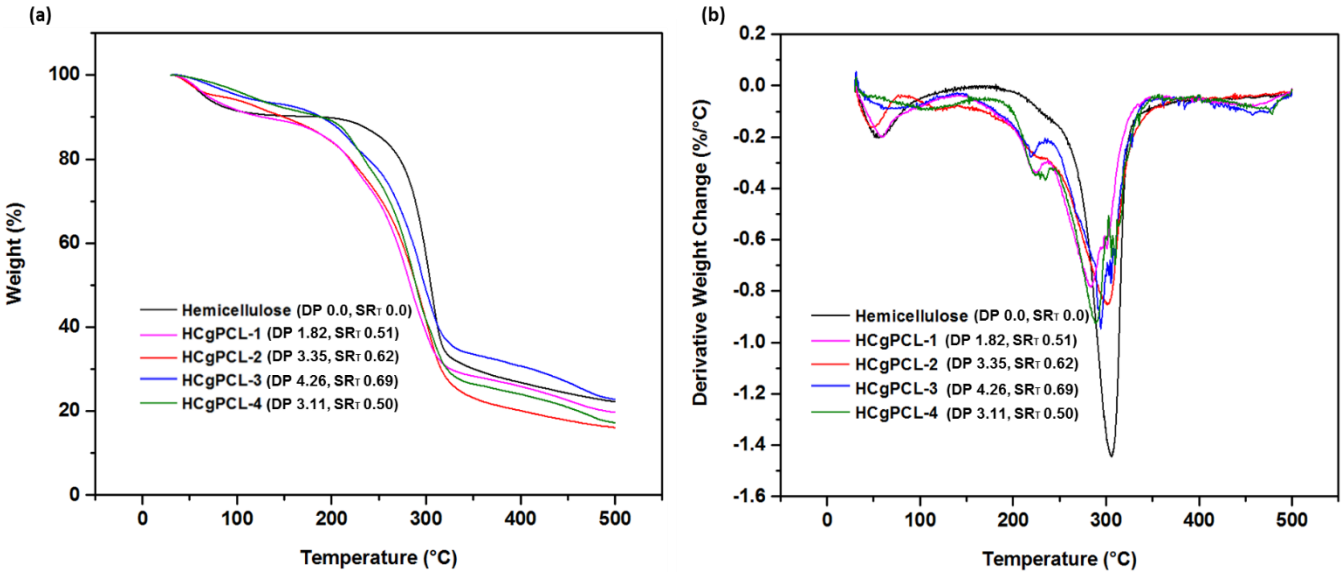

Figure 7. Thermogravimetric results of hemicellulose and its derivatives. (a) TGA curves, and (b) DTG curves.

Our results indicated that the T_{onset} and T_{max} of HC_gPCL copolymers are lower than those of the unmodified hemicellulose. The increased PCL grafting actually induces a reduction of both T_{onset} and T_{max}, providing a clear indication of the reduction in the thermal stability after grafting. The reduced thermal stability of hemicellulose derivatives can be explained by the incorporation of PCL sidechains onto the hemicellulose backbone, which will break the H-bonding between hemicellulose chains, thereby lead to a reduction in the thermal stability [47].

Furthermore, the degradation (second stage) proceeds in one step for hemicellulose and in two steps for HC_gPCL copolymers, indicated by the two peaks in the DTG traces (Figure 7b). This observation can be attributed probably to the different decomposition temperatures of PCL side chains and hemicellulose backbone. Actually, the decomposition proceeding at about 225°C is probably attributed to the decomposition of PCL sidechains, while the degradation at about 310°C is probably due to the degradation of hemicellulose main chains [48].

In order to further investigate the mechanism of the thermal decomposition of hemicellulose and its derivatives, the gases produced from heating the materials (by TGA) were characterized by FT-IR spectroscopy. A representative 3D spectrogram from the TGA-IR is depicted in Figure 8. This diagram provides related information both as a function of wavenumber and temperature. The produced gases can be identified by the distinctive wavenumber peaks, while the yield history of the off-gasses can be determined by the absorbance against temperature.

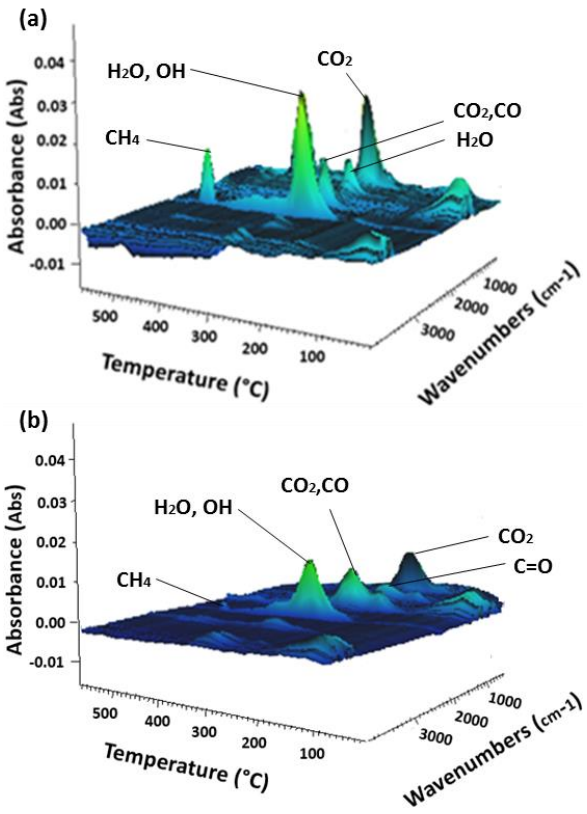

Figure 8. Corresponding gas absorption profile. (a) Native hemicellulose, and (b) HC_gPCL-3 (DP 4.26, SR_T 0.69) copolymer.

In agreement with the DTG curves, the majority of the gases were obtained between 200 and 400°C, confirming the decomposition of the materials in this range of temperatures. Figure 8a indicated that the native hemicellulose decomposition produces absorption profiles for H_2O, CH_4, CO_2, and CO. The absorption peaks at 3200 and 1400 cm^{-1} are attributed to the OH groups of water and alcohols. The absorption peaks of CO_2 were assumed to be at 2340 and 670 cm^{-1}. At higher temperatures, during charring reactions, a relatively high concentration of methane gas (CH_4) was produced (3100 cm^{-1}). Our results are in agreement with the findings of other research groups [49][50] in which they performed a detailed study of the thermal degradation mechanism of hemicellulose. On the contrary, HC_gPCL-3 copolymer shows a similar absorption gas profile to that of the native hemicellulose but with an additional absorption peak at 1765 cm^{-1} (Figure 8b) attributed to the carbonyl function of a carboxylic acid produced by pyrolysis of the grafted PCL ester functions [51]. Moreover, a significant reduction in the absorption band of water (3200 and

1400 cm^{-1}) in case of HC_gPCL-3 compared to the native hemicellulose, provides a further confirmation of the increased hydrophobicity of the HC_gPCL copolymers.

3.7. Film formation: Mechanical properties

Hemicellulose derivatives were studied for their film formation capability by compression molding. Unmodified hemicellulose did not form a continuous film probably due to its cross-linked nature favored by H-bonding [52]. In contrast, all the HC_gPCL copolymers show a strong ability towards film formation explained by the "*internal plasticization effect"* of the grafted PCL tails (Figure 9).

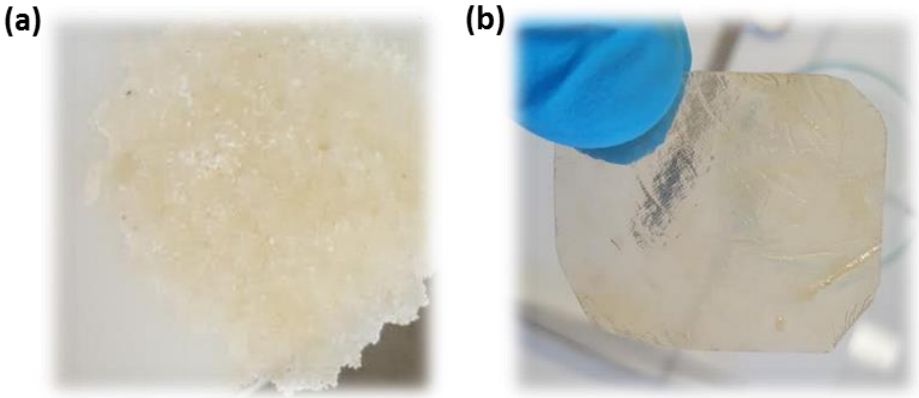

Figure 9. Film formation abilities as prepared using a manual press compression mold at 100° C. (a) native hemicellulose was not able to form a continuous film and (b) PCL grafted materials were able to form a continuous and flexible film materials

Tensile tests were performed on the various HC_gPCL copolymer films to estimate their mechanical properties in terms of tensile strength, Young's modulus, and elongation at break (Figure 10). The results revealed an extraordinary dependence of the mechanical properties on the DP and SR_T of the graft copolymers. HC_gPCL-1 (DP 1.82, SR_T 0.51) shows a tensile strength of 15.4 N/m^2, Young's modulus of 358 N/m^2 and elongation at break of 11.5%. The enhanced mechanical performance compared with pure hemicellulose (that was not able to form a continuous film) could be attributable to the thermoplastic nature of the PCL grafted materials which formed a melt that

allowed HC$_g$PCL polymer chains to diffuse past one another and upon cooling formed a continuous phase of entangled and interacting polymer chains. The increase in the DP and SR$_T$, in case of HC$_g$PCL-3 (DP 4.26, SR$_T$ 0.69), shows a reduction in both the tensile strength and Young's modulus of the films (3.9 and 67 N/m^2, respectively), while the elongation at break increased to 40%.

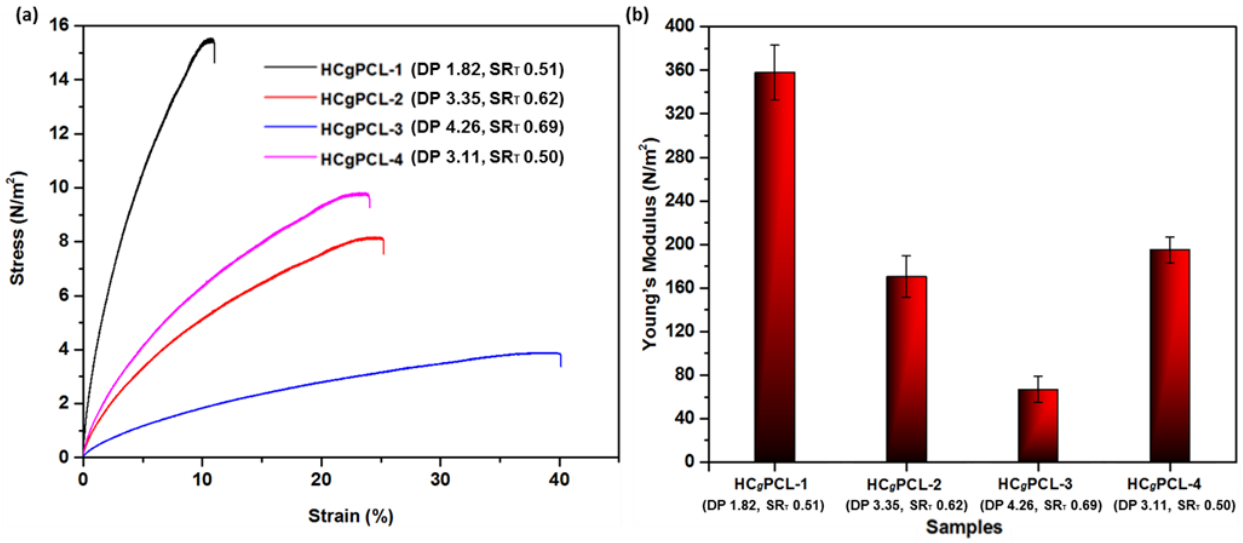

Figure 10. Mechanical properties of HC$_g$PCL films. (a) Stress-strain curves and (b) Young's modulus.

Furthermore, the existence of more and longer PCL tails (reflected by higher SR$_T$ and DP) will display an increased plasticizing effect and an increased ability to entangle intermolecularly which allows the film to be stretched to a higher extent. Strongly intermolecularly hydrogen bonded polymers do not show high elongation. Pure PCL displays rubber-like characteristics reflected by a low elastic modulus, low tensile strength, and high elongation at break. Actually, PCL grafting onto hemicellulose could improve the mechanical performance of the grafted copolymers. The increased DP and SR of the copolymer triggers a reduction of both the tensile strength and Young's modulus and an increase in the elongation at break of the films since the system under load can be considered to be a series of soft segments (PCL side chains) connected together between hemicellulose chains.

3.8. Films hydrophobic properties

The water contact angles of hemicellulose derivatives were examined as a function of time (Figure 11). The results revealed that the contact angle between the water droplet and copolymer films surface increases with the increase of DP and SR_T. For instance, HC$_g$PCL-1 (DP 1.82, SR_T 0.51) shows an average contact angle of 61° which increases to 81° in case of HC$_g$PCL-3 (DP 4.26, SR_T 0.69). It is anticipated that grafting of PCL onto hemicellulose backbone will influence the hydrophobic properties of the copolymer, which in turn can affect the contact angle and/or the adsorption of a water droplet [53].

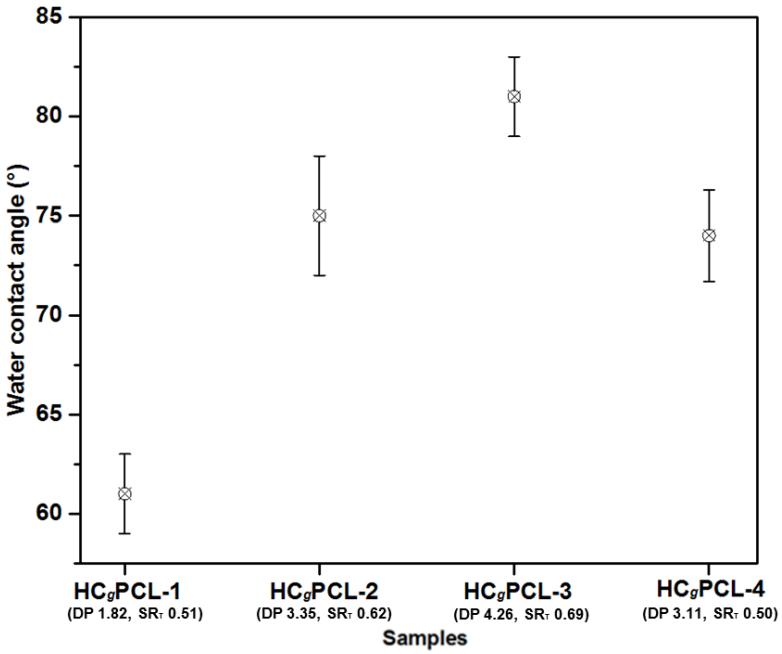

Figure 11. Water contact angle of HC$_g$PCl copolymer films collected at t=5s post contact of the water droplet with the copolymer film.

Contact angles can be influenced by two main features: polarity and surface roughness. Upon evaluating the static contact angles with water, nonpolar surfaces result in higher angles due to forces of repulsion [54]. Our results verify that the copolymer films with increased DP and SR_T show an increased hydrophobicity. Moreover, our results are in agreement with the finding of

Lönnberg et al. [55] in which the grafting of cellulose fibers with PCL increases the water contact angle of the cellulose-based material.

3.9. Biodegradability

In order to investigate the ecological impacts of the synthesized bio-based plastic materials, the kinetics of aerobic biodegradation of unmodified hemicellulose and its derivatives are depicted in Figure 12. All the studied materials exhibit a very high ultimate biodegradability ranging between 95.3-99.7% after 28 days of analyses. The predominate biodegradation of the hemicellulose and its derivatives is attributed to the activity of the different enzymes secreted by the diverse microorganism consortium presented in the activated sludge [56]. Our results are relatively higher than the findings of Cho et al. [57] in which they reported that the degradability of starch-PCL blend can reach a maximum of 88% under aerobic conditions.

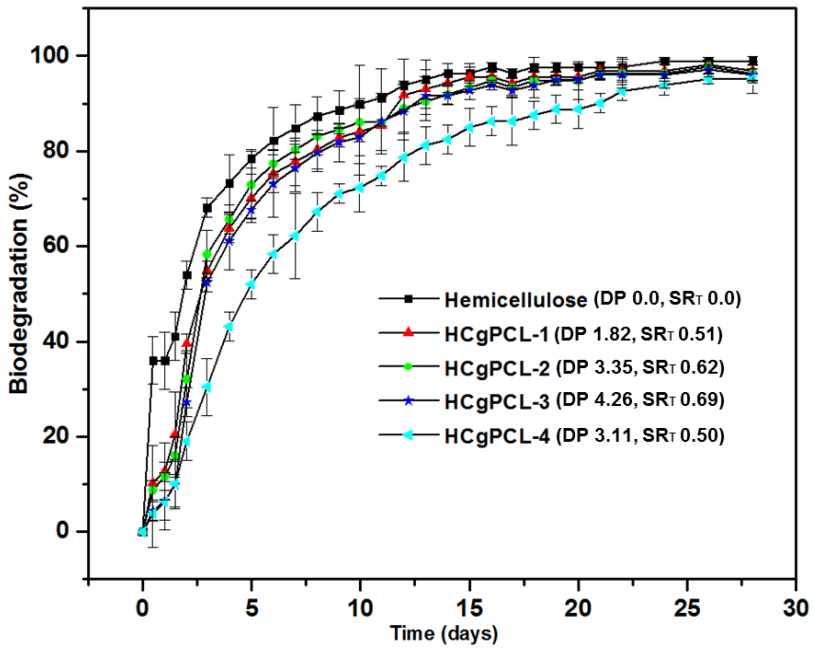

Figure 12. Evaluation of the ultimate aerobic biodegradability hemicellulose and its derivatives according to ISO 14,851 standard.

Furthermore, our results indicated a similar trend of the biodegradation of pure hemicellulose and its derivatives but with a higher degradation of unmodified hemicellulose at the first day of the assessment. The microorganisms presented in the activated sludge are probably more tolerant to pure hemicellulose than PCL. The presence of PCL will require the microorganisms to tolerate and then discharge the enzymes required for the combined degradation of PCL and hemicellulose. Moreover, the PCL content of the synthesized materials does not show a significant difference in the biodegradation properties of the copolymers.

The sample HC_gPCL-4 has the lowest biodegradability kinetics compared with the pure hemicellulose and the other copolymers. This can be attributed probably to the activity of the enzymes required to degrade the PCL. The enzymes secreted by the microorganisms to degrade the PCL have a slower activity than those required to degrade the hemicellulose. Thus, the materials show a slower biodegradability kinetics with higher PCL content. The increase in the DP and SR can reduce the kinetics of the biodegradability but not affect the final biodegradable properties of the designed HC_gPCL materials

In addition, the extracted and unmodified hemicellulose and the aliphatic polyester (PCL) were subjected to biodegradability tests. In fact, hemicellulose is entirely biodegradable under a vast variety of environmental conditions [58]. Also, in nature, the microorganisms can easily degrade PCL as a typical aliphatic polyester [57]. Hence, the combination of such polymers by the grafting of PCL onto hemicellulose can act as an alternative to the conventional thermoplastics and display an advanced technology in renewable and sustainable materials to reduce the environmental impacts produced by the current plastic wastes. Finally, additional studies are required to demonstrate the detailed mechanism and the properties of the degradation processes of HC_gPCL copolymer in order to have a full assessment of its biodegradability.

4. Conclusion

Thermoplastic hemicellulose materials were designed by ring-opening graft polymerization of caprolactone. In the current study we have reported the chemistry, syntheses, and characteristics of hemicellulose-graft-poly-(ε-caprolactone) prepared in solution using TBD as an organic catalyst. PCL was successfully grafted onto hemicellulose with various ranges of SR_T and DP adjusted by varying the molar ratios of the reactants, resulting in a maximum SR_T of 0.69 and DP of 4.26 at 1:2.6 molar ratio of *Xylp:CL*. The thermochemical properties of the grafted copolymers showed that the PCL grafts can act as an *internal plasticizer* and transform hemicellulose to a *thermoplastic material* with a T_g that ranges from 84.1 and 95.2 °C. The copolymers were able to form continuous films with good mechanical properties. The tensile test indicated that the tensile strength and Young's modulus of the copolymers decreased with the increase of SR_T and DP while the elongation at break increases. Furthermore, HC_gPCL-3 copolymer that exhibit the highest grafting efficiency reflected by the highest SR_T and DP also showed the highest hydrophobic nature, as confirmed through contact angle measurement. Finally, the synthesized materials exhibit high biodegrability and are exciting starting materials for the bioplastic and other industries.

References

[1] M.M. Bugge, T. Hansen, A. Klitkou, What is the bioeconomy? A review of the literature, Sustain. 8 (2016). doi:10.3390/su8070691.

[2] Bioeconomy council of the German Government, What is Bioeconomy?, (2017). http://biooekonomierat.de/home-en/bioeconomy.html.

[3] J.S. Golden, R.B. Handfield, J. Daystar, T.E. McConnell, An Economic Impact Analysis of the U.S. Biobased Products Industry: A Report to the Congress of the United States of America, (2015) 127. doi:10.13140/RG.2.1.2805.3603.

[4] T.S. Khoo, M.M. Ratnam, S. a. B. Shahnaz, H.P.S. Abdul Khalil, Wood Filler-recycled Polypropylene (WF-RPP) Composite Pallet: Study of Fastening Method, J. Reinf. Plast. Compos. 27 (2008) 1723–1731. doi:10.1177/0731684407087379.

[5] S.H. Alavi, B.K. Gogoi, M. Khan, B.J. Bowman, S.S.H. Rizvi, Structural properties of protein-stabilized starch-based supercritical ¯ uid extrudates, 32 (1999) 107–118.

[6] IEA Bioenergy, Bio-based Chemicals Value Added Products from Biorefinerie, (2012). www.ieabioenergy.com.

[7] S. Herrera, Industrial biotechnology—a chance at redemption, Nat. Biotechnol. 22 (2004) 671–675. doi:10.1038/nbt0604-671.

[8] W. Farhat, R.A. Venditti, M. Hubbe, M. Taha, F. Becquart, A. Ayoub, A Review of Water-Resistant Hemicellulose-Based Materials: Processing and Applications, ChemSusChem. 10 (2017) 305–323. doi:10.1002/cssc.201601047.

[9] T. Shahzadi, S. Mehmood, M. Irshad, Z. Anwar, A. Afroz, N. Zeeshan, U. Rashid, K. Sughra, Advances in lignocellulosic biotechnology : A brief review on lignocellulosic biomass and cellulases, Adv. Biosci. Biotechnol. 5 (2014) 246–251.

[10] Z. Anwar, M. Gulfraz, M. Irshad, Agro-industrial lignocellulosic biomass a key to unlock the future bio-energy: A brief review, J. Radiat. Res. Appl. Sci. 7 (2014) 163–173. doi:10.1016/j.jrras.2014.02.003.

[11] L. Christopher, Adding Value Prior to Pulping : Bioproducts from Hemicellulose, Glob. Perspect. Sustain. For. Manag. (2012). doi:10.5772/2634.

[12] F. Peng, J.L. Ren, F. Xu, J. Bian, P. Peng, R.C. Sun, Comparative study of hemicelluloses obtained by graded ethanol precipitation from sugarcane bagasse, J. Agric. Food Chem. 57 (2009) 6305–6317. doi:10.1021/jf900986b.

[13] L.M. Ferreira, L. Blanes, A. Gragnani, D.F. Veiga, F.P. Veiga, G.B. Nery, G.H.H.R. Rocha, H.C. Gomes, M.G. Rocha, R. Okamoto, Hemicellulose dressing versus rayon dressing in the re-epithelialization of split-thickness skin graft donor sites: a multicenter study, J. Tissue Viability. 18 (2009) 88–94. doi:10.1016/j.jtv.2009.06.001.

[14] A. Eduardo da Silva, H. Rodrigues Marcelino, M. Christine Salgado Gomes, E. Eleamen Oliveira, T. Nagashima Jr, E. Sócrates Tabosa Egito, Xylan, a Promising Hemicellulose for Pharmaceutical Use, Prod. Appl. Biopolym. (2012) 232. doi:10.5772/33070.

[15] W. Farhat, R. Venditti, N. Mignard, M. Taha, F. Becquart, A. Ayoub, Polysaccharides and lignin based hydrogels with potential pharmaceutical use as a drug delivery system produced by a reactive extrusion process, Int. J. Biol. Macromol. 104 (2017) 564–575. doi:10.1016/j.ijbiomac.2017.06.037.

[16] S. Daus, T. Heinze, Xylan-based nanoparticles: Prodrugs for ibuprofen release, Macromol. Biosci. 10 (2010) 211–220. doi:10.1002/mabi.200900201.

[17] C. Laine, A. Harlin, J. Hartman, S. Hyvärinen, K. Kammiovirta, B. Krogerus, H. Pajari, H. Rautkoski, H. Setälä, J. Sievänen, J. Uotila, M. Vähä-Nissi, Hydroxyalkylated xylans - Their synthesis and application in coatings for packaging and paper, Ind. Crops Prod. 44 (2013) 692–704. doi:10.1016/j.indcrop.2012.08.033.

[18] K.S. Mikkonen, M. Tenkanen, Sustainable food-packaging materials based on future biorefinery products: Xylans and mannans, Trends Food Sci. Technol. 28 (2012) 90–102. doi:10.1016/j.tifs.2012.06.012.

[19] X. Cao, X. Peng, L. Zhong, R. Sun, Multiresponsive hydrogels based on xylan-type hemicelluloses and photoisomerized azobenzene copolymer as drug delivery carrier, J. Agric. Food Chem. 62 (2014) 10000–10007. doi:10.1021/jf504040s.

[20] L.M. Ferreira, C.S. Sobral, L. Blanes, M.Z. Ipolito, E.K. Horibe, Proliferation of fibroblasts cultured on a hemi-cellulose dressing, J. Plast. Reconstr. Aesthetic Surg. 63 (2010) 865–869. doi:10.1016/j.bjps.2009.01.086.

[21] X. Zhang, H. Wang, C. Liu, A. Zhang, J. Ren, Synthesis of Thermoplastic Xylan-Lactide Copolymer with Amidine-Mediated Organocatalyst in Ionic Liquid, Sci. Rep. 7 (2017) 551. doi:10.1038/s41598-017-00464-6.

[22] X. Zhang, M. Chen, C. Liu, A. Zhang, R. Sun, Ring-opening graft polymerization of propylene carbonate onto xylan in an ionic liquid, Molecules. 20 (2015) 6033–6047. doi:10.3390/molecules20046033.

[23] C.G. Pitt, M. Chasin, A. Domb, E. Ron, E. Mathiowitz, R. Langer, K. Leong, C. Laurencin, H. Brem, S. Grossman, Polyanhydrides as Drug Delivery Systems, 1990. doi:10.1016/0223-5234(91)90162-G.

[24] Z. Terzopoulou, D. Baciu, E. Gounari, T. Steriotis, G. Charalambopoulou, D. Bikiaris, Biocompatible nanobioglass reinforced poly(ε-caprolactone) composites synthesized via in situ ring opening polymerization, Polymers (Basel). 10 (2018) 1–26. doi:10.3390/polym10040381.

[25] M.A. Woodruff, D.W. Hutmacher, The return of a forgotten polymer - Polycaprolactone in the 21st century, Prog. Polym. Sci. 35 (2010) 1217–1256. doi:10.1016/j.progpolymsci.2010.04.002.

[26] a. P. Pêgo, M.J. a. Van Luyn, L. a Brouwer, P.B. van Wachem, A. Poot, D.W. Grijpma, J. Feijen, In vivo behavior of poly(1,3-trimethylene carbonate) and copolymers of 1,3-trimethylene carbonate with D,L-lactide or epsilon-caprolactone: Degradation and tissue response., J. Biomed. Mater. Res. A. 67 (2003) 1044–1054. doi:10.1002/jbm.a.10121.

[27] P.R. Chang, Z. Zhou, P. Xu, Y. Chen, S. Zhou, J. Huang, Thermoforming starch-graft-polycaprolactone biocomposites via one-pot microwave assisted ring opening polymerization, in: J. Appl. Polym. Sci., 2009: pp. 973–2979.

[28] W. Farhat, R. Venditti, A. Quick, M. Taha, N. Mignard, F. Becquart, A. Ayoub, Hemicellulose extraction and characterization for applications in paper coatings and

adhesives, Ind. Crops Prod. 107 (2017) 370–377. doi:10.1016/j.indcrop.2017.05.055.

[29] F. Liebner, E. Haimer, M. Wendland, A. Potthast, T. Rosenau, Precipitation of hemicelluloses from DMSO/water mixtures using carbon dioxide as an antisolvent, J. Nanomater. 2008 (2008). doi:10.1155/2008/826974.

[30] S. Touhtouh, F. Becquart, C. Pillon, M. Taha, Effect of Compatibilization on poly-ε-caprolactone grafting onto poly(ethylene-co-vinyl alcohol), Polymers (Basel). 3 (2011) 1734–1749. doi:10.3390/polym3041734.

[31] B.Y. Colak, P. Peynichou, S. Galland, N. Oulahal, G. Assezat, F. Prochazka, P. Degraeve, Active biodegradable sodium caseinate films manufactured by blown-film extrusion: Effect of thermo-mechanical processing parameters and formulation on lysozyme stability, Ind. Crops Prod. 72 (2015) 142–151. doi:10.1016/j.indcrop.2014.12.047.

[32] X. Fu, C.-H. Tan, Mechanistic considerations of guanidine-catalyzed reactions, Chem. Commun. 47 (2011) 8210. doi:10.1039/c0cc03691a.

[33] L. Simón, J.M. Goodman, The mechanism of TBD-catalyzed ring-opening polymerization of cyclic esters, J. Org. Chem. 72 (2007) 9656–9662. doi:10.1021/jo702088c.

[34] B.A. Chan, S. Xuan, M. Horton, D. Zhang, 1,1,3,3-Tetramethylguanidine-Promoted Ring-Opening Polymerization of N-Butyl N-Carboxyanhydride Using Alcohol Initiators, Macromolecules. 49 (2016) 2002–2012. doi:10.1021/acs.macromol.5b02520.

[35] R. Sun, J.M. Lawther, W.B. Banks, Fractional and structural characterization of wheat straw hemicelluloses, Carbohydr. Polym. 29 (1996) 325–331. doi:10.1016/S0144-8617(96)00018-5.

[36] Y. Hishikawa, E. Togawa, T. Kondo, Characterization of Individual Hydrogen Bonds in Crystalline Regenerated Cellulose Using Resolved Polarized FTIR Spectra, ACS Omega. 2 (2017) 1469–1476. doi:10.1021/acsomega.6b00364.

[37] N.G. V Fundador, Y. Enomoto-Rogers, A. Takemura, T. Iwata, Syntheses and characterization of xylan esters, Polym. (United Kingdom). 53 (2012) 3885–3893. doi:10.1016/j.polymer.2012.06.038.

[38] F. Becquart, M. Taha, A. Zerroukhi, Y. Chalamet, J. Kaczun, L. Marie-France, ε-Caprolactone Grafting on a Poly(vinyl alcohol-co-vinyl acetate) in the Melt Without Added Initiator, J. Appl. Polym. Sci. 105 (2007) 2525–2531. doi:10.1002/app.

[39] R.C. Sun, J. Tomkinson, J.. Liu, Z.. Geng, Oleoylation of Wheat Straw Hemicelluloses in New Homogeneous System.pdf, Polym. J. (1999) pp 857_863.

[40] X. Zhang, M. Chen, C. Liu, A. Zhang, R. Sun, Homogeneous ring opening graft polymerization of caprolactone onto xylan in dual polar aprotic solvents, Carbohydr. Polym. 117 (2015) 701–709. doi:10.1016/j.carbpol.2014.10.061.

[41] R. Sun, J.M. Fang, J. Tomkinson, C.A.S. Hill, Esterification of hemicelluloses from poplar chips in homogeneous solution of N,N-dimethylformamide/lithium chloride, J. Wood Chem. Technol. 19 (1999) 287–306. doi:Doi 10.1080/02773819909349613.

[42] J.M. Fang, R. Sun, P. Fowler, J. Tomkinson, C.A.S. Hill, Esterification of wheat straw hemicelluloses in theN,N-dimethylformamide/lithium chloride homogeneous system, J. Appl. Polym. Sci. 74 (1999) 2301–2311. doi:10.1002/(SICI)1097-4628(19991128)74:9<2301::AID-APP20>3.0.CO;2-7.

[43] A. Ebringerová, T. Heinze, Xylan and xylan derivatives - Biopolymers with valuable properties, 1: Naturally occurring xylans structures, isolation procedures and properties, Macromol. Rapid Commun. 21 (2000) 542–556. doi:10.1002/1521-3927(20000601)21:9<542::aid-marc542>3.3.co;2-z.

[44] K.J. Zeleznak, R.C. Hoseney, The glass transition in starch, Cereal Chem. 64 (1987) 121–124. doi:10.1094/CCHEM.2002.79.1.138.

[45] S. Tiptipakorn, N. Keungputpong, S. Phothiphiphit, S. Rimdusit, Effects of polycaprolactone molecular weights on thermal and mechanical properties of polybenzoxazine, J. Appl. Polym. Sci. 132 (2015) 1–11. doi:10.1002/app.41915.

[46] F. Becquart, M. Taha, A. Zerroukhi, J. Kaczun, M.F. Llauro, Microstructure and properties of poly(vinyl alcohol-co-vinyl acetate)-g-caprolactone, Eur. Polym. J. 43 (2007) 1549–1556. doi:10.1016/j.eurpolymj.2006.12.035.

[47] C. Yan, J. Zhang, Y. Lv, J. Yu, J. Wu, J. Zhang, J. He, Thermoplastic cellulose-graft-poly(L-

lactide) copolymers homogeneously synthesized in an ionic liquid with 4-dimethylaminopyridine catalyst, Biomacromolecules. 10 (2009) 2013–2018. doi:10.1021/bm900447u.

[48] L. Song, Y. Yang, H. Xie, E. Liu, Cellulose Dissolution and in Situ Grafting in a Reversible System using an Organocatalyst and Carbon Dioxide, ChemSusChem. 8 (2015) 3217–3221. doi:10.1002/cssc.201500378.

[49] K. Werner, L. Pommer, M. Broström, Thermal decomposition of hemicelluloses, J. Anal. Appl. Pyrolysis. 110 (2014) 130–137. doi:10.1016/j.jaap.2014.08.013.

[50] Y. Ding, O.A. Ezekoye, S. Lu, C. Wang, Thermal degradation of beech wood with thermogravimetry/Fourier transform infrared analysis, Energy Convers. Manag. 120 (2016) 370–377. doi:10.1016/j.enconman.2016.05.007.

[51] O. Persenaire, M. Alexandre, P. Degée, P. Dubois, Mechanisms and Kinetics of Thermal Degradation of Poly(ε-caprolactone), Biomacromolecules. 2 (2001) 288–294. doi:10.1021/bm0056310.

[52] F.R.S. Mendes, M.S.R. Bastos, L.G. Mendes, A.R.A. Silva, F.D. Sousa, A.C.O. Monteiro-Moreira, H.N. Cheng, A. Biswas, R.A. Moreira, Preparation and evaluation of hemicellulose films and their blends, Food Hydrocoll. 70 (2017) 181–190. doi:10.1016/j.foodhyd.2017.03.037.

[53] A. Svärd, E. Brännvall, U. Edlund, Modified and thermoplastic rapeseed straw xylan: A renewable additive in PCL biocomposites, Ind. Crops Prod. 119 (2018) 73–82. doi:10.1016/j.indcrop.2018.03.067.

[54] J. Hartman, A.C. Albertsson, J. Sjöberg, Surface- and bulk-modified galatoglucomannan hemicellulose films and film laminates for versatile oxygen barriers, Biomacromolecules. 7 (2006) 1983–1989. doi:10.1021/bm060129m.

[55] H. Lönnberg, Q. Zhou, H. Brumer, T.T. Teeri, E. Malmström, A. Hult, Grafting of cellulose fibers with poly(ε-caprolactone) and poly(L-lactic acid) via ring-opening polymerization, Biomacromolecules. 7 (2006) 2178–2185. doi:10.1021/bm060178z.

[56] F. Jbilou, C. Joly, S. Galland, L. Belard, V. Desjardin, R. Bayard, P. Dole, P. Degraeve,

Biodegradation study of plasticised corn flour/poly(butylene succinate-co-butylene adipate) blends, Polym. Test. 32 (2013) 1565–1575. doi:10.1016/j.polymertesting.2013.10.006.

[57] H.S. Cho, H.S. Moon, M. Kim, K. Nam, J.Y. Kim, Biodegradability and biodegradation rate of poly(caprolactone)-starch blend and poly(butylene succinate) biodegradable polymer under aerobic and anaerobic environment, Waste Manag. 31 (2011) 475–480. doi:10.1016/j.wasman.2010.10.029.

[58] J. Pérez, J. Muñoz-Dorado, T. De La Rubia, J. Martínez, Biodegradation and biological treatments of cellulose, hemicellulose and lignin: An overview, Int. Microbiol. 5 (2002) 53–63. doi:10.1007/s10123-002-0062-3.

Chapter 6. Investigation of Stimuli-responsive Biomaterials: Synthesis and Characterization of Xylan-based Thermoreversible Networks

1. Introduction

Physically and chemically crosslinked polymeric materials "*gels*" are of great interest due to their outstanding mechanical and thermal properties [1]. In general, these materials, known as thermosets, are hardly deformable, they lack re-fabrication ability after their synthesis, and are not able to be reprocessed and repaired after fracture. This represents an important environmental and recycling concerns [2]. To overcome such issues, stimuli-responsive polymers have become a chief topic in the field of material science and engineering in the last several decades [3][4][5]. It is a strategy in which external stimuli (e.g. temperature, light, pH, etc.) are used to encourage the alteration in the polymeric structural features; for instance, the switch of a polymer due to temperature change between the crosslinked "*gel*" and non-crosslinked "*non-gel*" state is a typical example [6]. These materials can be used in many applications that include drug delivery [6][7], wound sealing [8] shape memory [9], and self-healing materials [10].

The reversible transition can provide a tunable processability of the polymeric materials. Based on the conditions, these materials exhibit either thermoplastic or thermosetting features. Temperature-dependent polymer crosslinking-decrosslinking can be performed by Diels-Alder reaction (DA) [11], which is the focus of this study. DA reaction is well entrenched in various domains of organic and material chemistry [12]. It is an organic reaction; specifically, a [4+2] cycloaddition, between a conjugated diene and a dienophile to form a substituted cyclohexene adduct. The reaction is typically favored when the diene and dienophile are engaged to electrodonor and electroattractive groups, respectively. Many have reported the use of furan/maleimide couple as a diene/dienophile system because of its good reactivity [10][13][14]. DA reaction is a very attractive chemistry mainly due to its thermoreversibility [12][15][16]. The temperature serves an important role in

determining the favored equilibrium direction. Generally, the forward DA condensation reaction dominates up to about 60 °C. However, the reverse backward decomposition of the DA (retro-DA (rDA)) predominate at above 100 °C [17].

Rheological properties are very promising to distinguish a gel, whose existence arises from chemical or physical cross-linking, from a vastly viscous non-gel material[19]. A gel is a solid-like material that can be examined by classical rheological methods. Oscillatory shear techniques are commonly used to analyze the rheological behavior of a gel. In fact, frequency sweep tests are frequently used to investigate the properties of a crosslinked material [20][21]. In a frequency sweep test, the materials are exposed to different frequency values at a constant stress and temperature and the storage (G') and loss (G") modulus are recorded as a function of frequency. The predominant modulus at a certain frequency will figure out whether the material seems to be elastic or viscous. For instance, a crosslinked material will present a marked elastic character even at very low frequencies, where G' is higher than G". In contrast, in the same range of frequencies, a lower G' than G" is an indication of a viscous solution or liquid-like material. However, experimental assessment to the very low frequencies data remains a tricky issue for such thermo-sensitive material and dynamic rheological data often reduces to information on local dynamics of the gel.

Creep-recovery is another rheological assessment method that can examine the dimensional stability of the polymeric materials by understanding their long-term viscoelastic deformation behavior under constant stress and temperature [22]. In the creep-recovery test, an instantaneous step in the creep phase raises the stress to a constant value for a certain duration of time and is then completely removed in the following recovery phase. The resulting strain is recorded as a function of time at a fixed temperature. The material will first show (in the creep phase) an immediate, elastic deformation (rubber behavior) followed by a transient behavior (retardation spectrum) and finally, for several samples, a steady flow of the material can be observed. In the following recovery phase, only the crosslinked elastic network will tend to recover completely while the viscoelastic uncrosslinked (or partially crosslinked) materials will recover only a part of the deformation, that is they will not show a complete strain recovery in the recovery phase [23].

In our work we decided to use creep tests to investigate the gelling and the thermoreversible behavior of the designed materials. We assumed that at low temperature (80°C) the samples will

exhibit a complete recovery due to the solid viscoelastic behavior of the fully crosslinked materials; however, at higher temperature (150°C) the tested specimens will lose part of their elastic behavior and will be converted to a liquid viscoelastic materials in response to the decrosslinking as induced by the opening of the DA adduct at such high temperature.

Gel point (GP) also known as the Sol-Gel Transition Point is the point where there is a sudden loss of flow due to unexpected alteration in viscoelastic properties from an initially liquid like state to a solid-like state. A well-known technique for investigating the GP is by evaluating the moment at which G′ and G″ cross each other in an oscillatory shear experiment with constant frequency[24].

Polymers from renewable resources have been attracting ever-increasing attention over the past two decades, principally for two reasons: the first being environmental concerns and the second being the realization that the fossil resources are soon to be depleted [25]. Hemicelluloses are debatably the second most abundant renewable component of lignocellulosic biomass after cellulose [25]. In the plant cell wall, hemicelluloses form a complex network by hydrogen bonds to cellulose and covalent bonds (mainly α-benzyl ether linkages) with lignin [26]. Unlike cellulose in which the monomer units are homogenous consisting of glucose residues, hemicelluloses are heterogeneous branched group of polysaccharides made up of pyranoses and furanoses sugar units.

Hemicellulose polymers contain xylans (arabinoxylans and 4-O-methyl-glucuronoxylans), galactomannans, glucomannans, β-D-glucans (3- and 4-linked), β-D-glucan-calluses (3-linked), and xyloglucans (4-linked β-D-glucans with attached side chains) [25][26]. Xylan is the most abundant hemicellulose, consisting of β-(1,4)-D-xylopyranosyl backbone [27]. It is estimated to count for one-third of all renewable organic carbon available on earth [28]. Despite its availability, xylan has not yet found broad industrial applications. In the paper industry, much of the xylan is discarded as a waste material during pulping, bleaching and other operations or used for energy [29]. However, in order to improve the value extracted from biomass, it would be beneficial to pre-extract hemicellulose prior to the pulping process and develop a number of bio-products. This could be an important part of a forest-based biorefinery that offers technologies enabling the conversion of biomass into a wide range of marketable materials [30].

In fact, the potential use of xylan in the plastic industry is one of the major concerns of the current research activity [31][32][33][34]. However, native xylan is not thermoplastic [35]. As other polysaccharides and hydroxyl rich polymers, xylan polysaccharide have strong inter and

intramolecular hydrogen bonds created during the drying and the storage process of the extracted polymer [36]. These hydrogen bonds can reduce the chain mobility and form stiffer chains that hinder water solubility and processability of this macromolecule for value-added applications. Xylan properties can be modified by introducing thermoplastic functions into its backbone. Its chemical modification by graft polymerization can reduce hydrogen bonds. The structural modification of xylan can enhance its thermal and mechanical properties [35][37]. In our recent reported work [38] we demonstrated that the modification of xylan by grafting small poly-(ε-caprolactone) (PCL) chains onto its backbone can reduce H-bonds and improve both the processability and the thermomechanical properties of the modified xylan.

To the best of our knowledge, xylan derivatives have not been crosslinked by DA reactions to create thermoreversible networks. Herein, we report the synthesis of xylan-based thermoreversible network by means of DA chemistry. Polymeric xylan was first converted into a thermoplastic material to enhance its processability. Xylan-g-PCL (thermoplastic xylan) was formed by the grafting of polycaprolactone (PCL) side chains onto the polymeric xylan via ring opening graft polymerization of ε-caprolactone. Xylan-g-PCL was then grafted by the diene (furan) moieties and allowed to form a thermoreversible network via the reaction with the bifunctional dienophile crosslinker (bismaleimide (BMI)) by means of DA reaction. The thermoreversibility of the designed materials can be addressed solely by controlling the temperature. Rheology and solubility tests were used to examine the temperature dependent reversibility of the designed materials

.

2. Experimental Part:

2.1. Materials

Maleic anhydride ≥ 99.0% (CAS 108-31-6), 2-Furanmethanethiol ≥ 97% (CAS 98-02-2), Triflic acid 98% (CAS 1493-13-6), Hexylamine 99% (CAS 111-26-2), and Acetone ≥ 99.9% (CAS 67-64-1) were obtained from Sigma-Aldrich. Xylan type hemicellulose was isolated from bleached hardwood using 10% NaOH treatment to recover a pure xylan with 11% average percent yield based on the original pulp mass. The recovered xylan has an average M_n of 9200 g/mol as

determined by GPC [31], and with about 90% xylose content as determined by sugar compositional analysis.

2.2.Analysis techniques

2.2.1. Proton Nuclear magnetic resonance (^{1}H NMR)

^{1}H NMR analysis was recorded using Bruker Avance II spectrometer with a frequency of 400 MHz equipped with a 5 mm multinuclear broad band probe (BBFO+) with a z-gradient coil. The samples (30 mg) were dissolved in DMSO-d6 (1 mL) and the spectra were recorded at 25°C with 128 scans. Chemical shifts, in ppm were expressed relative to the resonance of tetramethylsilane TMS (δ = 0 ppm). For samples S-10, S-20, S-30, and S-40, 1 drop of TFA (Trifluoroacetic Acid) was added to shift the labile protons to lower fields.

2.2.2. Size Exclusion Chromatography (SEC)

The molar masses of xylan-g-PCL and its furan-grafted derivatives were determined by SEC using DMSO as eluent (flow rate of 0.5 mL/min, 70°C). The analysis was performed on a Malvern Viscotek HT GPC 350 system equipped with refractive index (RI) and viscometer detectors. PSS-GRAM columns with a range of 100–1000000 g/mol were used. Molecular weights were calculated referring to a universal calibration with pullulan polysaccharide standards.

2.2.3. Film preparation

Films for mechanical testing were prepared using a hydraulic manual press compression mold. The materials were loaded into a square Teflon board and subsequently compression molded under 100 bar for 2 min and then under 200 bar for 5 min at the molding temperatures of 160°C. After molding, the specimens were cooled at room temperature. The materials were stored for five days at room temperature prior to the mechanical assessment to allow the re-crosslinking via the DA

chemistry. The thickness of the obtained films was 0.2–0.4 mm. Measurements of the thickness of the films did not show any significant difference.

2.2.4. Mechanical tensile properties

Mechanical tensile testing of the films (35×4×0.3mm) was conducted at room temperature using a Shimadzu Autograph AG-500A (Shimadzu Corporation, Kyoto, Japan). A crosshead speed of 10 mm/min and a 12 mm distance between grips were the parameters used. Five independent measurements were collected and standard deviation were calculated.

2.2.5. Hydrolytic degradation test

The hydrolytic degradation of the designed materials was studied by immersing the pre-weighed samples into 10 mL of phosphate buffer solution PBS (pH 7.4) at 37°C (similar to physiological conditions) and mass loss versus time was determined. Prior to the immersion, the materials were conditioned to a minimum weight at 37°C in an oven with desiccant. Samples were removed at regular intervals: 5, 10, 20, and 33 days, being taken out of the solution and washed with distilled water, blotted on filter paper to remove excess solution on the surface, weighed and then dried under vacuum (0.2 mbar) at 40°C for 5 days, and weighed again, taking an average of three readings. The percentage weight loss of the material in PBS was determined according to the following equation:

$$\text{Weight loss } (\%) = \frac{W_i - W_f}{W_i} \times 100 \quad (1)$$

Where W_f is the final dry sample weight and W_i is the initial dry sample weight.

2.2.6. Rheological studies

The Dynamic rheological analysis was performed with an Advanced Rheometric Expansion System (ARES-G2) rheometer using a parallel-plate geometry with 8 mm diameter. The materials were first subjected to maturation tests to ensure the crosslinking DA equilibrium [32]. Maturation tests were done at 80°C for 2h, in the linear viscoelastic region, as measured earlier by strain sweep tests. Creep-recovery measurements were performed by exposing the test specimens to an applied stress of 500 Pa for 30 min followed by a recovery period of 80 min at an isothermal temperature.

Independent creep-recovery measurements were recorded at different temperatures (80 or 150°C). Temperature sweep experiments were done at a 1 rad/s frequency and a heating/cooling rate of 2°C/min.

2.3. Synthesis

2.3.1. Synthesis of xylan-grafted-poly(ε-caprolactone) (Thermoplastic xylan)

Xylan-g-PCL was synthesized via ring-opening graft polymerization (ROP) of ε-caprolactone onto xylan backbones. ROP is an attractive chemistry due to its efficiency and simplicity [33]. The ring opening of lactones can be initiated by the xylan hydroxyl groups with the help of a co-initiator. Oven-dried xylan (5.00 g) was poured into a 300 mL glass reactor (60 mm diameter, with a 3-necked steel cover, the steel cover anchor stirrer operating with IKA motor) containing 10 mL of DMSO solvent with silicon oil bath at 80 °C. The mixture was stirred at 60 rpm until a homogeneous and transparent viscous solution was obtained. The silicon oil bath temperature was then increased to 110 °C and the ε-caprolactone monomer (10 g) was introduced into the solution and mixed for 30 min. Then 1,5,7- triazabicyclodecene [4.4.0] catalyst (TBD, 1% of the total mass of the reactants) was introduced into the reaction mixture and the reaction was kept for 4 h under the flow of nitrogen gas. The solution was cooled at room temperature and precipitated in an excess volume of diethyl ether in an ice bath. The material was then subjected twice to solubilization/precipitation using alternatively DMSO and diethyl ether. The obtained material was poured into an aluminum pan and dried under vacuum (0.2mbar) at 60 °C for 2 days.

2.3.2. Synthesis of 3-((furan-2-ylmethyl)thio)dihydrofuran-2,5-dione (F-MA)

The diene molecule (F-MA) was synthesized based on the thiol-ene click chemistry. An equimolar mixture (6 mmol) of furfuryl mercaptan and maleic anhydride were poured into 50 mL three-necked flask containing 15 mL of acetone solvent. The reaction was launched by the addition of three drops of hexylamine catalyst at 25°C and kept overnight under stirring and nitrogen flow. The solvent was then evaporated at 45°C under 0.2 mbar pressure to recover a pure product. The

^{1}H NMR (400 MHz, DMSO-d_6) of F-MA is reported in Figure 1. Prior to reaction, maleic anhydride resonances were at 7.1 ppm (2H) and furfuryl mercaptan resonances were at δ ppm 7.6 (1H), 6.4 (1H), 6.2 (1H), 3.6 (2H). The labile proton was shifted to lower fields by adding one drop of TFA.

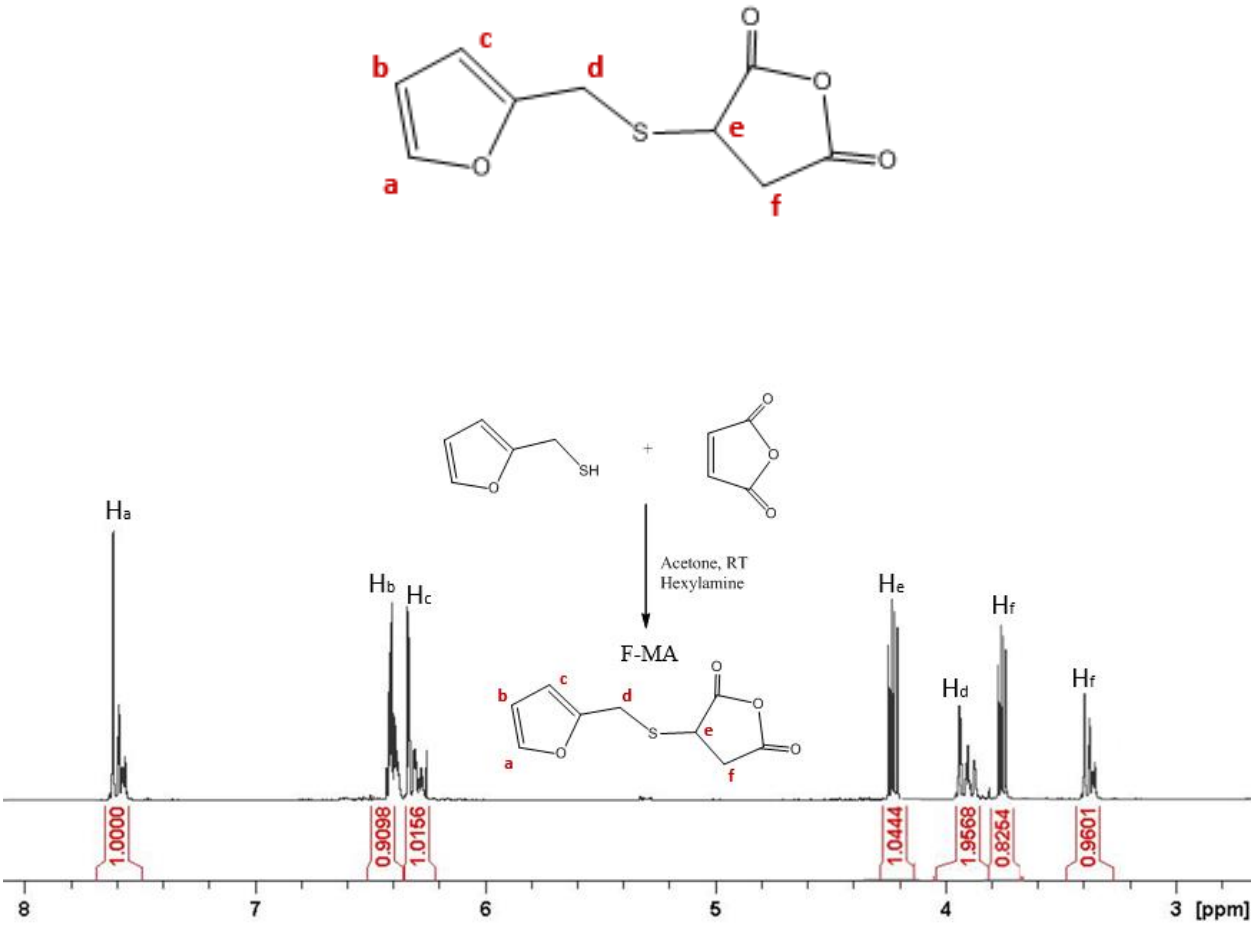

Figure 1. ^{1}H NMR spectrum of F-MA in DMSO-d_6 at 25°C and 400 MHz

2.3.3. Grafting of F-MA onto thermoplastic xylan

The grafting of the furan ring onto the xylan-g-PCL was performed according to the molar ratios of xylan-g-PCL:F-MA as listed in Table 1. Xylan-g-PCL (4.00 g) was poured into a 50 mL three-necked flask containing 20 mL of DMSO solvent at 50°C for 10 min. The F-MA was introduced

into the solution and mixed for 10 min. The reaction was initiated by the addition of 3-5 drops of trifluromethane sulfonic acid (Triflic acid) as catalyst and kept 90 min under a flow of nitrogen. The solution was cooled at room temperature and precipitated in cold ethanol. The materials were then washed with cold water and ethanol to entirely remove any unreacted F-MA. Finally, the obtained products were dried under vacuum (0.2 mbar) at 45°C for 2 days. The OH_{furan} (%) representing the theoretical molar percentage of the hydroxyl groups in the xylan-g-PCL bearing furan moieties are listed in Table 1.

Table 1. Molar ratio of xylan-g-PCL to F-MA

Sample	Molar ratio (Xylan-g-PCL/F-MA)	OH_{furan} (%)
HCgPCL	n.a.	0
S-10	1:7.4	10
S-20	1:14.8	20
S-30	1:22.2	30
S-40	1:29.6	40

S-X corresponds to FM-A grafted Xylan-g-PCL samples where X is the OH_{furan} (%) representing the theoretical molar percentage of the hydroxyl groups in the Xylan-g-PCL bearing furan moieties. n.a. is not applicable

2.3.4. Synthesis of 1,1'-(hexane-1,6-diyl)bis(1H-pyrrole-2,5-dione) (BMI)

The bifunctional dienophile (BMI) was synthesized as reported by our previous work [32]. It was obtained from the reaction between 1,6-diaminohexane with maleic anhydride in the presence of acetic anhydride, nickel acetate and triethylamine. The obtained molecule had a reaction yield of 85%. The ^{1}H NMR of BMI is reported in Figure 2.

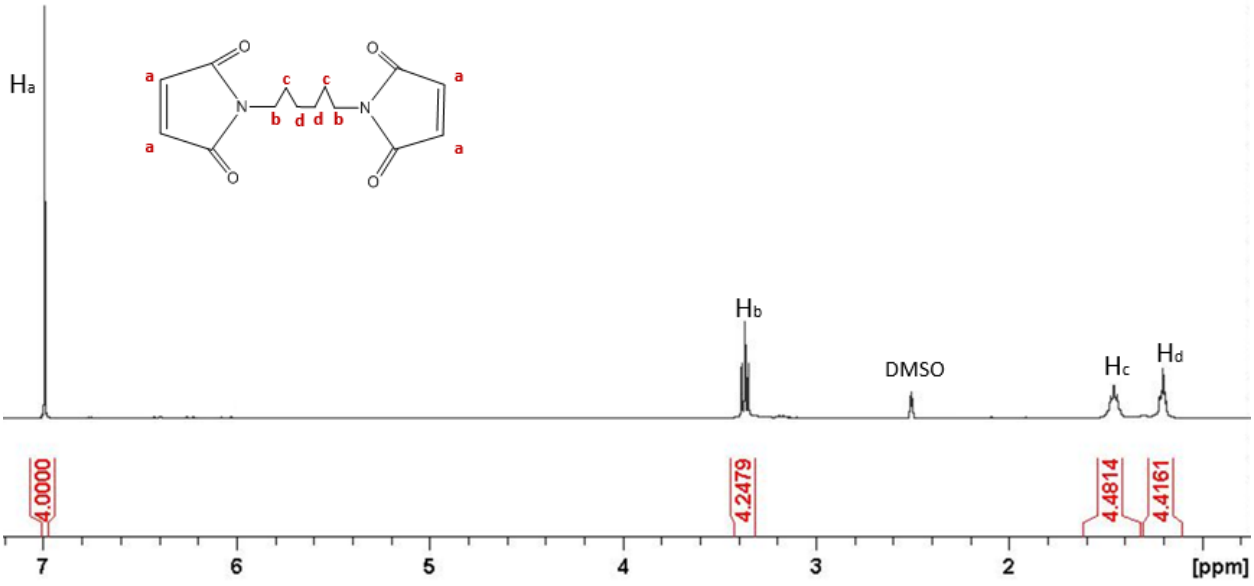

Figure 2. ^{1}H NMR signal of BMI in DMSO-d_6 at 25°C and 400 MHz

2.3.5. Synthesis of xylan-grafted-poly(ε-caprolactone) networks by Diels-Alder chemistry

The furan coupled xylan-g-PCL samples were crosslinked via Diels-Alder reaction using BMI. Stoichiometric amounts of furan functions and maleimide groups were used. Briefly, furan coupled xylan-g-PCL was poured into 50 mL three-necked flask containing 15 mL of DMSO under the flow of nitrogen at 80°C. The components were mixed until a homogeneous solution was obtained. The temperature was then reduced to 30°C and the BMI was added. The reaction was carried out

for 48 h. The obtained materials were washed with cold ethanol and cold water and then dried under vacuum (0.2 mbar) at 55°C for 2 days. These materials were labeled DA-10, DA-20, DA-30, and DA-40 in accordance with the labeling of the furan grafted polymers.

3. Results and Discussion

3.1.Synthesis of xylan-grafted-poly(ε-caprolactone)

In order to improve the processability of xylan, xylan-g-poly-(ε-caprolactone) copolymer was synthesized by ring opening graft polymerization of ε-caprolactone onto xylan polysaccharide (Figure 3) as described in our previous work [31]. PCL was successfully grafted onto xylan with an average PCL polymerization degree of 3.35, hemicellulose substitution ratio of 0.62, and an average molecular weight (M_n) of 22100 g/mol. This material was obtained by adjusting the molar ratio of the anhydroxylose repeating units (XylP) to ε-caprolactone (CL) monomers (XylP:CL) at 1:1.8. The grafting of PCL onto the xylan molecule reduces the T_g of the system from 144.9°C (unmodified xylan) to 84.1°C (PCL grafted xylan). Pure PCL has been reported to have a T_g of -50°C [44]. Thus, when grafted onto xylan, the system T_g is expected to be lower than that of pure xylan as already governed by Fox Law [45]. In fact, the ordered arrangement of grafted PCL tails will reduce the capability of xylan to form hydrogen bonds and thereby, act as an "*internal plasticizer*" to the xylan, forming a thermoplastic material. The detailed analysis of the structural and physicochemical properties of the synthesized xylan-g-poly-(ε-caprolactone) copolymer were reported in our previous work [31].

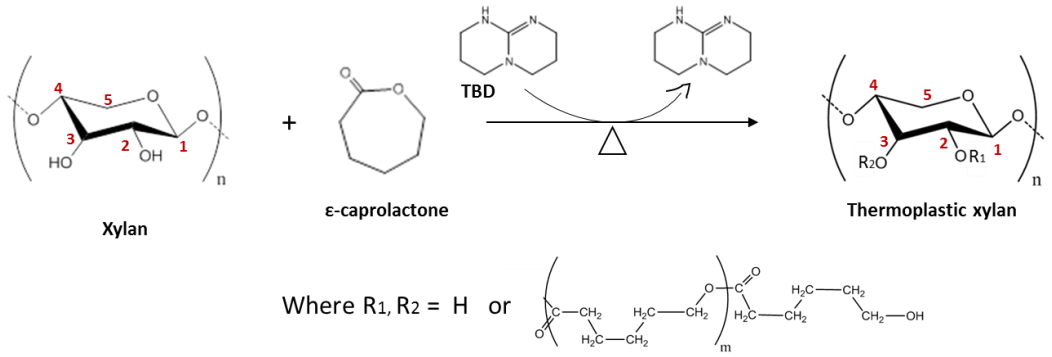

Figure 3. Synthesis of thermoplastic xylan (xylan-g-PCL) by ring-opening polymerization of ε-caprolactone onto xylan using TBD as an organic catalyst [31].

3.2.Grafting of furan onto the thermoplastic xylan

The furan ring was successfully grafted onto the xylan-g-PCL according to the reaction depicted in Figure 4. The hydroxyl groups of the xylan-g-PCL will react with the anhydride group of the furan ring via esterification reaction allowing the grafting of the furan onto the xylan-g-PCL. The furan rings can be grafted either onto free hydroxyl group of the xylan or onto the hydroxyl terminal of the grafted PCL tails. The amount of grafted furan is listed in Table 2. The grafting was confirmed by ^{1}H NMR (Figure 5).

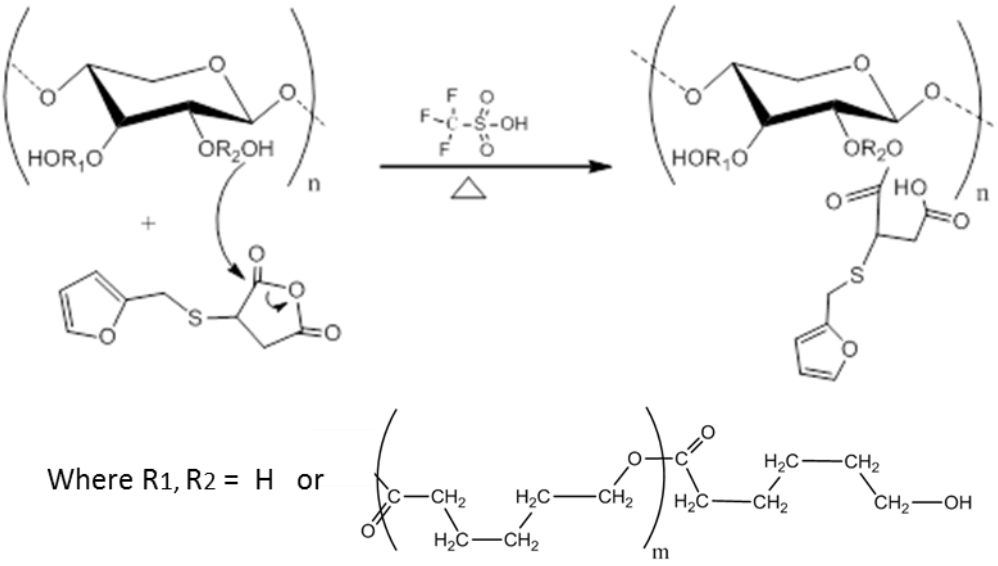

Figure 4. Grafting of the furan ring onto the xylan-g-PCL using triflic acid as catalyst.

Un-grafted F-MA were removed by extensive purification and hence, these remaining furan moieties are covalently linked to the xylan-g-PCL. All peaks were assigned: the resonances from 1-5.5 ppm are attributed to the xylan-g-PCL copolymer as discussed in our previous work [31]. The resonances between 6.2 and 7.8 ppm are assigned to the aromatic protons of the grafted furan rings (a, b, and c) [32][34]. The d, e, f, and f' resonances of the grafted furan are overlapped with the resonances of the xylan-g-PCL between 3.2 and 4.4 ppm. The molar percentage of the grafted furan can be estimated based on the ^{1}H NMR peak intensity of the corresponding resonances according to the following equation:

$$\mathrm{OH_{furan}}(\%) = \frac{\mathrm{OH_{furan}}}{\mathrm{OH_{Total}}} \times 100 = \frac{\mathrm{I(H_a)}}{2 \times \mathrm{I(H_2)_{Total}}} = \frac{\mathrm{I(H_a)}}{2 \times \mathrm{I(H_2 + H_{2g})}} \times 100 \quad (2)$$

Where, OH_{furan} (%) is the percentage of the hydroxyl groups in the xylan-g-PCL that are grafted with furan rings, OH_{Total} is the total number of hydroxyl groups in the xylan-g-PCL, and (I) is the

integral (area) of the selected proton. H_{2g} corresponds to the proton at PCL substituted C_2 of xylan and H_2 is the proton at C_2 of un-grafted xylan [31].

The furan functionality, representing the number of furan rings per polymer chain, can be established according to the following equation:

$$\bar{f}_{furan} = 2 \times \mathrm{DP} \times \frac{\mathrm{OH_{furan}}(\%)}{100} \quad (3)$$

Where, DP is the number of repeating units of the xylan-g-PCL.

Furthermore, the gel conversion, representing the molar percentage of the reactants that is required to reach gelation, can be determined using Macosko-Miller equation [14].

$$\mathrm{P_{gel}^2} = \frac{1}{\mathrm{r}(\bar{f}_{\mathrm{furan}} - 1)(\bar{f}_{\mathrm{Maleimide}} - 1)} \quad (4)$$

Where, $\bar{f}_{\mathrm{furan}}$ and $\bar{f}_{\mathrm{Maleimide}}$ are the average furan and maleimide functionalities, respectively. In addition, r is the molar ratio between furan and maleimide functions.

Table 2. Characteristics and structural features of the xylan-g-PCL and its furan grafted derivatives.

Sample	Theoretical OH_{furan} (%)	Experimental OH_{furan} (%)*	Theoretical $\bar{f}_{\mathrm{furan}}$	Experimental $\bar{f}_{\mathrm{furan}}$	Gel conversion (%)	Molecular weight ($g.mol^{-1}$)
Xylan-g-PCL	n.a.	n.a.	n.a.	n.a.	n.a.	22 100
S-10	10	8.5	7.4	6.3	43.6	23 480
S-20	20	15.6	14.8	11.5	30.8	24 700
S-30	30	23.3	22.2	17.2	24.9	26 050
S-40	40	31.2	29.6	23.1	21.2	27 400

*The molar percentage of grafted furan is the amount of the hydroxyl groups in the xylan-g-PCL reacted with the furan, calculated by ^{1}H NMR. $\bar{f}_{\mathrm{furan}}$ is the furan functionality per polymer chain. n.a. not applicable

As indicated in Table 2, the theoretical and experimental results are not identical. This is attributed to the fact that the furan grafting is incomplete. For S10, 85% of the expected conversion is achieved and 77-78% the other samples. In addition, the average number of furan functions per xylan-g-PCL chains are 6.3, 11.5, 17.2 and 23.1 for S10, S-20, S-30 and S-40, respectively. The gel conversion indicated a high possibility to crosslink these functional copolymers in which it is required about 43.6-21.2% conversion of the reactant to reach gelation.

The molar masses (M_n) of xylan-g-PCL and its furan grafted derivatives were determined by SEC (Table 1). Our results indicated that the M_n is influenced by furan grafting. The M_n of the xylan-g-PCL is 22100 g/mol and this increased to 27400 g/mol in the case of S-40. The grafting of furan rings stimulates a significant reduction in the elution time and hence an increase in the M_n of the copolymer. The increased M_n correlates with increased grafting and is an indication of the success of the furan grafting reaction.

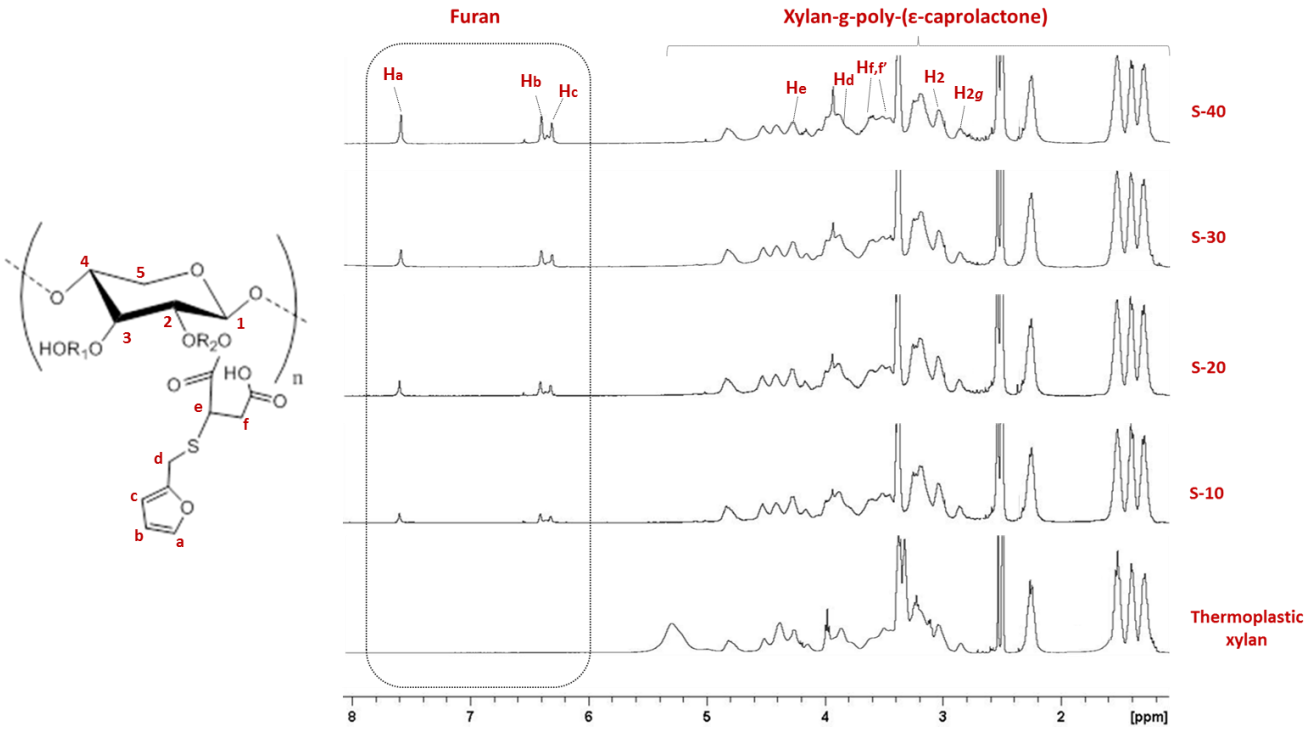

Figure 5. ^{1}H NMR spectra of furan grafted thermoplastic xylan based on the percentage of the grafted furan (solvent: DMSO-d_6 at 25°C and 400 MHz).

3.3. Synthesis of Diels-Alder materials

The temperature dependent reversibility of the DA chemistry has been used in the design of novel polymeric materials, particularly in the manufacture of thermoreversible crosslinked polymers [10][35]. In this study, the DA crosslinking reaction is expected to occur between the furan group of furan grafted xylan-g-PCL materials and bismaleimide (BMI) (Figure 6).

The qualitative solubility tests of the dried DA crosslinked materials at room temperature in DMSO are reported in Table 3. After 4 h of mixing, DA-10 was totally soluble unlike DA-20, DA-30, and DA-40; in which they showed a high tendency to form insoluble gels. This observation was based on the amount of the grafted furan. In fact, the sample with the lowest furan content (DA-10) and with a functionality of 6.3 was not able to form a gel in the reaction medium. However, all the other samples DA-20, DA-30, and DA-40 were able to form gels. This observation can be attributed to the inability of the material with low furan content (DA-10) to reach the gel point as discussed by Flory-Stockmayer theory [36][37]. As unexpected, this material was probably incapable to reach the required conversion percentage to form a network in the synthesis condition. In fact, DA-10 showed the highest gel conversion (43.6%, Table 2) and most probably it was not able to reach this conversion due to the reaction condition at 30°C. The other samples, due to the lower gel conversion (30.8-21.2%), were able to reach gelation at 30°C.

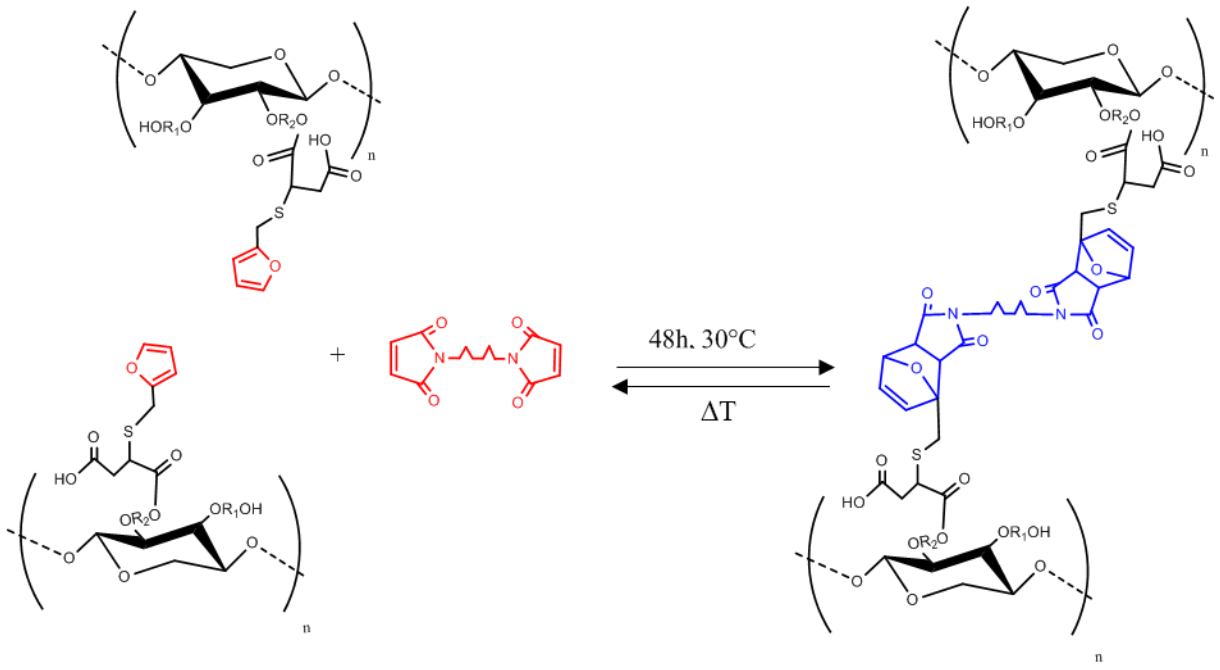

Figure 6: Schematic illustration of DA /rDA reaction between furan-grafted xylan-g-PCL and bismaleimide (BMI). △T represent the increase in temperature.

Table 3. Qualitative solubility tests at room temperature in DMSO

Sample (produced by DA reaction)	Furan grafted xylan-g-PCL starting material	Gel formation (?)*
DA-10	S-10	×
DA-20	S-20	√
DA-30	S-30	√
DA-40	S-40	√

*(×) refers that the sample was not able to form a gel in DMSO and (√) represents the ability of the sample to form a gel as observed in DMSO at room temperature after 4 h under magnetic stirring.

3.4. Tensile mechanical properties

The tensile tests of the designed materials (furan grafted copolymer and the DA crosslinked materials) are reported in Figure 7. The tensile strength indicates the maximum stress and provides a measure of the integrity and stiffness of the produced materials and hence, provides an indication of the material performance from being crosslinked or not. Our results showed that all the furan grafted copolymers (S-10, S-20, S-30, and S-40) have similar tensile strengths (8.2-9.3 N/m^2) and

a similar tensile strain (24.2-26.1%). This reveals that the grafting of furan with different percentages onto the xylan-g-PCL has no significant effect on the mechanical properties.

However, DA crosslinked materials showed much increased tensile strength and much lower strain to break than the non-crosslinked materials (Figure 7). The increase in the percentage of the grafted furan in the xylan-g-PCL influences the tensile strength of the DA crosslinked samples. Comparatively, sample DA-10 (S-10 starting material) showed the lowest strength (17 N/m^2) with a moderate elongation at break (9.2%) (compared with the other DA crosslinked materials). In addition, sample DA-40 (S-40 starting material) had the highest tensile strength (36.2 N/m^2) and the lowest strain (6%). This is attributed to the increase in the grafted furan which probably induces an increase in the crosslink density upon the reaction with BMI [38][39].

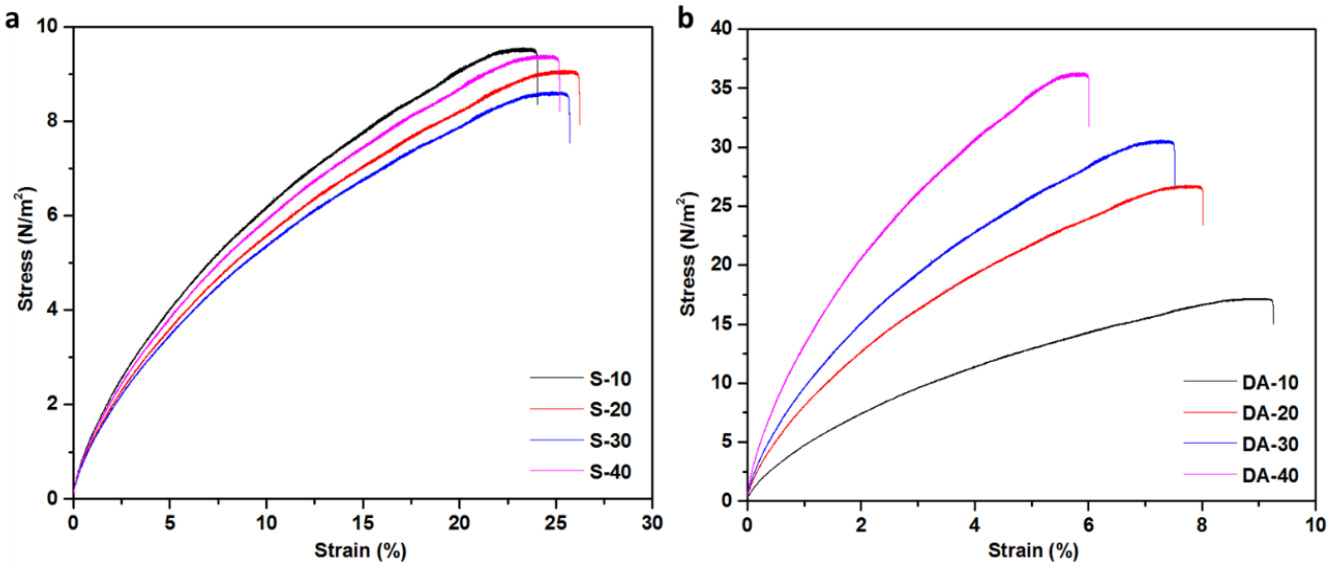

Figure 7. Stress-strain curves at a crosshead speed of 10 mm/min of (a) furan grafted xylan-g-PCL and (b) Diels-Alder crosslinked materials

3.5. Hydrolytic degradation

The hydrolytic degradation of these materials in phosphate buffer solution PBS (pH 7.4) at 37°C (similar to physiological conditions) over a period of 33 days is reported in Figure 8. In general, biodegradable polymers, during hydrolytic degradation, experience a hydrolytic bond cleavage. This allows the formation of water-soluble degradation intermediates that show high tendency to

dissolve in an aqueous environment, and subsequently cause polymer erosion [40]. According to Engineer *et al*. [40] the degradation process of polyesters occur in four stages. In the first stage, water diffuses into the polymeric matrix and followed by an auto-catalyzed hydrolysis reaction, most probably of the ester linkage, in the second stage resulting in release of oligomers. A critical molecular weight is achieved at the beginning of third stage, and oligomers start to diffuse out from the polymeric matrix. Water inters into the holes formed by the elimination of the oligomers, which in turn boosts the diffusion of the oligomers. Stage three exhibited a remarkable reduction in the polymer molecular weight. In last stage, the polymeric matrix become extremely porous and degradation proceeds homogeneously and more slowly [40]. Others have demonstrated that native xylan can degrade in its xylose monomer under hydrolytic degradation [18].

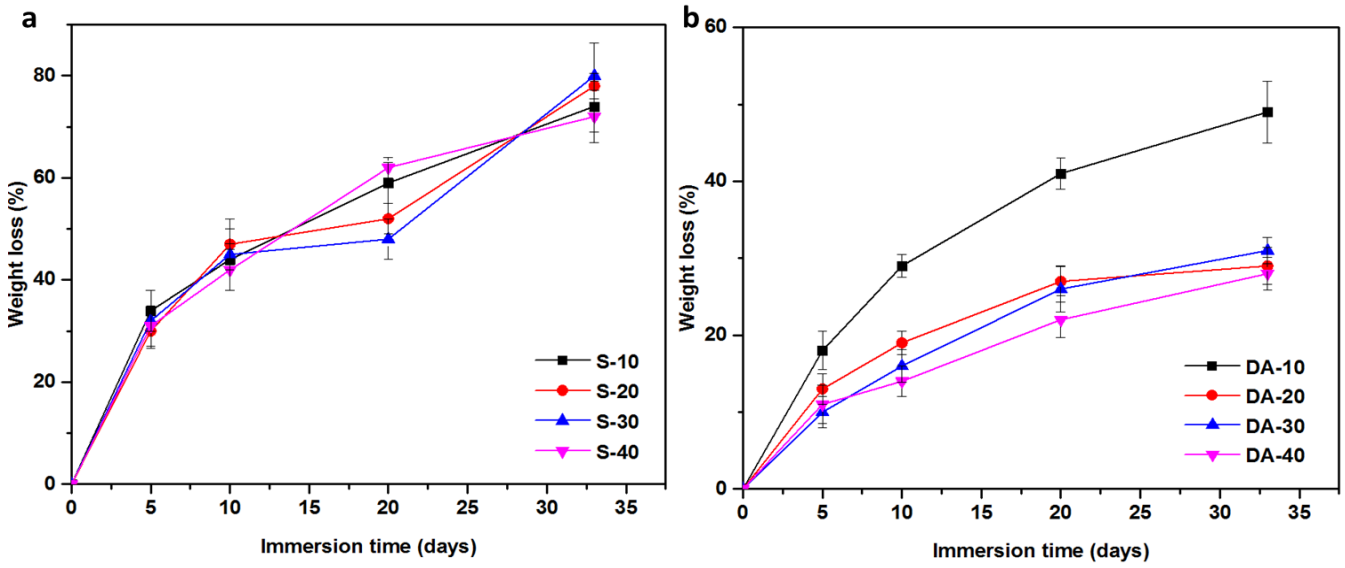

Figure 8. Weight loss as a function of immersion time in phosphate buffer solution (PBS) over a period of 33 days at 37°C: (a) furan grafted xylan-g-PCL and (b) Diels-Alder crosslinked materials.

Hydrolysable polymers tend to resist water degradation once crosslinked [41][42]. Herein, the un-crosslinked furan grafted copolymers showed a high degradation (74-80% weight loss) in PBS after 33 days (Figure 8a). The crosslinking by DA chemistry significantly reduces the hydrolytic degradation (25-49% weight loss) after 33 days (Figure 8b). In fact, sample DA-10 showed the highest degradation (49% weight loss) compared with the other DA crosslinked materials.

However, the increase in the percentage of the grafted furan (DA-20, DA-30, and DA-40) reduces the degradation of the materials to 31-25%., which limits the hydrolytic degradation in PBS. The high degradation of the furan grafted xylan-g-PCL is attributed to the autohydrolysis and solubilization of xylan and PCL side chains into their monomeric constituent as discussed before. The reduced degradation of the DA crosslinked materials is attributed the stabilized material strunction and hence, provide a further evidence on the success of the crosslinking.

3.6. Assessment of thermoreversibility

3.6.1. Solubility tests

In order to investigate the thermoreversibility of the designed networks by DA-rDA, the materials were first subjected to solubility test at different temperatures. DA-20 is presented in Figure 9 as an example. The samples were immersed in DMSO at 30 °C under magnetic stirring. After 4h of mixing, the materials did not dissolve and they were able to form a gel (only DA-10 was soluble as previously mentioned). This is attributed to the fact that the samples are crosslinked at such low temperature (30°C). The samples solubilize and form a homogeneous mixture upon heating at 150°C for 4h. The solubilization of the materials is attributed to the opening of the DA adduct by rDA upon heating at 150°C. In contrast, the samples were able to retune to the gel form by keeping them at 30°C for 2 days. Herein, the solubility test provides an evidence of thermoreversibility of the designed networks.

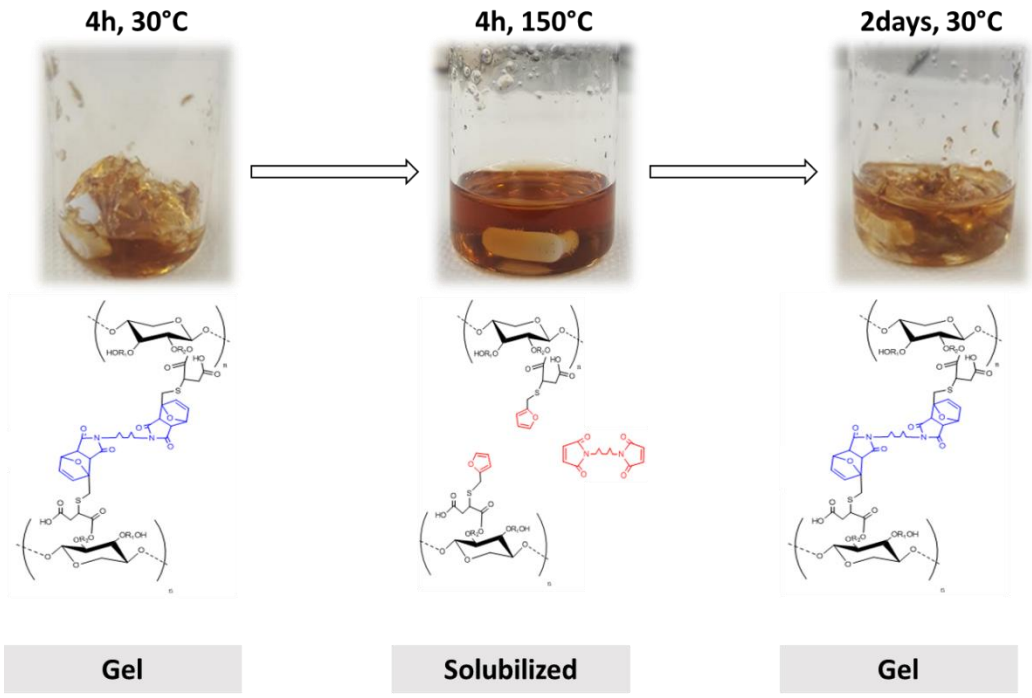

Figure 9. Evidence of the material (DA-20) thermoreversibility by solubility test in DMSO at 30 and 150°C.

3.6.2. Creep tests

To provide a quantitative confirmation of the temperature dependent reversibility of the manufactured networks, rheological studies were performed. The samples were first subjected to a maturation test to reach the maximum DA equilibrium. The maturation test was done at 80°C for 2 h at a fixed strain (Figure 10). Full maturation was reached as evidence of constant elastic modulus.

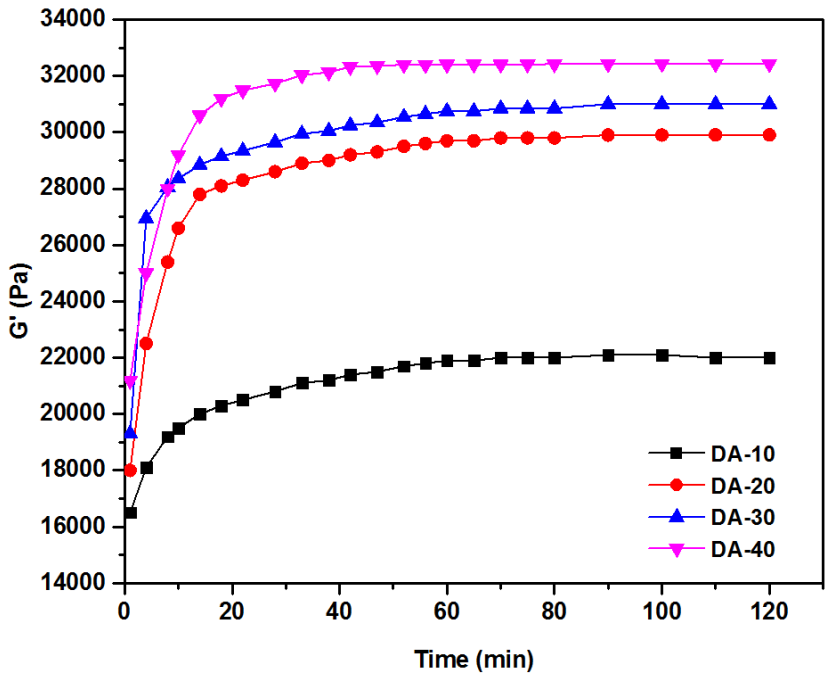

Figure 10. Maturation test at 80°C. Plots of G' of the different network materials versus time

The thermoreversibility of the designed materials were investigated by creep-recovery tests after maturation. To the best of our knowledge, this is the first report to use the creep-recovery test to confirm the temperature dependent reversibility of the DA networks. Creep-recovery assessments are adopted to examine the dimensional stability of the polymeric materials by understanding their long-term viscoelastic deformation behavior under constant stress and temperature [43]. In the creep-recovery test, an instantaneous step in the creep phase raise the stress to a constant value (500 Pa in our case) for a certain duration of time (herein, is 30 min) and is then completely removed in the following recovery phase. The resulting strain is recorded as a function of time at an isothermal temperature. The material will first show (in the creep phase) an immediate, elastic deformation (rubber behavior) followed by a transient behavior (retardation spectrum) and finally, for several samples, a steady flow of the material can be observed. In the following recovery phase, only the crosslinked elastic network will tend to recover completely while the viscoelastic uncrosslinked (or partially crosslinked) specimens will recover only a part of the deformation, that is they will not show a complete strain recovery in the recovery phase [44]. Chemical crosslinks create large molecules with long relaxation times and creep test gives opportunity to access the long term behavior without using time temperature superposition non applicable in the present

case of rheological complex systems. Moreover, compared to dynamic measurements, creep test allows to suppress any ambiguity on the origin of the rubbery behavior usually observed in the range on temperature and frequency used.

The creep-recovery test was applied to the designed networks at two different temperatures; (80°C) and (150°C), respectively. We assumed that at low temperature (80°C) the samples will exhibit a complete recovery due to the solid viscoelastic behavior of the crosslinked materials; however, at higher temperature (150°C) the tested specimens will lose part of their elastic behavior and will be converted to a liquid viscoelastic materials in response to the decrosslinking as induced by the opening of the DA adduct at such high temperature. The curves of the furan grafted thermoplastic xylan are reported in the Figure 11. The creep-recovery curves at 80°C and 150°C of the DA crosslinked materials are shown in Figure 12.

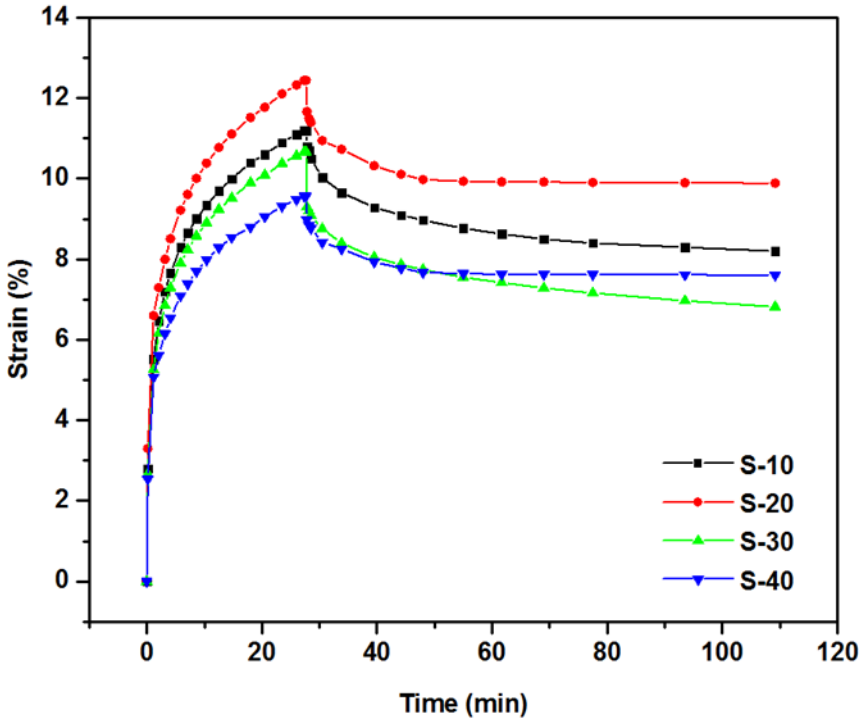

Figure 11. Creep-recovery response of the furan grafted copolymers at 80°C

Herein, the results of the creep-recovery test confirmed our hypothesis. In fact, all the furan grafted copolymers showed a partial recovery at 80°C, which confirms the liquid viscoelastic behavior of

such noncrosslinked or partially crosslinked materials (Figure 11). However, the majority of the DA fully crosslinked materials exhibited a complete recovery at 80°C (DA-20, DA-30, and DA-40) (Figure 12a). In contrast, these materials were not able to recover completely at 150°C. Instead, they were able to recover only 12.4, 19.3, and 16.8% of the original deformation, respectively (Figure 12b). The obtained results revealed that the tested specimens DA-20, DA-30, and DA-40 are viscoelastic solids at 80°C, attributed to their crosslinked structure. The increase in the temperature to 150°C induces a switch in their performance and the samples behave as liquid viscoelastic materials due to the partial or total decrosslinking induced by the opening of the DA adduct.

On the other hand, sample DA-10 was not able to recover completely at 80°C. However, it recovered 67% of the deformation. This result was in accordance to the outcomes of the tensile and degradation tests. This sample is probably not able to form a continuous network attributed to the furan content and DA crosslinking efficiency. As it was determined by ^{1}H-NMR and presented in Table 2, S-10 bears more than 6 furan functions, sufficient to generate full network. Despite that, it was not able to reach gelation. We strongly believe that for this sample the DA reaction was not efficient to crosslink the material and generate a full network.

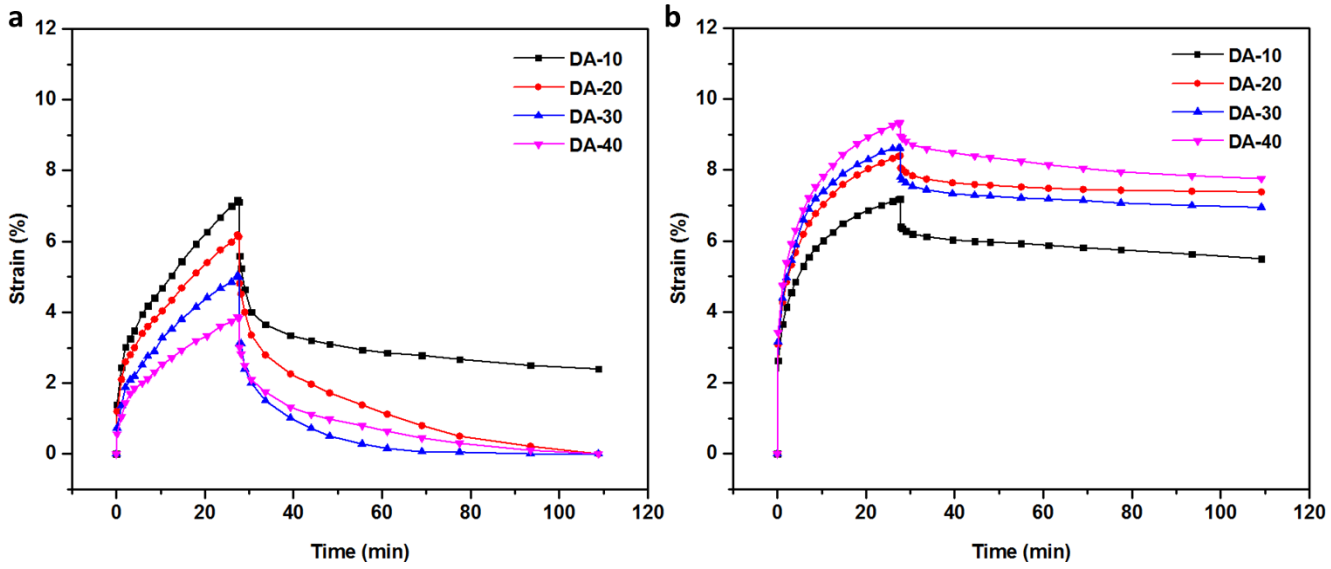

Figure 12. Creep-recovery response of the designed materials. (a) shows the creep-recovery at 80°C and (b) is the creep-recovery response at 150°C.

Temperature sweep tests were used to investigate the crosslinking/decrosslinking performance of the designed networks. Actually, a predominant elastic behavior results in a G′ higher than G″. In contrast, a liquid viscoelastic behavior indicates a G′ lower than G″. Herein, G′ was higher than G″ at lower temperatures. Then, both moduli values reduced with increasing temperature until the curves crossed ($T_{crossover}$) where G′ becomes lower than G″ as evidence of the opening of the DA adduct at higher temperatures by considering the creep results. By this dynamic test, we were able to determine the $T_{crossover}$ representing the point at which the DA/rDA reactions predominate. We believe that at $T_{crossover}$ the materials are neither in the fully crosslinked nor in the fully decrosslinked states. At this point the materials reached an average amounts of DA adduct opening sufficient to allow the partially decrosslinked networks to flow and behave as viscoelastic liquid materials. For this particular reason, we strongly believe that the determination of $T_{crossover}$ is not sufficient to provide a quantitative description the DA branching density of such covalent reversible materials, although it is commonly observed in literature. The $T_{crossover}$ of the uncroslinked furan grafted polymer (S-40) is shown in Figure 13.

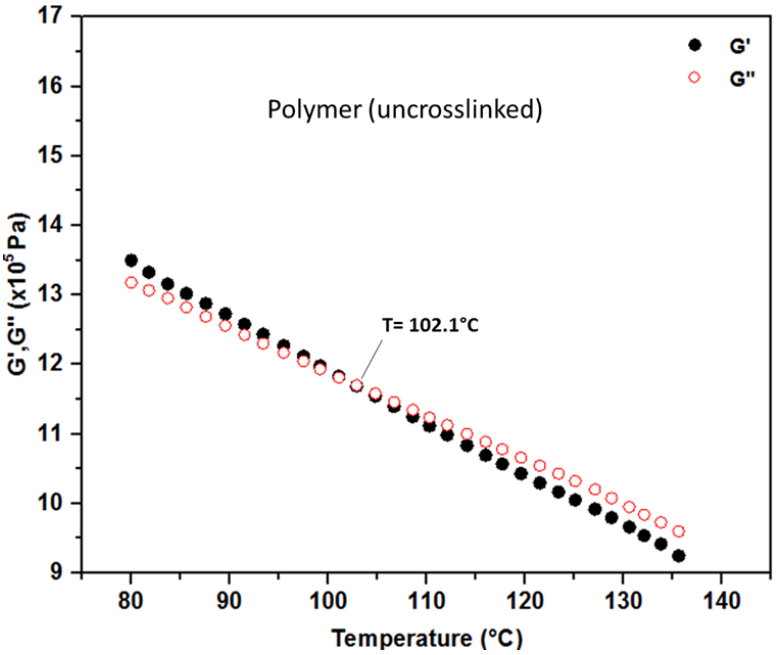

Figure 13. Temperature-sweep response of Furan grafted polymers (S-40) at 1 rad/s frequency

The $T_{crossover}$ of DA-10, DA-20, DA-30, and DA-40 was 108.6, 116.1, 120.2, and 127.6°C, respectively (Figure 14). Our results revealed a strong dependence of the crossover temperature on the furan content. In fact, the increase in the furan content induces a significant increase in the $T_{crossover}$. This is attributed to the increase of average relaxation times which stem from increase of crosslinking density with higher furan content.

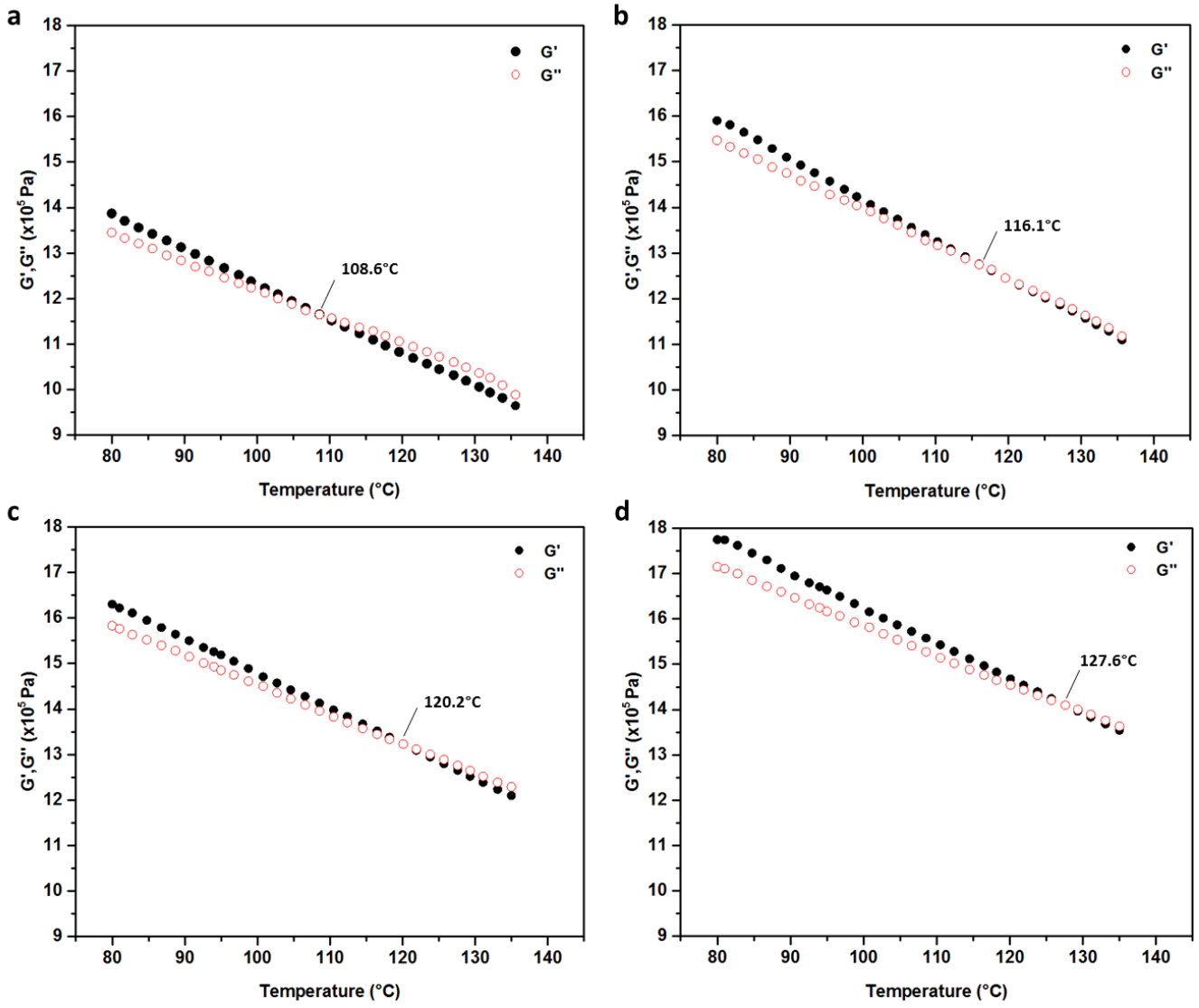

Figure 14. Temperature-sweep response of the designed networks at 1 rad/s frequency. (a) DA-10. (b) DA-20, (c) DA-30, and (d) DA-40.

4. Conclusion

Thermally reversible networks were formed from xylan type hemicellulose using Diels-Alder reaction. Short PCL chains were first grafted onto the xylan by ring opening polymerization to facilitate its use as a thermoplastic material. Thermoplastic xylan was then crosslinked by DA reaction to introduce thermoreversible properties to the material. Herein, we have used the furan/maleimide couple as a diene/dienophile system because of their good reactivity. Different amounts of furan moieties (6-22 furan ring/chain) were grafted onto the pre-synthesized xylan-g-PCL and allowed to form chemical networks via the reaction with BMI. The networks physicochemical and mechanical characteristics were explored by determining their solubility in PBS and their tensile properties. As expected, denser networks were obtained from furan-rich polymers characterized by higher tensile strength of 36.2 N/m^2, lower elongation at break of 6%, and lower solubility in PBS as in the case of DA-40. The thermoreversible characteristics of the designed networks were investigated by studying their solubility in DMSO at 30 and 150°C and by creep-recovery tests at 80 and 150°C proving that the thermoreversibily is reached in this range. Crossover temperatures ($T_{crossover}$) were examined and they were in the range of 109-128°C depending on the amount of furan moieties in the initial polymer.

References

[1] R.F. Patterson, A. Kandelbauer, U. Müller, H. Lammer, Crosslinked Thermoplastics, Third Edit, Elsevier, 2014.

[2] K. Roos, E. Dolci, S. Carlotti, S. Caillol, Activated anionic ring-opening polymerization for the synthesis of reversibly cross-linkable poly(propylene oxide) based on furan/maleimide chemistry, Polym. Chem. 7 (2016) 1612–1622. doi:10.1039/C5PY01778E.

[3] C.J. Kloxin, T.F. Scott, B.J. Adzima, C.N. Bowman, Covalent adaptable networks (CANs): A unique paradigm in cross-linked polymers, Macromolecules. 43 (2010) 2643–2653. doi:10.1021/ma902596s.

[4] C.O. Kappe, S.S. Murphree, A. Padwa, Synthetic applications of furan Diels-Alder chemistry, Tetrahedron. 53 (1997) 14179–14233. doi:10.1016/S0040-4020(97)00747-3.

[5] J.W. Kamplain, C.W. Bielawski, Dynamic covalent polymers based upon carbene dimerization., Chem. Commun. 16 (2006) 1727–9. doi:10.1039/b518246h.

[6] J. Brandt, J. Lenz, K. Pahnke, F.G. Schmidt, C. Barner-Kowollik, A. Lederer, Investigation of Thermoreversible Polymer Networks by Temperature Dependent Size Exclusion Chromatography, Polym. Chem. (2017). doi:10.1039/C7PY01262D.

[7] R.M.K. Ramanan, P. Chellamuthu, L. Tang, K.T. Nguyen, Development of a temperature-sensitive composite hydrogel for drug delivery applications, Biotechnol. Prog. 22 (2006) 118–125. doi:10.1021/bp0501367.

[8] N. Bayat, Y. Zhang, P. Falabella, R. Menefee, J.J.W. Iii, M.S. Humayun, M.E. Thompson, A reversible thermoresponsive sealant for temporary closure of ocular trauma, Sci. Transl. Med. 3879 (2017).

[9] T. Defize, R. Riva, J.M. Raquez, P. Dubois, C. Jérôme, M. Alexandre, Thermoreversibly crosslinked poly(e-caprolactone) as recyclable shape-memory polymer network, Macromol. Rapid Commun. 32 (2011) 1264–1269. doi:10.1002/marc.201100250.

[10] Y.-L. Liu, T.-W. Chuo, Self-healing polymers based on thermally reversible Diels–Alder chemistry, Polym. Chem. 4 (2013) 2194. doi:10.1039/c2py20957h.

[11] J. Ax, G. Wenz, Thermoreversible networks by diels-alder reaction of cellulose furoates with bismaleimides, Macromol. Chem. Phys. 213 (2012) 182–186. doi:10.1002/macp.201100410.

[12] A. Gandini, The furan/maleimide Diels-Alder reaction: A versatile click-unclick tool in macromolecular synthesis, Prog. Polym. Sci. 38 (2013) 1–29. doi:10.1016/j.progpolymsci.2012.04.002.

[13] N. Okhay, N. Mignard, C. Jegat, M. Taha, Diels-Alder thermoresponsive networks based on high maleimide- functionalized urethane prepolymers, Des. Monomers Polym. 16 (2013) 475–487. doi:10.1080/15685551.2012.747166.

[14] D. Djidi, N. Mignard, M. Taha, Thermosensitive polylactic-acid-based networks, Ind. Crops Prod. 72 (2015) 220–230. doi:10.1016/j.indcrop.2014.09.035.

[15] A. Gandini, A.J.D. Silvestre, D. Coelho, Reversible Click Chemistry at the Service of Macromolecular Materials. 2. Thermoreversible Polymers Based on the Diels-Alder Reaction of an A-B Furan/Maleimide Monomer, J. Polym. Sci. Part A Polym. Chem. 48 (2008) 2053–2056. doi:10.1002/pola.

[16] N. Mignard, N. Okhay, C. Jegat, M. Taha, Facile elaboration of polymethylmethacrylate/polyurethane interpenetrating networks using Diels-Alder reactions, J. Polym. Res. 20 (2013). doi:10.1007/s10965-013-0233-2.

[17] A. Gandini, Polymers from Renewable Resources: A Challenge for the Future of\rMacromolecular Materials, Macromolecules. 41 (2008) 9491–9504. doi:10.1021/ma801735u.

[18] W. Farhat, R.A. Venditti, M. Hubbe, M. Taha, F. Becquart, A. Ayoub, A Review of Water-Resistant Hemicellulose-Based Materials: Processing and Applications, ChemSusChem. 10 (2017) 305–323. doi:10.1002/cssc.201601047.

[19] W. Farhat, R. Venditti, A. Quick, M. Taha, N. Mignard, F. Becquart, A. Ayoub, Hemicellulose extraction and characterization for applications in paper coatings and adhesives, Ind. Crops Prod. 107 (2017) 370–377. doi:10.1016/j.indcrop.2017.05.055.

[20] X. Zhang, M. Chen, C. Liu, A. Zhang, R. Sun, Homogeneous ring opening graft

polymerization of caprolactone onto xylan in dual polar aprotic solvents, Carbohydr. Polym. 117 (2015) 701–709. doi:10.1016/j.carbpol.2014.10.061.

[21] F. Peng, J.L. Ren, F. Xu, J. Bian, P. Peng, R.C. Sun, Comparative study of hemicelluloses obtained by graded ethanol precipitation from sugarcane bagasse, J. Agric. Food Chem. 57 (2009) 6305–6317. doi:10.1021/jf900986b.

[22] T. Shahzadi, S. Mehmood, M. Irshad, Z. Anwar, A. Afroz, N. Zeeshan, U. Rashid, K. Sughra, Advances in lignocellulosic biotechnology : A brief review on lignocellulosic biomass and cellulases, Adv. Biosci. Biotechnol. 5 (2014) 246–251.

[23] W. Farhat, R. Venditti, N. Mignard, M. Taha, F. Becquart, A. Ayoub, Polysaccharides and lignin based hydrogels with potential pharmaceutical use as a drug delivery system produced by a reactive extrusion process, Int. J. Biol. Macromol. 104 (2017) 564–575. doi:10.1016/j.ijbiomac.2017.06.037.

[24] C. Laine, A. Harlin, J. Hartman, S. Hyvärinen, K. Kammiovirta, B. Krogerus, H. Pajari, H. Rautkoski, H. Setälä, J. Sievänen, J. Uotila, M. Vähä-Nissi, Hydroxyalkylated xylans - Their synthesis and application in coatings for packaging and paper, Ind. Crops Prod. 44 (2013) 692–704. doi:10.1016/j.indcrop.2012.08.033.

[25] K.S. Mikkonen, M. Tenkanen, Sustainable food-packaging materials based on future biorefinery products: Xylans and mannans, Trends Food Sci. Technol. 28 (2012) 90–102. doi:10.1016/j.tifs.2012.06.012.

[26] X. Cao, X. Peng, L. Zhong, R. Sun, Multiresponsive hydrogels based on xylan-type hemicelluloses and photoisomerized azobenzene copolymer as drug delivery carrier, J. Agric. Food Chem. 62 (2014) 10000–10007. doi:10.1021/jf504040s.

[27] L.M. Ferreira, C.S. Sobral, L. Blanes, M.Z. Ipolito, E.K. Horibe, Proliferation of fibroblasts cultured on a hemi-cellulose dressing, J. Plast. Reconstr. Aesthetic Surg. 63 (2010) 865–869. doi:10.1016/j.bjps.2009.01.086.

[28] X. Zhang, H. Wang, C. Liu, A. Zhang, J. Ren, Synthesis of Thermoplastic Xylan-Lactide Copolymer with Amidine-Mediated Organocatalyst in Ionic Liquid, Sci. Rep. 7 (2017) 551. doi:10.1038/s41598-017-00464-6.

[29] A. Ebringerová, T. Heinze, Xylan and xylan derivatives - Biopolymers with valuable properties, 1: Naturally occurring xylans structures, isolation procedures and properties, Macromol. Rapid Commun. 21 (2000) 542–556. doi:10.1002/1521-3927(20000601)21:9<542::aid-marc542>3.3.co;2-z.

[30] X. Zhang, M. Chen, C. Liu, A. Zhang, R. Sun, Ring-opening graft polymerization of propylene carbonate onto xylan in an ionic liquid, Molecules. 20 (2015) 6033–6047. doi:10.3390/molecules20046033.

[31] W. Farhat, R. Venditti, A. Ayoub, F. Prochazka, C. Fernández-de-alba, N. Mignard, M. Taha, F. Becquart, Towards thermoplastic hemicellulose : Chemistry and characteristics of poly- (ε -caprolactone) grafting onto hemicellulose backbones, Mater. Des. 153 (2018) 298–307. doi:10.1016/j.matdes.2018.05.013.

[32] S. Mhiri, N. Mignard, M. Abid, F. Prochazka, J.C. Majeste, M. Taha, Thermally reversible and biodegradable polyglycolic-acid-based networks, Eur. Polym. J. 88 (2017) 292–310. doi:10.1016/j.eurpolymj.2017.01.020.

[33] K.M. Stridsberg, M. Ryner, A.-C. Albertsson, Controlled Ring-Opening Polymerization: Polymers with designed Macromolecular Architecture, Degrad. Aliphatic Polyesters. 157 (2002) 41–65. doi:10.1007/3-540-45734-8_2.

[34] N. Teramoto, Y. Arai, M. Shibata, Thermo-reversible Diels – Alder polymerization of difurfurylidene trehalose and bismaleimides, Carbohyd Polym. 64 (2006) 78–84. doi:10.1016/j.carbpol.2005.10.029.

[35] C. Gaina, O. Ursache, V. Gaina, E. Buruiana, D. Ionita, Investigation on the thermal properties of new thermo-reversible networks based on poly(vinyl furfural) and multifunctional maleimide compounds, Express Polym. Lett. 6 (2012) 129–141. doi:10.3144/expresspolymlett.2012.14.

[36] W.H. Stockmayer, Theory of molecular size distribution and gel formation in branched polymers: II. General cross linking, J. Chem. Phys. 12 (1944) 125–131. doi:10.1063/1.1723922.

[37] A. Matsumoto, Y. Kitaguchi, O. Sonoda, Approach to Ideal Network Formation Governed

by Flory−Stockmayer Gelation Theory in Free-Radical Cross-Linking Copolymerization of Styrene with *m* -Divinylbenzene, Macromolecules. 32 (1999) 8336–8339. doi:10.1021/ma990368k.

[38] W.N.E. Van Dijk-Wolthuis, J.A.M. Hoogeboom, M.J. Van Steenbergen, S.K.Y. Tsang, W.E. Hennink, Degradation and release behavior of dextran-based hydrogels, Macromolecules. 30 (1997) 4639–4645. doi:10.1021/ma9704018.

[39] H.A. Khonakdar, J. Morshedian, U. Wagenknecht, S.H. Jafari, An investigation of chemical crosslinking effect on properties of high-density polyethylene, Polymer (Guildf). 44 (2003) 4301–4309. doi:10.1016/S0032-3861(03)00363-X.

[40] C. Engineer, J. Parikh, A. Raval, Review on Hydrolytic Degradation Behavior of Biodegradable Polymers from Controlled Drug Delivery System, 25 (2011) 79–85.

[41] J.A. Jung, B.K. Kim, Controls of solubility parameter and crosslinking density in polyurethane acrylate based holographic polymer dispersed liquid crystal, Opt. Commun. 247 (2005) 125–132. doi:10.1016/j.optcom.2004.11.063.

[42] E.M. Ahmed, Hydrogel: Preparation, characterization, and applications: A review, J. Adv. Res. 6 (2015) 105–121. doi:10.1016/j.jare.2013.07.006.

[43] F. Daver, M. Kajtaz, M. Brandt, R.A. Shanks, Creep and recovery behaviour of polyolefin-rubber nanocomposites developed for additive manufacturing, Polymers (Basel). 8 (2016). doi:10.3390/polym8120437.

[44] C. Yan, D.J. Pochan, Rheological properties of peptide-based hydrogels for biomedical and other applications., Chem. Soc. Rev. 39 (2010) 3528–40. doi:10.1039/b919449p.

Conclusions and Future Perspective

Naturally occurring renewable and sustainable materials have become well known in the design of bio-based products. Biomass, which includes all plants and plant derivatives, has been widely used in many disciplines, and converted into a wide range of marketable products. Currently, the interest in replacing synthetic polymers with natural polymers for applications that interact with humans or the environment is based on human health, environmental impacts at end of life, the use of renewable resources, and for national security. Hemicellulose materials are arguably the second most abundant renewable component of biomass after cellulose. They are relatively underutilized hetero-polysaccharides present in lignocellulosic materials. Chapter 1. In this dissertation comprehensive approaches towards the extraction, modification and application of hemicellulose has been presented. Research in which hemicellulose derivatives or combinations of hemicelluloses with modified derivatives are used with to prepare biomaterials is considered in this chapter. An overview of the various isolation methods that have been used to separate hemicellulose from biomass are also discussed. In addition, the most useful pathways to change the character of hemicelluloses into a processable and hydrophobic material are reviewed. Several applications of these materials are presented. In fact, Hemicelluloses show high potential for utilization in remarkable applications. Unique properties, such as being branched hetero-polymers with several structures based on the different sources and the ability to be modified by several physical and chemical reactions, provides hemicelluloses with an ability to be used in the manufacturing of unique products. In Chapter 2, an alkaline treatment was optimized for the extraction of polymeric hemicellulose from fully bleached hardwood pulp (B-HWP) and partially delignified switchgrass (SWG). The hemicellulose extracted from B-HWP was relatively pure with zero percent lignin and 89.5% xylose content; whereas, the partially delignified SWG hemicellulose contained about 6-3% lignin and 72–82% xylose, depending on the NaOH concentration during extraction (3–17% NaOH solution). A maximum molecular weight of SWG hemicellulose of 64,300 g/mol was achieved for the 10% NaOH solution extraction. We have demonstrated that the residual lignin in SWG hemicellulose lowered the system T_g and this might be utilized as a way to increase the applications of hemicellulose in high value biomaterials. Furthermore, the technical and economic analysis for the extraction process was investigated. The

analysis was performed to determine the economic feasibility of building a commercial biorefinery for the co-production of dissolving pulp and hemicellulose using bleached pulp as a starting raw material. In Chapter 3, hemicellulose was crosslinked with zirconium to develop a water resistant gel for coating or adhesive applications. Our results showed that the loading stress required to break an hemicellulose based adhesive connection between two paper surfaces was 0.89, 2.02, 2.75, 3.46, and 3.11 (MPa) for 2, 4, 6, 8 and 10% AZC samples, indicating that up to about 8% AZC crosslinker in the hemicellulose increases the adhesive behavior of the material. The hemicellulose crosslinked with AZC has a good potential for coating and adhesive applications and may be an important higher valued byproduct for the biorefinery. In Chapter 4, we have provided a novel study for the processing of hemicellulose and other natural polymers. In this research we described the development of drug delivery hydrogels from the natural polymers, hemicelluloses, starch, and lignin by means of reactive extrusion. The hydrogels show a strong swelling ability dependent on pH which may be used to control diffusion rates of water and small molecules in and out of the gel. Also, the hydrogels degradation rates were studied in a physiological solution (pH 7.4) for 15 days. The results indicated that for all three macromolecules, the higher level of plasticizer increase the rate of weight loss of the hydrogels. The degradation was extremely reduced when the polymers were extruded in the presence of a catalyst. The dynamic mechanical analysis revealed that the degradation of the hydrogels induce a significant reduction in the compressive modulus. This part of the dissertation demonstrates the characteristics and potential of hemicellulose and other natural polymers as a drug release system. In Chapter 5, hemicellulose was subjected to a chemical modification by ring-opening graft polymerization of ε-caprolactone (CL) to improve its processability. Hemicellulose-graft-poly-(ε-caprolactone) (HC_gPCL) copolymers were synthesized using 1,5,7-triazabicyclodecene [4.4.0] (TBD) as an organic catalyst. The extent and length of grafted PCL sidechains in HC_gPCL copolymers were controlled by adjusting the molar ratios of CL monomer to anhydroxylose residues. The various characterization analysis of the physicochemical and mechanical properties of HC_gPCL materials revealed a successful grafting. The NMR analysis indicated that the degree of polymerization (DP) of the grafted PCL can range between 1.82 and 4.26 based on the changes in the molar ratio of the reactants. Furthermore, results indicated that the mechanical and the hydrophobic properties of the materials were enhanced by PCL grafting onto hemicellulose. The biodegradability measurements indicated a remarkable (95.3–99.7%) materials biodegradation. Finally, Chapter 6 provided the

synthesis of thermally reversible hemicellulose-based network, crosslinked by means of Diels-Alder chemistry. The thermoplastic hemicellulose presented by HC_gPCL copolymer were functionalized with a different amount of furan rings and allowed to react with bismaleimide through Diels-Alder reaction. The temperature dependent reversibility of the designed networks was addressed by solubility and rheological assessments. Our results indicated that the temperature at which the networks disassemble varies based on the amount of the furan moieties in the initial copolymer and can range between 108.6-127.6°C. The designed networks display a promising molecular and synthetic features for the production of high-performance temperature-responsive polymers from renewable resources. We strongly believe that the advancement in the scope of sustainable biomaterials is essential to solve environmental and economic issues currently impacting present and future generations. For this purpose, more work must be done on significant projects in the field of green materials as these chief issues can probably be addressed by imaginative scientific ideas. Our results in all the investigation areas presented here shed light on vital features of the use of the natural polymer hemicellulose in the sustainable and renewable biomaterials, representing a step forward towards the expansion of value-added biomaterials that might solve future economical and ecological problems.